UNIVERSITÀ DI PARMA

UNIVERSITA' DEGLI STUDI DI PARMA

DOTTORATO DI RICERCA IN DRUG SCIENCES

CICLO XXXVI

DESIGN, SYNTHESIS, AND PRELIMINARY INVESTIGATION ON THE MODE OF ACTION FOR A SERIES OF NOVEL ANTIMICROBIAL PEPTIDOMIMETICS

Coordinatore:

Chiar.mo Prof. Marco Mor

Tutore:

Chiar.mo Prof. Marco Pieroni

Dottoranda: Diletta Bergamo

Anni Accademici 2020/2021 – 2022/2023

[This page is intentionally left blank]

Ai miei genitori e a mia sorella,

punti cardinali nella mia vita.

[This page is intentionally left blank]

Index

[This page is intentionally left blank]

Abstract

Over the years, many antibiotics with different mechanisms of action have been developed. However most of them succumb to antimicrobial resistance, especially when their mechanism of action depends on enzymatic inhibition. Nowadays it is recognized that a non-specific mechanism, such as physical disruption of the membrane, is less susceptible to resistance. This can be achieved through specific molecules, including antimicrobial peptides (AMPs). Despite their unique mode of action, the antimicrobial activity of AMPs is limited, primarily due to their high susceptibility to proteolytic degradation by endogenous or microbial enzymes. To counteract proteolytic degradation and to improve the knowledge around these antibacterial agents, we planned to synthetize a library of antimicrobial peptides mimetics overcoming specific weaknesses related to this class of molecules, such as their metabolic instability. Additionally, our goal is to develop compounds that not only mimic peptides but also possess membranolytic properties similar to AMPs, enabling direct disruption of the bacterial membrane. The molecular template for the development of our library of peptidomimetics compounds is represented by Brilacidin which is a defensin-mimetic molecule. This molecule was showed to have activity against *S. aureus*, *Enterococcus faecium*, *E. Coli*. Taking inspiration by the Brilacidin structure and relevant literature, we identified a hypothetical pharmacophore for synthesizing structurally related analogues. The modification of side arm lengths is crucial to achieving the specific conformation required for perpendicular insertion into phospholipid bilayers. Before synthesizing other analogues, I have focused my interest on the comprehensive biological characterization of the molecules synthesized. Therefore, the compounds were tested on a wide panel of clinically relevant pathogens showing encouraging antimicrobials activity and preliminary investigations on the mode of action confirmed the hypothesised membranolytic mechanism of action.

[This page is intentionally left blank]

Acknowledgments

During these three long and hard years of PhD I had the great pleasure to work with awesome people that I'm pleased to thank for all their support and devotion in doing their research. I first thank my supervisor prof. Marco Pieroni for being the person who main supported me during these years always welcoming my ideas and requests, for being such a passionate researcher who helped enriching my scientific knowledge and provide me with the basic skills to afford the scientific word. I had the great opportunity to experience two period abroad supported and encouraged by him and I'll be always thankful for accomplish my requests of experiencing new research realities. I'd like to thank as well prof. Costantino for giving me the opportunity to carry out my PhD studies in his lab.

I like to thank all my PhD colleagues and friends for their support during these years, in particular a special thanks to Laura for being a wonderful college and friend helping me with the first steps in the life of a PhD student and for being always present and available. I'd like to thank as well the whole research group colleagues, among them Gianna, Chiara, Grazia, Lisa, Francesca, Kelly, it has been a great pleasure shearing these years working with you, and I'll be always tankful for all the help.

Since I had the awesome opportunity to join prof. Brimble Lab at the University of Auckland in New Zealand I'm pleased to thank Margaret for giving me the opportunity to join her lab enriching my scientific knowledge and living at the same time the most awesome life experience ever. I would like to thank all the wonderful people who I worked with, among them Paul, Yan and Alan for being amazing mentors leading me to love my work even more thanks to their passion for research. Moreover a special thanks to all the PhD students I had the pleasure to work with, Juliana, Saawan, CJ, Rolland, Tony, Yubing Christy

,Suzie ,Polly Emily ,Cat, Dennise, Julia and who ever contributed in making this experience the most incredible.
I'd like to thanks prof.Muller as well for giving me the opportunity to join his lab at Helmholtz Institute where I performed the second part of my project and Katarina for supervising me with patience and dedication in teaching to a chemistry researcher the biology word. I would like to thank all the PhD students and postdoc researchers I worked with among them Franzi, Sari, Timo, Felix and my wonderful office mates and friends Jeenu, Sumeire, Kamal, Vida and Asfandyar.

Infine, voglio ringraziare i miei genitori per essere stati da sempre il mio esempio e punto di riferimento e per avermi sempre guidato verso la luce anche nei momenti piu bui di questi anni di dottorato. Grazie per essere sempre presenti, per tutto il supporto che ricevo costantemente e per credere in me piuù di chiunque altro insegandomi a vedere sempre il lato positivo in ogni cosa che faccio anche quando sembra che non ci siano soluzioni. Grazie per avermi insegnato, e continuare ad insegnarmi, che una soluzione c'è sempre a tutto perché è grazie a voi e agli insegnamenti che mi avete trasmesso se oggi sono arrivata a questo punto della mia carriera. Sono fiera dei genitori che siete e grata di avervi come punti cardinali nelle mie scelte di vita.

Abbreviations

6-Cl-HOBt	6-chloro-1-benzotriazole
AA	amino acid
Ac_2O	acetic anhydride
Ala	alanine
All	allyl
Alloc	allyloxycarbonyl
AMPs	antimicrobial peptides
AMR	antimicrobial resistance
Arg	arginine
Boc	tert-butoxycarbonyl
Boc_2O	di-tertbuthyl-dicarbonate
BOP	benzotriazol-1-yloxytris(dimethylamino)phosphonium hexafluorophosphate Bzl benzyl
Cbz	carbobenzoxy
CH_2Cl_2	dichloromethane
CH3CN	acetonitrile
$CHCl_3$	chloroform
$ClCO_2iBu$	isobutyl chloroformate
CLipPA	Cysteine Lipidation on a Peptide or Amino acid
Cys	cysteine
Dab	2,4-diaminobutyric acid
DCC	N,N'-dicyclohexylcarbodiimide
DCM	dicloromethane

DCU	N,N'-dicyclohexylurea
Dde	1-(4,4-dimethyl-2,6-dioxocyclohexylidene)ethyl
DIC	N,N'-diisopropylcarbodimide
DIPEA	N,N-diisopropylethylamine
DMAP	2,2-dimethoxy-2-phenylacetophenone
DMSO	dimethyl sulfoxide
EDT	1,2-ethanedithiol
EP	petroleum ether
ESI-MS	electron-spray ionisation mass spectrometry
EtOAc	Ethyl acetate
Et_2O	diethyl ether
EtOH	ethanol
Fmoc	9-fluorenylmethoxycarbonyl
HATU	O-(7-azabenzotriazol-1-yl)-N,N,N′,N′-tetramethyluronium hexafluorophosphate
HBr	hydrogen bromide
HBTU	O-(benzotriazol-1-yl)-N,N,N′,N′-tetramethyluronium hexafluorophosphate
HCTU	O-(6-chlorobenzotriazol-1-yl)-N,N,N′,N′-tetramethyluronium hexafluorophosphate
HF	hydrogen fluoride
HRMS	high resolution mass spectrometry
IC_{50}	half maximal inhibitory concentration
LiOH	Lithium hydroxide
Ile	isoleucine
LPS	lipopolysaccharides
MDR	Multidrug resistant

MeOH	methanol
MHBII	Mueller-Hinton broth
MIC	minimum inhibitory concentration
MoA	Mechanism of action
MRSA	methicillin-resistant Staphylococcus aureus
MS	mass spectrometry
MS/MS	tandem mass spectrometry
Mtt	4-methyltrity
NaOH	sodium hydroxide
NH_3	Ammonia
NMM	*N*-methyl morpholine
NMP	1-methyl-2-pyrrolidinone
NMR	nuclear magnetic resonance
$Pd(PPh_3)_4$	tetrakis(triphenylphosphine) palladium (0)
$PhSiH_3$	phenylsilane
PMB	PMB
PMBN	polymyxin B nonapeptide
PyAOP	(7-azabenzotriazol-1-yloxy)tripyrrolidinophosphonium hexafluorophosphate
PyBOP	benzotriazole-1-yl-oxy-tris-pyrrolidino-phosphonium hexafluorophosphate
RP-HPLC	reverse-phase high performance liquid chromatography
RT	Room temperature
SAR	structure-activity relationships
SEM	Scanning Electron Microscopy
SPPS	solid-phase peptide synthesis

tBu	tert-butyl
TEM	Transmission Electron Microscopy
TFA	trifluoroacetic acid
TFAA	trifluoroacetic anhydride
THF	tetrahydrofuran
Thr	threonine
TIPS	triisopropylsilane
Trp	tryptophan
Trt	trityl
VRE	vancomycin resistant Enterococci
WHO	World Health Organisation

List of Figures

[This page is intentionally left blank]

List of Schemes

List of Tables

[This page is intentionally left blank]

Chapter1_Introduction

[This page is intentionally left blank]

1.1.Antibiotics history

The privilege for the humanity to get into the "Antibiotic era" began less than a century ago with the discovery and clinical use of penicillin. The outstanding success of the antibiotic chemotherapy started the antimicrobial development rush, culminating with the golden period of the antibacterial drug discovery (1940-1960), when many of the currently used antibacterial agents were studied and introduced in the clinical use.

Despite what we are led to believe, penicillin wasn't the first antimicrobial molecule in the human history, but it was the one that mainly impacted the antimicrobial future discovery since it was the first molecule presenting more antimicrobial than toxic activity [1].

The use of different substances that might play a role in the prevention of diseases diffusion dates back thousands of years. It might be worth mentioning the use of mouldy bread and medicinal soil to treat wounds in the ancient Serbia, China, Greece and Egypt. [2]

Despite these rudimentary remedies, the upcoming centuries reserved to the humanity the terrible experience due to the plague caused by the *Yersinia pestis*, which showed up several times with different alias such as "Bubonic plague", "Justinian plague" or "Black death", proving how the introduction of efficient medical solutions was highly needed to guarantee human beings livelihood.[3]

Along those centuries, different scientists begun to assume that there were specific causes behind the diffusion of this human illness and that some precautionary measures could be implemented. It was in 1546 that Girolamo Fracastoro envisaged the idea that specific diseases could be caused by transferable, undetectable seed-like particles. Only a few centuries later the

Hungarian physician Ignaz Semmelweis emphasized the relevance of hand washing and hygiene in the hospitals.[4]

The first time the existence of microscopic living organism was detected was more than a century later, in 1676 by Antonie van Leeuwenhoek, through a microscope he designed. However, the actual breakthrough in the field of microbiology came with Koch and Pasteur, when for the first time the association between individual species of bacteria and disease was demonstrated. [5]

Between 1854 and 1859 Antonie Béchamp synthetized aniline and by reacting it with arsenic acid he obtained Atoxyl, initially used in the treatment of trypanosomes and syphilis. [6] In 1871, Joseph Lister identified the inhibitory activity of *Penicillium glaucum* extract against bacterial growth allowing the treatment of an injury and consequently proving that bacteria were somehow liable for human infections.[3] Between 1882 and 1884 Koch, Fisher and Gaffky, isolated the *Mycobacterium tuberculosis* and the *Vibrio cholerae*.[4] In 1887 Jules François Joubert discovered as *Bacillus anthracis* growth was inhibited when co-cultivated with other aerobic bacteria present in urine samples.[1]
The first natural molecule with antimicrobial activity has been identified in 1893 by Bartolomeo Gosio from *Penicillium glauucum*, it was the so-called mycophenolic acid that inhibits the growth of *Bacillus anthracis*. However, the structure has been unidentified until 1952 and the total synthesis was obtained only in 1969.[4] Consequently in 1897 Ernest Duchesne discovered the inhibition of *Escherichia coli* by *Penicillium glaucum*.

Therefore it can be said that there were numerous evidences that bacteria or plants might produce some self-defence molecules with antibacterial activity against other microbes, however none of these molecules has been purified, and the first antimicrobial compound was chemically synthetized.[1]

Paul Ehrlich and his collaborators in 1909 rationally synthetized a new molecule based on the arsenic-derivate structure Atoxyl previously studied by

Béchamp, which was showed to be selectively active against *Treponema pallidum* for the treatment of syphilis. The chemotherapeutic era had begun. This molecule was named Salvarsan and was used as the main prescribed antimicrobial drug until the discovery of penicillin. Chemical modifications of this starting molecule led to develop a more soluble compound called Neosalvarsan, even though we have to wait till mid-1930 to have a safe antibacterial compound, when Gerard Domagk synthesized the first sulfamic drug, Prontosil. Since then, thousands of derivatives named azo-compounds such as sulfamethoxazole were prepared and they are nowadays still used in clinical use.[6]

As it is well known, the first antibiotic was discovered serendipitously by Alexander Flemming in 1928. He found out that a fungus called *Penicillium notatum* was able to inhibit the growth of a *Pseudomonas aeruginosa* strain. However, since the difficulties in the isolation and purification of the molecule, and the need to set up a scalable process, relegated Penicillin to oblivion. During World War II, and thanks to the contribution of H. W. Florey and E. B. Chain, who practically isolated the compound, discovered the structure, designed and scaled up the synthesis, Penicillin G was introduced in the market in 1941 becoming the first antibiotic in the history.[3]

Afterward, the golden era of antibiotic drug discovery started in 1940 when Selman Waksman discovered as the soil bacteria actinomycetes had the ability to produce metabolites which inhibit the growth of other pathogens, allowing him to develop a screening platform based on a set of culture techniques and strategies and called “Waksman platform”. Nowadays, over 90% of the antibiotics in clinical use originated from actinomycetes, making these microbes a golden source of antibiotics. This extraordinary intuition allows him to isolate most of the major antimicrobial compounds such as actinomycin, streptothricin, neomycin, fumigacin and clavacin and this approach became the milestone in the rising pharmaceutical industry. Indeed the rational screening techniques led to the discovery of most of the antibiotic compounds between ’40s and ’70s,

some of them still used today such as actinomycin, neomycin and streptomycin.[1,3,6]

Some examples of all the new antimicrobial molecules isolated from microbes and introduced in these decades are here reported. In 1939 **Gramicidin D** was isolated from *Bacillus brevis* and active against Gram-positive and some Gram-negative, it unfortunately successively showed haemolytic properties after clinical introduction. In 1943 **streptomycin** was isolated from *Actinomyces griseus* and classified as the first molecule of the aminoglycoside class. In 1945 **tetracyclines**, was isolated from *Strep. aureofaciens* active on gram+/- they pursue bacteriostatic activity by binding to the ribosome at the 30S site leading to the inhibition of the bacterial protein synthesis.

In 1952 **erythromycins** presenting macrolide structures were isolated from *Saccharopolyspora erythraea* and their bacteriostatic or bactericidal activity was due to the binding to the 50S subunit of the ribosome. In 1953 **vancomycin** was extracted from *Strep. orientalis* and it soon became the main representative

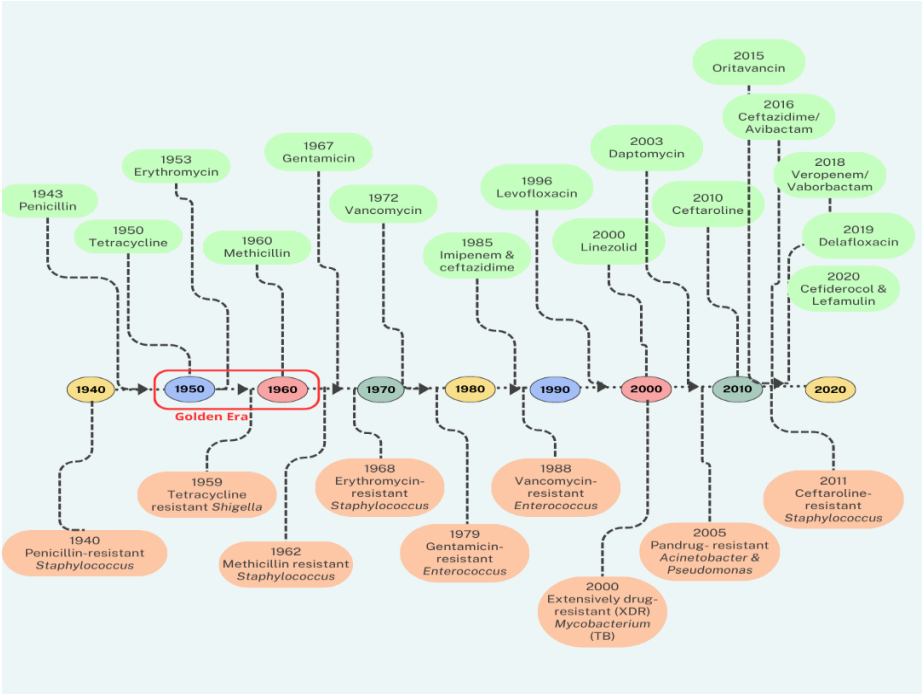

Figure 1 *Main antibiotic discoveries and related developed resistance. Adapted from Ref.7.*

of a new class called glycopeptides and introduced in clinical use in 1958 but later substituted by other derivatives for toxicity reasons. In the same year (1953) was also discovered **streptogramin** from the *Strep. Graminofaciens* which acts by binding the 50s ribosomal subunit and became commercially available in 1973 for the treatment of Streptococci and Staphylococci infections.[4] The first lipopeptide compound was discovered in 1947 as **polymyxin E**, isolated from *Paenibacillus polymyxa*, despite the efficacy their use was really limited as a consequence of their adverse effects, only in the last years they have been reconsidered and chemically modified to obtain new derivatives.[6]

By the early '60s, the discovery of new scaffolds based on natural bacterial compounds was getting harder since most of them showed toxicological and pharmacological issues and the antimicrobial resistance could be easily detected for most of the new molecules. This led to the beginning of the medicinal chemistry era which allowed to the development of new molecules based on the synthetic modification of natural compounds previously discovered. [7] This resulted in the lack of new antimicrobial classes for the next 50 years.[3] Examples of this new medicinal chemistry approach are represented by **Trimethoprim** and **nalidixic acid** synthetized in 1962, the latest allow the development of quinolones that were later replaced by fluoroquinolones as **ciprofloxacin**. Another example of this new approach is represented by semisynthetic studies based on erythromycin which led to the development of the new ketolide class including **telithromycin** discovered in 1997 and active against gram positive bacteria. Last but not least example is represented by **telavancin** that was semi synthetically derived from vancomycin and became part of the lipoglycopeptides class and approved by FDA in 2009, it acts interfering with the cell wall precursor lipid II. [4]

Despite the new antimicrobial molecule discovered in the last decades, none of them represented a completely innovative antibiotic class, with oxazolidinones, discovered in 1987, representing the last antimicrobial class introduced in

therapy, [1,3] with blockbuster **Linezolid** introduced in the market in 2003.[1] The last antibiotics compounds discovered after many decades were **teixobactin** in 2015, active against gram positive interacting with the bacterial wall synthesis, and more recently **lugdunin** isolated from *Staph. lugdunensis*.[4]

At the moment, despite a clear increase in the number of antibacterial drugs approved by EMA and FDA compared with non-bacterial drugs[8] in the last decades (2010-2022) only 14 antibiotics were approved.[9] Among them between 2009 and 2022 some of the FDA/EMA approved drugs for the treatment of gram positive and gram negative infections are glycopeptides (Telavancin, Oritavancin, Dalbavancin), cephalosporin (Ceftaroline,Cefiderocol), pleuromutilin (Ceftaroline), fluoroquinolones (Delafloxacin), Aminoglycosides (Plazomicin, Fidaxomicin, Bezlotoxumab), Oxazolidinones (Tedizolid), tetracycline (Eravacycline). [10]

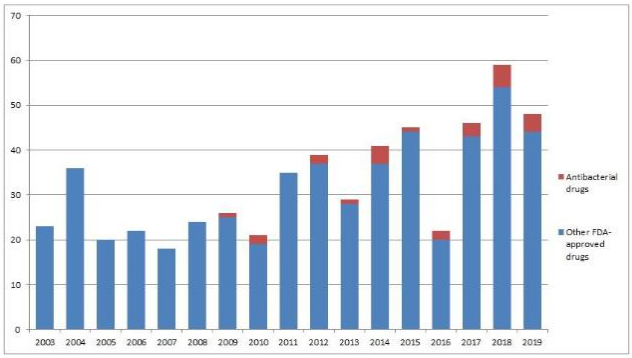

Figure 2 *Novel FDA-approved antibacterial drugs in the last 17 years. Adapted from Ref.9.*

Being intended as an at-hand remedy for every kind of infection, the misuse of antibiotics, combined with the loss of interest by pharmaceutical company to devote money and time to antibiotic research, have led to the raise of a potentially dreadful phenomenon, antibiotic resistance

1.2. Antimicrobial resistance (AMR)

The discovery and introduction of antibacterial molecules has allowed humanity to survive a high number of infections. Simultaneously as a response to the human attack, bacteria managed to fight back, developing a series of counter-defense actions to escape antibacterial effect.

Antimicrobial resistance (AMR) is the capacity of bacteria to survive exposure to a defined concentration of an antimicrobial substance.[11]

AMR is a natural defense mechanism in bacteria, indeed genes encoding resistance to glycopeptides, tetracyclines, and β-lactam antibiotics have been discovered in Canada's frozen sediments dating back 30,000 years.[12,13] Vancomycin intrinsic resistant enterococci naturally exist in nature. Moreover, they have proven to be less susceptible to penicillin.[14] Additionally, they have been identified in the gut flora of individuals who have been isolated from the modern society and the use of antibiotics.[15]

Despite the natural resistant strains, the unproper use of antimicrobials represents one of the main drivers of AMR, considering that it occurred since the introduction of the first antimicrobial molecule in 1945 resulting in many bacterial strains resistant to the new wonder drug.[3,12,14] For instance, in the 1950s, there were many bacterial strains showing resistance to some of the most common antibiotics such as tetracycline, streptomycin, or chloramphenicol. Moreover, the first methicillin-resistant *S. aureus* (MRSA) strain was discovered in 1961 only a few months after the introduction of the drug (1959). Resistance to Linezolid and Daptomycin was identified after 5 years from the market introduction.[15]

Thereafter it was clear that bacteria where able to evolve resistance to most of the new antimicrobial molecules, moreover some of them were already resistant even before the market introduction **(*Figure3*).**[12]

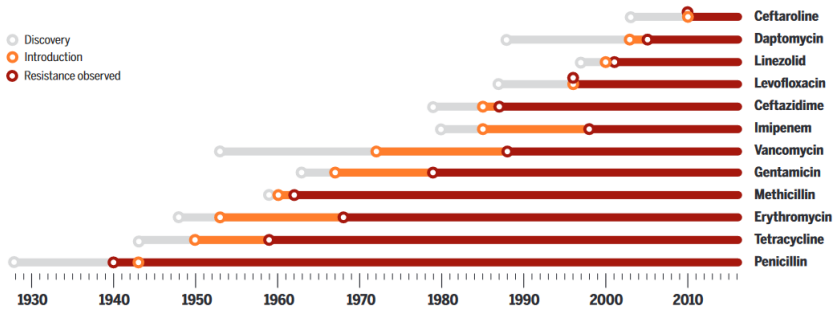

Figure 3. *Antibiotics and their relative antimicrobial resistance. Adapted from Ref 13..*

Over the years, figures related to AMR have increased and nowadays it's considered one of the 3 global health issues encountered by the humanity.[16] Additionally, it has been predicted that by 2030, the global human consumption of antibiotics is set to increase by more than 30%. The strengthen and diffusion of AMR is establishing a new set of "Super bugs" against which the current antimicrobial compounds might be no longer effective.[17] Additionally, second-line and third-line antibiotics are increasingly affected by AMR, and this data has predicted to grow the most until 2030 **(*Figure4*).**[18]

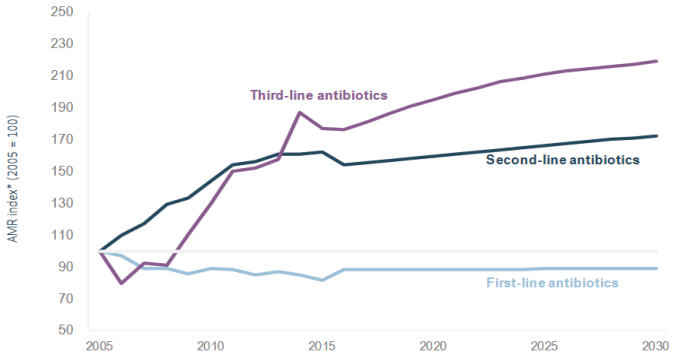

Figure 4. *AMR to second-line and third-line antibiotics will grow the most in EU/EEA countries. Adapted from Ref.19.*

In the European countries more than 670 000 infections per year are related to resistant bacteria and every year 33 000 people die **(*Figure5*).** Moreover, the total cost of AMR for the European health care systems is about 1.1 billion Euros.[18]

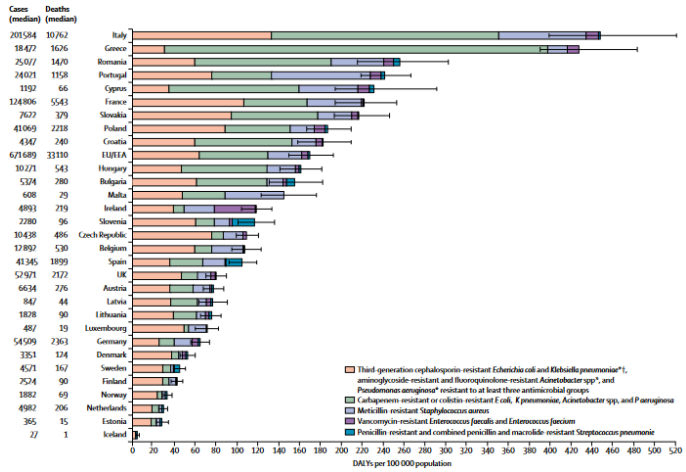

Figure 5. *Impact of infections related to antibiotic-resistant bacteria. Adapted from Ref.20*

To note, Italy and Greece had higher number of infections related to antibiotic-resistant bacteria than other EU countries, particularly carbapenem-resistant or colistin-resistant bacteria cause a larger number of infections in Greece than in Italy. [19] Infections (expressed in disability-adjusted life-years_DALYs) caused by AMR bacteria are comparable to the combination of influenza, tuberculosis and HIV/AIDS infections and nearly 40% of the health burden of AMR is caused by infections with bacteria resistant to last-line antibiotics.**(*Figure* 6)** [19]

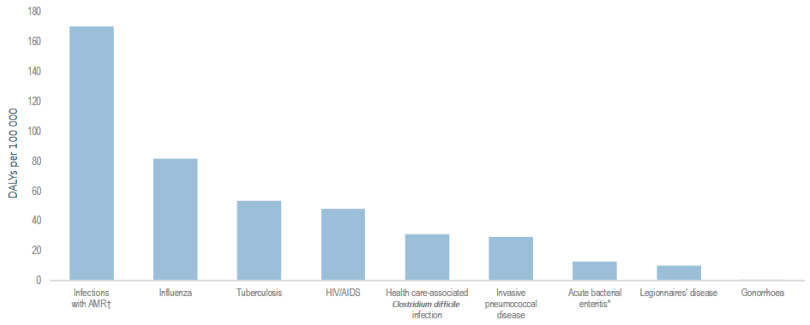

Figure 6. *Infections due to bacteria with AMR (in 2015) compared to other communicable diseases (average 2009-2013), EU/EEA. Adapted from Ref.19.*

1.2.1. AMR drivers

From the introduction of the first antimicrobial agent, this class of drugs has been widely used for clinical purposes, then released in the environment, and disseminate by animals and atmospheric agents. Indeed it has been estimated that millions tons of antibiotics have been released into the ecosystem [20] most of the time related to the unregulated waste disposal system.[15]

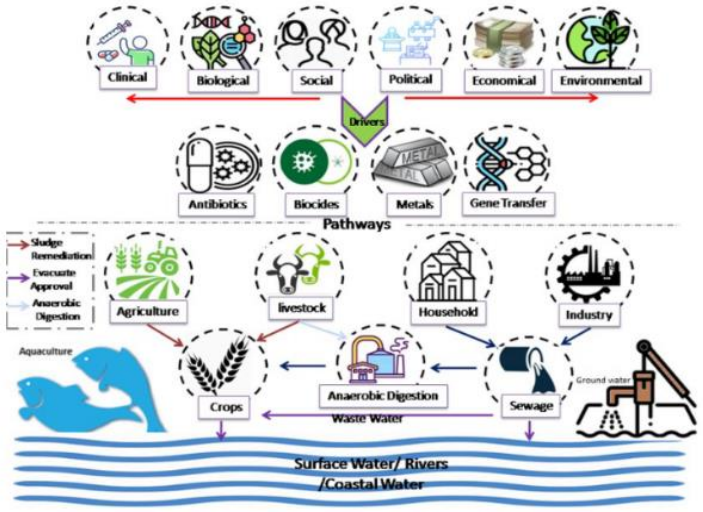

Figure 7. *Relationship between antimicrobial resistance and its environmental drivers. Adapted from Ref.26*

It is supposed that the spread of resistance is mainly related to the excessive use of antibiotics in human healthcare. Unfortunately this is not the main driver of antimicrobial resistant development,[21] since over half of the overall antibiotics produced are employed in alternative applications different from the therapeutic use. Antibiotic use for growth enhancement and prophylactic use in animals, aquaculture, household pets and agriculture are some of the prominent examples. Sometimes they can be found also in hand care and household cleaning products.[20]

Human activities favour the development of reservoirs of genes responsible for the resistance affecting the incidence of antibiotic resistance.[15] Indeed, ever since the industrial revolution's inception, human beings have discarded toxins and heavy metal in the natural environment inducing bacteria to develop the earliest extrusion systems to avoid the accumulation of those toxic molecules.[20] Particularly, chemicals released in the aquatic environment can generate mutations which enhance resistant bacteria.[21]

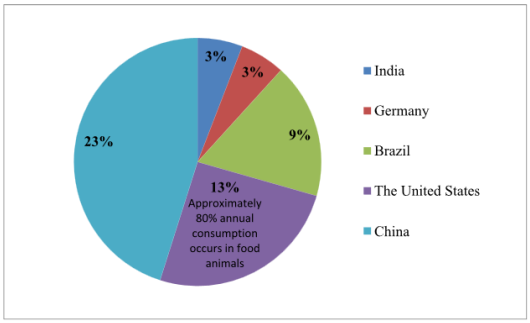

Figure 8. *Main antibiotics consumers countries in food-animal production. Adapted from Ref.26.*

Nonmedical uses of antibiotics are clearly increasing the selection and transmission to humans of antibiotic-resistant bacteria. For instance, it has been reported the transfer of resistance genes through companion animals or food production animals to human. This is proven by the fact that highly resistant genes have been found in humans and chicken meat bacteria. Moreover, it is evident that bacteria that infect humans exhibit genes inherited from aquaculture bacteria such as some resistant genes found in the human pathogen Salmonella Typhimurium as well as in some fish species.[22]

Based on these evidences, it became clear that the persistence and spread of AMR are determined by socioeconomic risk factors which are strictly correlated[21] and lead to AMR impact in a different way in High incoming countries (HICs) and in low and middle incoming countries (LMICs).[23] For instance, in LMICs the relevant impact of AMR is mainly related to the absence of an appropriate regulation which results in improper use of antibiotics in humans, animals, agriculture, and irresponsible handling of the pharmaceutical waste. Additionally, disparities in healthcare costs, poverty, infrastructure, education, governance[21],poor sanitation and easy access to antibiotics contribute to AMR diffusion.[23,24]

The increase in antimicrobial consumption in LMICs countries is related to the growing economies and most of the times to the increase consume of meat which implies the increased administrations of antibiotics in poultry and livestock to promote the growth acceleration and prevent the spread of disease. This is reflected in 131,000 tons of antibiotics consumed per year in the last decade, and this is set to rise to 200,000 tons by 2030.[21,25]

Despite the different impact of AMR in LMICs and HICs countries, there are common reasons for the increased dissemination of resistance worldwide: inadequate regulations, unsuitable use of antibiotics (50% of the prescriptions are considered inappropriate and the use without prescription is still widely diffused), loss of therapy compliance or the usage of this molecules as prevention or growth promoters. Additionally, the lack of adequate hygienic precautions, the release of antibiotics in the environment through inadequate waste disposal or manure are other significant risk factors.[26]

1.3. Mechanisms of resistance

Currently, the various antibiotics in use can be classified in 5 different classes based on their mechanism of action.

- Inhibition of the protein synthesis by affecting the bacterial ribosome at the 30s or 50s subunit (Aminoglycosides, Tetracyclines; Chloramphenicol, Lincosamides, Macrolides, Oxazolidinones, Streptogramins);
- Alteration of cell wall synthesis (Beta-lactams (Carbapenems, Cephalosporins, Monobactams, Penicillins) and Glycopeptides),
- Interference with nucleic acid synthesis leading to the alteration of bacteria replication and genomic integrity (Quinolones, Fluoroquinolones),
- Disruption of metabolic pathways such as folate biosynthesis (Sulfonamides, Trimethoprim),

- Depolarization of cell membranes (Lipopeptides). [21,27,28]

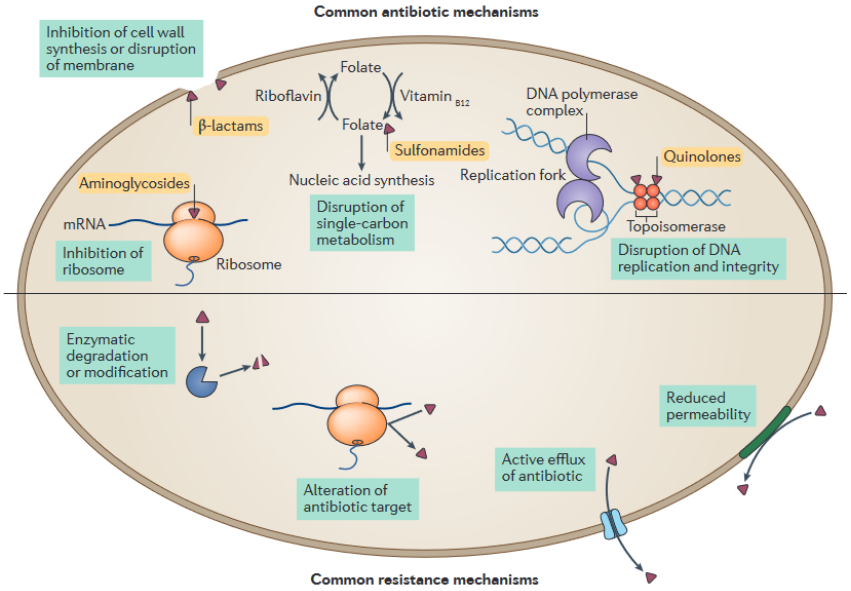

Figure 9. *Mechanisms of antibiotic action and antibiotic resistance. Adapted from Ref.27.*

On a similar vein, in order to withstand antibiotics, bacteria have elaborated a number of strategies based on the different types of antibacterial actions.

In general, when referring to AMR, this can be subdivided in:

- Intrinsic (related to innate characteristics of bacteria),
- Acquired (determined by mutations or acquisition of a new genetic pool from the environment and mainly represented by the horizontal gene transfer),
- Adaptive (this is the less alarming one since it is transitory and it depends on a specific signal coming from the environment and once subsided it reverts to the original state). [27,29]

Intrinsic resistance

Bacteria possess an innate capability to defend themselves against competitors, phages and predators from a molecular, cellular and multicellular point of view. At a molecular level bacteria produce specific molecules geared to destroy the harmful agents produced by other species. At cellular level bacteria present different elements which create a barrier against powerful killing agents such as membranes, lipopolysaccharide (LPS), capsules, efflux pumps, vesicles (that bind and deactivate toxic elements) or motility systems that allow the bacteria to escape the hazardous environment. At a multicellular level the primary defence pathway is represented by the biofilm formation, though other defence mechanisms are also relevant such as those activated by cell populations that lead to the degradation of enemy cells or agents, the start of widespread counter-attacks or the self-destruction to protect the community.[30]

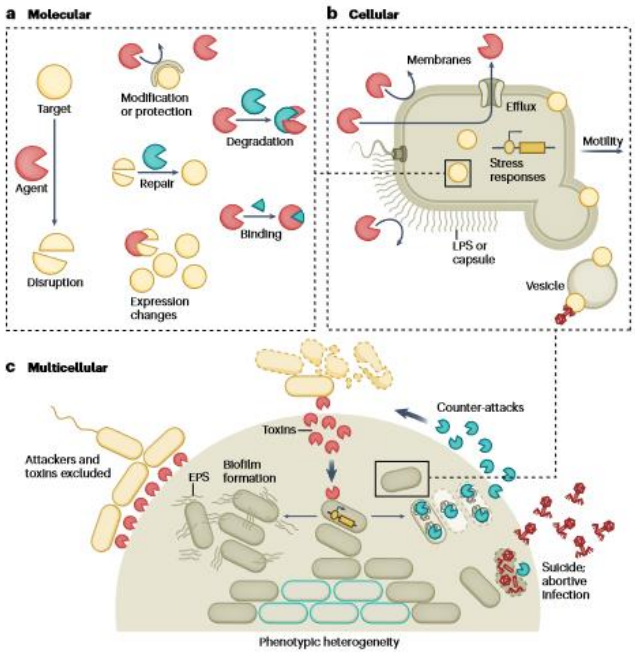

Figure 10. *Multiple lines of bacterial defence. Adapted from Ref. 30.*

Acquired resistance

Among the three types of resistances, acquired resistance is responsible for the development and dissemination of resistant strains and it is related to the acquisition of new antibiotic resistance genes (ARGs). It includes (1) the association of a gene with insertions sequences obtaining its mobilization in the genome that can consequently (2) be relocated to a genetic element such as a plasmid that can (3) be transferred to another pathogen through different routes, and (4) finally the bacterium hauling the ARG can be relocated to humans or other animal species. [31]

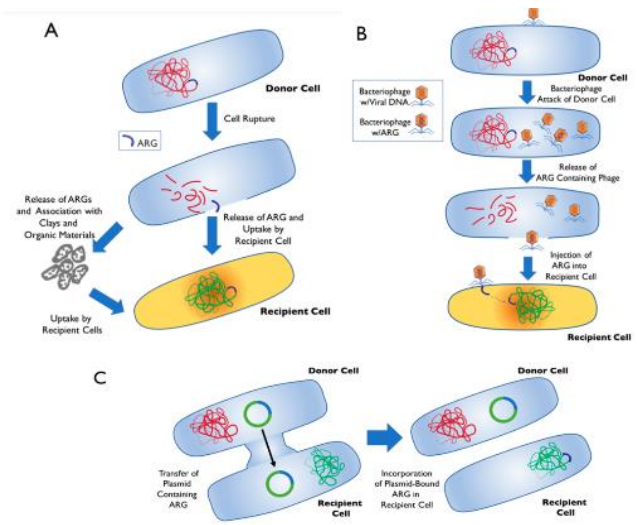

Figure 11. *Mechanisms of horizontal gene transfer (HGT). (A) Transformation, (B) Transduction, and (C) Conjugation. Adapted from Ref.32.*

Additionally, resistance transmission can occur through vertical and horizontal gene transfer (HGT). The first pathway refers to the transition of resistant genes (ARGs) from one generation to the next within the same bacterial family. [26,32] The second one represents the most common mechanism of AMR dissemination, and it can occur by three main routes which are:

A. Transformation (ability of bacteria to include in their genome free DNA from the environment)

B. Transduction (DNA transfer mediated by bacteriophages)

C. Conjugation (transfer of plasmids from a bacterium to another by direct physical contact through a sex pilus).[33]

They are well knowing mechanism in ideal conditions but it is clear that in the natural environment many other factors can interfere resulting in more complicated mechanisms. [26]

The mechanisms though which bacteria acquire resistance to a given antibiotic can be summarized as follows: [28] [29,34,35]

(1) **Destruction of antibiotic** by hydrolytic enzymes is a mechanism carried out especially against β-lactam (by β-lactamases enzymes) and tetracyclines. Similarly, the deactivation by addition of protective groups such as acyl, phosphate, nucleotidyl and ribitoyl groups may occur against aminoglycosides, chloramphenicol, streptogramins, and fluoroquinolones;[28]

(2) **Target modification** is the most common mechanism to withstand the action of the drugs, and the one conferring the highest level of resistance.[33] One of the main examples of this kind of defense are the alterations concerning the penicillin-binding proteins involved in the bacterial cell wall synthesis allowing to the resistance to β-lactams. [28] Drugs that target the ribosomal subunit such as aminoglycosides, oxazolidinones, tetracyclines can undergo antimicrobial resistance related to the ribosomal mutation or protection.[36] Similarly, fluoroquinolones can encounter resistance due to DNA gyrase or topoisomerase IV modifications. [37]

(3) **Reduction of the concentration** of the molecule inside the bacterial cell. This can be obtained through 2 different mechanisms:

Diminishing of the cellular permeability and the drug uptake. Usually this is related to the bacterial intrinsic characteristics, as for in gram negative the

LPS confers an innate resistance to specific molecules;[28] in mycobacterium the high hydrophobic components of the membrane confer resistance to hydrophilic molecules and mycoplasma results intrinsically resistant to b-lactams and glycopeptides because of the lack of the cell wall[38], staphylococcus aureus creates a chunky cell wall that confers it resistance to vancomycin.[39] Additionally, gram negative bacteria can reduce the number or induce modifications in the porins channels preventing the access of specific hydrophilic molecules. This results in Enterobacteriaceae which are resistant to carbapenems[40]; in E. aerogenes resistant to imipenem and cephalosporins[41], and in Neisseria gonorrhoeae resistant to β-lactams and tetracycline.[28]

Overexpression of efflux pumps. In recent decades, the analysis of this resistance mechanism has captured the attention of numerous researchers.By extruding the drugs out of the cell, efflux pumps usually confer a low-level resistance phenotype. However, the reduction of the concentration of the drug might predispose the bacterial cell to mutations, therefore leading to high level of resistance. Therefore, block of efflux pumps might represent a way to restore the susceptibility of resistant strains and prevent the onset of resistance in the native cells. Moreover, efflux pumps are sometime responsible for the misleading interpretation of biological data when a novel panel of antibacterial agents is screened. In fact, the lack of activity might be not due to the intrinsic inefficacy of the molecules, but to its propensity to be substrate of efflux pumps, resulting in a false negative and compromising the development of interesting hits. Efflux pumps are naturally present in bacteria in five main groups: the ATP-binding cassette (ABC) family, the multidrug and toxic compound extrusion (MATE) family, the small multidrug resistance (SMR) family, the major facilitator superfamily (MFS), and the resistance-nodulation-cell division (RND) family. In gram negative bacteria multicomponent pumps can easily been identified such as MacAB-TolC and EmrAB-TolC. Additionally, all

the five families are present in the membrane even if the RND family is the most important. In gram positive bacteria the main representative families are MATE and MFS.[28]

A more detailed description on how efflux systems work is reported in ***chapter 4.***

1.4.Resistant pathogens and their main features

It worth mentioning the WHO in the last few years has compiled a list of resistant pathogens which have different priority based on their hazard. This is aimed to focalize the research on the development of new and efficient treatments specific targeted against these strains.[42] Three different priority categories have been identified: [43]

Critical → it includes multidrug resistance Gram-negative pathogens such as *Acinetobacter baumannii* (carbapenem-resistant), *Pseudomonas aeruginosa* (carbapenem-resistant), *Enterobacteriaceae* (carbapenem-resistant), *Klebsiella pneumoniae, Escherichia coli, Enterobacter spp., Serratia spp., Proteus spp., Providentia spp., Morganella spp*. (third generation cephalosporin-resistant).

High → Gram-positive pathogens such as *Enterococcus faecium* (vancomycin-resistant (VRE)) and *Staphylococcus aureus* (methicillin-resistant (MRSA), vancomycin intermediate and resistant), *Helicobacter pylori* (Clarithromycin-resistant), *Campylobacter* (Fluoroquinolone-resistant), *Salmonella spp.* (Fluoroquinolone-resistant), *Neisseria gonorrhoeae* (Third generation cephalosporin-resistant, Fluoroquinolone-resistant).

Medium → *Streptococcus pneumoniae* (Penicillin-non-susceptible), *Haemophilus influenzae* (Ampicillin-resistant), *Shigella spp*. (Fluoroquinolone-resistant).

Among these a group of 6 pathogens is of great interest since they are developing a growing multidrug resistance and virulence and they are collected

under the name ESKAPE: ***E****nterococcus faecium*, ***S****taphylococcus aureus*, ***K****lebsiella pneumoniae*, ***A****cinetobacter baumannii*, ***P****seudomonas aeruginosa*, and ***E****nterobacter spp*. They are capable of escape the antimicrobial effect of antibiotic compounds, based on resistance mechanisms previously described, and responsible for most of the nosocomial infections. Additionally they are associated with the highest risk of mortality consequently leading to the increase of the healthcare costs.[44] ESKAPE strains are mostly present in hospital environmental even if sometimes they have also been isolated from extra-hospital reservoirs such as soil, food, various water sources, plants and sewage or municipal waste.[42]

A brief introduction to the main characteristics of these bacteria is herein reported.

E*nterococcus faecium*: two different subpopulations have been identified a population of commensal bacteria which colonize the gastrointestinal tract in humans and animals and are not responsible for clinical infections and a pathogenic one which is responsible for opportunistic and nosocomial infections. *Enterococci* have shown to be resistant to a myriad of antibiotics such as cephalosporins, low concentrations of clindamycin, trimethoprim, amino glycosides and β-lactams. Enterococci of higher concern are the high-level gentamicin-resistant and vancomycin-resistant *E. faecium* (VRE) strains. Particularly the latest have been described as the most challenging MDR Enterococcus to treat that it has been necessary to introduce new therapeutic compounds for the treatment of VRE infections such as tigecycline, linezolid, and daptomycin (mainly used in the treatment) .[42]

S*taphylococcus aureus*: this bacterial strain exists as a commensal that is naturally present on the human skin. But at the same time, it can show either intrinsic or acquire resistance. The first occurs for instance as aminoglycoside resistance due to a decreased permeability of the OM or as penicillin resistance determined by the beta-lactamase expression. On the other hand, the acquired

resistance is related to mutations resistance genes, biofilm formation or persistence. Acquired resistance has been reported against methicillin (MRSA strains), vancomycin (VRSA strains), daptomycin and linezolid. MRSA and VRSA strains can be responsible for critical clinical conditions resulting in alarming scenarios since vancomycin is considered the final resource against VRSA. It has been reported that Sa is the main responsible for bacterial skin-and-soft tissue infections moreover it is also implicated in pneumonia, musculoskeletal infections, and endocarditis and is also easily found in the environment especially in sewage, untreated water, and raw milk. [42]

K*lebsiella pneumoniae*: responsible for various infections such as tract infections and bloodstream infections; additionally, it is usually correlated to hospital-related infections such as endophthalmitis, pyogenic liver abscess, meningitis, or brain abscess. The first line treatments are β-lactams, polymyxins or cephalosporins. Unfortunately, *K. pneumoniae* strains show intrinsic resistance to penicillin related to specific penicillinases, moreover carbapenems enzymes are also responsible for mechanisms of resistance since they can easily hydrolyze monobactams, cephalosporins, carbapenems and β-lactam inhibitors. [42]

A*cinetobacter baumannii*: related with nosocomial infections such as pneumonia, bacteremia, meningitis, gastrointestinal infections this bacterial strain is intrinsically resistant to glycopeptides, macrolides, streptogramins and lincosamides. Carbapenems and polymyxins have been active and are still used again infectious caused by this pathogen even if resistance is increasing. Additionally, it can survive in harsh environments in dry or damp conditions for such long periods of time.

P*seudomonas aeruginosa*: opportunistic bacterium associated with several infections such as septicemia, endocarditis, pneumonia and cystitis, this bacterium possesses various mechanisms to elude antimicrobial molecules such as overexpression of porins, efflux pumps, mutations in the targets or in the

activity of enzymes which result in resistance against chloramphenicol, colistin, rifampin, trimethoprim-sulfamethoxazole, tetracycline, and β-lactams. Consequently, the main classes of antibiotics still effective against it are Cephalosporins, monobactams, carbapenems, fluoroquinolones, aminoglycosides, polymyxins.

***E**nterobacter spp.:* natural commensal in human and animal gastrointestinal tract it is also responsible for meningitis, pneumonia, cerebral abscess, wound infections, septicemia, and intestinal/abdominal cavity infections. This bacterium developed resistance to quinolones, penicillins, and third generation cephalosporins but carbapenems and fourth generation cephalosporins are still active.[42]

1.5.Strategies to counteract antimicrobial resistance

Considering the high impact of AMR, in the last years many governments and international health organizations have taken action to address this problem applying different strategies. Some of them are intended to modify customs and bad habits of individuals: for instance, the banning of antibiotics as growth promoters[42]; the enhancement of hygiene rules in clinics and hospitals; the restricted control on the antibiotic prescription. On a different vein, innovative research approaches have come out. As an example, the use of alternative therapies such as antibiotics in combination or with adjuvants, bacteriophage therapy, antimicrobial peptides, photodynamic therapy, antibacterial antibodies, phytochemicals and nanoparticles as antibacterial agents;[44]

Various global initiatives and surveillance programs have been introduced especially in the US and in the EU. Among these, starting from 2015, the World Health Organization (WHO) has constituted the Global Action Plan for managing AMR (GAP-AMR) and the Global Antimicrobial Resistance and Use Surveillance System (GLASS)[45] in order to offer a “standardized approach to the collection, analysis, interpretation and sharing of data by countries and seeks

to actively support capacity building and monitor the status of existing and new national surveillance systems". [46] Different plans at global level are based on the One Heath approach which promotes interdisciplinary collaboration between the public health, animal health, and environmental health sectors since it is based on the evidence that there is a clear correlation between human and animal health and the natural environment.[23] Indeed some of the aims of this approach is to introduce specific rules to monitor the use of antibiotics in animals, eliminate the use of antibiotics as growth promoters and promote prescription drugs.[24,45,47]

Among the most encouraging approaches fuelling antibacterial research, the study of antimicrobial peptides (AMP) has recently sparked strong interest among scientists since their peculiar characteristics. An in-depth description of their structure, mechanism of action, and updates in their development are reported in the next chapter.

[This page is intentionally left blank]

Chapter2_Antimicrobial peptides (AMPs) and peptidomimetics

[This page is intentionally left blank]

2.1.General features and classification

AMPs are considered ideal candidates for the development of new drugs to counteract antimicrobial resistance. They are naturally produced by all multicellular organisms, from amphibia to mammals and they are also named "Host defence peptides" since their role in the immunomodulatory system.[48] Despite the different structural properties, origins and mechanisms of action, AMPs share some common features: most of them are short aminoacidic structures with less than 100 aa, they generally display a positive net charge and they are characterized by an amphipathic structure which allow them to be soluble in aqueous environments.[49]

Based on their structural features they target preferentially bacterial membrane instead of the eukaryotic cell membrane and most of the AMPs exert inhibitory activity through interactions with the bacterial phospholipidic bilayers. As a result of membrane binding, antimicrobial peptides alter its structural features leading to complete disruption of the membrane which is one of the reasons that confer them a rapid broad-spectrum activity also against antibiotic resistant bacteria.[50] This reflects in some advantages in being used as therapeutic agents such as low incidence of side effects, predictable metabolism, high potency, easily reproducible by synthetic strategies. Despite these favourable characteristics, liabilities such as enzymatic degradation and fast kidney clearance represent a heavy drawback and, at the same time, a chance for medicinal chemistry research. . [51]

AMPs classification is based on source, activity, structural characteristics, and amino acid-rich species.[52]

In the last decades, more than 1,200 AMPs have been isolated from various organisms. [53]Mammalian AMPs have been identified in human, sheep, cattle, and they include mainly cathelicidins and defensins. Amphibian AMPs include magainin from the frog's skin and cancrin. Insects AMPs comprise cecoprin and jellein. AMPs from microorganisms such as bacteria and fungi include nisin and

gramicidin from Lactococcus lactis, Bacillus subtilis, and Bacillus brevis. It is noteworthy that biological production of AMPs is acquiring importance as a consequence of high cost of peptides synthesis.[52]

Additionally, AMPs showed a broad activity spectrum which include antibacterial, antifungal, antiviral and anticancer activity. Most of the antibacterial peptides show a wide inhibitory activity against pathogens of great concern such as VRE, Acinetobacter baumannii, and MRSA for instance Nisin, cecropins and defensines have displayed interesting activity against gram+ and gram-.[52] Antiviral peptides include molecules as defensines, LL-37, gramicidin D, caerin 1, maximin 3, magainin 2, dermaseptin-S1, dermaseptin-S4, siamycin-I, siamycin-II which act in different ways acting on the interaction of the virus with the membrane, disrupting the virus envelope or preventing the replication. Anticancer AMPs also acts on different ways indeed they can stimulate the immune system employing immune cells, generate necrosis or apoptosis processes, prevent angiogenesis, and activate regulatory functional proteins involved in growth and metastasis. Examples of anticancer molecules include indolicidin and puroindoline A.[52]

The different amino acids constituting the molecular AMPs backbone are responsible for size and conformational structures. [53] Indeed, different types of AMPs can be identified:

- proline rich peptides (PrAMPs) which don't act disrupting the bacterial membrane but interacting with a specific transporter which allow them to reach the cytoplasm and consequently the ribosomes;
- tryptophan and arginine rich peptides in which arg allow the interaction with the negatively charged residues in the membrane and trp helps in the insertion of the molecule in the phospholipidic bilayer;
- histidine rich peptides which increase the bacterial cell membrane permeability and glycine rich peptides which have an important effect on the three dimensional structure of the peptide.[52]

In this scenario, the **electrostatic charge** represents a peculiar aspect for the AMPs classification indeed two different groups of AMPs can be identified: **cationic peptides** with a total net positive charge and **non-cationic** peptides. The latest are the less represented[54] and they are mostly negatively charged AMPs with a net negative charge between -1 and -8 with less than 70 aa. Most of them are the result of the proteolysis even if some are encoded by genes [55]

Positively charged AMPs are the great majority and can be classified based on various properties, although the most common classification refers to their secondary structures: alfa-helical, beta-sheet, mixed and cyclic peptide.[53,54]

The α-helical peptides are the most studied and they include cathelicidins such as magainin, mellitin and LL-37. These are considered small peptides with less than 40 aa and a net charge between +2 and +9.[55] This peptide structure is characterized by a distance between aa of 0.15 nm and an angle of 100° and it promotes the peptide interaction with the bacterial membrane since hydrophilic and hydrophobic portion of the molecule are situated on the alpha-helix's opposing sides. Additionally alfa-helical structure is related with haemolysis and toxicity to mammalian cells for this reason one of the synthetic strategies in the peptide synthesis include the substitution of L-aa with D-aa or the introduction of lysin residues.[56]

Beta-sheet peptide structures are constituted of two beta-strands linked together by disulphide bonds which stabilized the structure, for this reason they do not withstand structural modifications after the interaction with the bacterial membrane. They include beta-hairpin, and α-β-defensines, which play a great role in the innate immune system.[48]

Finally, the alfa-helix/beta-sheet mixed structures are characteristic of some antimicrobial polypeptides and it consists of an alfa-helix and a beta-sheet made by three anti-parallel strands.[56]

Another important AMPs feature is represented by the amphipathicity which is known as one of the most important parameter related to AMPs activity not

necessary in a good way since a good amphipathicity could result in both bactericidal activity and cytotoxicity.[48]

2.2.Host defence peptides melittin and magainin

For the purpose of this PhD project, it is worthy to deeply describe the main features of two specific host defence peptides which are Magainin and Melittin. Both showed the capacity to acquire an α-helical conformation in the anisotropic environment of the bacterial membrane which seems to be essential for the alfa-helical structure formation since peptides are mainly unstructured in solution. [57]

Melittin is one of the most studied AMPs discovered in the '70s as the major component (it accounts for 52% of dry mass)[58] of the honeybee *Apis mellifera* venom. It classified as a toxin and haemolytic polypeptide[59]. It is naturally synthetized as an inactive precursor containing 70 amino acid residues and converted by a multistep process in a 26 amino acids active peptide. Among these 20 are hydrophobic amino acids and 6 are hydrophilic [58], specifically at the N-terminus are mainly hydrophobic with +4 charges and at the C-terminal hydrophilic with +2 charges resulting in a total charge of +6 for the whole molecule .[59]

The crystal structure of melittin has been determined by Terwilliger and Eisenberg in 1982 as an amphiphilic α-helix.[60] It has been demonstrated that in aqueous solutions melittin forms a random coil while an α-helix structure is reached after the interaction with the bacterial membrane.[58] The α-helical conformation is promoted by the first 20 residues of the sequences, and stabilized by the presence of positively charged residues at the C-terminus while the presence of a proline residue in position 14 is responsible for the formation of a kink in the structure.[61] Indeed after binding to the membrane it acquire a bent conformation with two α-helical portions (Gly^{1} to Thr^{10} and Pro^{14} to Gln^{26}) connected by a non α-helical kink region (Thr^{11} to Gly^{12}). This results

in an amphipathic helix in which the hydrophobic groups are located on the inside of the structure as strictly as possible from one another while the positive charged groups lied far from each other are projected toward the solvent. [62]

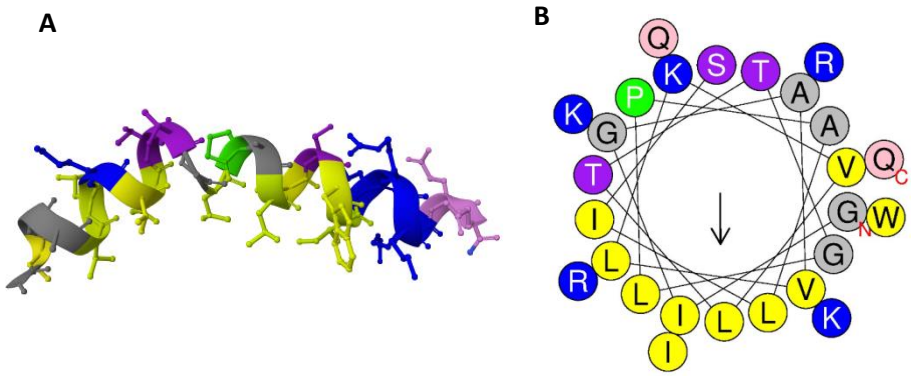

Figura 12. *α-helical structure generated by RCSB PDB server (A) and helical wheel representation generated by HeliQuest server (B) of melittin. Colour coding for residues: yellow for hydrophobic, purple for Ser (S)and Thr (T), blue for Lys (K) and Arg (R), red for acidic, pink for Gln (Q), grey for small residues (Ala,A and Gly,G), green for Pro (P), light blue for His (H). C and N letter in red represent the C and N terminal dominium respectively. UniProt access number P01501 MEL_APIME.*

Despite many efforts have been made in the past decades to define the exact mechanism of action of this natural peptide, it is still poorly understood, probably related to the small molecular weight of the molecule (2840 Da[58]). Many studies have been carried out to investigate the molecular dynamic of the peptide-membrane interaction, but it has been proven that it is rather complex to experimentally obtain a direct observation of this process. Nevertheless, it is generally recognized that it is a multi-steps process which starts with the binding of the molecule to the membrane surface leading to the consequent accumulation, after reaching a specific concentration the peptides molecule slowly reorient on the surface and insert perpendicularly into the membrane leading to the formation of transmembrane pores and allowing us to include this mechanism in the barrel-stave or toroidal model typical of other positive charged antimicrobial peptides.[59]

Melittin has been shown to possess a broad-spectrum bactericidal activity even against antibiotic-resistant bacteria, such as *A. baumannii* and *P. Aeruginosa* [63] For this reason it is widely used as a starting point for the development of new antimicrobial molecules and as a positive control to define the antimicrobial activity of new natural or synthetic AMPs and peptidomimetic molecules.[59]

The **magainins** family has been discovered in 1987 by M.Zasloff from the skin of and African clawed frog (*Xenopus laevis*). They have been named magainin 1 and 2 based on the Hebrew word "magain" meaning "shield" to underline their possible antimicrobial role in the protection against microorganisms, acting as a shield.[64]

These two peptides differ for the presence of two different residues in position 10 and 22 (G and K for magainin I, K and N for magainin II), based on these differences magainin II has been showed to display a wider activity spectrum than magainin I consequently receiving more attention from the scientific community as a potential antimicrobial molecule.[65]

Magainin II is a 23 amino acid residues peptide with a molecular mass of 2466.9 g/mol. It has an overall basic nature indeed it presents a net positive charge of +4 at physiological pH which allow it to easily interact selectively with the negative charged membrane of bacteria through electrostatic interactions.[66]

This molecule adopts facially amphiphilic conformation consequently showing hydrophilic and hydrophobic residues located in two opposite regions of the helix. The hydrophobic residues (Phe,Leu) face the membrane interface driving the molecule to insert deeply into the hydrophobic region of the membrane, while the hydrophilic groups (Lys) are located on the opposite side interacting with the hydro- carbon chains of the negatively charged lipids contributing to the formation of a global amphiphilic structure.[66,67] It worth mention that it has been demonstrated as increasing the hydrophobicity results in an higher antibacterial but also higher haemolytic activity[68]

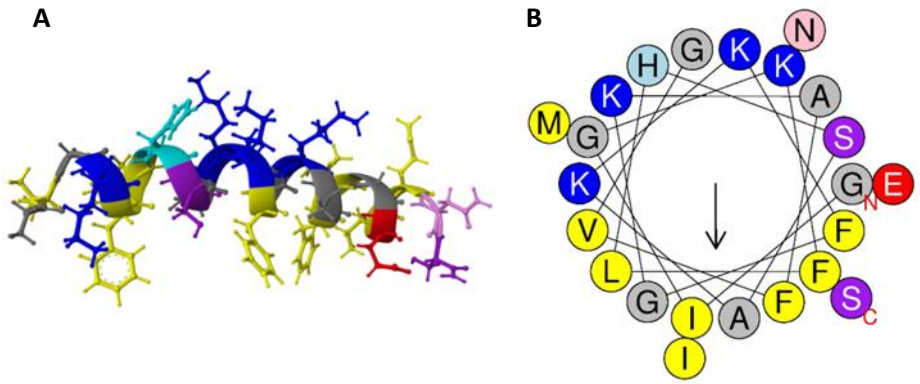

Figure 13. *α-helical structure generated by RCSB PDB server (A) and helical wheel representation generated by HeliQuest server (B) of magainin II.. Colour coding for residues: yellow for hydrophobic, purple for Ser (S)and Thr (T), blue for Lys (K) and Arg (R), red for acidic, pink for Asn (N), grey for small residues (Ala,A and Gly,G), green for Pro (P), light blue for His (H). C and N letter in red represent the C and N terminal dominium respectively.) UniProt acess number P11006 MAGA_XENLA..*

Additionally several studies underline as this molecule appears as unstructured in aqueous solution but it acquires an α-helical conformation upon the interaction with the acidic phospholipid bilayer.[69] This structure can be stabilized in analogues which show an increased number of Arg and Lys residues and α-disubstituted amino acids leading to the improvement of antimicrobial activity.[70]

Another important feature of magainin related to its antimicrobial activity is represented by the polar angle θ (angle subtended by the α-helix face) which is provide by the presence of the positively charged lysine in the natural magainin II structure and its account for 120°, molecular analogues with larger angles (180° instead of 120) showed eight times improved antibacterial activity. Unfortunately at the same time also the haemolytic effect has shown to be increased.[71]

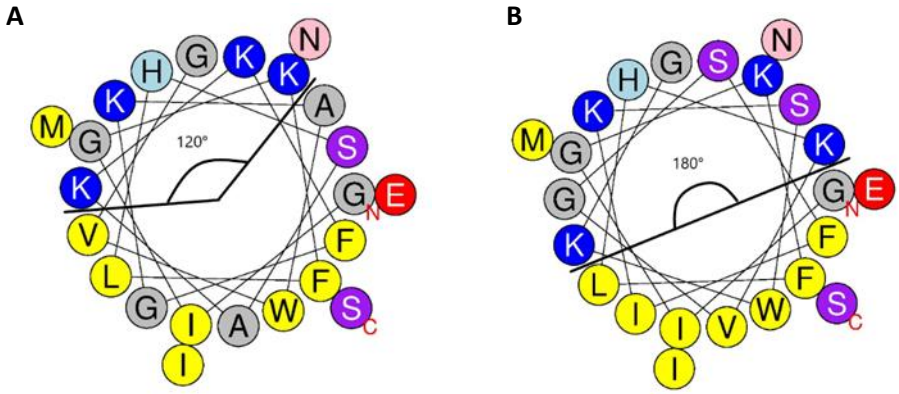

Figure 14. *Angle subtended by the positively charged residues in the structure of magainin2 analogues. Adapted from Ref.66.*

It has been demonstrated that magainin possess antimicrobial properties against various species of Gram-positive and Gram-negative bacteria acting toward a toroidal pore model which consists of the formation of 2–3 nm in diameter pores where the wall is lined with both magainin molecules and membrane phospholipids.[72] After the membrane permeation it induces cell apoptosis. [73]

2.3.Mode of action

Although the extensive number of different AMPs and the various described categories, the majority of them share the affinity for negative charge prokaryotic membranes based on their positive net charge which is the main requirement for bacterial cells selectivity and the basis for the membrane disruption.[74] AMPs can act through different mechanisms of action which are most of the time related to the peptide's sequence, although they show some common aspects.[74] The positive net charge and the hydrophobic features of the molecule play a pivotal role in the activity promoting the bacterial killing or toxicity against the human cells indeed, a relevant positive charge is responsible for increasing the haemolytic effect. At the same time hydrophobicity influences the target affinity and the toxicity for eukaryotic cells.[74]

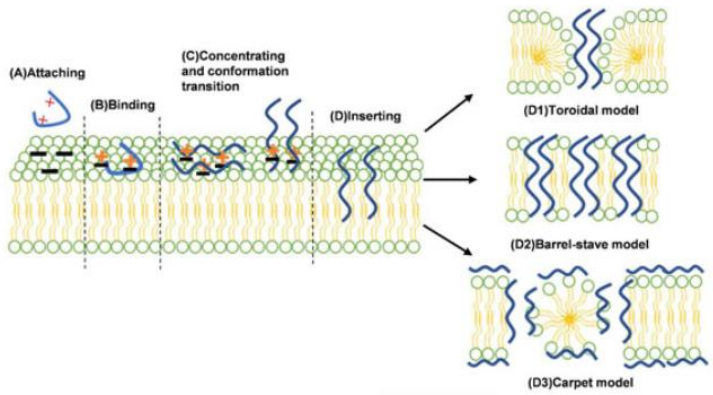

Figure 15. *Antimicrobial peptides interactions with the bacterial membrane. Adapted from Ref.48.*

The specific mechanism of interaction of the AMPs with the bacterial membrane hasn't been clearly defined for all the AMPs.[75] However, it was established that the first step in the AMPs-membrane interaction results in the association between the peptide and a great number of phospholipids in the membrane outer layer. Particularly, they interact with the membrane acquiring a parallel orientation to the phospholipidic bilayer leading to the destabilization of

the membrane physical properties. In a second moment, after reaching a specific concentration, they reorient perpendicularly in the membrane acquiring the specific orientation which promote the consequent AMPs penetration and the pores formation.[76]

AMPs likely possess two main mechanisms of action: "membrane acting peptides" which destabilize the bacterial membrane leading to its disruption and "non-membrane acting peptides", which migrate through the membrane without destabilizing it to perform their activity interacting with intracellular targets.[49] Both the two mechanisms are based on the electrostatic interactions between the positive net charge on the peptide structure and the negative charge of teichoic acid in the cell wall of Gram-positive or the LPS in the outer membrane of Gram-negative supported by the important role played by the molecule hydrophobicity.[49,77]

Different models to describe the membrane interacting peptides action have been proposed and they can be now subdivided into two main categories: transmembrane pore and non-pore formation peptides. [78] Transmembrane pore models include:

Barel-stave pore models→ after reaching a specific concentration on the membrane surface peptides insert perpendicularly into the bilayer leading to the pore formation due to the alfa-helical, beta-sheet amphipathic structures.[78] Indeed these structures play a crucial role in the pore formation since they are arranged one close to the other with peptide-peptide interactions and the hydrophobic portions of the structure interacting with the hydrophobic membrane regions whereas the hydrophilic ones form the inner surface of the pore core.[55] The main feature of this mechanism is the maintenance of the hydrophilic and hydrophobic organization of the phospholipidic bilayer.[78]

Toroidal pore models→ this model is quite similar to the previous one although the main difference is the absence of peptide-peptide interactions since after the peptide concentration increased on the membrane surface, peptides start to form

pores which are made of both peptides and phospholipids.[79] This result in peptide-lipids bindings which lead to the formation of pores destroying the hydrophobic and hydrophilic arrangement.[78]

Non-pore formation models mainly refer to the *"carpet model"*. AMPs, after orienting parallel to the membrane surface and reaching a specific concentration, lead to the bacterial cell destruction in a detergent-like manner. This process is strong enough that pores formation and insertion into the bilayer are not involved in the mechanism of action, nevertheless they lead to formation of micelles and the consequent total disruption of the cell. AMPs which assume this mechanism of action include cecropin, indolicidin, aurein 1.2, and LL-37.[78,79]

Among the "Non-membrane acting peptides" **Indolicin**, human beta-defensins4 and human alfa defensins1 first interact with the cytoplasmic membrane without destroy it and accumulating in the cytoplasm where they interfere with important cellular mechanisms[78] indeed they can act on the nucleic acids directly binding to the DNA or indirectly interfering with the DNA replication; they can also act on proteins synthesis, enzymes activity or cell wall synthesis [55]interfering with the precursor molecule lipid II.[78]

2.4.AMPs under clinical investigation

Despite the thousands of AMPs described, currently only few natural AMPs have entered the market and mostly for topic infections. Indeed, nisin, polymyxin, gramicidin, daptomycin and melittin,[80] the only five natural AMPs currently in clinical use, show hemolytic properties along with neurotoxicity and nephrotoxicity, therefore their application is suggested only as ointment for topic infections.[81]

Nisin is produced by Lactococcus lactis bacterium, it interacts with lipid II leading to the inhibition of the cell wall synthesis and the formation of pores; it

is used in dental care products for topical application or for the treatment of stomach ulcers or colon infections.

Gramicidin is a natural peptide produced by bacillus brevis and it acts through the membrane depolarization against various Gram-positive and is used essentially for ophthalmic treatments.

Polymixins B and E are cyclic peptides produced by *Paenibacillus polymyxa* which are active against Gram-negative bacteria such as *P.Aeruginosa* and *E.Coli* owing to the interaction with the lipid A presents in the LPS on the outer membrane of these pathogens. Polymixin B is used in the treatment of eyes infections while polymyxin E in infected wounds, both are responsible for neurotoxicity and nephrotoxicity consequently they are used as a last-line treatment.

Daptomicin is a cyclic lipopeptide produced by *Streptomyces roseosporus* which inhibit the cell wall synthesis in Gram-positive bacteria. Melittin is the main component of Apis mellifera's venom and it has been approved by the FDA for the treatment of specific symptoms related to rheumatoid arthritis, tendinitis, and multiple sclerosis.[80]

Aside those in the market, 34 AMPs are currently in preclinical trials and 27 in clinical trials **(*Figure* 16).**[82]

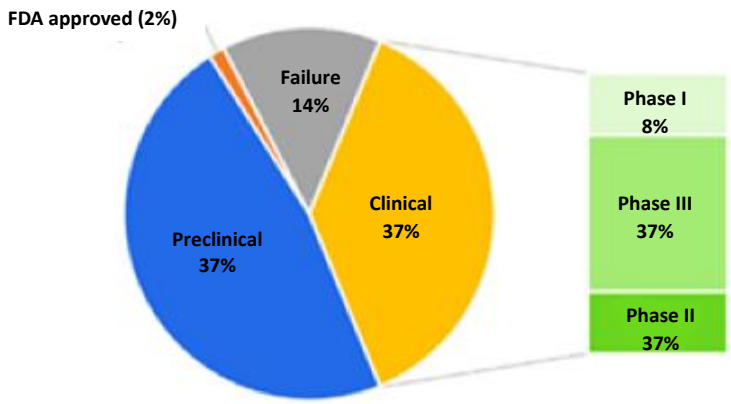

Figure 16. *AMPs in preclinical and clinical trials. Adapted from Ref.82.*

The reason for this poor success in overcoming the preclinical phases of research can be sought in the various weaknesses exhibited by AMPs. Indeed, they present high susceptibly to proteases activity resulting in short lifetime coupled with rapid kidneys clearance. Additionally they show poor oral bioavailability and absorption across membranes related to their hydrophobicity, consequently most of the AMPs with antimicrobial activity are implicated in topical formulations which are responsible to generate an immunogenic reaction leading to the necessity to focus the research on stabilise them and make them efficient.[51,83] Some studies also reported AMPs haemolytic activity due to their interaction with eukaryotic cells especially erythrocytes, leading to cytotoxicity.[84] It has also been demonstrated that higher hydrophobicity and amphipathicity increase the haemolytic activity of these molecules but at the same time the relationship between these two characteristics is so delicate that it required a perfect balance which is difficult to predict in advance to avoid the cytotoxic effect. [84]Moreover AMPs might lose their antimicrobial activity in physiological environments in relation with the presence of salts which interfere with the electrostatic interactions between the AMPs and the bacterial membrane, alternatively they can bind to specific proteins present in the serum resulting in a reduced number of AMPs interacting with bacteria.[80] Another issues in the AMPs production is that they are commonly obtained by two different routes which are the extraction from natural microorganism or the AMPs total synthesis which are both extremally expensive in terms of time and costs. [85]

2.5.Peptidomimetics origins and classification

Over the last decades peptidomimetics features, classification and synthesis have been extensively described. According to Vagner et al. "*Peptidomimetics are compounds whose essential elements (pharmacophore) mimic a natural*

peptide or protein in 3D space and which retain the ability to interact with the biological target and produce the same biological effect." [86]

Historically peptidomimetics have always been classified in three different categories based on their structural and functional features:[87,88]

- **Type I** → structural mimetics: showing a high similarity to the parent peptide indeed they mimic the topography maintaining almost the same amino acid backbone and differentiating only for side substituent.
- **Type II** → functional mimetics which don't have apparent structural analogies with the parent peptide they just interact similarly in the target site.
- **Type III** → structural-functional: mimetics with a different scaffold from the parent peptide, the similarity is based on interactions with the target most of the time due to specific portions of the molecule strategically oriented to achieve the same target interactions of the parent peptide.

Nevertheless, the old classification does not account the recent progresses in the field and does not consider new approaches developed in latest years, consequently a new classification based on the degree of their similarity to the natural peptide has been introduced by Grossman at al.[89,90] :

- **Class A** → this class includes the previous type I class which are the most similar to the parent peptide structure with only a limited number of modified amino acids to reduce the susceptibility to the proteolytic enzymes.
- **Class B** → these molecules present various non-natural amino acids and relevant backbone alterations and they include foldamers, such as b- and a/b-peptides and peptoids.
- **Class C** → this class includes molecules in which the peptide backbone is completely substituted by a central scaffold which mimic the spatial orientation of the relevant residues of the parent peptide. This class is strictly related to the type II class of the old classification.

- **Class D** → they mimic the mode of action of a peptide without any relation with the functional groups of the parent peptide, particularly these molecules can be obtained from hit-to-lead approaches or screening of virtual libraries.
-

2.6. From peptides to peptidomimetics: modifications of AMPs

Since the drawbacks showed by these natural structures, over the years the scientific community has focused its attention on the necessity to overcome AMPs problems. This could be done through the introductions of specific modifications on the AMPs structures to improve their stability and bioavailability while maintaining the biological activity. [82]

The majority of the modifications cannot be applied directly on the structure of the natural peptide but incorporated during the chemical synthesis. Most common modifications include:

a) Substitution of one or more aminoacidic residues with non-classic amino acids such as D-amino acids, N-methyl-α-amino acids, β-amino acids, γ-amino acids, α-substituted amino acids, β-substituted α-amino acids;
b) Modification of the peptide bonds with other chemical portions which result in N-alkylation, substitution of the carbonyl function with a methylene group, a sulfur atom or phosphonamide, NH group substitution with oxygen (depsipeptide), sulfur (thioester) or methylen (ketomethylene);
c) Capping reactions such as N-acetylation or C-amidation at the C or N terminus domain or the PEGylation;
d) Cyclization which allows to the formation of a peptide bond between the C and N terminals but it is usually avoid since it leads to important structural modifications in the molecule that can totally modify the activity;
e) Elimination of specific amino acids susceptible to the proteolytic activity or introduction of modifications which allow the realization of prodrugs

characterized by the presence of an unstable portion which protects the molecule from the proteases activity but can easy been removed nearby the peptide active site.[52,83]

In other cases, completely new molecules can be designed and synthetized based on the chemical structure of the bioactive natural peptide leading to the development of the so-called **peptidomimetics compounds**, where the activity of the natural peptide is maintained whereas the structure is modified in strategic points susceptible to protease activity. [82]

2.6.1. Brilacidin: a specific case study of peptidomimetic host defence peptide mimetic

As previously reported host defence peptides acquire an α-helical structure only after the interaction with the phospholipid bilayer since they are mostly unstructured in solution. Consequently all the main features of an antimicrobial peptide are essential in the definition of the specific structure they acquired inside the phospholipid bilayer.[57] Based on the fact that the α-helical structure is important for their action, during the past decades many attempts to develop α-helical-like synthetic peptides and peptidomimetics have been done. Among these one of the most representative example is the rational design approach that lead to the development of the antimicrobial peptidomimetic molecule called Brilacidin.[91] (considered as a new antibiotic class called host defence

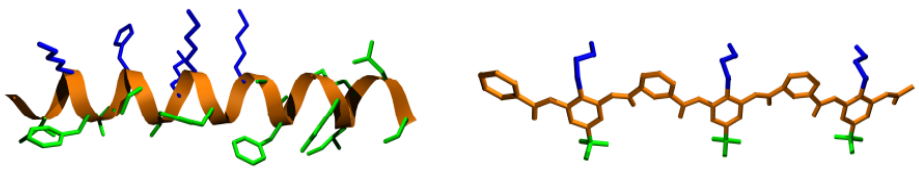

Figure 17. *Structures of magainin compared to the arylamide polymer mimic. Hydrophobic side chains (green) on one side and hydrophilic (blue) on the other prove the amphiphilic structure. Adapted from Ref.91.*

protein mimetics, or HDP-mimetics).[92]

The rational approach which lead to the development of this antimicrobial molecule, actually in phase III clinical trials, was proposed more than 2 decades ago by De Grado and coworkers.[91] At the time various non-natural facially amphiphilic peptides with specific designed conformation mimicking the structure and biological function of magainin, had been developed. These molecules where essentially β-peptide analogues extremely expensive to synthetize, consequently De Grado et al. designed a series of facially amphiphilic arylamide polymers which were easily to prepare from cheap monomers supposed to mimic the physical and biological properties of AMPs as magainin.[91]

Based on the evidence that the facial segregation of hydrophobic and hydrophilic residues is a typical feature of natural antimicrobial peptides it was hypothesized that to reproduce the properties of a natural AMP would have been necessary to introduce this property in a small molecule. [93]

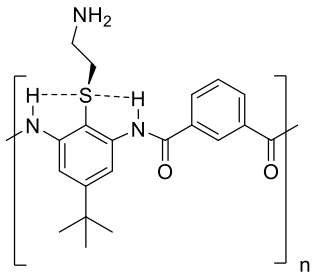

Figure 18. *General structure of arylamide foldamers.*

In the design of these molecule a diamine aromatic portion was chosen as central core based on the advantages it can bring to the synthesis and its conformational properties. Additionally, a thioether portion was chosen in order to obtain the methylene bond to the thioether group located out of the plane of the aromatic ring, reducing the possibility to create hydrogen bonds with the side amide groups. [91]

All the initial supposition were then confirmed by computational studies which played a pivotal role in the design of the above-mentioned polymers. In particular one of the most important features to determine was the torsional hindrance responsible for the rotation of bonds within the arylamide structure and it was confirmed that the attachment of the methylene to the thioether portion would locate out of the plane of the phenyl ring. [91]

Biological activity analysis for these oligomers (n = 2, 3, 8) such as MIC evaluation underlined as they didn't show a great antimicrobial activity since it ranged around 15 ug/mL for the selected strains *E. coli, K. pneumoniae, B. subtilis*. Additionally, they have proven to not selectively target the bacterial cells instead of the mammalian cells, and higher analogues (n = 60) were totally inactive.[93]

Consequently, it was clear that a deeply design analysis involving charge and hydrophobicity modification of the side chains was necessary to obtain more active compounds which might be able to mimic the properties of AMPs such as magainin and melittin.[91]

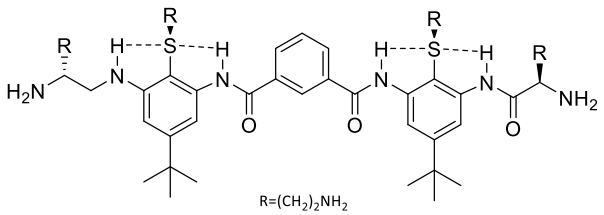

Figure 19. *Generic structures of conformationally restrained antimicrobial arylamide foldamers Adapted from Ref.94.*

Based on the consideration that an appropriate balance of conformational rigidity, hydrophobicity and distribution of charged side chains in the mimetic peptide are fundamental to mimic the activity of the natural peptide, in the following years the research group developed a library of analogues of a short triaryl amide **(*Figure* 19),** moving away from the development of polymers

series which might be too hydrophobic to discriminate between mammalian and bacterial cells and focusing in small oligomer molecules.[94] ω

The triaryl amide structure served as a template for the optimization of these series of compounds. It is constituted of three aromatic rings linked together through peptide bonds and showing on both sides a free amine portion which allows for further functionalization. Additionally, hydrogen bonds between the sulphur atoms and the side amide groups stabilize the amphiphilic structure. [93,94]

The side amines have been functionalized by the addition of aminoacidic residues leading to the conclusion that hydrophobic substituents (Leu,Phe,Trp) supported antimicrobial activity but they were shown to obtain toxic molecules against red blood cells; on the other side the introduction of polar substituents (Arg,Lys) reduced the toxicity whereas increasing the potency and the safety of these molecules. [94]

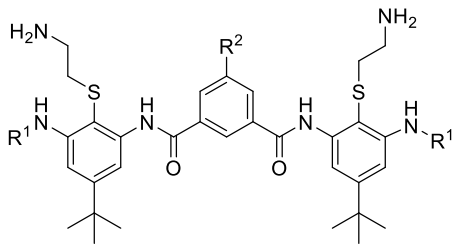

Figure20. *General structure for 5-monosubstituted arylamide foldamers. Adapted from Ref.94.*

Consequently, based on the fact that a greater selectivity could be obtained by increasing the number of positive charges a second series of analogues has been developed characterized by the addition of a positively charged amino alkyl chain to the central aromatic ring. This modification increased the selectivity for bacterial cells regardless the nature of the side aminoacidic substituent [94].

Since the interesting results, in the following years De Grado et al. continued to investigate the structure activity relationship of arylamide derivatives. In particular they focused the attention in increasing the rigidity of the structure since X/Ray crystal structures analysis showed as the involvement of the thioether portion in the hydrogen bonds allow to restrict the rotation of the N–C torsional angle between the amide nitrogen and the phenyl ring, but it was not efficient in determine the proper rigidity of the molecule showing a significant torsional flexibility of the above mentioned angle. Consequently a 4,6-dialkoxy-substituted isophthalic acid was used as central core properly substituted to provide intramolecular hydrogen bonds. The side amine residues were then functionalized by the introduction of more polar cationic substituent (Arg, Lys). Both these structural modification allow to increasing both affinity and selectivity for bacterial cell.[95]

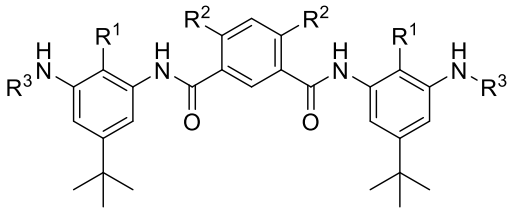

Figure 21. *General structure for 4,6-disubstituted arylamide foldamers substituted at the amine sites. Adapted from Ref.95.*

Simultaneously Tew and coworkers based on the new founding related to the importance of the molecule's spatially rigidity, to increase the hydrogen bonds and restrict the rotation around the aryl–CO bond, decide to replace the central aromatic ring with a pyrimidine ring presenting two nitrogen atoms acting as hydrogen bonding acceptors, allowing to increase the rigidity and the facial amphiphilicity of the molecule.[93,96]

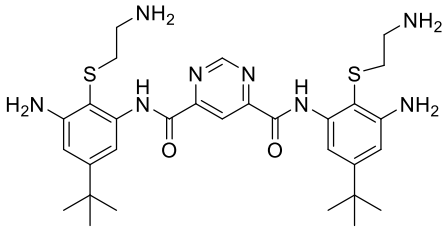

Figure 22. *General structure of analogues presenting the pyrimidine ring. Adapted from Ref.93.*

Finally, based on the previously studies conducted by Tew et al., De Grado developed different analogues presenting a pyrimidine central ring and side amine portions functionalized with positively charged substituent leading to the development of the final structure of Brilacidin which has then been patented and is actually in the phase III clinical trial. [95,97]

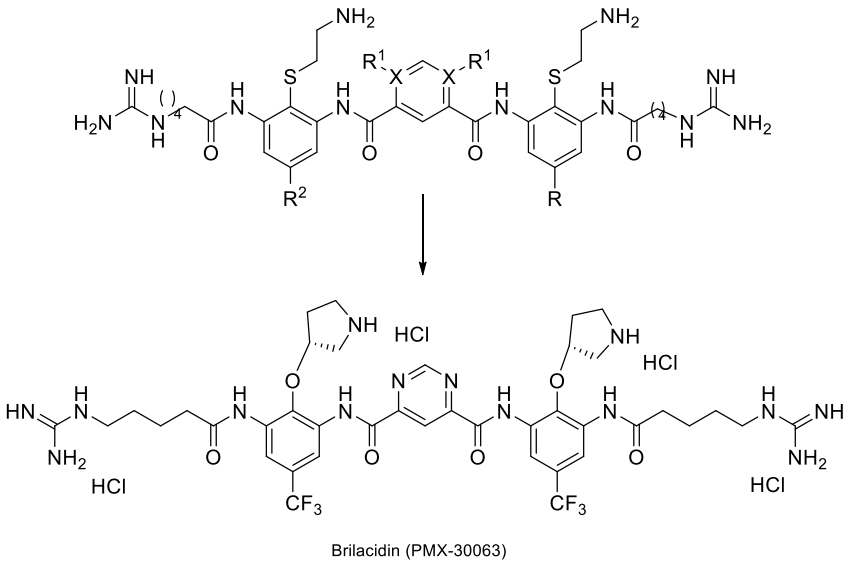

Figure 23. *General structure characterized by a pyrimidine central ring and guanidinic side moieties which led to the synthesis of Brilacidin Adapted from Ref.95.*

The above-described rational design of this molecule is one of the main examples of the development of a peptidomimetic molecule based on the features of the natural antimicrobial peptide. The optimization of the total charge and the hydrophobic features increases both potency and safety indeed it has proved to be important to obtain compounds highly active and non-toxic. [98]

Chapter 3_ Synthesis of peptidomimetics

[This page is intentionally left blank]

3.1.Background

3.1.1. Peptidomimetics design approaches

Several approaches have been undertaken to develop new peptidomimetic molecules. The most representative are:

- The rational design based on the structure of the parent peptide;
- The random screening of large peptidomimetic libraries.[87]

From a medicinal chemistry perspective, the rational approach represents the most interesting one consequently it will be deeply described in the following sections.

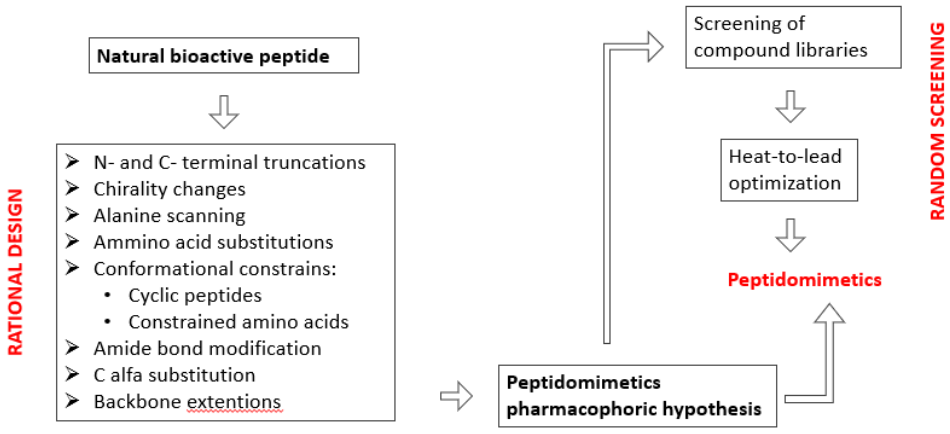

Figure 24. *Peptidomimetics design approaches. Interconnected role of rational design and random screening*

According to the rational approach, this can be accomplished through four main steps, aimed at the definition of the **role of each amino acid** and to the identification of the pharmacophore. The main steps are here reported:

a) *Size reduction*, aimed to identify the peptide residues involved in target interactions. This step is generally carried out starting from the systematic removal of specific amino acids from C or N termini of the peptide aminoacidic sequence to define ether or not they play an essential role in

the antimicrobial activity. Once the removal of an amino acid doesn't affect the molecule's activity this is excluded from the aminoacidic structure of the new synthesized molecule with the purpose to define the minimal peptide sequence responsible for di bioactivity which cannot be further modified.[90]

b) *Alanine scanning*, performed by substitution of some specific residues of the natural peptide with alanine to define if that specific functional group was essential for the bioactivity. Over the year this scanning technique has been widely used to investigate peptides since the introduction of a proline in the aminoacidic structure provide the substitution of a side functional group with a methyl group which could make a relevant difference in the biological activity of the compound most of the time resulting in a loss of bioactivity proving that the parent residue was essential for the drug-target interactions.[90,99]

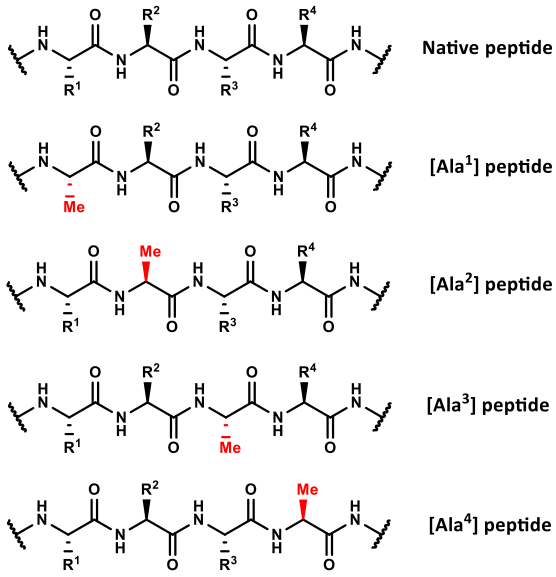

Figure 25. *Systematic combinatorial alanine scan. Adapted from Ref. 90.*

c) *D-amino acid scanning,* quite similar to the alanine scanning this step is carried out to identify which of the parent peptides residues are essential for the biological activity and also to verify how a non-natural amino acid impacts on the structural conformation most of the time leading to an implemented metabolic stability.[90]

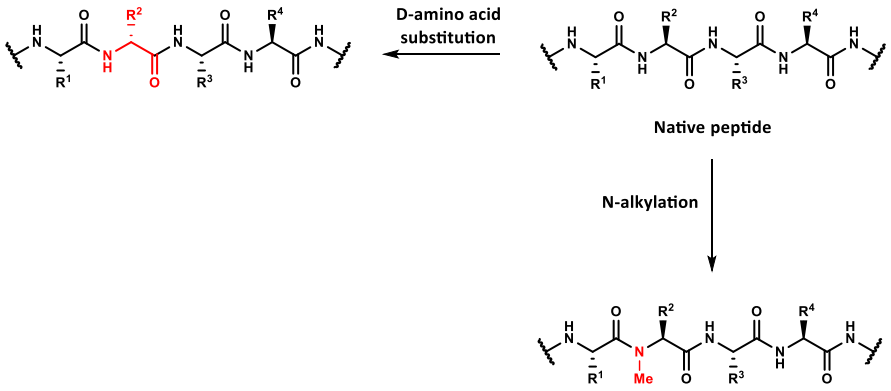

Figure 26. *Substitution of wild-type L-amino acid with D-amino acid and site-specific N-alkyl peptide. Adapted from Ref.90.*

d) *N-methylation,* the alkylation approach of the ammine group is extremely important to identify the amino acids acting as hydrogen bonds donor during drug-target interactions helping to define the relationship between the **conformational disposition** of the peptide and **bioactivity.** Additionally, it has been demonstrated that N-methylation has a role in the definition of cis/trans balance nearby the amide bond, particularly it promotes the cis-peptide bonds leading to the optimization of the conformational aspect of the molecule. [90]

e) *Modifications.* Once the pharmacophore represented by the minimal peptide sequence has been identified, **local and global structural modifications** of the molecule are introduced to define the optimal bioactive conformation with a reduced peptide character, an improved binding affinity for the target and PD/PK profile.[100] All the modifications described are typically

implicated in the development of peptidomimetic molecules as a result of a slight modification of the parent peptide structure or the generation of a pure nonpeptide.[101]

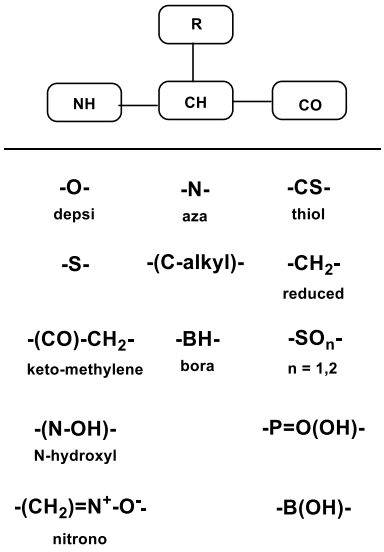

Figure27. *Isosteric local modification of the amino acid structure. Adapted from Ref.100.*

Local modifications generally occur on a single amino acid most of the time involving a specific functional group:

The amino group can be replaced with isosteric atoms or groups, such as oxygen, keto-methylene or N-hydroxyl moieties.

- the alpha carbon can be replaced with nitrogen atoms, C-alkyl to achieve quaternary amino acids, or boron atoms;
- the carbonyl group has been replaced with thiol, methylene, phosphinic and boronic groups.
- the original amino and carboxylic groups positions can be reversed leading to obtain a Retro-inverse peptide.

These local alterations of the peptide structure can be grouped into backbone and side-chain modifications**.**

Backbone modifications are achieved though the introduction of amide bond surrogates (also called bioisosters) to mimic the peptide bond structural features improving the metabolic stability. A great amount of classical and non-classical amide bioisoster classes are known, including **1,2,3triazole**, **oxadiazole, imidazole,** tetrazole, pyrazole, indole, pyridine, pyrazine, **retroinverted and reverse amide**, urea, **olefin**, fluoroalkene, **ester, sulfonamide**, thioamide, and carbamate. [102]

To date the triazol moiety is considered an excellent peptide bond surrogate which possesses characteristics that can lead to the realization of peptidomimetics molecules resistant to proteases activity and with improved biological activity. Some of the major features are the ability to mimic the trans amide bond configuration and present a planarity, dipole moment and hydrogen bonding properties which are analogous to those of an amide. [102]

Additionally, oxadiazole is another heterocyclic amide surrogate composed of two carbons, two nitrogens, and one oxygen atom with a weak basic nature. It is resistant to cleavage mediated by proteases, oxidation, hydrolysis, and nucleophilic attack but it undergoes nucleophilic substitution. The introduction of this moiety in the molecular structure can improve the metabolic stability, membrane permeability, and bioavailability. Many isosteres are known but the 1,2,4-isomer and 1,3,4-isomer are the most common indeed they can mimic the molecular planarity and dipole moment of an amide.[103]

Imidazole is also a structure used as amide bond surrogate. It works as hydrogen bonds donator (HBD-if the nitrogen is unsubstituted) and hydrogen bond acceptors HBA. It mimics the charge of the amide nitrogen consequently it can replace the amide bond leading to increase the basicity

of the molecule promoting the formation of water-soluble salts as demonstrated for the main representative molecule containing an imidazole portion which is midazolam. [102,104]

The introduction of retro inverted and reverse amide in the peptide structure is an additional technique to increase the metabolic stability of peptidomimetic compounds maintaining the amide bond geometry and conformational flexibility.[102]

Sulfonamide are structurally similar to the amide structure since it is replaced by an isosteric sulfonyl group but they show an increased water solubility and provide Hydrogen bond acceptors (HBAs).[102]

The last example of peptide bond surrogate here considered is represented by the olefine structure which consisted of a nonhydrolyzable alkene group which mimic the planar feature of an amide bond, but it is not involved in the definition of hydrogen bonds (it is not HBAs or HBDs) because of the lack of heteroatoms. It is resistant to proteases, oxidation and hydrolysis.[102,105]

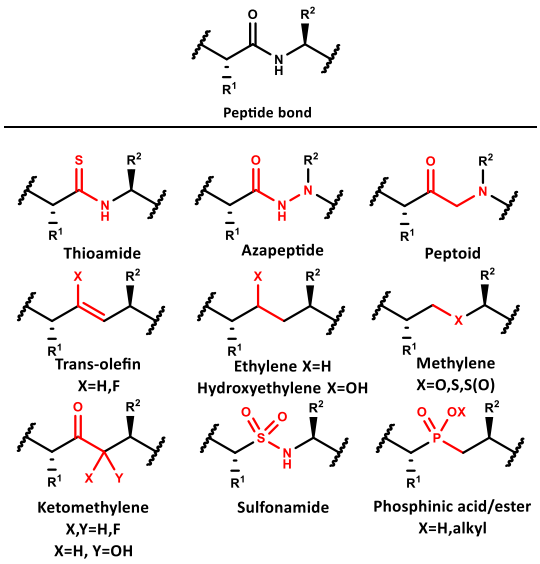

Figure 28. *Peptide bond isosteres. Adapted from Ref.90.*

Side chain modifications have been introduced to modify the conformational aspect of the peptide in order to control the rotatable bonds flexibility. These modifications allow to modify the electronic interactions occurring in the active site indeed they could involve the introduction of hydrophobic or polar side residues increasing or reducing the interactions with the target site. These modifications include:

- *C-alfa or N-alkylation*: this substituted amino acids are introduced in the molecular structure with the aim of constrain the torsional freedom of angles φ, ψ or ω. The main example of this type of amino acids is the alfa-Me-alanine which can contribute for the reduction of the rotational torsion of 90% when inserted into a peptide.
- *Cyclized amino acids*: these amino acids are commonly considered proline mimetics since it is the only amino acid presenting a cyclic structure and able to give a cis/trans isomerization. Consequently they are characterized by the presence of a bond between C-alfa and N-alfa which allow to the formation of a cycle responsible for the reduced conformational freedom, moreover the steric hindrance between the proline mimetic and adjacent residues afect the overall conformational disposition of the molecule.[90]

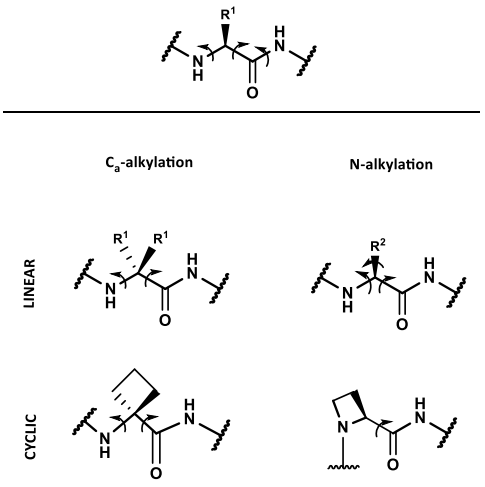

Figure 29. *Side chain modifications: Cα- and N-alkylation to give acyclic or cyclic constraint structures. Adapted from Ref.90.*

Global modifications include the possibility to cyclize a linear peptide. Cyclization leads to the alteration of the entire peptide profile for this reason it is different from the introduction of cyclic portions in the peptide structures which implies a local modification. It has been demonstrated that cyclization is very effective in increasing potency and stability against proteases in relation to the presence of a relevant number of cis amide bonds and absence of free C and N termini. The resulted constrained conformational structure increases the receptor selectivity and the binding affinity.[100] Cyclisation can occur in four different ways based on the peptide's features:

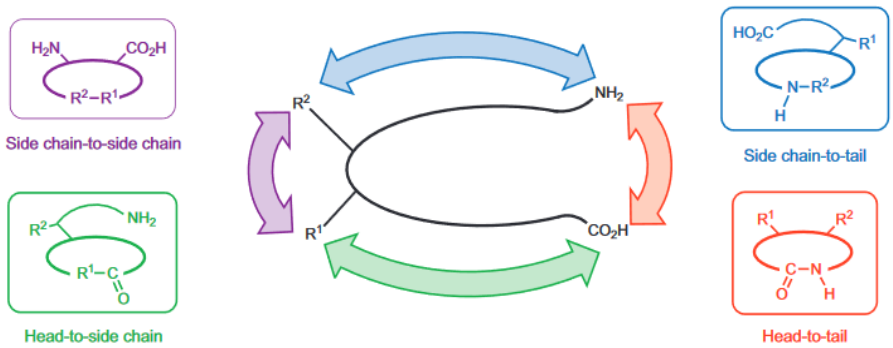

Figure 30. *The four possible ways a peptide can be constrained in a macrocycle. Adapted from Ref.106.*

- **Head-to-tail.** N- and C-terminal ends cyclized with an amide bond.
- **Head-to side chain**. N-terminal amino group and a nitrogen atom linked by a spacer.
- **Side chain-to-tail**. Two amide nitrogen atoms tethered by a linker.
- **Side-chain-to-side-chain.** Cα and α nitrogen atom connected by a chemical junction.

Among these the most common technique is the head-to-tail cyclization of a linear peptide through the formation of a peptide bond under standard peptide chemistry conditions.[106]

3.1.2. Different types of peptidomimetics

The combination of both local and global modifications allows for the development of different types of peptidomimetics.

Mimetics of Turn Structures. Peptidomimetic structures characterized by the presence of turn region which has been defined as specific portion of the molecule that allow a polypeptide chain to fold back on itself in a totally different conformation compared to β-sheet and α-helices. This type of mimetic structures can be obtained by most of the modification previously described in ***section 3.1.1.*** which include cyclization, *N*-methylation or introduction of amino acids which are able to induce a turn in the structure and confer rigidity such as the proline.[89]

Figure 31. *General stabilization of turn structures.* **a)** *Macrociclization.* **b)** *N-methylation.* **c)** *Turn inducing amino acids. Adapted from Ref.89.*

Mimetics of β-Sheets. β-sheet are highly involved in the formation of proteins tertiary structure and are the result of the parallel or antiparallel alignment of various β-strands stabilized by an extensive number of hydrogen bonds. There are three main approaches that can be undertaken to develop peptidomimetic structures of β-sheet which are:

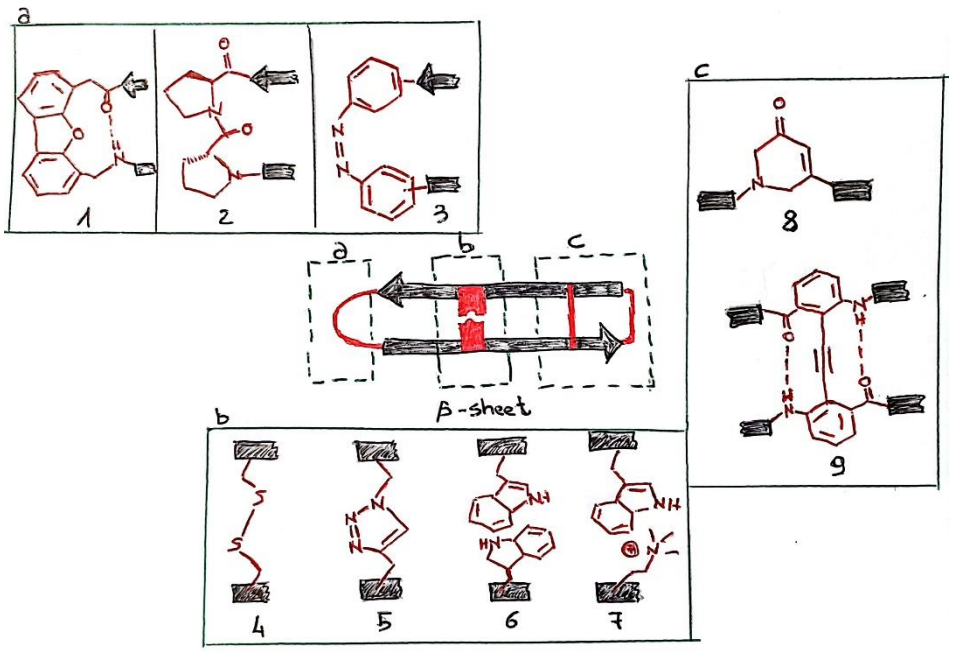

Figure 32. *General strategies to afford b-sheet mimetics.* ***a)Turn mimetics***, **1**. *Dibenzofuran derivatives,* **2**.*Oligourea derivatives,* **3**.*Azobenzene.* **b)*β-strand enforcing amino acids***, **4**.*Side chain to side chain cross-link with a disulfide and* **5**.*1,2,3-triazole ring,* **6**.*Side chain to side chain π– π interaction and* **7***Cation– π interaction* . **c)** ***Macrocyclization***: **8**. *4.1,6-dihydro-3(2H)-pyridinone,* **9**. *Diphenylacetylene building block. Adapted from Ref.89.*

- the use of turn mimetics which induce the formation of β-sheet structures such as D-amino acid or *N*-alkylated amino acids, proline residues or small scaffolds such as dibenzofuran oligourea, azobenzene derivatives;
- macrocyclization obtained by head to tail approach, side chain to side chain, cross-link with a disulfide and 1,2,3-triazole ring, side chain to side chain π–π interaction (Trp–Trp) and cation–π interaction (Nd-trimethylornithine–Trp);
- the use of specific amino acids which induce the β-strand formation reproducing the typical hydrogen-bonding pattern of a β-sheet for instance 1,6-dihydro-3(2H)-pyridinone or diphenylacetylene building block.[89]

Mimetics of Helices (foldamer and peptoids): αHelices in nature are repetitive secondary structures stabilized by intramolecular hydrogen bonds. Different approaches have been utilized over the years to develop α-helical mimetics such as:

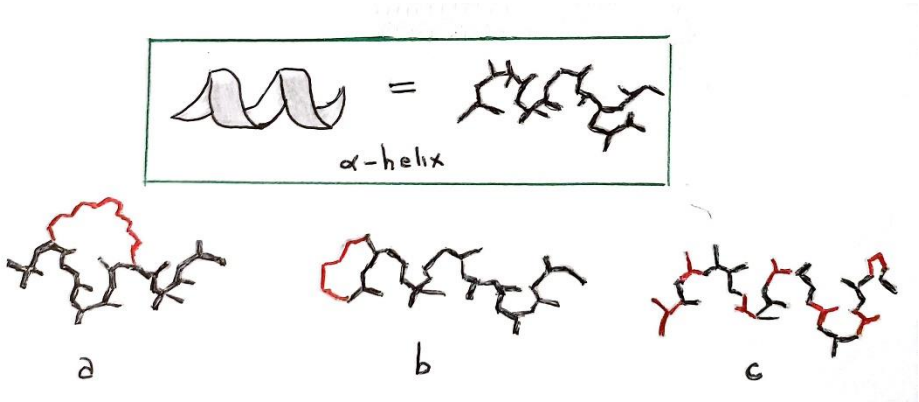

Figure 33. *General strategies of α-helix stabilization and mimicry.* **a)** *Side chain to side chain cross link.* **b)** *N-terminal cap.* **c)** *Foldamers. Adapted from Ref.89.*

- Side chain to side chain cross-linking of peptides that can be obtained through the formation of salt bridges between for instance glutamic acid and lysine, disulfide bridges between two cysteine residues, lactam cross-link due to the formation of an amide bond between lysine and aspartic, thiazole cross-link resulting in enhanced protease stability.
- Introduction of stabilizing *N*-terminal caps: constituted of linkers such as hydrazones and thioethers capable of stabilizing several turns of an α-helix.

- **Foldamers** are non-natural oligomeric structures which possess the folding properties of an α- helix with an increased proteolytic stability and they include b-peptides, peptoids, hybrids α/β-peptides. More in detail:
    - **β-peptides** are the most studied and are synthesized by coupling reactions between β-amino acids presenting an additional methylene group linked to the backbone if compared with an α-amino acid. Their folding ability in aqueous environment is lower than α-peptides. Consequently, different approaches have been considered to increase it such as the introduction of cyclic β -amino acids, intramolecular salt bridges, hydrocarbon or diether cross-links.
    - **α/ β -peptides** are given by the combination of α- and β -amino acids with predictable folding properties, α-amino acids play a role in the surface recognition, while the β -amino acids define the helical conformation.
    - **Peptoids** are composed of α-amino acids presenting the side chain directly linked to the amide nitrogen instead of to the α-carbon of the aminoacidic structure. These features lead to obtain a variety of structures which are resistant to proteolysis and with an improved cell permeability. Peptoids can also adopt a chiral structure where the amide bonds adopt a cis conformation allowing to support the idea that hydrogen bonds are not involved in the helical conformation.

- **structural mimetics**: include scaffold which specific substituents able to reproduce the same steric hindrance present in an α-helix.[89]

Isosteric replacement of the amino functionality leads to obtain various types of different molecules such as:

- **Dipeptide isosteres**. Molecules obtained by chemical modification of the peptide backbone aimed to constrain the conformational freedom fixing the φ, ψ or ω angles rotations and improving the peptidomimetic stability. This result can be achieved by substituting the amide moiety with specific structures included cyclic structures (lactams, piperazinones and imidazolinones) mimicking the structure of the peptide bond. Dipeptide obtained by the introduction of lactams as conformational constraints are the most common dipeptide isosteres. [100]
- **Depsipeptides.** Characterized by the replacement of one or more amino groups in the peptide chain by an oxygen atom which results in an ester-like structure with decreased ability on creating hydrogen bonds. Depsipeptides also show a reduced resonance delocalization consequently they have an increased freedom in the rotational angles which results in a more flexible structure.
- **Tiodepsipeptide.** Are the result of the substitution of the amide nitrogen with a sulfur atom and are obtained by thioesterification of a cysteine thiol group by the carboxylic group of amino acids, *N*-alkylamino acids or hydroxy acids.[107]

Retroinverso peptides. This strategy is based on the backbone modification "by replacing one or more L-amino acids with the parent enantiomer, and at the same time inverting the backbone direction from $N \rightarrow C$ to $C \rightarrow N$." The obtained molecules are not more rotational constrained but the modification of the amide bonds confer them an higher in vivo stability. [100]

AA-peptides. N-acylated-N-aminoethyl amino acids and they include to different subclasses: α-AApeptides and γ-AApeptides depending on the position

of the chiral side chains which are attached in γ position in γ-AApeptides and in α position in α-AApeptides. The whole structure resembles two adjacent α-peptides with one side chain attached to the α-carbon and the other to the to the adjacent amide nitrogen [108,109]

Azapeptides. Obtained by modification at the α-carbon in particular the replacement of the rotatable α carbon-CO with a rigid urea Nα–C(O) leading to obtain significant changes in chemical and biological properties. This eliminates chirality at the α-position and decreases the electrophilicity of the carbonyl group.

3.1.3. Amphipathic α-helical antimicrobial peptides

Many factors can impact on the architecture of a peptide such as presence of helix-stabilizing (e.g., Leu, Ala, Lys) or -destabilizing residues (e.g., Pro), capping effects, interaction of charged residues with the helix dipole, salt-bridging between residues with opposite charges, interaction of residues in the hydrophobic sector with the acyl chains of phospholipids in the membrane bilayer. [57]

Helix formation, hydrophobic interactions with the lipid bilayer and its rearrangement provide stabilization for the helical peptide insertion into membranes. This is due to the formation of hydrogen bonds in the phospholipidic bilayer which reduces the energy required to introduce peptide bonds into the bilayer. [57]

It has been demonstrated that the net charge of the antimicrobial peptides is strictly correlated with their antimicrobial activity potency but at the same time an excessive charge has a negative effect on the activity hindering the heliacal formation, indeed the optimal average charge is around +4.[57] For instance, the increased charge in magainin analogues results in smaller, less stable pores, and a quicker peptide translocation through the membrane.[110]

Another important feature of this peptides is their hydrophobicity which is more complicated to define since most of the time peptides show side tails which are not involved in define the hydrophobicity in a reliable manner.[111] Additionally it has been demonstrated that an increased hydrophobicity is responsible for the reduced selectivity for bacterial membranes since hydrophobic residues can easily interact with both acidic and neutral membranes.[57]

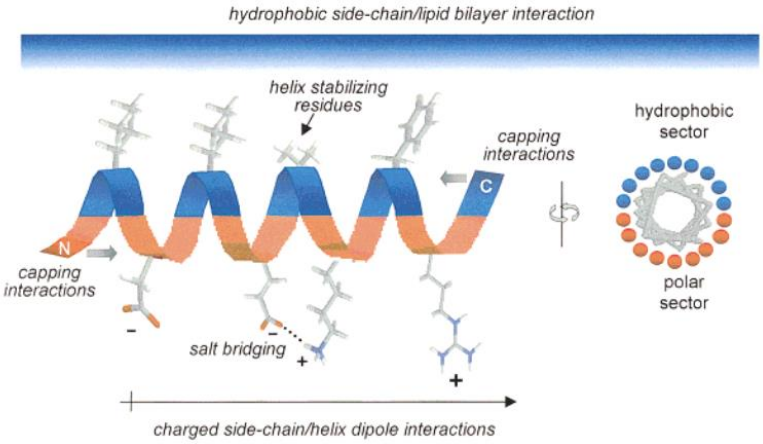

Figure 34. *Amphipathic features of a-helical AMPs. Adapted from Ref.56.*

All the amphiphilic α-helical peptides are by the presence of spatially separate hydrophobic and positively charged surfaces, but they differ in sequence and in their detailed secondary structure. Additionally, all of them lead to the formation of pores and the consequent disruption of bacterial membrane.[94]

[This page is intentionally left blank]

3.2. Aim of the project

While peptidomimetics like Brilacidin may represent a valuable resource in the battle against resistant bacterial strains, an extensive literature search has revealed a lack of a solid foundation for structure-activity relationships. Additionally, there is no available information regarding the selectivity of these agents toward various bacterial strains.

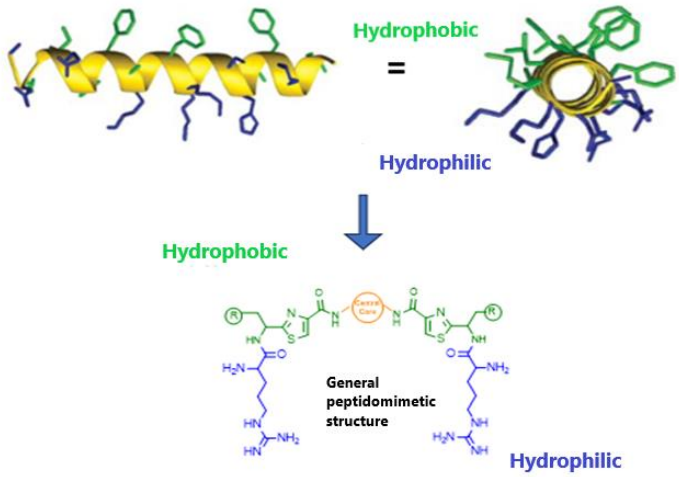

Figure 35. *Side and end on representation of magainin base on which the general structure of our peptides was designed.*

Therefore, we deemed of interest to plan the synthesis of a series of antimicrobial peptidomimetic compounds that can mimic the facially constrained disposition of magainin's structure. The design of the molecules took inspiration from the general considerations above reported whereas the synthesis was planned in order to optimize time, yields, and allow for the production of numerous molecules following a modular synthetic scheme.

Looking at the side and end-on representations of magainin structures, it is clear that hydrophilic and hydrophobic residues are located in two opposite regions of the helix and carefully balanced. Indeed, many studies underline as the specific steric conformational disposition of different residues in the molecule is responsible for the amphipathicity of the molecule and, in turn, for the antimicrobial activity. This inspired us to design and synthesize a library of molecules which can be considered as peptidomimetic compounds since they mimic the structure of a natural peptide. We aimed at introducing specific key residues and peptide bond surrogates responsible for intramolecular electrostatic interactions, in order to maintain a specific conformational structure of the molecule.

Overall, the design was aimed to reach two main goals.

First, to reproduce the structural features of magainin through the introduction of different modifications in the peptide structure. As a second aspect, the synthesis was aimed to obtain molecules which can mimic not only the conformational structure of AMPs but also their mechanism of action. Indeed,[63,64] AMPs exert their antimicrobial activity through membrane lysis and consequent direct disruption of cellular components, an effect obtained by the selective interaction with the bacterial membrane due to their neat positive charge and the balanced lipophilicity of the molecules.

Once the improvements in the synthetic procedure have led to the synthesis of a reasonable number of different analogues, another important aim was the determination of antimicrobial activity in order to define a structure activity relationship study that would allow the identification of a pattern of specific portions essential for the activity.

Finally, we deemed of interest to collect additional information on the biological characteristics of these molecules related to their interaction with the bacterial cell. Therefore, I investigated whether the mechanism of action is comparable to that of magainin (interaction and disruption of the bacterial membrane) or if it depends on the interaction with a specific membrane or

intracellular target. For this purpose, I planned a series of biological experiments, which have been carried out during the period spent at Helmholtz institute, under the supervision of prof. Müller, including membrane depolarization assay, time killing assay, ATP assay, scanning electron microscopy, lysis assay and affinity based proteomic (refer to **chapter4** for detailed description of the mode of action studies).

[This page is intentionally left blank]

3.3. Results and discussion

3.3.1. Design approach

The rational design of these peptidomimetic molecules was based on data deriving from literature and rational designs that inspired the synthesis of Brilacidin **(*Section 2.6.1*.).**

The rationale used to design the molecules of interest started from well-established knowledge about the role of positive charge and hydrophobicity on the antimicrobial potential of AMPs. The positive charge enables the cationic molecules to interact with the negatively charged phospholipids on the bacterial surface through electrostatic interactions, whereas hydrophobic portions facilitate the deeply insertion of the molecules into the lipid bilayer of the membrane, hence perturbing or destroying the bacterial membrane architecture leading to the cell death.[50,112]

Based on this notion, three main features could be considered peculiar for the new designed structures: 1) a central core to serve as the linker between the two charged portions; 2) an amide bond surrogate to mimic the peptide bond containing the lipophilic amino acid, and 3) a charged portion.

It is worth mentioning that the proposed design takes into consideration a separate disposition of the hydrophilic and hydrophobic residues as it is for the natural AMPs.

Central core showing an aromatic ring is the focal point of the molecule essential for the linkage of the symmetric and asymmetric side tails. Symmetricity of the positive charges is one of the main features of this molecule that plays a pivotal role in the definition of the spatial distribution of the molecule itself, nevertheless the synthesis of asymmetric molecules has been investigated incorporating two different aminoacidic branches into the structure. Different structures were chosen as central core in such a way to obtain sufficient variability and, in case, offer a better discernment of SAR

characteristics. Therefore aromatic, heteroaromatic, polycyclic or aliphatic structures were selected as linker since their different steric and chemical characteristics. All of these structures were adorned with two side amino groups essential to create a peptide bond or link a mimetic surrogate. (as showed in ***Figure 36***)

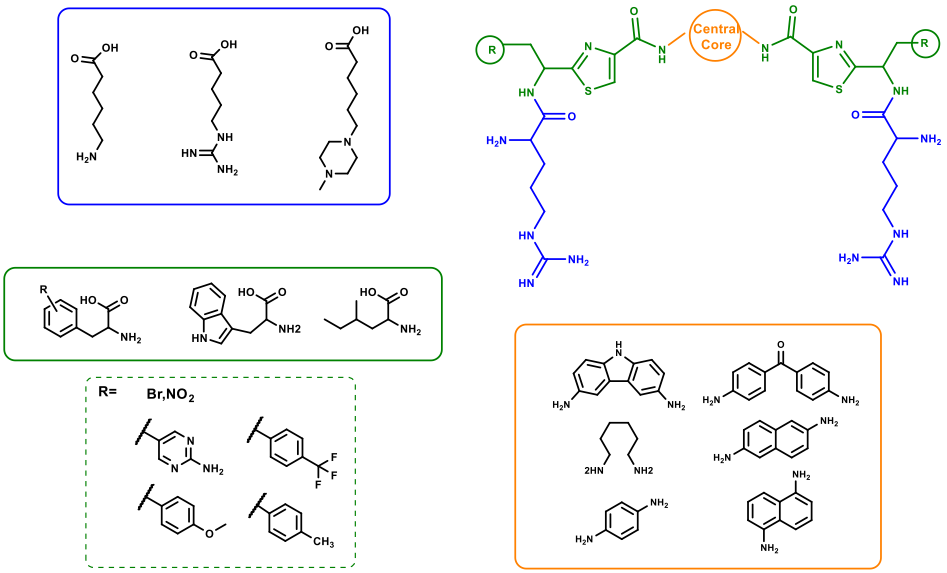

Figure 36. *Three focal points in the designed peptidomimetic structure and relative modifications investigated.*

An amide bond surrogate was necessary to safeguard molecule stability. In this case, we chose to introduce the thiazole moiety as peptide surrogate based on the fact that, as reported in ***Section 3.1.1*****,** thiazole is considered one of the main amides bioisoster and it allows to obtain a conformational restriction in the molecule which prevent it from proteolytic degradation. This is due to the presence of nitrogen and sulphur atoms in the structure which act as hydrogen bond donor (HBD) and acceptors (HBA) respectively, leading to the formation of intramolecular electrostatic interactions with the carbonylic group of the side amides resulting in a conformational constricted structure. This part of the molecule, in our vision, was supposed to hold the lipophilic character of the molecule. It is known that hydrophobic amino acids, including, leucine (L),

isoleucine (I), tryptophan (W), phenylalanine (F), valine (V) or alanine (A), play a pivotal role in helping the insertion of the molecule into the membrane due to π-π interactions. In this regard, we decided to use phenylalanine and tryptophan to adorn the lipophilic face of our molecules, essentially for 3 reasons.

From one side, these are lipophilic and bulky amino acids, that could be used to balance the polarity of the charged tails.

On a second instance, the presence of the aromatic might have offered additional chemical modification, through the introduction of small functional groups or more elaborated aromatic substituents.

Finally, molecules with tryptophan residues display a great antimicrobial activity.[113] We wanted to investigate the possibility to synthesize both symmetric and asymmetric molecules, maintaining the same specific spatial conformation. For this reason, a different synthetic procedure was studied as reported in the following section.

Positively charged moieties confer a net positive charge to the molecule allowing to mimic the positive charge of natural AMPs and are essential for the antimicrobial activity.

Positive amino acids such as lysine (K), arginine (R) and histidine (H) are generally responsible for the positive charge of many natural molecules. Therefore, for our preliminary investigation, arginine was selected as it has proved to be the most effective for antimicrobial activity.[114] However, besides the arginine-containing molecules, and considering the synthetic strategy adopted, also a small set of compounds were tested where the arginine was not introduced, and another set with a Boc-protected arginine. The rationale is that for all of these molecules, an appreciable positive charge, of variable intensity, could be obtained.

3.3.2. Synthetic strategy

The developed synthetic strategy which allows to obtain the final general structure **i**, involves 8 steps all performed through in-solution synthetic procedures and reported in ***Scheme1.***For complete structures, see ***Figur*e 37,*Figure* 38** and the experimental part.

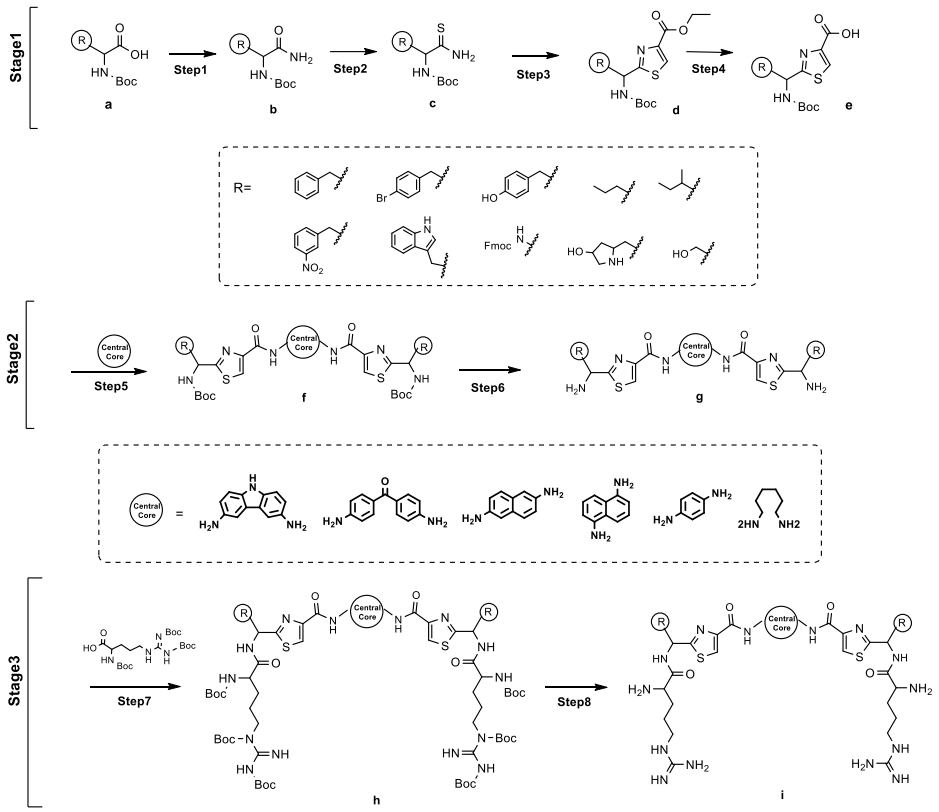

Scheme1. *General synthetic strategy. Reagents and conditions:* **Step1**. *Isobutylcloroformate, N-methylmorpholine, THFdry, rt, 4h; 30%NH_4OH, 0°C, 2h.* **Step2.** *Lawesson's reagent THFdry, 50°C, 4h.* **Step3**.*Ethyl bromo pyruvate, $KHCO_3$, DME, TFAA, pyridine, 0°C, 2h.* **Step4**. *LiOH, THF/MeOH/H_2O, RT,2h.* **Step5.** *HATU, DIPEA, DMF, rt,4h.* **Step6**. *TFA, DCM, rt,2h.* **Step7.** *HATU, DIPEA, DMF, 4h.* **Step 8**. *TFA, DCM, rt, 12h.*

The first stage led to the synthesis of the modified aminoacidic portion characterized by the thiazole moiety as amide bond surrogate presenting an amino acid branch in position R with the amino group protected by the tert-butyloxycarbonyl (Boc) group. The commercially available N^{α}protected N-(Boc)-amino acid **a** undergoes a substitution reaction where N-methyl morpholine and isobutyl chloroformate react together to form an intermediate which deprotects the carboxylic group consequently the nucleophilic NH_4OH attacks the negatively charged carbon leading to the amide formation **b.**

The obtained amide **b** was then treated with Lawesson's reagent, a thionating agent which is commonly used to convert amides in thioamides, to obtain compound **c**. The reaction with the carbonyl atom leads to a thiaoxaphosphetane intermediate where the driving force is the formation of a stable P=O bond which promotes a cycloreversion step where the sulphur atom substitutes the carbonyl oxygen.

Compound **d** characterized by the thiazole moiety has been obtained accordingly to a modified Hantzsch thiazole synthesis.[115] The synthetic procedure known as Hantzsch thiazole synthesis which lead to the formation of thiazole was discovered in 1889 but the original reaction conditions (refluxing ethanol) allow to the formation of hydrogen halide responsible for a loss of optical purity. Consequently, a two-step procedure, called Holzapfel–Meyers–Nicolaou modification, was then introduced. It consists of a cyclocondensation reaction between the thioamide **b** and ethyl bromo pyruvate under basic conditions which produces the hydroxythiazoline intermediate, then converted in thiazole by a dehydration step performed by trifluoroacetic anhydride (TFAA) and pyridine.[116]

The final acidic thiazole molecule **e** obtained by the first stage of the synthesis results from the basic hydrolysis reaction carried out by using LiOH in $THF/MeOH/H_2O$.The second stage involves a classic coupling reaction between compound **e** obtained in the first stage and the central core. Compound **5** was

treated with the coupling agent HATU in basic conditions offered by DIPEA, then the central core was added to the solution to form compound **6**. Different building block have been used as central core, such as 9H-carbazole-3,6-diamine, 4,4'-diamminobenzophenone, naphthalene-2,6-diamine, benzene-4-diamine and hexan-1,6-diamine in order to offer variability. Compound **f** undergoes an acidic hydrolysis to remove the two Boc protecting group to obtain compound **g**.

Once obtained compound **g,** two different synthetic routes have been investigated to synthetize the final compound **i** which have been compared in terms of time and yields.

The two routes are reported in ***Scheme2***:

- **Route A** includes 3 steps, and it involves the arginine protected moiety Boc-Arg(Z)$_2$-OH in a coupling reaction with compound **g** to get compound **h.1.** The last underwent a Pd/C-catalysed hydrogenative deprotection of *N*-Benzyl groups by using the Parr shaker hydrogenators apparatus to obtain compound **h.2.** This reaction step has been performed and optimized by using different conditions indeed various combinations of accelerating factors (high pressure and acids HCl, CH_3COOH..) has been used getting to different outcomes.

  Finally, compound **i** has been obtained from compound **h.2** by acid removal of the Boc protecting group.

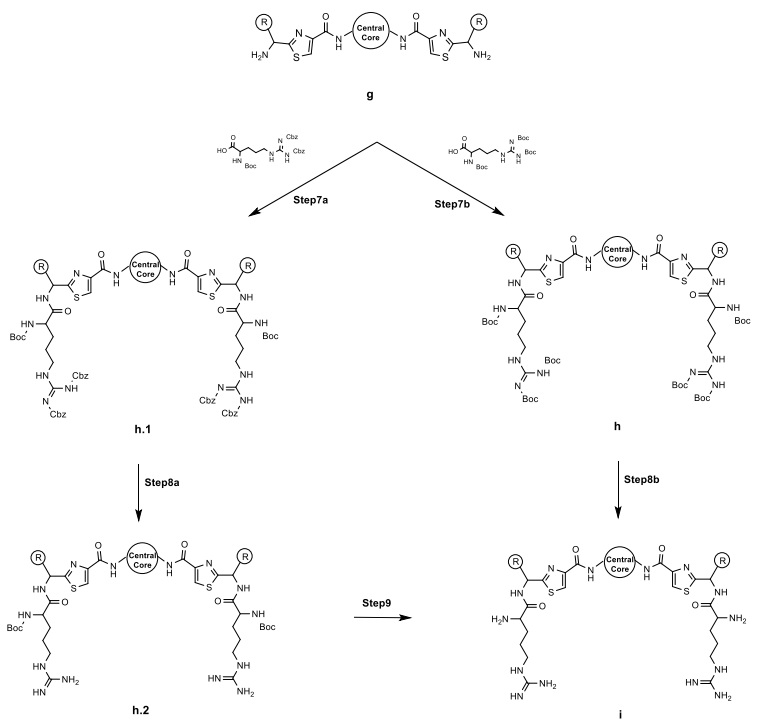

Scheme 2 *Reagents and conditions:* **Step7a**. *Boc-Arg (Boc)$_2$-OH ,HATU, DIPEA, rt, 1h.*__Step7b__.*Boc-Arg(Z)$_2$-OH*__,__*HATU,DIPEA,rt,1h.*__Step8a.__*Pd/C,MeOH/EtOAc/ CH3COOH, hydrogen atmosphere, rt, 15h* **Step8b.** *TFA, THF/MeOH/H$_2$O ,0°C then rt, 3h.* **Step9**. *TFA, THF/MeOH/H$_2$O ,0°C then rt, 3h.*

Route B includes only one coupling reaction step between the obtained intermediate **g** and the positively charged and protected portion represented by Boc-Arg (Boc)$_2$-OH to obtain compound **h.** Then compound **i** was obtained by acid removal of the Boc protecting group. As reported above, after setting an efficient synthetic methodology to synthetize the final desired compound, the intermediate structure **g** and **h.2** were also identified as general structures for the development of two more series of derivatives 1) derivatives with the N $^{\alpha}$ protected arginine moiety 2) intermediates without arginine.

It is easy to understand that general molecule **e** is a key product to guarantee chemical variability to the whole set of compounds planned. Indeed, playing

with the different starting amino acid **a**, or with the charged portion attached, or with a different central core, the modular synthesis of many analogues can be performed.

Although the simple reactions, however the designed synthesis and the following purification resulted very challenging in nearly all the steps, leading to focus the attention on the optimization of both reaction and purification steps.

Commercially available amino acids or N^{α}protected amino acids have been used as starting materials **a** for the development of the thiazole modified amino acids derivatives **e**, among these Boc-L-Phe-OH, Boc-Trp-OH, Boc-Phe-(3-NO_2)-OH, L-Isoleucine, Fmoc-Hpy-OH, N-Boc-4-bromo-L-phe-OH, Fmoc-Gly-OH and DL-Norvaline. Compound **b** (**Step 1**) synthesis was properly modified in order to reduce the time required to obtain the desired compound, indeed the reaction was first performed by following the procedure already reported which assumes to treat the commercially available N^{α}protected N-(Boc)-amino acid **a** with N-methyl morpholine and isobutyl chloroformate at -20C (by using liquid nitrogen) for 4h, then after adding NH_4OH the reaction was stirred at room temperature for 3 more hours. Nevertheless, during the optimization step it was tried to furnish a -10C cold environment by using ice bath instead of liquid nitrogen and the reaction time was reduced to 1h in both the two reaction steps allowing us to obtain the desired final compound in an optimal yield (97%).

Additionally, the synthesis of the thioamide derivate compound **c** (**Step 2**) was also performed accordingly to the reported procedure which presumes to stir the starting compound **b** together with 2 eq of Lawesson's reagent in THF_{dry} for 16h at 50°C. In this case the reaction time was reduced from 16h to 2h since it has been verified that such a long reaction time is not necessary to get to the reaction completion. Based on the challenging purification step the amount of Lawesson's reagent was also reduced from 2eq to 1.2eq leading to obtain a final reaction mixture presenting less impurities deriving from the Lawesson's reagent action which was way easily to purified by flash column

chromatography. These modifications allow to increase the yield from 38% to 65% as reported in ***section 3.5.***

The thiazole acidic derivatives **e** (**step 3**) were synthesized following the procedures reported by Bertram et al. and Singh et al. [117,118] properly modified in some steps to increase the total yield. This was certainly one of the most challenging steps of this synthetic procedure. The three steps modified Hantzsch method reported by Singh et al. was first followed. Compound **c** was reacted with ethyl bromopyruvate (-15 °C for 12h) to obtain the intermediate 4,5-dihydrothiazole **c.1**, then filtered, resuspended in DME and treated with trifluoroacetic anhydride (TFAA) and 2,6-lutidine (for 12h) to furnish the thiazole product **d**. According to Singh *et al*. the second step could allow to the N-trifluoro acetylation of amide NH consequently the treatment of the reaction mixture with freshly prepared sodium ethoxide (for 6h) was carried out.

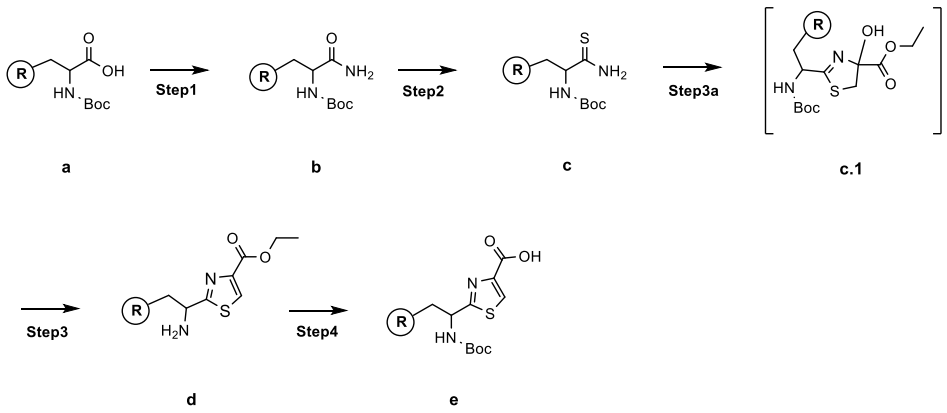

Scheme3. *4,5-dihydrothiazole intermediate formation during Hantzsch synthesis.*

Following this procedure, it was possible to obtain the final intermediate only once with a low yield of 30%, whereas other attempts failed to give the desired molecular structure. Consequently, based on the fact that this reaction was time-consuming, low yield and the fact that the sodium ethoxide deacetylation step was redundant, a different and more concise synthetic procedure was followed according to Wahyudi et al.[119] so to obtain the desired product **d** through a 1h reaction step and to increase the yield to 67% .

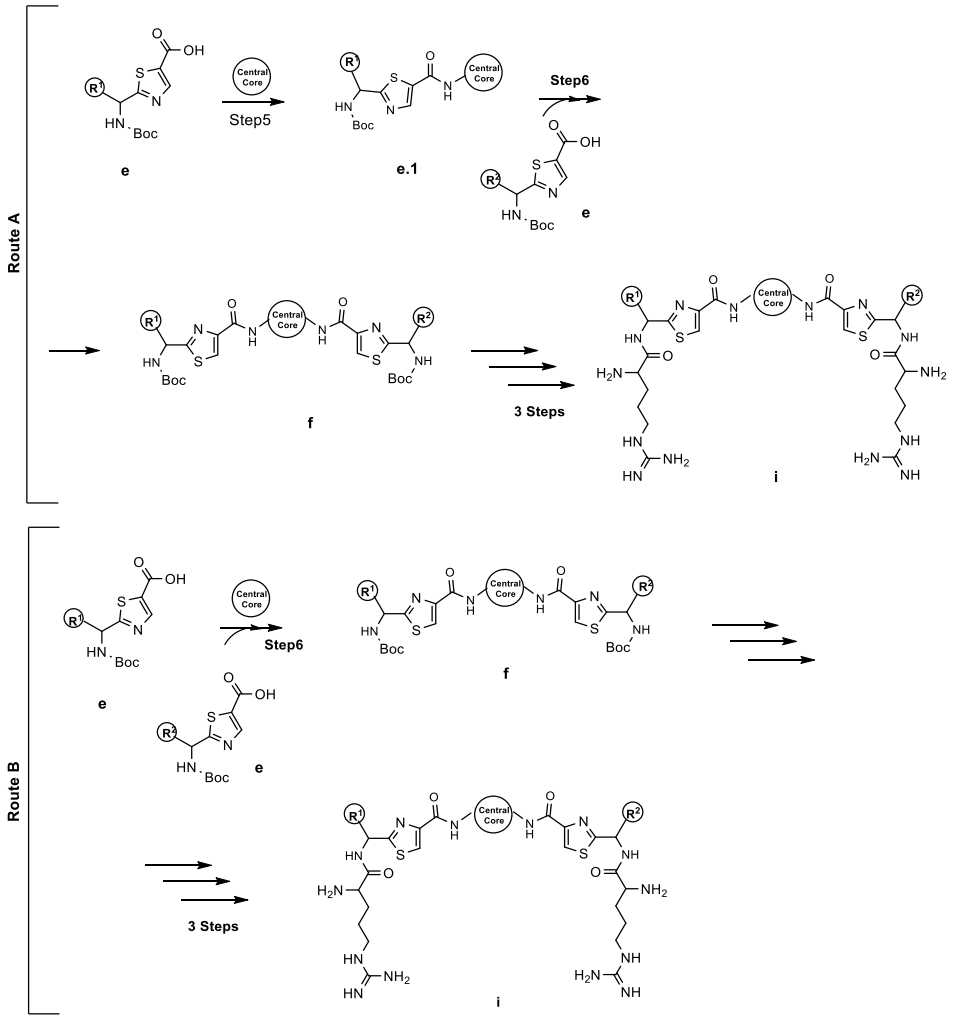

Scheme4. *Two coupling strategies (RouteA and routeB) in the synthesis of intermediate structure* ***f.*** *Reagents and conditions: HATU, DIPEA, rt, 1h.*

The synthetic steps which allow to obtain compounds **f** and **h** are both coupling reactions were the acid molecule, respectively compound **e** and Boc-Arg$(Z)_2$-OH or Boc-Arg$(Boc)_2$-OH, is activated with a coupling agent and DIPEA then added to the basic central core. For the coupling reactions different conditions have been used leading to the modification of reaction solvents and coupling reagents including HBTU in DCM, HOBt/EDC in DMF and HATU in DMF resulting in the identification of HATU as the best coupling reagent for these reactions based on the different obtained yields.

Concerning the synthesis of asymmetric derivatives, two different coupling strategies **(Route A and B**) were attempted.

Both the strategies require the previous synthesis of the two different thiazole acidic moieties **e**. Another common feature is represented by the reagent's equivalents used, that must be carefully considered. Therefore, 2 eq of central core and 1 eq of thiazole moiety were used.

The main difference in this synthesis is represented by the method employed which involves two different steps in the first procedure **(Route A)** and one step in the second **(Route B).** In particular in Route A one of the acidic thiazole portion **e** was first added to the central core then after purification and characterization of intermediate **e.1** the second thiazole portion was added. On the contrary Route B requires the separate and simultaneous activation of the two different thiazole moieties that are then contemporary added to a solution of central core. The second procedure allowed to obtain the final compound in a faster way, but the yield was extremely lower if compared to procedure A which was consequently chosen as the favourite one. Since the preliminary scope of this investigation, we preferred to to focus mainly on the synthesis of symmetric derivatives, as that of asymmetric derivates was too time-consuming.

The antimicrobial activity of the synthetized compounds with intermediate structure **g**, intermediate structure **h.2,** and the final compounds with structure **i**, were evaluated and the results are deeply analysed in chapter 4. For the sake of clarity, two summary tables of all the tested compounds are reported below.

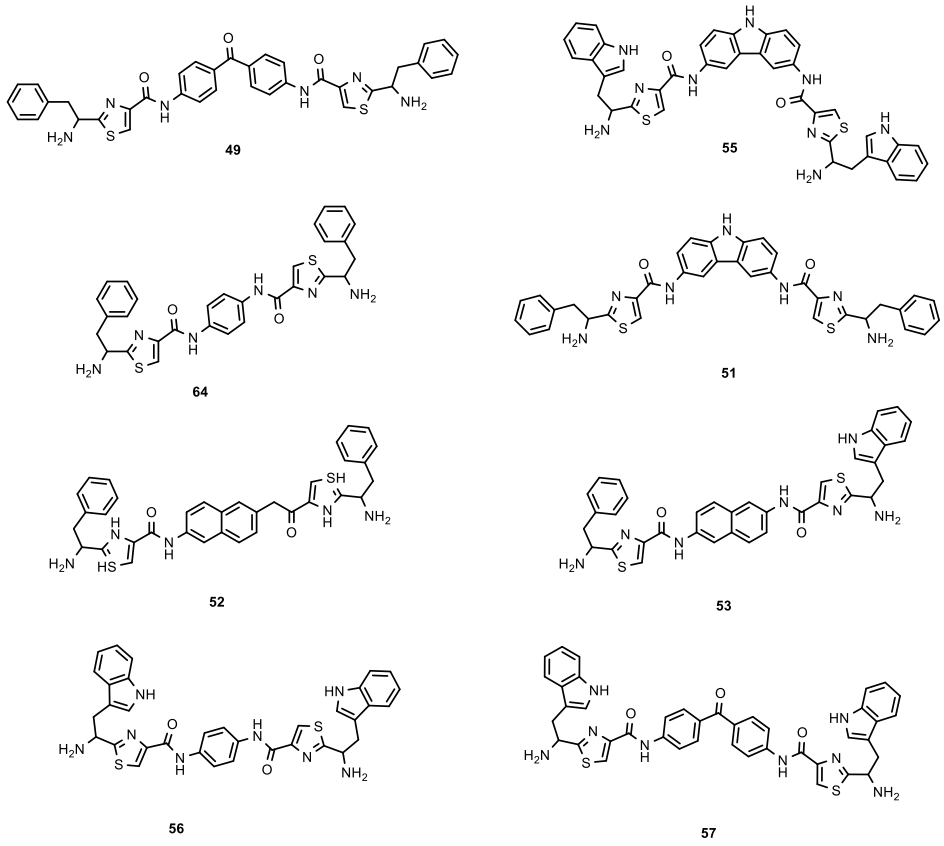

Figure 37. *Tested compounds with general structure **g***

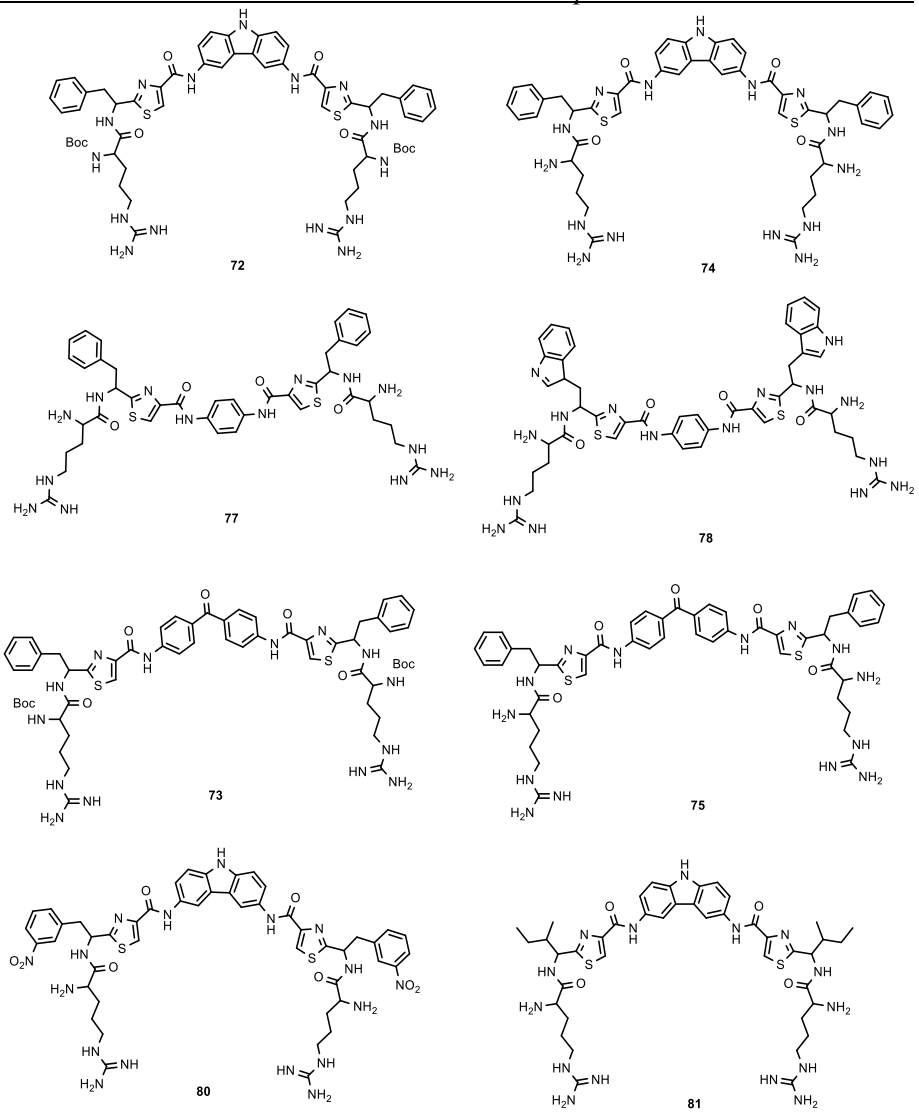

Figure 38. *Tested compounds with general structure* ***i***

[This page is intentionally left blank]

3.4.Conclusion

The first part of this project led to the synthesis of a series of antimicrobial peptides with a novel structure. I have managed to obtain amphiphilic structures to mimic that of magainin, where the charged polar portion was constituted by arginine. Along with such compounds, also some intermediated were tested based on the assumption that the compounds still carried a basic character. The designed synthetic strategy tourned out to be tedious and led to low yields, therefore I was successful in the optimization leading to increase the yield and reduction of the reaction times. Before undertaking additional synthetic efforts, I preferred to biologically characterize the molecules synthesized, investigating the mechanism of action of the synthetized peptidomimetic molecules. Therefore, a comprehensive MIC evaluation and specific biological assays (including proteomic analysis) were planned and carried out, as discussed in the following chapter.

[This page is intentionally left blank]

3.5.Experimental procedures

3.5.1. Solvents and chemicals

Commercial reagents were purchased as reagent grade and used without further purification. Solvents for RP-HPLC were purchased as HPLC grade and used without further purification. Solvents and chemicals were all purchased from Sigma–Aldrich, Fluorochem, Honeywell or Carlo Erba reagents.

3.5.2. General methods for purification and analysis

Analytical thin-layer chromatography (TLC)

TLC was performed using Kieselgel F254 200 μm(Merck) silica plates. In order to enhance the difference of Rf between reagents, products and any possible impurity, mobile phases have been optimized and EP/EtOAc was identified as the best solvents combination for the synthesized molecules. TLC spots were then visualized by UV florescence lamp at 254 nm and 365 nm or by $KMnO_4$ staining followed by heating of the plate.

Flash column chromatography

Flash chromatography is performed packing Merck silica gel (40−63 μm) in a variable size glass column and flushing with air. The final product is purified from the reaction mixture by using an eluent mixture optimized through TLC analysis.

1.1.1 Automated flash column chromatography

1.1.2 Automated flash column chromatography was carried out with the CombiFlash *Sep®Rf* automated flash column chromatography by using Silica Redi*Sep®Rf* cartridges(direct phase) and C18 Redi*Sep®Rf* cartridges (reverse phase).

Nuclear magnetic resonance (NMR)

Spectra were recorded on a Bruker AVANCE 400 spectrometer at 400 MHz for ^{1}H nuclei and 100 MHz for ^{13}C nuclei at RT in $CDCl_3$ and CD_3OD All chemical shifts are reported in parts per million (ppm) and refers to the residual chloroform peak (δ 7.26 ppm) for ^{1}H NMR or the residual chloroform peak (δ 77.1 ppm) for ^{13}C NMR. The ^{1}H NMR shift values are reported as chemical shift δ, multiplicity (s=singlet, d= doublet, t=triplet, q=quartet, m=multiplet, dd=doublet of doublets, td=triplet of doublets, qd=quartet of doublets) and coupling constant (J inHz). ^{13}C NMR values are reported as chemical shift δ.

Mass spectrometry

ESI-mass spectra were recorded on UHPLC/ESI-MS system (ACQUITY Ultra Performance LC; ESI, positive ions, Single Quadrupole analyzer) and are reported in the form of (m/z). Isocratic gradient 10%B (MeOH), run time 5 min, injection volume 10µL.

HPLC-ESI-MS/MS

Purity of the final compounds was analysed by HPLC-ESI-MS/MS performed by using an Accela UHPLC system (Thermo, USA), equipped with a Synergy Fusion C18 80Å RP-column (2.0 × 100 mm, 4 µm; Phenomenex, USA) at a flow rate of 0.35 mL/min. The injection volume was 10 µL and the total run 30 min. The reported gradient was used: 95 %B between 0 and 4 min; linear gradient to 5 %B from 4 to 14 min; 5 %B between 14 and 20 min; 0 %B between 20 and 22 min and returning to 95 %B in 2 min where it last for 6 min. Solvent A: H_2O+0.1% TFA and solvent B: ACN +0.1% TFA

3.5.3. General synthetic methods

General synthetic method for Boc-AA-OH (*Method* A)

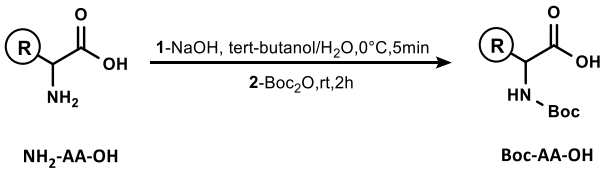

To a solution of NH_2-AA-OH (1eq) in tert-butanol/H_2O (50/50 v/v) at 0°C (ice bath) was added NaOH (3.5 eq.). The reaction was stirred for 5 min at 0 °C then di-tertbuthyl-dicarbonate (Boc_2O) (4 eq.) was added and the mixture was allowed to reach room temperature (rt) and stirred for 2h. The obtained suspension was washed with $KHSO_4$ 1M then extracted with EtOAc. The organic solution was dried over Na_2SO_4 and the solvent was removed under reduced pressure obtaining the product as a withe solid filtered with a mixture of EP/Et_2O.

General synthetic method for Boc-AA-OH amide derivates (*Method* B)

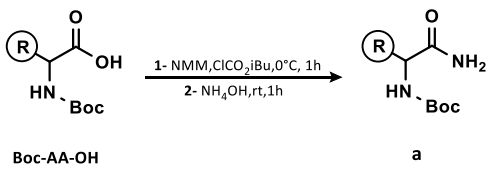

To a solution of Boc-AA-OH (1eq.) in THF_{dry} was added *N*-methyl morpholine (NMM) (1.2 eq.) and isobutyl chloroformate ($ClCO_2iBu$) (1.2 eq.). The solution was stirred at 0°C for 1h. Then NH_4OH was added, and the solution was stirred at rt for 1h. The obtained mixture was washed with $KHSO_4$ 1M then extracted

with EtOAc. The organic solution was dried over Na_2SO_4 and the solvent was removed under reduced pressure obtaining the product as a withe solid filtered with a mixture of EP/Et_2O.

General synthetic method for thioamide derivates (*Method C*)

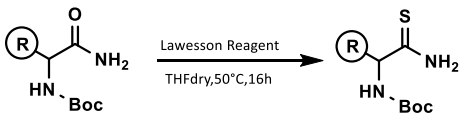

a **b**

To a solution of **a** (1 eq.) in THF_{dry} under a nitrogen atmosphere was added the Lawesson Reagent (1.5 eq.). The solution was stirred at 50°C for 16h. The mixture was washed with saturated $NaHCO_3$ and Brine then extracted with EtOAc. The organic solution was dried over Na_2SO_4, the solvent was removed under reduced pressure and the product was purified by flash silica gel column chromatography (EP/EtOAc 7:3) or CombiFlash *Sep®Rf* automated flash column chromatography (A: EP and B: EtOAc) by using Silica Redi*Sep®Rf* cartridges obtaining the product as a pale green solid.

General synthetic method for thiazole derivates (*Method D*)

b c

To a solution of **b** (1eq.) in DME_{dry} (mL), under a nitrogen atmosphere, was added $KHCO_3$ (8 eq.). The solution was vigorously stirred for 5 min. Then ethyl bromopyruvate (EBP) (3 eq.) was added and the reaction was stirred for 1 min. The suspension is placed at 0°C and was added a solution of pyridine (8.5 eq.) and TFAA (4 eq.) in DME (mL). The solution was stirred 1h at rt. The mixture was washed with H_2O and Brine then extracted with EtOAc. The organic solution was dried over Na_2SO_4, the solvent was removed under reduced pressure and the product was purified by flash silica gel column chromatography (EP/EtOAc 8:2) or CombiFlash *Sep®Rf* automated flash column chromatography (A:EP and B:EtOAc) by using Silica Redi*Sep®Rf* cartridges obtaining the product as a with solid.

General synthetic method for thiazole acidic derivates (*Method E*)

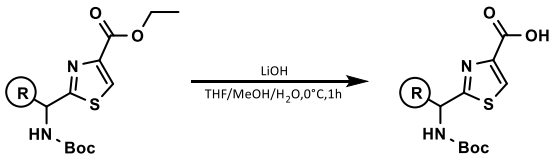

c d

To a solution of **c** (1 eq.) in THF/MeOH/H_2O at 0°C was added LiOH (4 eq.). The mixture was stirred at rt for 1h. The obtained mixture was washed with

$KHSO_4$ 1M and was extracted with EtOAc. The organic solution was dried over Na_2SO_4 and the solvent was removed under reduced pressure obtaining the product as a withe solid filtered with a mixture of EP/Et_2O.

General coupling methods

Method F

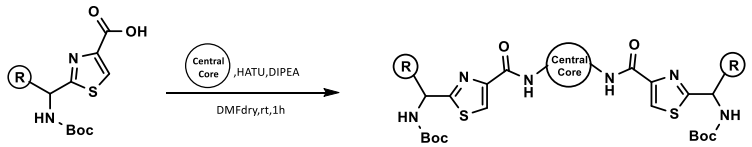

d e

To a solution of **e** (2eq.) in $DMF_{dry,}$ under a nitrogen atmosphere at rt were added HATU (2.2eq.) and DIPEA (5 eq.). The mixture was stirred at rt for 10 min. Then **central core** (1eq.) was added, and the solution stirred at rt for 1h. The mixture was washed with H_2O and Brine then extracted with EtOAc. The organic solution was dried over Na_2SO_4, the solvent was removed under reduced pressure and the product was purified by flash silica gel column chromatography (DCM/MeOH 99:1) obtaining the product as a yellow solid.

Method F_bis

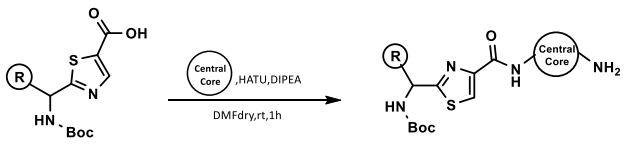

d e

To a solution of **e** (1eq.) in $DMF_{dry,}$ under a nitrogen atmosphere at rt were added HATU (1.2eq.) and DIPEA (5eq.). The mixture was stirred at rt for 10

min. Then **central core** (2eq.) was added, and the solution stirred at rt for 1h. The mixture was washed with H_2O and Brine then extracted with EtOAc. The organic solution was dried over Na_2SO_4, the solvent was removed under reduced pressure and the product was purified by flash silica gel column chromatography (EP/EtOAc 6:4) obtaining the product as a yellow solid.

Method G

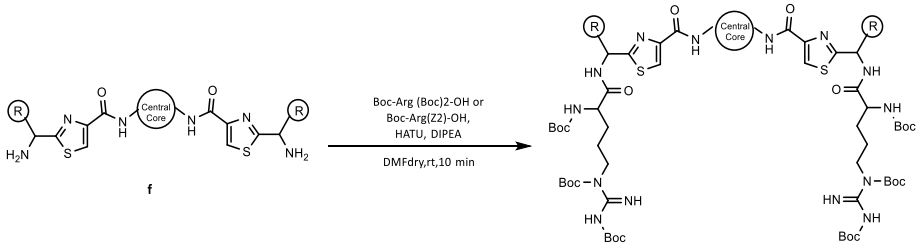

To a solution of Boc-Arg $(Boc)_2$-OH or Boc-Arg(Z_2)-OH (2 eq.) in $DMF_{dry,}$ under a nitrogen atmosphere at rt were added HATU (2.2 eq.) and DIPEA (5 eq.). The mixture was stirred at rt for 10 min. Then **f** (1 eq.) was added and the solution stirred at rt for 1h. The mixture was washed with H_2O and Brine then extracted with EtOAc. The organic solution was dried over Na_2SO_4, the solvent was removed under reduced pressure and the product was purified by flash silica gel column chromatography (DCM/MeOH 98:2+ 0.2% NH_3) obtaining the product as a pale brown solid.

General Boc deprotection methods

Method H

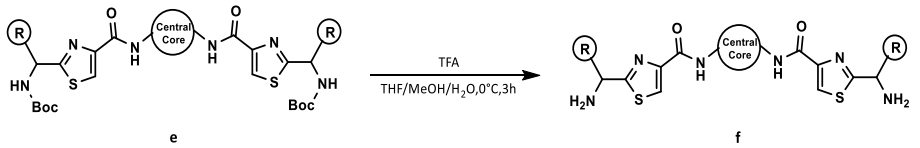

To a solution of **e** (1 eq.) in THF/MeOH/H_2O at 0°C was added TFA (30eq.). The mixture was stirred at rt for 3 h. The obtained mixture was washed with NaOH 2M and was extracted with EtOAc. The organic solution was dried over Na_2SO_4 and the solvent was removed under reduced pressure obtaining the product as a yellow solid filtered with a mixture of EP/Et_2O.

Method I

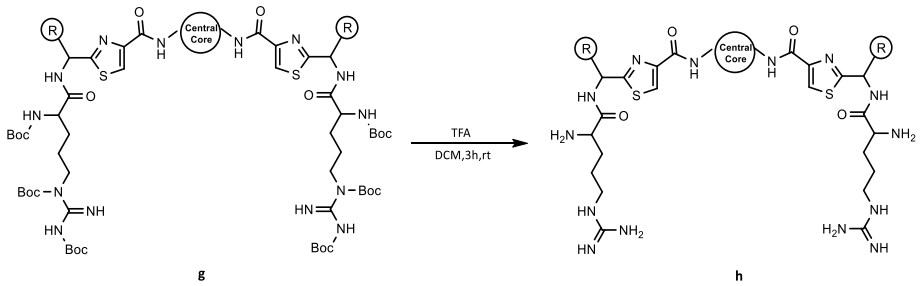

To a solution of **g** (1 eq.) in DCM was added TFA (30 eq.). The mixture was stirred at rt for 3h. The solvent was removed under reduced pressure and the product was purified with CombiFlash *Sep®Rf* or Biotage Isolera One automated flash column chromatography (A:H_2O and B: ACN) by using C18 Redi*Sep®Rf* cartridges obtaining the product as a white solid.

General Cbz deprotection method (*Metod L*)

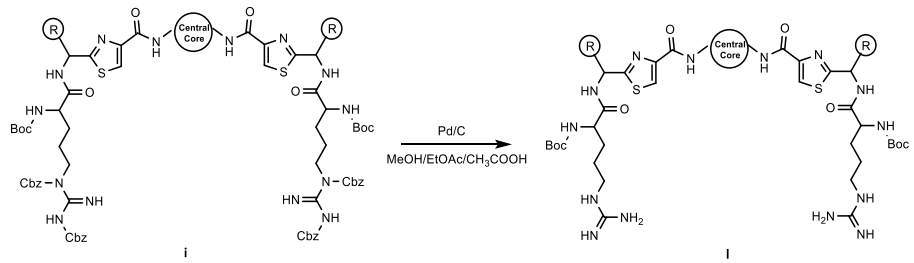

To a solution of i (1 eq.) in MeOH/EtOAc/CH_3COOH was added Pd/C (5eq.). The mixture was stirred under hydrogen atmosphere at rt for 15h. The reaction mixture was filtered in vacuo, then the solvent was removed under reduce pression and the product was purified with CombiFlash *Sep®Rf* or Biotage Isolera One automated flash column chromatography (A:H_2O and B:ACN) by using C18 Redi*Sep®Rf* cartridges obtaining the product as a white solid.

3.5.4. General synthetic procedures

Synthesis of compound 1

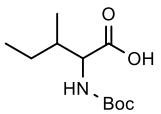

Compound **1** was obtained from DL-isoleucine (2g, 15 mmol, 1eq.) using **Method A**, as a white solid (3.44g, 1.4 mmol, 93% yield).

ESI-MS (m/z): 231.29 $[M+H]^+$.

^1H NMR (600 MHz,$CDCl_3$): δ 9.35(s, 1H), 5.92(s, 1H), 5.03(dd, J=13.6.Hz, 6.0Hz, 1H), 4.39(dd, J=14Hz,J=8.8Hz,1H), 1.95(d, J=8.8Hz,1H), 1.42(s, 9H), 0.95(m, 6H)

Synthesis of compound 2

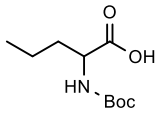

Compound **2** was obtained from DL-norvaline (1g, 8.5 mmol, 1eq.) using **Method A**, as a white solid (1.6g, 7.8 mmol, 92% yield).

ESI-MS (m/z): 217.26 $[M+H]^+$.

^1H NMR (400 MHz,$CDCl_3$): δ 5.07-502(m, 1H), 4.24-4.21(m, 1H), 3.49-3.46(m,1H), 1.82-1.73(m,2H), 1,62-1.59(m, 1H), 1.45(s, 9H), 0.96(q, J=7.9Hz, 3H).

Synthesis of compound 3

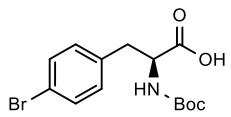

Compound **3** was obtained from L-p-Bromo-Phe-OH (2 g, 8.1 mmol, 1eq.) using **Method A,** as a white solid (2.72g, 7.2mmol, 88% yield).

ESI-MS (m/z): 374.27 $[M+H]^+$.

^1H NMR (400 MHz,$CDCl_3$): δ 7.46(d, J=8.2Hz, 2H), 7.14(d,J=7.8Hz, 2H), 5.06(s,1H), 4.38(s,1H), 3.06-3.03(m,2H), 1.43(s,9H).

Synthesis of compound 4

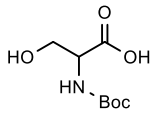

Compound **4** was obtained from DL-serine (0.500g, 4.7 mmol, 1eq.) using **Method A**. The mixture was washed with H_2O and Brine then extracted with EtOAc. The organic solution was dried over Na_2SO_4, the solvent was removed under reduced pressure and the product was purified by flash silica gel column chromatography (DCM/MeOH 99:1+ 0.1% TFA) and obtained as a white solid (0.150 g, 7.8 mmol, 16% yield).

ESI-MS (m/z): 205.21 $[M+H]^+$.

^{1}H NMR (400 MHz,$CDCl_3$): δ 5.41(s, 1H), 4.64-4.60(m, 1H), 4.53-4.49(m,1H), 4.40-4.37(m,2H), 1.48(s, 9H).

Synthesis of compound 5

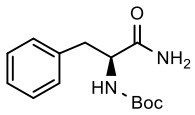

Compound **5** was obtained from Boc-Phe-OH (5.00g, 18.8mmol, 1eq.) using **Method B**, as a white solid (4.98g, 18.8mmol, 99% yield).

ESI-MS (m/z): 264.32 [M+H]+ .

^{1}H NMR (400 MHz,$CDCl_3$): 7.29-7.26(m,4H), 7.21-7.19(m,1H), 7.01(s,1H), 6.82(d,J=8.7Hz,1H), 4.12-4.10(m,1H), 2.98(dd, J=4.4Hz, J=13.7Hz, 1H), 2.76(dd, J=3.6Hz, J=10.2Hz,H1), 1.30(s, 9H).

Synthesis of compound 6

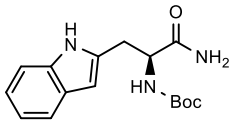

Compound **6** was obtained from Boc-Trp-OH (5.00g, 16.4mmol, 1eq.) using **Method B**, as a white solid (4.78g, 15.7mmol, 98% yield).

ESI-MS (m/z): 303.36$[M+H]^+$.

^{1}H NMR (400 MHz,$CDCl_3$): δ7.13(s,1H),7.73(d,J=8Hz,1H), 7.40(d,J=8Hz,1H), 7.26-7.24(m,4H), 5.75(s,1H), 5.31(s,1H), 4.51(s,1H), 3.36-3.33(m, 2H), 1.45(s, 9H)

Synthesis of compound 7

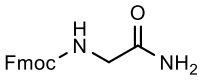

Compound **7** was obtained from Fmoc-Gly-OH (0.500 g, 1.68 mmol, 1eq.) using **Method B**, as a white solid (0.280 g, 0.94 mmol, 56% yield).

ESI-MS (m/z): 297.31$[M+H]^+$.

^{1}H NMR (400 MHz,DMSO-d_6): δ 7.91(d, J=8Hz,2H), 7.73(d,J=8Hz,2H), 7.45-7.43(m,2H), 7.35-7.30(m,2H), 4.30(d,J=8,2H), 2.25-2.23(m,1H), 3.56(d, J=4Hz,2H).

Synthesis of compound 8

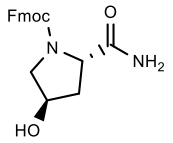

Compound **8** was obtained from Fmoc-Hpy-OH (0.500 g, 1.41 mmol, 1eq.) using **Method B**, as a white solid (0.266 g, 0.75 mmol, 53% yield).

ESI-MS (m/z): 353.37$[M+H]^+$.

^{1}H NMR (400 MHz,DMSO-d_6):δ 7.92(t, J=6.8Hz,2H),7.69(t,J=6.4Hz,2H),7.45-7.40(m,2H),7.36-7.30(m,2H),7.09(s,1H),6.92(s,1H),5.15(s,1H),4.31(s,1H), 4.23(m,2H), 3.53(m,2H), 2.30(m,1H), 2.07(m,1H).

Synthesis of compound 9

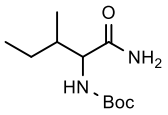

Compound **9** was obtained from compound **1** (0.375 g, 1.62 mmol, 1eq.) using **Method B**, as a white solid (0.340 g, 1.47 mmol, 91% yield).

ESI-MS (m/z): 230.31$[M+H]^+$.

^{1}H NMR (400 MHz,$CDCl_3$):δ 6.07(s,1H), 5.64(s,,1H), 5.07(m,1H), 4.18(m,1H), 1.98(m,1H), 1.46(s,9H), 0.99-0.95(m,6H).

Synthesis of compound 10

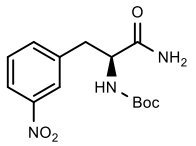

Compound **10** was obtained from Boc-Phe($3NO_2$)-OH (0.300 g, 0.967 mmol, 1eq.) using **Method B**, as a white solid (0.287 g, 0.927 mmol, 96% yield).

ESI-MS (m/z): 309.32$[M+H]^+$.

^{1}HNMR(400MHz,DMSO-d_6): δ8.20(s,1H),8.10(d,J=4Hz,1H),7.61(t,J=8Hz,1H), 7.45(s,1H),7.07(s,1H),6.95(d,J=8Hz,1H),6.49(s,1H),4.174.14(m,1H),3.14(dd,J= 4Hz,J=13.6Hz),2.89(dd,J=4H,J=12Hz,2H), 1.26(s,9H).

Synthesis of compound 11

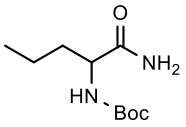

Compound **11** was obtained from compound **2** (3g, 14.0 mmol, 1eq.) using **Method B**, as a white solid (1.6g, 7.8 mmol, 92% yield). The mixture was washed with $KHSO_4$ 1M and Brine then extracted with EtOAc. The organic solution was dried over Na_2SO_4, the solvent was removed under reduced pressure and the product was purified by flash silica gel column chromatography (DCM/MeOH 98:2, 97:3, 96:4) and obtained as a white solid (0.204 g, 0.94 mmol, 20% yield).

ESI-MS (m/z): 216.28 $[M+H]^+$.

^{1}H NMR (400MHz,$CDCl_3$):δ6.17(s,1H),5.59(s,1H), 5.04(s,1H),4.14(s,1H),1.87-1.85(m,1H),1.65-1.64(m,1H),1.46(s,9H),1.43-1.42(m,2H),0.98(t,J=7.2Hz,3H).

Synthesis of compound 12

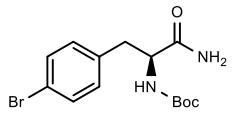

Compound **12** was obtained from compound **3** (2.7 g, 7.2mmol, 1eq.) using **Method B**, as a white solid (2.25 g, 6 mmol, 83% yield).

ESI-MS (m/z): 372.29 $[M+H]^+$.

^{1}HNMR(400MHz,$CDCl_3$):δ7.46(d,J=8.4Hz2H),7.14(d,J=8Hz,2H),5.91(s,1H),5.50(s,1H),4.37(s,1H),3.06(d,J=6.8Hz,2H),1.43(s,9H).

Synthesis of compound 13

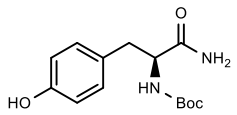

Compound **13** was obtained from Boc-tyr-OH (1 g, 3.5 mmol, 1eq.) using **Method B**, as a white solid (0.715g, 2.5 mmol, 71% yield).

ESI-MS (m/z): 280.32 $[M+H]^+$.

^{1}HNMR(400MHz,DMSO-d_6):δ7.38(s,1H),7.30(d,J=8.3Hz,1H),7.13 (d,J=6.7Hz1H),7.00(s,1H),6.82(d,J=8.7Hz,1H),4.11-4.09(m,1H),2.98 (dd,J=4.4Hz,J=9.4Hz,1H),2.77(dd,J=3.6Hz,J=10.2Hz,1H), 1.30(s,9H).

Synthesis of compound 14

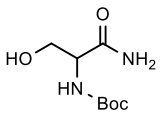

Compound **14** was obtained from compound **4** (0.500 g, 2.4 mmol, 1eq.) using **Method B**, as a with solid (0.354 g, 1.7 mmol, 71% yield).

ESI-MS (m/z): 280.39 $[M+H]^+$.

^{1}H NMR (400 MHz,$CDCl_3$):δ 6.52(s,1H),6.21(s,1H),5.56(d,J=7.6Hz,1H),4.47-4.44(m,2H),4.25-4.23(m,1H),1.45(s,9H).

Synthesis of compound 15

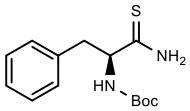

Compound **15** was obtained from compound **5** (5 g, 19.0 mmol, 1eq.) using **Method C**, as a green pale solid (3.5 g, 12.4 mmol, 65% yield).

ESI-MS (m/z): 280.39 $[M+H]^+$.

^{1}HNMR(400MHz,$CDCl_3$):δ7.59(s,1H),7.49(s,1H),7.31-7.25(m,5H),5.41(s,1H), 4.72-4.65(m,1H),3.16-3.10(m, 2H),1.41(s, 9H).

Synthesis of compound 16

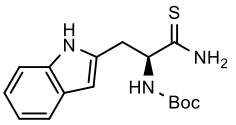

Compound **16** was obtained from compound **6** (3 g, 9.88 mmol, 1eq.) using **Method C**, as a green pale solid (1.6 g, 5 mmol, 51% yield).

ESI-MS (m/z): 319.42 $[M+H]^+$.

^{1}HNMR(400MHz,$CDCl_3$):δ7.76(d,J=7.0Hz,1H),7.39(d,J=7.8Hz,2H),7.24-7.20(m,1H),7.17-7.13(m,2H),7.11(d,J=2.2Hz,1H),5.45(s,1H),3.40-3.29-3.26 (m,2H),1.43(s,9H).

Synthesis of compound 17

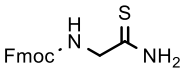

Compound **17** was obtained from compound **7** (0.278 g, 0.935 mmol, 1eq.) using **Method C**, as a green pale solid (0.182 g, 0.614 mmol, 66% yield).

ESI-MS (m/z): 296.32 $[M+H]^+$.

^{1}HNMR(400MHz,DMSO-d_6):δ 9.69 (s,1H), 9.05 (s,1H),7.91 (d,J=7.5Hz,2H), 7.74(d,J=7.4Hz,2H),7.64(t,J=6.1Hz,1H),7.44(t,J=7.5Hz,2H),7.44(t,J=6.3Hz,2H, 4.31(d,J=7.5Hz,2H), 7.44 (t,J=6.7Hz,1H), 3.90 (d,J=6.1Hz,2H).

Synthesis of compound 18

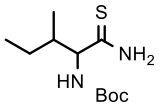

Compound **18** was obtained from compound **9** (1.44 g, 6.2 mmol, 1eq.) using **Method C**, as a green pale solid (0.704 g, 2.8 mmol, 66% yield).

ESI-MS (m/z): 246.37 $[M+H]^+$.

^{1}HNMR(400 MHz,$CDCl_3$): δ 7.72(s, 1H), 7.58 (s,,1H), 5.22-5.13 (m,1H), 4.36-4.18(m,1H),2.18-1.77(m,2H),1.46(s,9H),0.99(t,J=7.0Hz,3H),0.93 (t,J=7.4Hz,3H).

Synthesis of compound 19

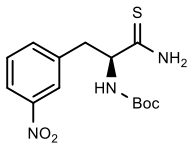

Compound **19** was obtained from compound **10** (1.37 g, 4.4 mmol, 1eq.) using **Method C**, as a yellow/green pale solid (0.900 g, 2.7 mmol, 61% yield).

ESI-MS (m/z): 325.38 $[M+H]^+$.

^{1}H NMR(400MHz,DMSO-d_6):δ 8.38 (s, 1H), 8.07 (d,J=7.8Hz,2H), 8.00 (s,1H), 7.60(d,J=7.0Hz,1H), 7.45 (d,J=7.9Hz,1H), 5.79-5.72 (m,1H), 3.13-3.07 (m,1H), 1.27 (s,9H).

Synthesis of compound 20

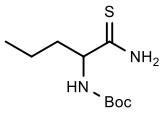

Compound **20** was obtained from compound **11** (2.86 g, 4.4 mmol, 1eq.) using **Method C**, as a yellow/green pale solid (1.7 g, 7.3 mmol, 56% yield).

ESI-MS (m/z): 232.34 $[M+H]^+$.

^{1}H NMR (400 MHz,$CDCl_3$): δ 7.87 (s,1H), 7.55 (s,1H), 5.44-5.39 (m,1H), 1.92-1.87(m,1H),1.75-1.69(m,1H),1.46(s,9H),1.42-1.38(m,1H), 0.98 (t,J=7.4Hz,3H).

Synthesis of compound 21

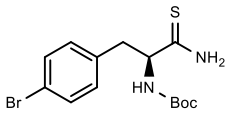

Compound **21** was obtained from compound **12** (0.104 g, 0.270 mmol, 1eq.) using **Method C**, as a yellow/green pale solid (0.049 g, 1.30 mmol, 48% yield).

ESI-MS (m/z): 360.27 $[M+H]^+$.

^{1}H NMR (400 MHz,$CDCl_3$): δ 7.45 (d, J=8.3Hz 2H), 7.39 (s,1H), 7.15 (d, J=8.4Hz, 2H), 4.62-4.57 (m,1H), 3.14 (d,J=7.2Hz,2H), 1.42 (s,9H).

Synthesis of compound 22

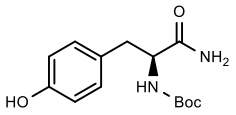

Compound **22** was obtained from compound **13** (0.949 g, 3.4 mmol, 1eq.) using **Method C**, as a white solid (0.235 g, 0.792 mmol, 23% yield).

ESI-MS (m/z): 296.38 $[M+H]^+$.

^{1}HNMR(400MHz,DMSO-d_6):δ9.14(s,1H),7.03(d,J=8.1Hz,2H),6.65 (d,J=8.4Hz,2),4.01-3.98(m,1H),2.28 (dd, J=4.6,J=9.3,1H), 1.31 (s,9H).

Synthesis of compound 23

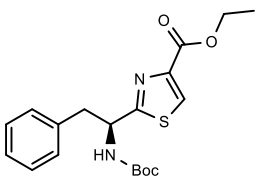

Compound **23** was obtained from compound **15** (1 g, 3.57 mmol, 1eq.) using **Method D**, as a yellow solid (0.860 g, 2.28 mmol, 64% yield).

ESI-MS (m/z): 376.47 $[M+H]^+$.

^{1}H NMR (400 MHz,$CDCl_3$): δ 8.06(s,1H), 7.31-7.24 (m,3H), 7.14-7.11 (m,2H), 5.30 (s, 1H), 4.48 (q, J=7.1 Hz,2H), 3.40 (d, J=6 Hz ,2H)., 1.41 (s, 9H)

Synthesis of compound 24

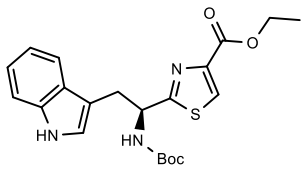

Compound **24** was obtained from compound **16** (2.65 g, 8.30 mmol, 1eq.) using **Method D**, as a orange solid (2.2 g, 5.20 mmol, 63% yield).

ESI-MS (m/z): 417.52 $[M+H]^+$.

^{1}HNMR(400MHz,$CDCl_3$): δ8.03(s,1H),7.51(d,J=7.9Hz,1H),7.37 (d,J=8Hz,1H), 7.22 (t,J=5.8 Hz, 1H), 7.12 (t,J=6.9Hz, 1H),5.41 (s, 1H), 4.48 (q, J=7.1 Hz,2H), 3.40 (d, J=6 Hz ,2H)., 1.41 (s, 9H).

Synthesis of compound 25

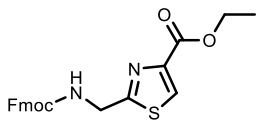

Compound **25** was obtained from compound **17** (0.180 g, 0.607 mmol, 1eq.) using **Method D**, as a yellow solid (0.060 g, 0.142 mmol, 23% yield).

ESI-MS (m/z): 422.49 $[M+H]^+$.

^{1}H NMR(600MHz,$CDCl_3$):δ8.11(s,1H),7.75(d,J=6.6Hz,1H),7.58(d,J=7.8Hz,1H, 7.40 (t,J=7.2 Hz, 1H), 7.30 (t,J=7.2Hz, 1H), 5.58 (s, 1H), 4.71 (d, J=6.3 Hz,2H), 4.46 (d, J=6.9 Hz ,2H)., 4.43 (q, J=7.1Hz ,2H)., 4.22 (t,J=7.2Hz, 1H), 1.40 (t,J=7.2Hz, 3H).

Synthesis of compound 26

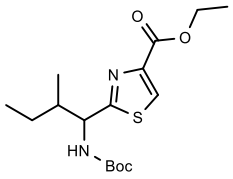

Compound **26** was obtained from compound **18** (0.700 g, 2.8 mmol, 1eq.) using **Method D**, as a yellow solid (0.452 g, 1.3 mmol, 46% yield).

ESI-MS (m/z): 342.45 $[M+H]^+$.

^{1}H NMR (400 MHz,$CDCl_3$): δ9.14(s,1H),7.77(s,1H),4.39 (m,2H), 2.53 (q,J=7.2 Hz, 1H), 1.28 (s, 9H), 1.29 (d,J=6.8 Hz, 1H),1.00 (m, 3H), 0.94 (t, J=7.3 Hz,6H).

Synthesis of compound 27

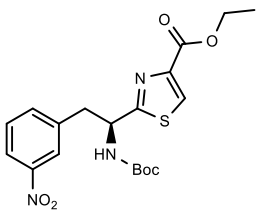

Compound **27** was obtained from compound **19** (0.481 g, 1.4 mmol, 1eq.) using **Method D**, as a yellow solid (0.261 g, 0.610mmol, 43% yield).

ESI-MS (m/z): 421.46 $[M+H]^+$.

^{1}HNMR(400MHz,$CDCl_3$):δ8.12(d,J=6.1Hz,2H), 8.06 (s,1H), 7.54 (d,J=8.9,1H), 7.48 (t,J=7.5 Hz, 1H), 5.34 (s, 1H), 4.48 (q,J=6.8 Hz, 1H), 3.59-3.54 (m, 1H), 3.40-3.35 (m, 1H), 1.45 (t, J=7.4 Hz,6H), 1.40 (s, 9H).

Synthesis of compound 28

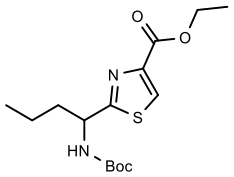

Compound **28** was obtained from compound **20** (0.166 g, 0.710 mmol, 1eq.) using **Method D**, as a yellow solid (0.085 g, 0.258 mmol, 38% yield).

ESI-MS (m/z): 328.42 $[M+H]^+$.

^{1}HNMR(600MHz,$CDCl_3$): δ 8.04 (s,1H), 5.21 (s,1H), 4.99 (s,1H), 4.40 (q, J=7.1 Hz, 1H), 2.08 (s, 1H), 1.79-1.73 (m, 2H), 1.41 (s, 9H), 1.38 (t, J=7.1 Hz,6H), 0.93 (t, J=7.3 Hz,6H).

Synthesis of compound 29

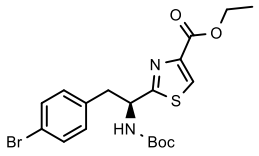

Compound **29** was obtained from compound **21** (0.049 g, 0.130 mmol, 1eq.) using **Method D**, as a yellow solid (0.023 g, 0.05 mmol, 38% yield).

ESI-MS (m/z): 457.38 $[M+H]^+$.

^{1}HNMR(400 MHz,CD_3OD): δ 8.32 (s,1H), 7.46 (d,J=8.3Hz,2H), 7.24-7.20 (m, 2H), 5.58 (q,J=5.7 Hz,1H), 4.44 (q, J=7.2Hz,2H), 3.57 (dd,J=5.8 Hz, 13.9 Hz, 1H), 3.48 (dd,J=4.8 Hz,13.8Hz, 1H), 1.43 (t, J=7.1 Hz,6H), 1.38 (s, 9H).

Synthesis of compound 30

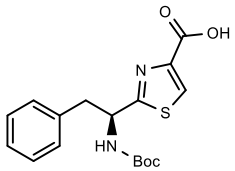

Compound **30** was obtained from compound **23** (0.160 g, 0.400 mmol, 1eq.) using **Method E**, as a white solid (0.140 g, 0.425 mmol, 94% yield).

ESI-MS (m/z): 348.41 $[M+H]^+$.

^{1}H NMR (400 MHz, DMSO-d_6): δ 13.0 (s,1H), 8.36 (s,1H), 7.31-7.30 (m, 2H), 7.24-7.21 (m, 1H), 5.02-4.96 (m,1H), 3.41 (q, J=7.0, 1H), 3.03-2.97 (m,1H), 1.31 (s, 9H).

Synthesis of compound 31

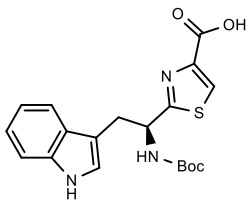

Compound **31** was obtained from compound **24** (0.200 g, 0.479 mmol, 1eq.) using **Method E**, as a yellow solid (0.171 g, 0.441 mmol, 92% yield).

ESI-MS (m/z): 387.45 $[M+H]^+$.

^{1}HNMR(400MHz,$CDCl_3$):δ8.12(s,1H),7.70(d,J=7.9Hz,1H),7.41(d,J=7.9Hz,1H, 7.24-7.21 (m, 2H), 7.16-7.09 (m, 1H), 4.77-4.74 (m,1H), 4.49 (q, J=7.1Hz, 2H),3.56-3.47 (m, 1H), 3.13-3.07 (m,1H), 1.46 (t,J=7.1,3H), 1.45 (s, 9H).

Synthesis of compound 32

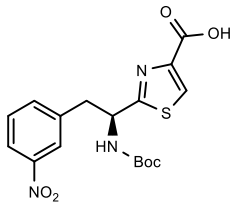

Compound **32** was obtained from compound **27** (0.211g, 0.520 mmol, 1eq.) using **Method E**, as a yellow solid (0.177 g, 0.450 mmol, 86% yield).

ESI-MS (m/z): 393.41 $[M+H]^+$.

^{1}HNMR(400 MHz,$CDCl_3$): δ 8.24 (s,1H), 8.14-8.07 (m, 2H), 7.55-7.48 (m, 1H), 5.40-5.36 (m,1H), 3.60-3.54 (m,1H), 3.52-3.38 (m, 1H), 1.40 (s, 9H).

Synthesis of compound 33

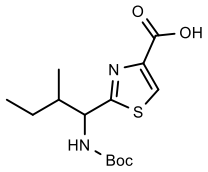

Compound **33** was obtained from compound **26** (0.024 g, 0.073 mmol, 1eq.) using **Method D**, as a yellow solid (0.020 g, 0.066 mmol, 90% yield).

ESI-MS (m/z): 300.11 $[M+H]^+$.

^{1}HNMR(400MHz,$CDCl_3$): δ 8.21 (s,1H), 5.29-5.27 (m, 1H), 5.04-5.02 (m, 1H), 2.09-2.03 (m,1H), 1.85-1.79 (m,1H),1.45 (s, 9H).

Synthesis of compound 34

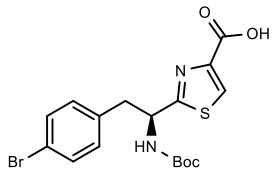

Compound **34** was obtained from compound **29** (0,090g, 0.198 mmol, 1eq.) using **Method D**, as a white solid (0,048g, 0.113mmol, 57% yield).

ESI-MS (m/z):426.02 $[M+H]^+$.

^{1}HNMR(400 MHz, DMSO-d_6): δ 8.24 (s,1H), 7.49-7.47 (m, 2H), 7.30-7.27 (m, 1H), 5.01-4.96 (m,1H), 3.22-3.16 (m,1H), 2.98-2.92 (m, 1H), 1.30 (s, 9H).

Synthesis of compound 35

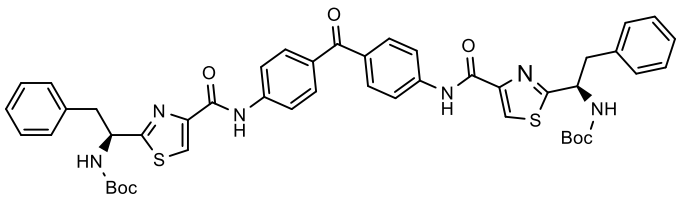

Compound **35** was obtained from compound **30** (0.500 g, 1.43 mmol, 2 eq.) through **Method F**, using as central core 4-4' diamminobenzophenone (1eq). It was purified by flash silica gel column chromatography (Esane/EtOAc 6:4) obtaining the product as a yellow solid (0.522 g, 0.597 mmol, 42% yield).

ESI-MS (m/z): 873.05 $[M+H]^+$.

^{1}HNMR(400MHz,$CDCl_3$):δ 9.33 (s,2H), 8.16 (s, 2H), 7.91-7.86 (m, 8H), 7.34-7.30 (m,6H), 7.16-7.14 (m,4H), 5.36-5.23 (m, 2H), 3.36-3.32 (m, 2H), 1.45 (s, 18H).

Synthesis of compound 36

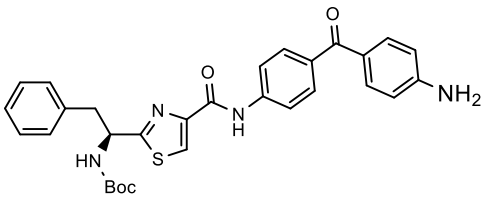

Compound **36** was obtained from compound **30** (0.200 g, 0.574 mmol, 1 eq.) through **Method F_bis**, using as central core 4-4' diaminobenzophenone (1eq). It was purified by flash silica gel column chromatography (EP/EtOAc 5:5) obtaining the product as a yellow solid (0.250 g, 0.461 mmol, 80% yield).

ESI-MS (m/z): 542.19 $[M+H]^+$.

^{1}H NMR (400 MHz,$CDCl_3$): δ 9.28 (s,2H), 8.16 (s, 1H), 7.84 (s, 4H), 7.76 (d, J=8.6Hz, 2H), 7.32 (d, J=7.6Hz, 2H), 7.15 (d, J=8.0Hz, 2H), 6.73 (d, J=8.4Hz, 2H), 5.35 (s,1H), 5.17 (s,1H), 3.39-3.34 (m,2H), 1.45 (s, 9H).

Synthesis of compound 37

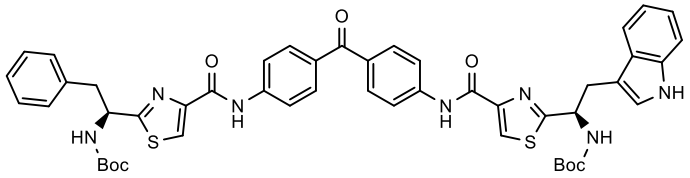

Compound **37** was obtained from compound **31** (0.100 g, 0.258 mmol, 1 eq.) and compound **36** (0.140 g, 0.258 mmol, 1 eq) through **Method F**. It was purified by flash silica gel column chromatography (EP/EtOAc 1:1) obtaining the product as a yellow solid (0.157 g, 0.172 mmol, 67% yield).

ESI-MS (m/z): 912.09 $[M+H]^+$.

^{1}HNMR(400MHz,$CDCl_3$): δ 9.36 (s,1H), 9.32 (s,1H), 8.16 (s, 1H), 8.14 (s, 1H), 7.92-7.86 (m, 8H), 7.50 (d, J=7.8Hz, 2H), 7.40 (d, J=8.0Hz, 2H), 7.32-7.31 (m,1H), 7.25-7.21 (m,1H), 7.15-7.13 (m, 4H), 5.44-5.30 (m,4H), 5.53-5.49 (m,2H), 3.39-3.32 (m,2H), 1.46 (s, 18H).

Synthesis of compound 38

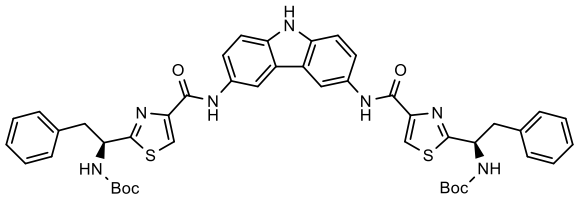

Compound **38** was obtained from compound **30** (0.626 g, 1.70 mmol, 2 eq.) through **Method F**, using as central core 9H-carbazole-3,6-diamine (1eq). It was purified by flash silica gel column chromatography (DCM/MeOH 98:2) obtaining the product as a yellow solid (0.349 g, 0.406 mmol, 40% yield).

ESI-MS (m/z): 858.24 $[M+H]^+$.

^{1}H NMR (400 MHz,$CDCl_3$): δ 9.25 (s,2H), 8.37 (s,2H), 8.16 (s, 2H), 8.08 (s, 1H), 7.72-7.70 (m, 1H), 7.41 (d, J=8.6Hz, 2H), 7.32-7.25 (m,5H), 7.17-7.15 (m,5H), 5.44-5.34 (m,4H), 3.68-3.63 (m,2H), 3.42-3.39 (m,2H), 1.40 (s, 18H).

Synthesis of compound 39

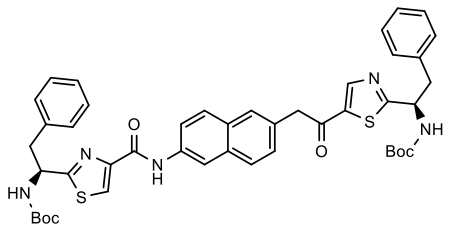

Compound **39** was obtained from compound **30** (0.500 g, 1.43 mmol, 2 eq.) through **Method F**, using as central core naphthalene-2,6-diamine (1eq). It was purified by flash silica gel column chromatography (DCM/MeOH 99:1) obtaining the product as a yellow solid (0.171 g, 0.208 mmol, 29% yield).

ESI-MS (m/z): 819.00 $[M+H]^+$.

^{1}HNMR(400MHz,$CDCl_3$):δ9.28(s,2H),8.44(s,2H),8.16 (s, 2H), 7.69(d,J=7.9Hz, 2H), 7.67 (d, J=8.0Hz, 2H), 7.35-7.32 (m,5H), 7.17-7.15 (m,5H), 5.37-5.21 (m,2H), 3.40-3.35 (m,4H), 1.45 (s, 18H).

Synthesis of compound 40

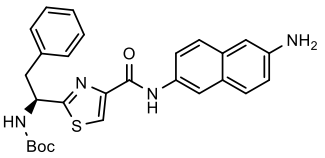

Compound **40** was obtained from compound **30** (0.097 g, 0.279 mmol, 1 eq.) through **Method F_bis**, using as central core naphthalene-2,6-diamine (6eq). It was purified by flash silica gel column chromatography (EP/EtOAc 5:5) obtaining the product as a yellow solid (0.250 g, 0.153 mmol, 55% yield).

ESI-MS (m/z): 488.60 $[M+H]^+$.

^{1}HNMR(400MHz,$CDCl_3$): δ 9.18 (s,1H), 8.28 (s,1H), 8.12 (s, 1H), 7.70 (d,J=8.4Hz, 2H), 7.64 (q, J=8.8Hz, 2H), 7.33-7.26 (m,4H), 7.15 (d,J=7.2Hz, 2H), 7.00 (d,J=8.8Hz, 2H), 5.35 (s,1H), 5.20 (s,1H),3.85 (s,2H), 3.40-3.35 (m,2H), 1.52 (s, 9H).

Synthesis of compound 41

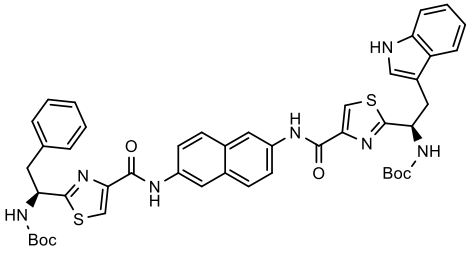

Compound **41** was obtained through a modified **Method F**. To a solution of compound **30** (0.078 g, 0.20 mmol, 1 eq.) in $DMF_{dry,}$ under a nitrogen atmosphere at rt were added HATU (0.091 g, 0.24 mmol, 1.2 eq.) and DIPEA (0.174 mL, 1 mmol, 5 eq.). The mixture was stirred at rt for 10 min.

To a solution of **31** (0.078 g, 0.20 mmol, 1 eq.) in $DMF_{dry,}$ under a nitrogen atmosphere at rt were added HATU (0.091 g, 0.24 mmol, 1.2 eq.) and DIPEA (0.174 mL, 1 mmol, 5 eq.). The mixture was stirred at rt for 10 min.

The two activated acidic solutions were then mixed together and added to a solution of naphthalene-2,6-diamine (0.095 g, 0.60 mmol, 3 eq.) in $DMF_{dry,}$ .The reaction mixture was then stirred at rt for 1h. The mixture was washed with H_2O then extracted with EtOAc. The organic solution was dried over Na_2SO_4, the solvent was removed under reduced pressure and the product was purified by flash silica gel column chromatography (DCM/MeOH 99:1) obtaining the product as a brown solid. (0.042g, 0.048 mmol, 42% yield).

ESI-MS (m/z): 857.30 $[M+H]^+$.

^{1}HNMR(400MHz,$CDCl_3$): δ 9.28 (s,2H), 8.44 (s,1H), 8.16 (s, 2H), 7.89 (d,J=8.8Hz, 2H), 7.68-7.66 (m,3H), 7.41-7.39 (m,1H), 7.34-7.30 (m, 3H), 7.25-7.21 (m, 1H), 7.16-7.12 (m,1H), 5.36-5.32 (m,4H), 3.54-3.51 (m,2H), 3.38-3.36 (m,2H), 1.46 (s, 18H).

Synthesis of compound 42

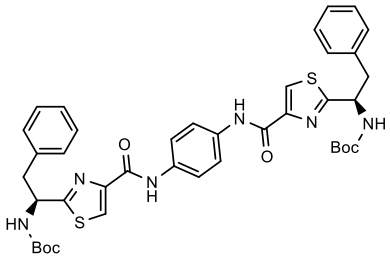

Compound **42** was obtained from compound **30** (0.340 g, 0.976 mmol, 2 eq.) through **Method F**, using as central core benzene-1,4-diamine (1eq). It was purified by flash silica gel column chromatography (EP/EtOAc 6:4) obtaining the product as a yellow solid (0.330 g, 0.428 mmol, 44% yield).

ESI-MS (m/z): 770.29 $[M+H]^+$.

^{1}HNMR(400MHz,$CDCl_3$): δ 9.17 (s,2H), 8.12 (s,1H), 7.78 (s, 4H), 7.32-7.29 (m,6H), 7.15-7.13 (m,4H), 7.36 (s, 1H), 7.24 (s, 1H), 3.36-3.32 (m,4H), 2.40-2.38 (m,2H), 1.45 (s, 18H).

Synthesis of compound 43

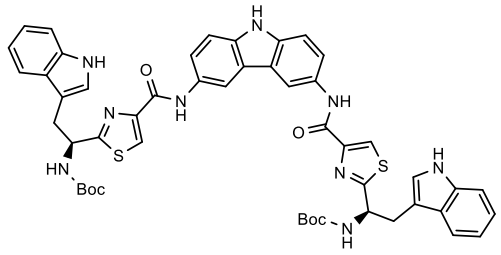

Compound **43** was obtained from compound **31** (0.340 g, 0.976 mmol, 2 eq.) through **Method F**, using as central core 9H-carbazole-3,6-diamine (1eq). It was purified by flash silica gel column chromatography (DCM/MeOH 98:2) obtaining the product as a yellow solid (0.098 g, 0.104 mmol, 27% yield).

ESI-MS (m/z): 936.11 $[M+H]^+$.

^{1}HNMR(400MHz,$CDCl_3$): δ 9.23 (s,2H), 8.38 (s,2H), 7.69 (d,J=8.8 Hz, 2H), 7.54 (d,J=8.4 Hz, 2H), 7.40-7.34 (m,4H), 7.22-7.20 (m,2H), 7.12-7.10 (m,2H), 6.87 (s,2H),3.70-3.64 (m,2H), 3.16 (q,J=7.2 Hz, 2H), 1.46 (s, 18H).

Synthesis of compound 44

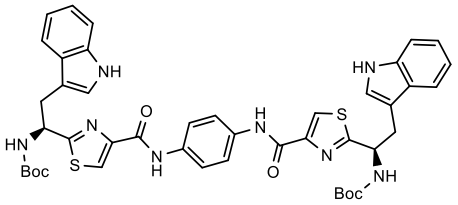

Compound **44** was obtained from compound **31** (0.250 g, 0.645 mmol, 2 eq.) through **Method F**, using as central core benzene-1,4-diamine (1eq). It was purified by flash silica gel column chromatography (DCM/MeOH 98:2) obtaining the product as a yellow solid (0.150 g, 0.177 mmol, 27% yield).

ESI-MS (m/z): 846.70 $[M+H]^+$.

^{1}HNMR(400MHz,$CDCl_3$):δ 9.17 (s,2H), 8.22 (s,2H), 7.77 (s, 4H), 7.51 (d,J=8.0 Hz, 2H), 7.40 (d,J=8.0 Hz, 2H), 7.24-7.20 (m,2H), 7.15-7.11 (m,2H), 6.90 (s,1H), . 5.44 (s,2H),5.32 (s,2H), 3.53-3.52 (m,2H), 1.46 (s, 18H).

Synthesis of compound 45

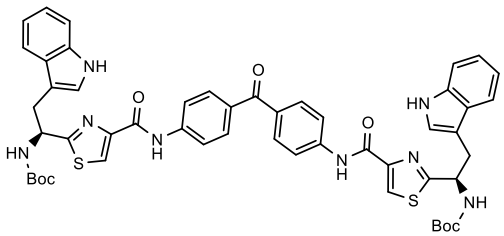

Compound **45** was obtained from compound **31** (0.200 g, 0.516 mmol, 2 eq.) through **Method F**, using as central core 4,4'-diamminobenzophenone (1eq). It was purified by flash silica gel column chromatography (DCM/MeOH 98:2) obtaining the product as a yellow solid (0.150 g, 0.158 mmol, 31% yield).

ESI-MS (m/z): 951.13 $[M+H]^+$.

^{1}HNMR(400MHz,$CDCl_3$): δ 9.37 (s,2H), 8.56 (s,2H), 8.11 (s,2H), 7.89-7.84 (m,6H), 7.49 (d,J=8.0, 2H), 7.38 (d,J=8.0 Hz, 2H), 7.22-7.18 (m,2H), 7.89-7.84 (m,6H), 7.13-7.09 (m,2H),6.90 (s,1H), 5.42 (s,4H), 3.50-3.49 (m,4H), 1.48 (s, 18H).

Synthesis of compound 46

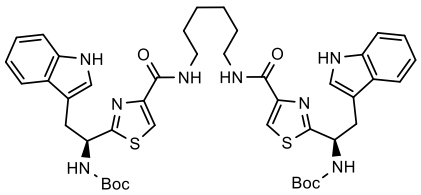

Compound **46** was obtained from compound **30** (0.170 g, 0.490 mmol, 2 eq.) through **Method F**, using as central core hexane-1,6-diamine (1eq). It was purified by flash silica gel column chromatography (DCM/MeOH 98:2) obtaining the product as a yellow solid (0.123 g, 0.144 mmol, 29 % yield).

ESI-MS (m/z): 855.08 $[M+H]^+$.

^{1}HNMR(400MHz,CDCl3): δ 8.15 (s,2H), 7.33-7.22 (m,10H), 5.59 (q,J=5.6 Hz, 2H), 3.63 (q,J=5.6 Hz, 2H), 3.44 (t,J=6.8 Hz,4H), 3.27 (q,J=10 Hz,2H), 1.69-1.65 (m,4H), 1.49-1.47 (m,4H), 1.44 (s,18H)..

Synthesis of compound 47

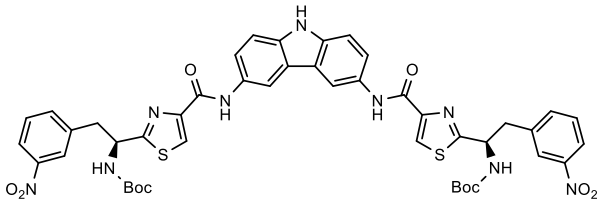

Compound **47** was obtained from compound **32** (0.100 g, 0.25 mmol, 2 eq.) through **Method F**, using as central core 9H-Carbazole-3,6-diamine (1eq). It was purified by flash silica gel column chromatography (EP/Acetone/MeOH 6.9:3:0.1) obtaining the product as a yellow solid (0.094 g, 0.095 mmol, 38% yield).

ESI-MS (m/z): 948.04 $[M+H]^+$.

^{1}HNMR(400 MHz,$CDCl_3$):δ 9.21 (s,2H), 8.30 (s,2H), 8.18-8.14 (m,6H), 7.74-7.72 (m,2H),7.58 (d,J=7.6 Hz, 2H), 7.51-7.49 (m,2H), 7.40 (d,J=8.4 Hz, 2H), 5.62 (s,2H), 3.50-3.60 (m,2H), 3.42-3.36 (m,2H), 1.44 (s, 18H).

Synthesis of compound 48

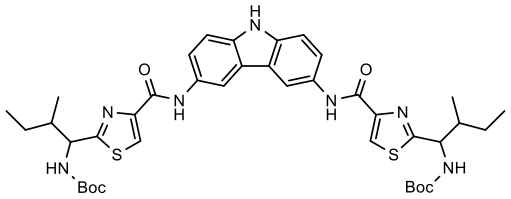

Compound **48** was obtained from compound **26** (0.100 g, 0.314 mmol, 2 eq.) through **Method F**, using as central core 9H- Carbazole-3,6-diamine (1eq). It was purified by flash silica gel column chromatography (EP/Acetone/MeOH 7.4:2.5:0.1) obtaining the product as a yellow solid (0.126 g, 0.150 mmol, 48%yield).

ESI-MS (m/z): 792.03 $[M+H]^+$.

^{1}HNMR(400 MHz,$CDCl_3$):δ 9.27 (s,2H), 8.39 (s,2H), 8.14 (m,2H), 7.80-7.77 (m,2H), 7.43 (d,J=8.8 Hz, 2H), 5.32-5.24 (m,2H), 5.10-4.99 (m,2H), 2.28-2.18 (m,2H), 1.51 (s, 18H), 1.08 (m,12H).

Synthesis of compound 49

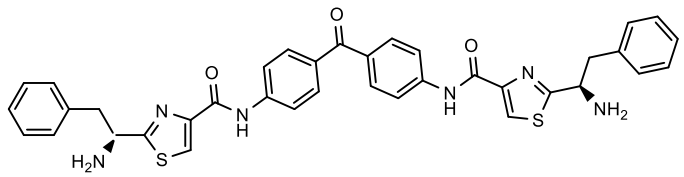

Compound **49** was obtained from compound **35** (0.500 g, 5.7 mmol, 1 eq.) through **Method H** obtaining the product as a yellow solid (0.362 g, 0.5938 mmol, 94% yield).

ESI-MS (m/z): 672.82 $[M+H]^+$.

^{1}HNMR(400 MHz,$CDCl_3$):δ 9.35 (s,2H), 8.20 (s,2H), 7.92-7.89 (m,10H), 4.61 (q,J=4.8, 2H), 4.61 (dd,J=4.4Hz, 13.6Hz,2H), 3.00 (q,J=5.2Hz,2H).

Synthesis of compound 50

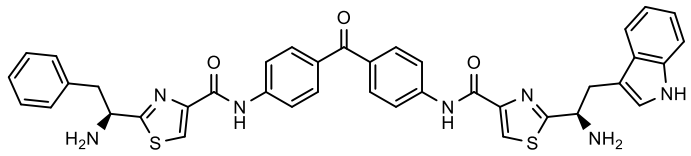

Compound **50** was obtained from compound **37** (0.072 g, 0.079 mmol, 1 eq.) through **Method H**. It was purified by flash silica gel column chromatography (DCM/MeOH 98:2+ 0.2%NH_3) obtaining the product as a yellow solid (0.016 g, 0.024 mmol, 28% yield).

ESI-MS (m/z): 711.86 $[M+H]^+$.

^{1}HNMR(400 MHz,$CDCl_3$):δ 9.42 (s,1H), 9.38 (s,1H), 8.19 (s,2H), 7.90 (s, 8H), 7.43-7.18 (m,10H), 4.73 (q, J=4.8 Hz, 2H)), 4.61 (q,J=4.4 Hz, 2H), 3.58 (dd,J=4.4Hz, 14.4Hz,1H), 3.43 (dd,J=4.8Hz, 13.6Hz,1H), 3.18 (q,J=8.8 Hz, 1H), 3.00 (q, J=9.2 Hz, 1H).

Synthesis of compound 51

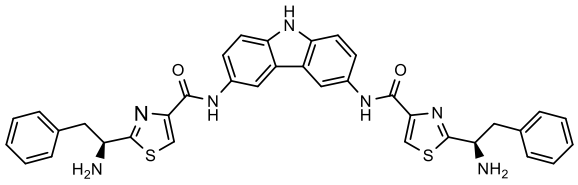

Compound **51** was obtained from compound **38** (0.303 g, 0.318mmol, 1 eq.) through **Method H.** It was purified by flash silica gel column chromatography (DCM/MeOH 98:2+ 0.2%NH_3) obtaining the product as a yellow solid (0.230 g, 0.350 mmol, 97% yield).

ESI-MS (m/z): 657.81$[M+H]^+$.

^{1}HNMR(400MHz,$CDCl_3$):δ 9.33 (s,2H), 8.46 (s,2H), 8.16 (s,2H), 7.81 (dd,J=8.4 Hz, 8.8Hz,1H), 7.45-7.30 (m,10H), 4.62 (q, J=4.4 2H), 3.49 (dd,J=13.6Hz,9.2Hz,1H),3.00(q,J=8.8,1H).

Synthesis of compound 52

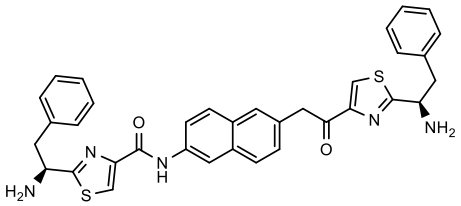

Compound **52** was obtained from compound **39** (0.283 g, 0.346 mmol, 1 eq.) through **Method H** obtaining the product as a yellow solid (0.114 g, 0.184 mmol, 67% yield).

ESI-MS (m/z): 618.77 $[M+H]^+$.

^{1}HNMR(400 MHz,$CDCl_3$):δ 9.33 (s,2H), 8.46 (s,2H), 8.19 (s,2H), 7.88 (d,J=8.8 Hz, 2H), 7.68 (dd,J=8.8 Hz, 8.8Hz,2H),7.40-7.30 (m,10H), 4.61 (q, J=4.4 2H), 3.49 (dd,J=13.6Hz, 13.6Hz,1H), 3.00 (q, J=9.2, 1H).

Synthesis of compound 53

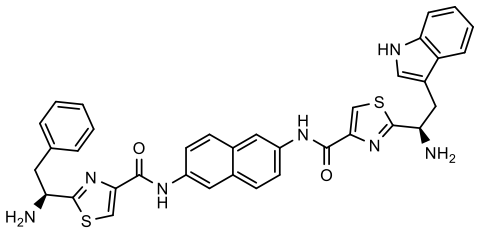

Compound **53** was obtained from compound **41** (0.056 g, 0.653 mmol, 1 eq.) through **Method H**. It was purified by flash silica gel column chromatography (DCM/MeOH 98:2) obtaining the product as a brown solid. (0.018g, 0.027 mmol, 41% yield).

ESI-MS (m/z): 657.81 $[M+H]^+$.

^{1}HNMR(400MHz,$CDCl_3$):δ 9.38 (s,1H), 9.33 (s,1H), 8.46 (s,2H), 8.19 (s,2H), 7.89 (d,J=8.8 Hz, 2H), 7.73-7.66 (m,2H), 7.45-7.18 (m,10H), 4.75 (q, J=4.4 1H), 4.62 (q, J=4.4 1H), 3.60 (dd,J=14.4Hz, 14.4Hz,1H), 3.46 (dd,J=13.6Hz, 13.6 Hz,1H), 3.20 (q, J=8.8, 1H), 3.01 (q, J=8.8, 1H).

Synthesis of compound 54

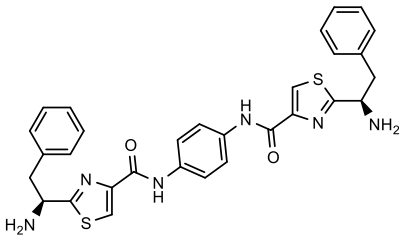

Compound **54** was obtained from compound **42** (0.324 g, 0.421 mmol, 1 eq.) through **Method H** obtaining the product as a white solid (0.230 g, 0.408 mmol, 97% yield).

ESI-MS (m/z): 570.18 $[M+H]^+$.

^{1}HNMR(400MHz,DMSO-d_6):δ 10.04 (s,2H), 8.29 (s,1H), 7.81 (s,4H), 7.34-7.21 (m,10H), 4.47 (q, J=4.4 2H), 2.37-2.33 (m,2H).

Synthesis of compound 55

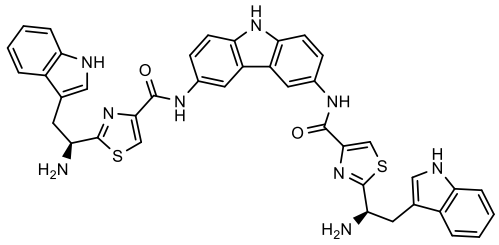

Compound **55** was obtained from compound **43** (0.156 g, 0.167 mmol, 1 eq.) through **Method H.** It was purified by flash silica gel column chromatography (DCM/MeOH 98:2+ 0.2%NH_3) obtaining the product as a white solid (0.020 g, 0.0214 mmol, 78% yield).

ESI-MS (m/z): 936.11 $[M+H]^+$.

^{1}HNMR(400MHz,MeOD):δ 8.46 (s,2H), 8.19 (s,2H), 7.70 (d,J=8.8 Hz, 2H), 7.56 (d,J=8.0 Hz, 2H), 7.49 (d,J=8.0 Hz, 2H), 7.38 (d,J=7.9 Hz,2H), 4.70 (t,J=7.1 Hz,2H), 3.47 (d,J=7.4 Hz,2H).

Synthesis of compound 56

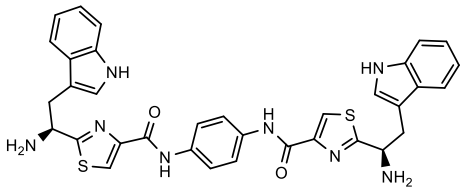

Compound **56** was obtained from compound **44** (0.133 g, 0.20 mmol, 1 eq.) through **Method H** obtaining the product as a yellow solid (0.102 g, 0.158 mmol, 79% yield).

ESI-MS (m/z): 646.78 $[M+H]^+$.

^{1}HNMR(400 MHz,CD_3OD): δ 8.19 (s,2H), 7.79 (s,4H), 7.53 (d,J=7.8 Hz, 2H), 7.37 (d,J=8.0 Hz, 2H), 7.13-6.99 (m,8H) (d,J=7.9 Hz,2H), 4.73 (t,J=6.8 Hz,2H), 3.43 (d,J=8.0 Hz,2H). 3.29 (d,J=8.0 Hz,2H).

Synthesis of compound 57

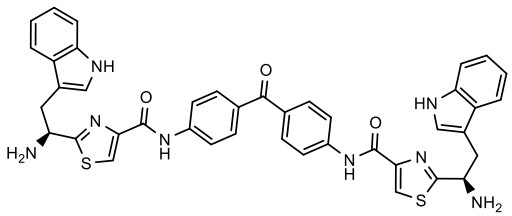

Compound **57** was obtained from compound **45** (0.150 g, 0.160 mmol, 1 eq.) through **Method H**. It was purified by flash silica gel column chromatography (DCM/MeOH 98:2+0.2% NH_3) obtaining the product as a yellow solid (0.035 g, 0.050 mmol, 31% yield).

ESI-MS (m/z): 696.20 $[M+H]^+$.

^{1}HNMR(400MHz,CD_3OD):δ 8.24 (s,2H), 7.97 (d,J=8.8 Hz, 2H), 7.91 (s,8H) 7.87 (d,J=8.8 Hz, 2H),7.53 (d,J=7.9 Hz,2H), 7.37 (d,J=8 Hz,2H), 7.12-7.08 (m,4H) 7.03-6.99 (m,2H) 4.71 (t,J=6.4 Hz,2H), 3.51(q,J=6.8 Hz,2H). 3.26 (q,J=8.0 Hz,2H).

Synthesis of compound 58

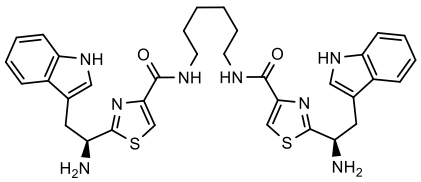

Compound **58** was obtained from compound **46** (0.159 g, 0.20 mmol, 1 eq.) through **Method H.** It was purified by flash silica gel column chromatography (DCM/MeOH 98:2+0.2% NH_3) obtaining the product as a yellow solid (0.063 g, 0.109mmol, 54% yield).

ESI-MS (m/z): 576.78 $[M+H]+$.

^{1}HNMR(400 MHz,CD_3OD): δ 8.15(s,2H), 7.33-7.22 (m,10H), 5.59 (q,J=5.6 Hz, 2H), 3.63 (q,J=5.6 Hz, 2H), 3.44 (t,J=6.8 Hz,4H), 3.27 (q,J=10 Hz,2H), 1.69-1.65 (m,4H), 1.49-1.47 (m,4H).

Synthesis of compound 59

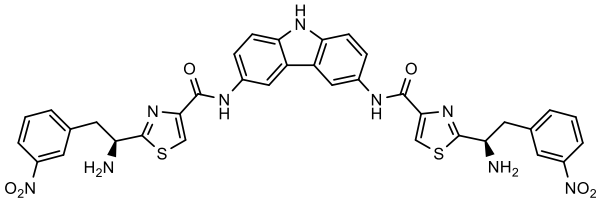

Compound **59** was obtained from compound **47** (0.090 g, 0.095 mmol, 1 eq.) through **Method H** obtaining the product as a yellow solid (0.057 g, 0.076 mmol, 80% yield).

ESI-MS (m/z): 749.82 $[M+H]^+$.

^{1}H NMR (400 MHz,CDCl3): δ 9.30 (s,2H), 8.46 (s,2H), 8.20 (s,2H), 7.84 (dd,J=8.8 Hz, J=8.8 Hz, 2H), 7.60-7.56 (m,6H), 7.48 (d,J=8.8 Hz, 2H), 4.68 (q,J=4.4 Hz, 2H), 3.68-3.66 (m,2H), .3.59 (dd,J=13.6 Hz, 2H), 3.19 (q,J=4.4 Hz, 2H).

Synthesis of compound 60

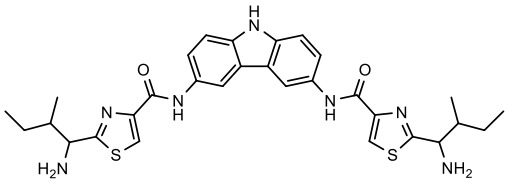

Compound **60** was obtained from compound **48** (0.400 g, 0.05 mmol, 1 eq.) through **method H**. It was purified by flash silica gel column chromatography (DCM/MeOH 98:2+0.2% NH_3) obtaining the product as a white solid (0.185 g, 0.320 mmol, 64% yield).

ESI-MS (m/z): 578.79 $[M+H]^+$

^{1}H NMR (400 MHz,CDCl3): δ 9.34 (s,2H), 8.44 (s,2H), 8.18(s,2H), 7.82-7.78 (m,2H), 7.45 (d,J=8.0 Hz, 2H), 4.32 (d,J=7.9 Hz, 2H), 4.27(d,J=4.4 Hz, 2H), 2.19-2.15(m,2H), 2.08-2.02. (m,2H), 1.40-1.37. (m,2H),1.33-1.28 (m,2H), 1.09-0.98 (m,12H).

Synthesis of compound 61

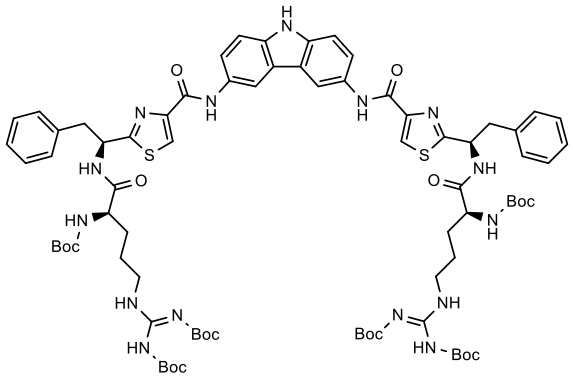

Compound **61** was obtained from compound **51** (0.105 g, 0.160 mmol, 1 eq.) through **Method G**. It was purified by flash silica gel column chromatography (DCM/MeOH 99.7:0.3) obtaining the product as a white solid (0.110 g, 0.070 mmol, 44% yield).

ESI-MS (m/z): 1572.90 $[M+H]^+$ 787.45

^{1}HNMR(400MHz,CDCl3):δ 9.29 (s,2H), 8.49 (s,2H), 8.13 (s,2H), 7.77-7.73 (m,2H), 7.59 (d,J=8.0 Hz, 2H), 7.45 (d,J=7.9 Hz, 2H), 7.31-7.18(m,10H), 6.07(s,1H), 5.79(s,1H), 3.64-3.59 (m,4H), 3.38-3.32 (m,2H), 1.80-1.72 (m,8H), 1.33-1.12(m,2H),1.46-1.42(m,54H)

Synthesis of compound 62

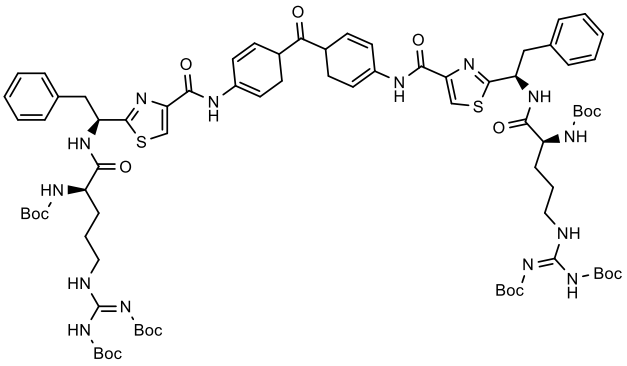

Compound **62** was obtained from compound **49** (0.200 g, 0.290 mmol, 1 eq.) through **Method G**. It was purified by flash silica gel column chromatography (DCM/MeOH 99.7:0.3) obtaining the product as a white solid (0.041 g, 0.026 mmol, 10% yield).

ESI-MS (m/z): 1585.90 $[M+H]^+$ 793.95.

^{1}HNMR(400MHz,CDCl3): δ 9.39 (s,2H), 9.30 (s,2H), 8.17 (s,2H), 7.90 (s,6H), 7.63 (d,J=8.0 Hz, 2H), 7.27-7.18 (m,10H), 6.11 (s,1H), 5.77 (d,J=8.0 Hz, 2H), 4.38-4.25 (m,2H), 1.81-1.76 (m,8H), 1.70-1.66 (m,4H), 1.50-1.42 (m,54H)

Synthesis of compound 63

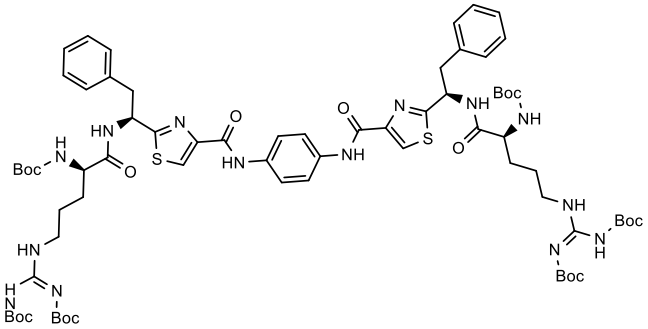

Compound **63** was obtained from compound **54** (0.130 g, 0.23 mmol, 1 eq.) through **Method G**. It was purified by flash silica gel column chromatography (DCM/MeOH 99.7:0.3) obtaining the product as a white solid (0.038 g, 0.026 mmol, 12% yield).

ESI-MS (m/z): 1481.68 $[M+H]^+$ 741.84.

^{1}HNMR(400MHz,CDCl3):δ 9.30 (s,2H), 9.27 (s,2H),8.14 (s,2H), 7.90(s,4H), 7.49 (d,J=8.0 Hz, 2H), 7.27-7.18 (m,10H), 6.11(s,1H), 5.77 (d,J=8.0 Hz, 2H), 5.38-5.29 (m,2H), 2.43-2.36 (m,8H), 2.08-1.99 (m,4H), 1.50-1.42 (m,54H).

Synthesis of compound 64

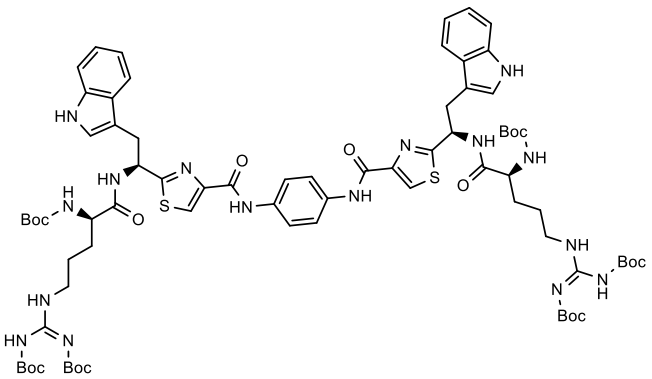

Compound **64** was obtained from compound **56** (0.090 g, 0.15 mmol, 1 eq.) through **Method G**. It was purified by flash silica gel column chromatography (DCM/MeOH 98.2:0.2) obtaining the product as a white solid (0.035 g, 0.022 mmol, 15% yield).

ESI-MS (m/z): 1558.71$[M+H]^+$; 780.35 $[M+2H]^{2+}$.

^{1}HNMR(400MHz,CD_3OD):δ 8.19 (s,2H), 7.77 (s,4H),8.14 (s,2H), 7.62-7.52 (m,2H), 7.35 (d,J=7.9 Hz, 2H), 7.13-6.99 (m,8H), 5.69-5.65 (m,2H), 4.10(s,2H), 3.85-3.80 (m,2H), 3.77-3.70 (m,8H), 3.56-3.50 (m,4H), 1.72-1.67(m,6H), 1.50-1.47(m,54H).

Synthesis of compound 65

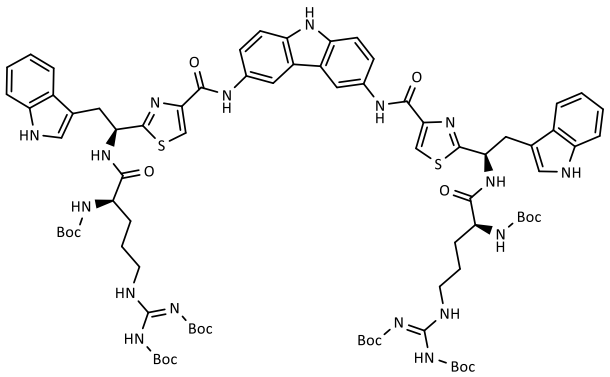

Compound **65** was obtained from compound **55** (0.041 g, 0.15 mmol, 1 eq.) through **Method G**. It was purified by flash silica gel column chromatography (DCM/MeOH 98.2:0.2) obtaining the product as a white solid (0.035 g, 0.022 mmol, 15% yield).

ESI-MS (m/z): 1647.73$[M+H]^+$; 824.86 $[M+2H]^{2+}$.

^{1}HNMR(400MHz,CD_3OD):δ 8.23 (s,2H), 8.14 (s,2H), 7.40 (m,6H), 7.46-7.42 (m,2H), 7.35 (d,J=7.9 Hz, 2H), 7.25-7.20 (m,8H), 4.06 (s,2H), 3.85-3.80 (m,2H), 3.77-3.70 (m,8H), 3.56-3.50 (m,4H), 1.72-1.67 (m,6H), 1.43-1.40 (m,54H).

Synthesis of compound 66

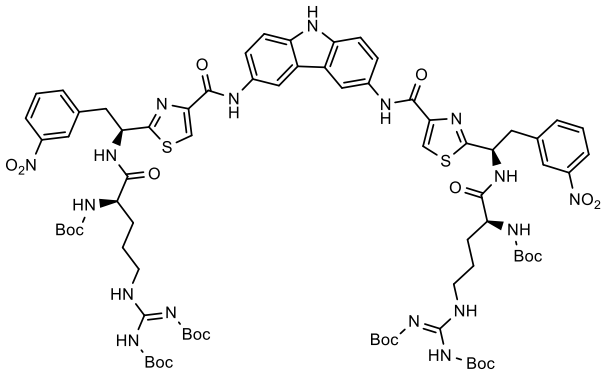

Compound **66** was obtained from compound **59** (0.100 g, 0.13 mmol, 1 eq.) through **Method G**. It was purified by flash silica gel column chromatography (DCM/MeOH 98:2+0.2%NH_3) obtaining the product as a white solid (0.122 g, 0.073 mmol, 56% yield).

ESI-MS (m/z): 1659.68$[M+H]^+$; 830.84 $[M+2H]^{2+}$.

^{1}HNMR(400MHz,CDCl3):δ 8.37 (s,2H), 8.16 (s,2H), 7.50-7.45 (m,2H), 7.39 (d,J=8.0 Hz, 2H), 7.34 (d, J=7.2 Hz, 2H), 7.31-7.18 (m,8H), 6.07 (s,1H), 5.79 (s,1H), 3.64-3.59 (m,4H), 3.38-3.32 (m,2H), 1.80-1.72 (m,8H), 1.33-1.12 (m,2H), 1.47-1.43 (m,54H)

Synthesis of compound 67

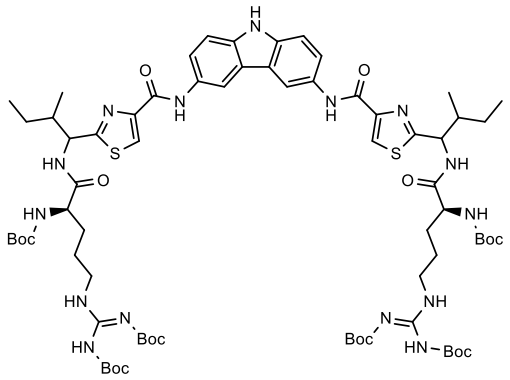

Compound **67** was obtained from compound **60** (0.85 g, 0.18 mmol, 1 eq.) through **Method G**. It was purified by flash silica gel column chromatography (DCM/MeOH 99.5:0.5) obtaining the product as a white solid (0.052 g, 0.034 mmol, 19% yield).

ESI-MS (m/z):1501.74 $[M+H]^+$; 751.87 $[M+2H]^{2+}$.

^{1}HNMR(400MHz,CDCl3):δ 8.49 (s,2H), 8.28 (s,2H), 7.72-7.69 (m,6H), 5.25 (d, J=6.9 Hz 1H), 4.17-4.14 (m,2H), 3.91-3.89 (m,4H), 2.32-2.23 (m,2H), 1.69-1.61 (m,10H), 1.57-1.55 (m,6H), 1.49-1.45 (m,54H), 1.04-0.98 (m,12H).

Synthesis of compound 68

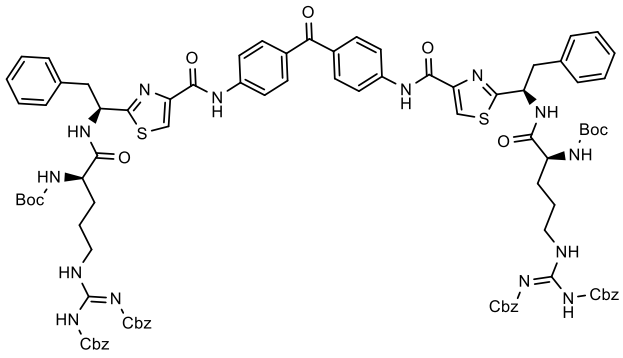

Compound **68** was obtained from compound **49** (0.023 g, 0.042 mmol, 1 eq.) through **Method G**. It was purified by flash silica gel column chromatography (EtOAc/EP 6:4) obtaining the product as a white solid (0.014 g, 0.008 mmol, 19% yield).

ESI-MS (m/z): 1720.65 $[M+H]^+$; $[M+2H]^{2+}$ .636.32

^{1}HNMR(400MHz,CDCl3):δ 9.36(m,6H), 8.13 (s,2H), 7.94-7.89 (m,8H), 7.43-7.38 (m,15H), 7.27-7.18 (m,10H), 7.12-7.04 (m,5H), 5.93(d, J=7.9 Hz 2H), 5.60-5.54 (m,2H), 5.32-5.23 (m,6H), 5.12 (d, J=8.8 Hz 2H), 4.37 (s,2H),3.81-3.67(m,4H),3.27-3.22(m,2H),1.76-1.72(m,4H),1.44(s,18H)

Synthesis of compound 69

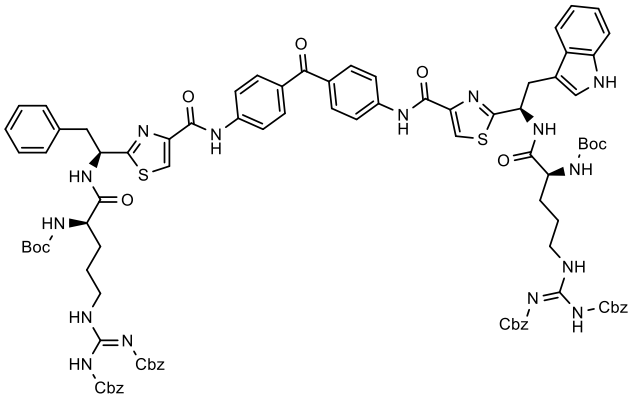

Compound **69** was obtained from compound **50** (0.017 g, 0.239 mmol, 1 eq.) through **Method G**. It was purified by flash silica gel column chromatography ($CHCl_3$/MeOH 99.5:0.5) obtaining the product as a white solid (0.020 g, 0.008 mmol, 19% yield).

ESI-MS (m/z): 1759.66 $[M+H]^+$; $[M+2H]^{2+}$ .880.83

^{1}HNMR(400MHz,CDCl3):δ 9.42 (m,4H), 8.13 (s,2H), 7.90-7.88 (m,8H), 7.42-7.38 (m,20H), 7.21-7.05 (m,10H), 5.92(d, J=8.4 Hz 2H), 5.29-5.12 (m,9H), 4.41-4.37 (m,1H), 4.29-4.26 (m,1H), 3.83-3.70 (m,4H), 3.46-3.38 (m,1H), 3.29-3.22 (m,2H), 3.00-2.87 (m,1H), 1.42 (s,18H).

Synthesis of compound 70

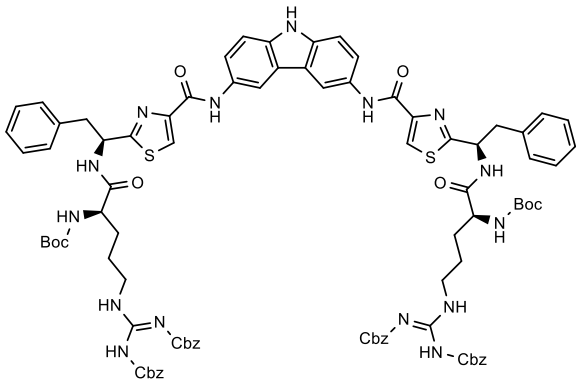

Compound **70** was obtained from compound **51** (0.232 g, 0.353 mmol, 1 eq.) through **Method G**. It was purified by flash silica gel column chromatography ($CHCl_3$/MeOH 98:2) obtaining the product as a white solid (0.415 g, 0.688 mmol, 69% yield).

ESI-MS (m/z): 1705.65 $[M+H]^+$; $[M+2H]^{2+}$ .853.82

^{1}HNMR(400MHz,CDCl3):δ 9.42 (m,4H), 9.30 (s,2H), 9.26 (s,2H), 8.47 (s,2H), 7.79 (d,J=8.2 Hz, 2H), 7.44-7.35 (m,20H), 7.26-7.18 (m,10H), 7.11-7.06 (m,5H), 5.87(d, J=7.6 Hz 2H), 5.62 (q, J=8.4 Hz 2H), 5.26-5.17 (m,6H), 5.15-5.10 (m,2H), 4.37-4.31 (m,2H), 3.82-3.72 (m,4H), 3.35-3.30 (m,2H), 1.61-1.55 (m,4H), 1.44 (s,18H).

Synthesis of compound 71

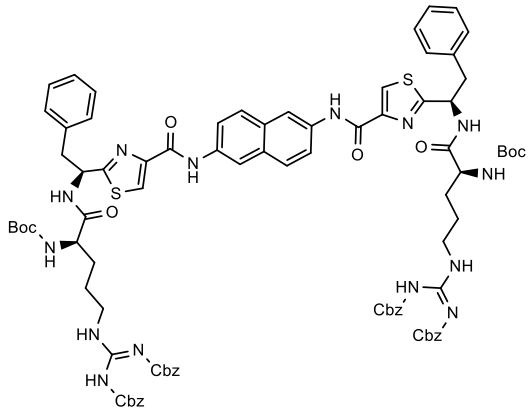

Compound **71** was obtained from compound **52** (0.056 g, 0.091 mmol, 1 eq.) through **Method G**. obtaining the product as a white solid (0.118 g, 0.070 mmol, 78% yield).

ESI-MS (m/z): 1666.64 $[M+H]^+$; $[M+2H]^{2+}$584.32

^{1}HNMR(400MHz,CDCl3):δ9.47(m,2H),9.43 (s,2H), 9.31 (s,2H), 8.47 (dd,J=7.9 Hz, 13.9 Hz, 1H), 8.12 (s,2H), 7.89 (d,J=7.9 Hz, 2H), 7.73-7.66 (m,2H), 7.43-7.36 (m,14H), 7.26-7.18 (m,7H), 7.13-7.06 (m,5H), 5.92 (d, J=7.9 Hz 2H), 5.62-5.56 (m,2H), 5.28-5.09 (m,7H), 4.38-4.27 (m,2H), 3.99-3.92 (m,1H), 3.81-3.71 (m,2H), 3.38-3.26 (m,2H), 3.00-2.89 (m,2H), 1.76-1.73 (m,2H),1.59-1.55(m,2H),1.43(s,18H).

Synthesis of compound 72

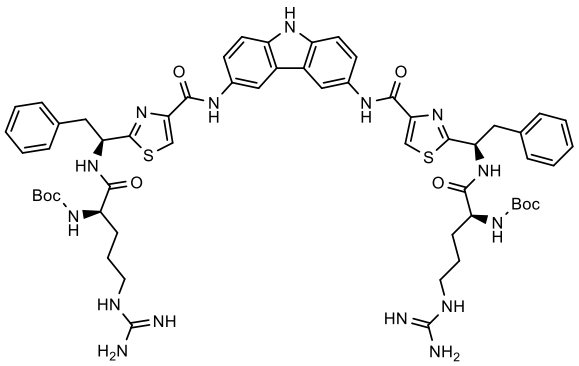

Compound **72** was obtained from compound **70** (0.100 g, 0.0586 mmol, 1 eq.) through **Method L**. (Gradient 10%B 2CV, 10-48%B 8.5CV, 48-55%B 1.4CV, 55-100%B 2CV, 100%B 2CV; flow rate 12 mL/min) obtaining the product as a white solid (0.083 g, 0.071 mmol, 82% yield).

ESI-MS (m/z): 1170.57 $[M+H]^+$; $[M+2H]^{2+}$ .585.94

^{1}HNMR(400MHz,CD_3OD):δ 8.58(d,J=4.8 Hz, 2H), 8.52 (d,J=4.9 Hz, 2H), 8.27 (s,2H), 7.80 (dd,J=8.8 Hz, 8.8 Hz, 1H),7.71 (dd,J=10 Hz, 13.6 Hz, 1H), 7.51 (d,J=8.8 Hz, 2H), 7.34-7.31 (m,8H), 7.27-7.22 (m,2H), 5.66-5.63 (m,2H), .4.11-4.08 (m,2H), 3.61 (dd,J=14 Hz, 8 Hz, 1H), 3.15 (t,J=6.4 Hz, 4H), 1.68-1.59 (m,4H), 1.56-1.50 (m,4H), 1.42 (s,18H).

Synthesis of compound 73

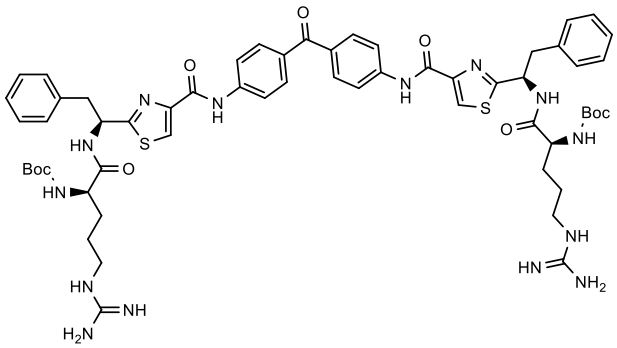

Compound **73** was obtained from compound **68** (0.290 g, 0.179 mmol, 1 eq.) through **Method L**. (Gradient 10%B 2CV, 10-48%B 8.5CV, 48-55%B 1.4CV, 55-100%B 2CV, 100%B 2CV; flow rate 12 mL/min) obtaining the product as a white solid (0.060 g, 0.051 mmol, 28% yield).

ESI-MS (m/z): 1184.50$[M+H]^+$; $[M+2H]^{2+}$ .593.25

^{1}HNMR(400MHz,CD_3OD):δ8.61(s,4H), 8.41 (s,2H), 8.31 (s,2H), 7.90 (d,J=8.8 Hz, 2H), 7.84 (d,J=9.2 Hz, 2H), 7.35-7.31 (m,10H), .7.26-7.24 (m,2H), 5.64-5.62 (m,2H), .4.10-4.07 (m,2H), 3.62 (dd,J=14 Hz, 6 Hz, 1H), 3.24-3.21 (m,1H),3.16 (t,J=7.6 Hz, 4H), 3..08-3.05 (m,1H), 1.66-1.60 (m,4H), 1.52-1.50 (m,4H), 1.43 (s,18H).

Synthesis of compound 74

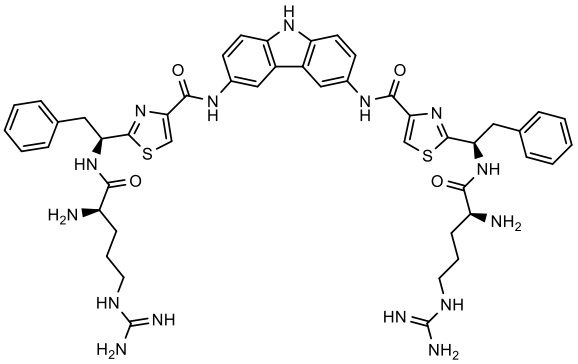

Compound **74** was obtained from compound **61** (0.091 g, 0.0587 mmol, 1 eq.) through **Method L**. (Gradient 10%B 2CV, 10-35%B 7.9CV, 35-60%B 2CV, 60-95%B 1CV, 100%B 2CV; flow rate 12 mL/min) obtaining the product as a white solid (0.042 g, 0.043 mmol, 74% yield).

ESI-MS (m/z): 970.66 $[M+H]^+$; $[M+2H]^{2+}$ .485.99

^{1}HNMR(400MHz,CD_3OD):δ 8.57(m,4H), 8.28 (s,2H), 7.68-7.63 (m,2H), 7.52 (d,J=8.8 Hz, 2H), 7.40-7.33 (m,8H), 7.29-7.24 (m,2H), 5.68-5.65 (m,2H), .4.01-3.93 (m,2H), 358-3.53 (m,2H), 3.39 (t,J=8.2 Hz, 4H), 3.21 (t,J=7.2 Hz, 2H), 3.16 (t,J=7.6 Hz, 4H), 3.03 (t,J=6.8 Hz, 2H), 2.00-1.94 (m,3H), 1.69-1.63 (m,4H), 1.52-1.50 (m,4H), 1..33-1.29 (m,1H).

Synthesis of compound 75

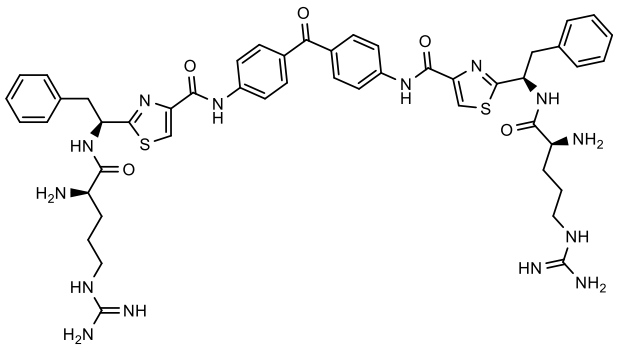

Compound **75** was obtained from compound **62** (0.027 g, 0.017 mmol, 1 eq.) through **Method L**. (Gradient 10%B 2CV, 10-55%B 10CV, 55-100%B 1CV, 100%B 2CV; flow rate 12 mL/min) obtaining the product as a white solid (0.018 g, 0.010 mmol, 59% yield).

ESI-MS (m/z): 985.20 $[M+H]^{+}$; $[M+2H]^{2+}$ .493.6

^{1}HNMR(400MHz,CD_3OD):δ 8.38 (m,1H), 8.34 (s,1H), 8.00 (d,J=7.2 Hz, 2H), 7.90 (d,J=8.8 Hz, 2H), 7.39-7.36 (m,8H), .7.28-7.26 (m,2H), 5.75 (q,J=6.0Hz, 1H), 5.68 (q,J=6.4 Hz, 1H),4.60 (s,2H),3.85-3.82 (m,2H), 3.71 (dd,J=10.4 Hz, 14 Hz, 1H), 3.59 (dd,J=14 Hz, 14 Hz, 1H), 4.60 (m,2H), 3.85-3.82 (m,2H), 3.71 (dd,J=10 Hz, 14 Hz, 1H), 3.60 (dd,J=14 Hz, 14 Hz, 1H),3.19-3.15 (m,4H), 3.03 (t,J=6.8 Hz, 2H).

Synthesis of compound 76

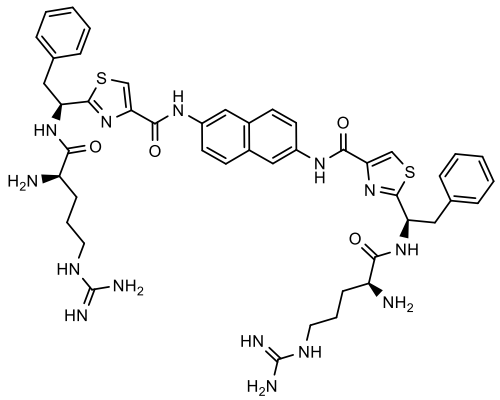

Compound **76** was obtained from compound **73** (0.028 g, 0.0248 mmol, 1 eq.) through **Method L**. (Gradient 10%B 2CV, 10-55%B 10CV, 55-100%B 1CV, 100%B 2CV; flow rate 12 mL/min) obtaining the product as a white solid (0.010 g, 0.011 mmol, 44% yield).

ESI-MS (m/z): 931.15 $[M+H]^+$; $[M+2H]^{2+}$ .466.57

^{1}HNMR(400MHz,CD_3OD):δ 8.50 (s,4H),.8.39-8.28 (m,2H), 7.88-7.78 (m,2H), 7.38-7.27 (m,10H), 5.67-5.63 (m,1H), 5.14-5.12 (m,1H), 3.92-3.89 (m,1H), 3.58-3.53 (m,1H), 3.26-3.18 (m,2H), 1.92-1.87 (m,4H), 1.66-1.62 (m,4H).

Synthesis of compound 77

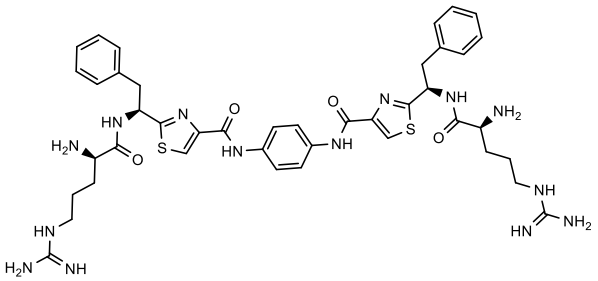

Compound **77** was obtained from compound **63** (0.006 g, 0.0248 mmol, 1 eq.) through **Method L**. (Gradient 10%B 2CV, 10-55%B 10CV, 55-100%B 1CV, 100%B 2CV; flow rate 12 mL/min) obtaining the product as a white solid (0.003 g, 0.0034 mmol, 85% yield).

ESI-MS (m/z): 881.4 $[M+H]^+$; $[M+2H]^{2+}$ .441.3

^{1}HNMR(400MHz,CD_3OD):δ 8.31(s,1H), 8.27 (s,2H), 7.79(s,4H),7.37-7.27 (m,10H),5.74-5.70(m,1H),5.66-5.62(m,1H),3.99-3.95(m,2H), 3.69-3.64 (m,1H), 3.57-3.49 (m,2H), 3.23-3.17 (m,4H), 3.01 (t, J=6.8 Hz 2H),3.96-3.92(m,4H), 1.64-1.61(m,4H).

Synthesis of compound 78

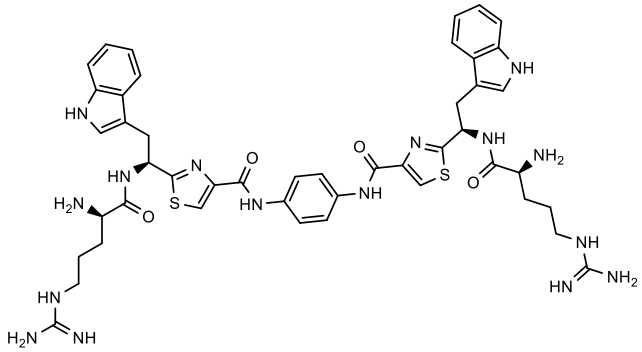

Compound **78** was obtained from compound **64** (0.017 g, 0.01 mmol, 1 eq.) through **Method L**. (Gradient 10%B 2CV, 10-55%B 10CV, 55-100%B 1CV, 100%B 2CV; flow rate 12 mL/min) obtaining the product as a white solid (0.002 g, 0.0034 mmol, 20% yield).

ESI-MS (m/z): 958.39$[M+H]^+$; $[M+2H]^{2+}$ .480.19

^{1}HNMR(400MHz,CD_3OD):δ8.50-8.47(m,4H),8.24(s,2H),7.78(s,4H),7.62 (d,J=8Hz,2H),7.34 (d,J=8.2 Hz,2H), 7.14-7.10 (m,4H), 7.06-7.01 (m,2H), 5.72-5.78 (m,2H), 3.66-3.58 (m,4H), 3.50-3.46 (m,6H), 3.15-3.13 (m,1H), .3.12 (t, J=7.9 Hz 2H), 1.69-1.61(m,4H), 1.54-1.49(m,4H).

Synthesis of compound 79

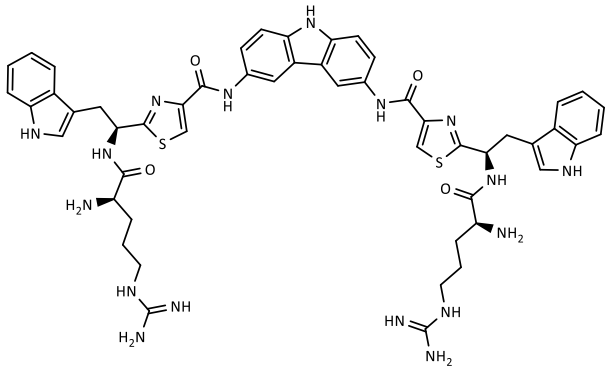

Compound **79** was obtained from compound **65** (0.0014 g, 0.008mmol, 1 eq.) through **method L**. (Gradient 10%B 2CV, 10-55%B 10CV, 55-100%B 1CV, 100%B 2CV; flow rate 12 mL/min) obtaining the product as a white solid (0.003 g,0,002 mmol, 52% yield).

ESI-MS (m/z): 1047.42$[M+H]^+$; $[M+2H]^{2+}$ .524.71

^{1}HNMR(400MHz,CD_3OD):δ 8.45 (s,4H), 8.14 (s,2H),7.73-7.70 (m,4H),7.47-7.45 (m,2H), 7.36-7.34 (m,4H), 7.30 (d,J=8.00 Hz, 2H), 4.06 (s,2H), 3.85-3.80 (m,2H), 3.77-3.70 (m,8H), 3.56-3.50 (m,4H), 1.72-1.67(m,4H).

Synthesis of compound 80

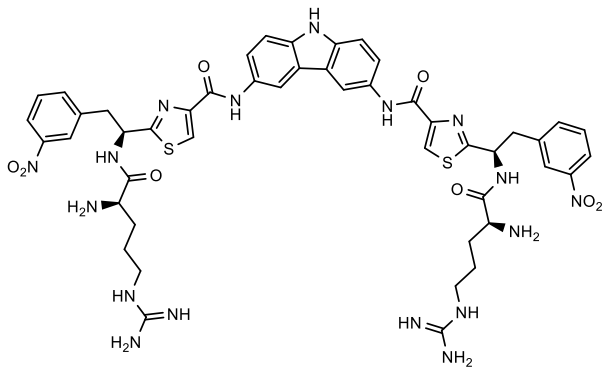

Compound **80** was obtained from compound **66** (0.100 g, 0.06 mmol, 1 eq.) through **method L**. (Gradient 10%B 2CV, 10-55%B 10CV, 55-100%B 1CV, 100%B 2CV; flow rate 12 mL/min) obtaining the product as a yellow solid (0.012 g, 0.011 mmol, 10% yield).

ESI-MS (m/z): 1060.18 $[M+H]^+$; $[M+2H]^{2+}$ 531.09

^{1}HNMR(400MHz,CD_3OD):δ8.56-8.53(m,2H),8.52-8.50(m,4H),8.32 (d,J=7.8Hz,2H), 7.83-7.77 (m,2H), 7.69-7.66 (m,4H), 7.62-7.58 (m,2H), 5.83 (q,J=6.8 Hz, 1H). 5.77 (t,J=7.8 Hz, 1H), 4.37-4.31 (m,2H), 4.01-3.96 (m,2H), 3.86-3.74 (m,2H), 3.52-3.47 (m,2H), 3.34-3.32 (m,2H), 3.23-3.19 (m,4H), 1.98-1.95(m,4H).

Synthesis of compound 81

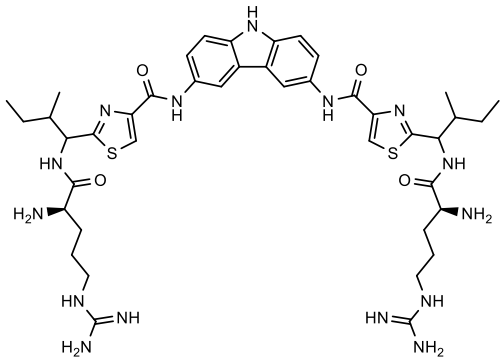

Compound **81** was obtained from compound **67** (0.052 g, 0.034 mmol, 1 eq.) through **method L**. (Gradient 10%B 2CV, 10-55%B 10CV, 55-100%B 1CV, 100%B 2CV; flow rate 12 mL/min) obtaining the product as a yellow solid (0.017 g, 0.018 mmol, 52% yield).

ESI-MS (m/z): 902.16 $[M+H]^+$; $[M+2H]^{2+}$ 452.08

^{1}HNMR(400MHz,CD_3OD):δ 8.59-8.52 (m,2H), 8.33 (s ,2H), 7.65-7.63 (m,2H), 7.53 (d,J=8.8 Hz, 2H), 5.44 (t,J=6.7 Hz, 1H),. 5.30 (d,J=8.2 Hz, 1H), 4.13-4.07 (m,2H), 3.20-3.17 (m,2H), 2.36-2.29 (m,2H), 2.03-1.92 (m,4H), 1.79-1.69 (m,4H), 1.64-1.60 (m,4H), 1.42-1.31 (m,4H), 1.05 (t, J=8.4 , 12H).

Chapter4_Mode of action studies

[This page is intentionally left blank]

4.1.1. Background

4.1.2. Gram- positive and Gram-negative bacteria overview

Bacteria are prokaryotic unicellular organisms present in every environment such as soil, plants, water including extreme conditions characterized by aridity, radiations, elevated temperatures (hot springs), extreme pH values and high salt concentrations. They can be classified based on the shape/size, cell wall and metabolism. [120] Moreover, based on the bacterial cell wall, it is possible to differentiate Gram-positive and Gram-negative bacteria. It is intended that this difference is important in order to design and synthesize selective molecules, as herein described.

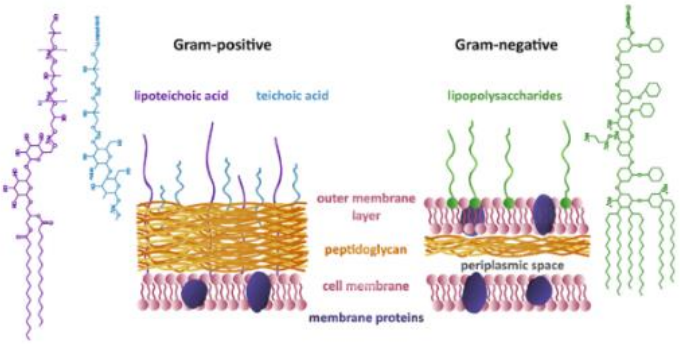

Figure 39. *Differences between Gram-positive and Gram- negative bacterial cell walls. Adapted from Ref.122*

Gram positive: the cell wall of Gram-positive bacteria lacks the outer membrane, for this reason they developed a thicker layer of protective peptidoglycan. It is made by anionic polymers such as called teichoic acids (glycerol phosphate, glucosyl phosphate, or ribityl phosphate repeated) and lipoteichoic acids.[121] It constitutes a glycan backbone, tetrapeptide side chains, and a pentapeptide cross-linking bridge.[122] Since there is no outer membrane, most of the protein are inside the inner membrane, anchored to the lipids or to the peptidoglycan. This class of bacteria includes, among others, *Streptococcus* spp., *Staphylococcus aureus*, *Clostridium botulinum*, and *Bacillus anthracis*. [121]

Gram negative: the cell wall of Gram-negatives is more elaborated, posing an additional challenge to the synthesis of selective antibacterials. Indeed, it is composed of three layers; (i) the inner membrane, (ii) the peptidoglycan, and (iii) the outer membrane. The two membranes delimitate the periplasmic region. The outer membrane is a lipid bilayer made of phospholipids on the inner side of the membrane and glycolipids such as lipopolysaccharide (LPS) on the outer side. Additionally, it contains important proteins, mainly lipoproteins and β-barrel, such as tolC, LptD, LptE, Bam or OmpF.[123,124] The peptidoglycan is made of repeated units of N-acetyl glucosamine-N-acetyl muramic acid, cross-linked by pentapeptide side chains. The outer membrane is clamped to the peptidoglycan layer through the Lpp lipoprotein, and it is the site where all the associated-membrane functions (energy production, lipid biosynthesis, protein secretion, and transport) proteins are located. *Escherichia coli*, *Salmonella enterica*, *Hemophilus influenzae*, *Neisseria gonorrhoeae* are representative Gram-negative bacteria of interest.[120,121]

4.1.3. Multidrug efflux systems

As briefly reported in ***chapter1***, efflux systems represent one of the most versatile antimicrobial resistance mechanisms. These systems constitute an innate defence mechanism in all bacterial species, and they are usually classified based on their structure, number of transmembrane regions, energy sources and substrates: ATP-binding cassette (**ABC**) family, major facilitator superfamily (**MFS**), the multidrug and toxin extrusion (**MATE**) family, the small multidrug resistance (**SMR**) family, the resistance-nodulation-cell division **(RND**) superfamily and the proteobacterial antimicrobial compound efflux (**PACE**) family **(*Figure* 40).**[125,126]

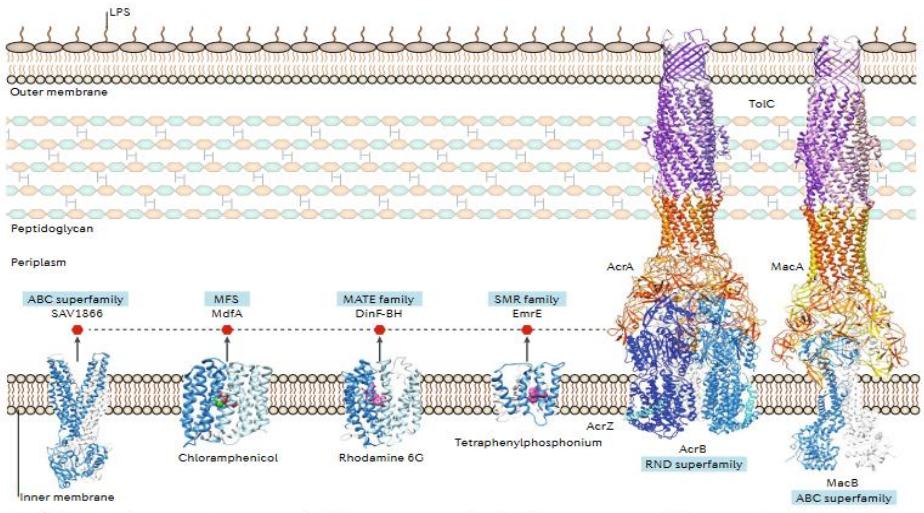

Figure 40. *Structure and location of the main families of MDR transporters in Gram positive and Gram negative. Adapted from Ref.126.*

To better understand some of the experiments carried out in this work, the most relevant efflux systems in Gram negative bacteria will be briefly described.[126]

The main contribution to intrinsic multi drug resistance (MDR) in Gram negative is given by the presence of RND efflux systems.[127] The most studied and well characterized RND efflux system in Gram negative bacteria is the Escherichia coli AcrAB-TolC system, which is composed of three elements: (I) outer membrane protein channel (TolC) (II)periplasmic adaptor protein (AcrA) and (III) inner membrane transporter (AcrB).[128]

The three-component efflux systems allow the passage of molecules across inner and outer membrane and their structure is highly conserved throughout Gram-negative strains. Indeed, RND systems characterized by high homology sequence have been reported in *E. coli* (AcrB), *Pseudomonas aeruginosa* (MexB), *Campylobacter jejuni* (CmeB*), Acinetobacter baumannii* (AdeB) and *Neisseria gonorrhoeae* (MtrD) [129]

Efflux system expression depends on a strict control by various transcription regulators. Mutations in the local and global transcriptional regulators which modify the regulatory system could lead to overexpression of efflux pumps, which can result in undesired efflux of metabolites. Most of these regulators belong to the TetR, MarR, or MerR family, which generally acts as transcriptional repressors located adjacent to the structural genes of efflux pumps **(*Figure* 41).** [126]

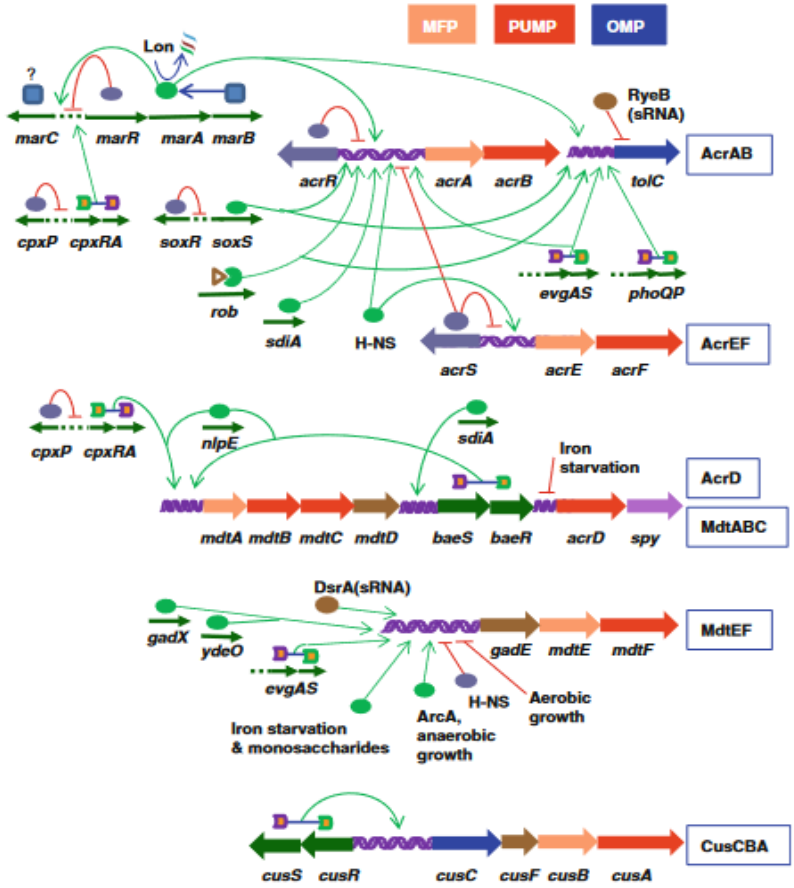

Figure 41. *RND regulation system in E.coli. Adapted from Ref. 126.*

For the sake of information completeness, a table showing the efflux systems and their related regulators is here reported. For any additional information the recent reviews on this topic can be consulted. [125,126,130]

Microrganism	*Efflux system*	*Efflux pump family*	*Regulator family*
A.baumannii	AdeABC	RND	AdeRS
B. subtilis	Bmr	MFS	BmrR
			Mta
	Blt	MFS	BltR
			Mta
E.coli	AcrAB	RND	AcrR
			AcrS
			MarA
			MarR
			SoxS
			Rob
			SdiA
	AcrD	RND	BaeSR
			CpxAR
	AcrEF	RND	H-NS
	EmrAB	MFS	EmrR
	EmrKY	EmrKY	EvgSA
			H-NS
	MdtABC	RND	BaeSR
			CpxAR
	MdtEF	RND	ArcAB
			CRP
			EvgSA
			H-NS
			GadE
			GadX
N.gonorrhoeae	FarAB	RND	FarR
	MtrCDE	RND	MtrR
			MtrA
P.aeruginosa	MexAB	RND	MexR
			NalD
	MexCD	RND	NfxB
	MexEF	RND	MexT
	MexXY	RND	MexZ
S. aureus	MepA	MATE	MepR
	QacA	MFS	QacR

Table 1. *Relevant efflux systems and regulators for bacteria of interest.*

4.1.4. Proteomic in new drug-targets discovery

In recent years, mass spectrometry (MS)-based proteomics has emerged as innovative technique in the identification of protein targets and drug modes of action, indeed it became a central technique employed in drug development programs.[131,132]

Proteomic approaches can be grouped in 3 different fields:

- ***Clinical proteomics*** employed in the discovery, identification and quantification of novel biomarkers responsible for specific diseases to allow the early detection and diagnosis.[131]
- ***Chemical proteomics*** involved in the analysis of a drug's mechanism of action based on the proteome expressed in the target cell.[133]
- ***Functional proteomics*** enables the characterization of interacting proteins providing an overall view of the specific biological pathways.[134]

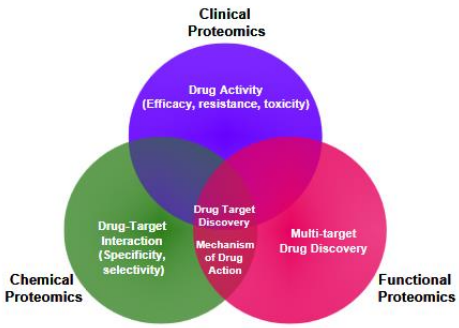

Figure 42. *Three main proteomic approaches. Adapted from Ref.131*

The three approaches are well interconnected in order to ensure the study of drug-target interaction and mode of action (MoA) **(*Figure* 42).**[131] For the purpose of this project, only the chemical proteomic approaches will be briefly described in the following section.

Chemical proteomic approaches to drug target identification and drug profiling

Chemical proteomic constitutes one of the most immediate approaches to investigate potential interactions of a drug with a wide number of proteins present in a lysate. Since low abundant proteins can bind specifically to the drug and high abundant protein can less specifically bind to the molecule, several approaches employing a variety of different experimental procedures have been developed over the last years. [135]

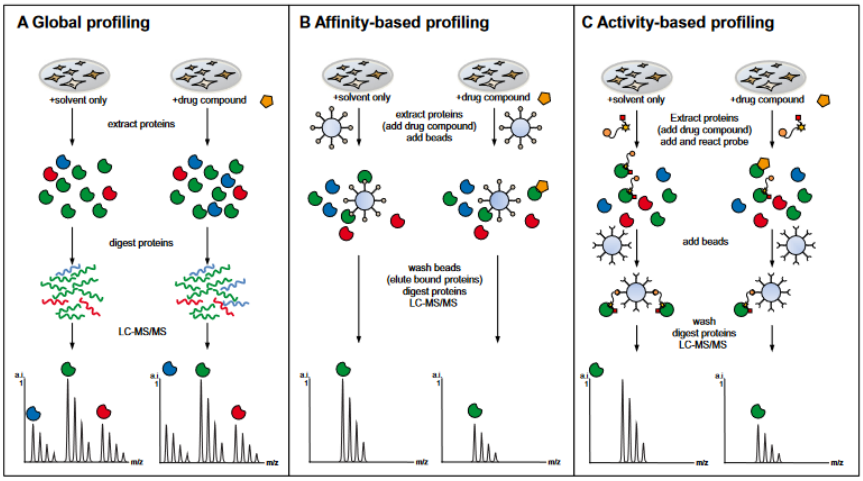

Figure 43. *Experimental workflow in chemoproteomics approaches. Adapted from Ref.136*

Among these three major approaches can be distinguished[133,136]:

- **Global proteomic** is oriented to the characterization of the cellular response to small molecules.[133]

  The specificity of the experiment is related to the number of proteins which can be differentially quantified since the results can be altered by the more abundant proteins. [136] For these reasons a global proteomic analysis could results in missing of low abundant protein consequently leading to prefer affinity based techniques. [135]

- **Activity- or affinity-based protein profiling (ABPP)** employs small chemical probes covalently capturing protein targets in a complex biological system. Based on the interaction type between the molecule and the ABPP and affinity-based protein profiling (AfBPP) can be performed.

  In presence of covalent inhibitors ABPP is employed. The molecules are chemically modified to carry a chemical probe in order to directly label the target proteins reacting in a mechanism-based way with an active site residue.

  For non-covalent inhibitors AfBPP is used. They are based on photo-affinity probes characterized by a photoreactive group which promotes the creation of a covalent bond with the target proteins under UV-irradiation. Then proteomic analysis or microscopy imaging can be carried out to identify the florescent target covalent bound to the relative proteins.

  With this technique, assuming a high affinity of the molecule for a determined molecular target, it is possible to elucidate the molecular mechanism of action.

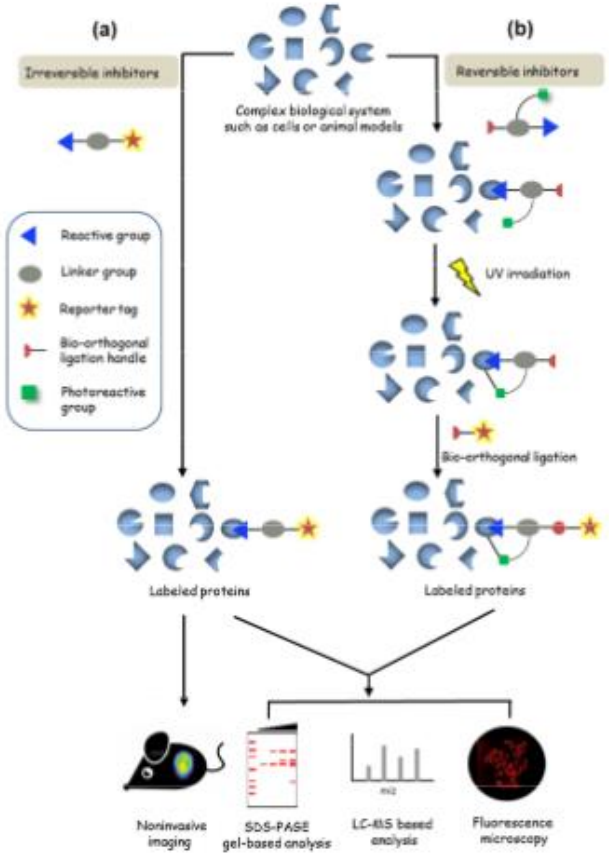

Figure 44. *General workflow of (a) activity-based protein profiling (ABPP) and (b) affinity-based protein profiling (AfBPP) strategy. Adapted from Ref.133*

4.2. Aim of the project

Relying on the fact that the new peptidomimetic structures were designed inspired by the structure of naturally occurring antimicrobial peptides, it has been speculated that they could perform their antimicrobial activity *via* a similar mechanism. Antimicrobial peptides (AMPs) interaction with membranes has been widely described **(Chapter1)**, nevertheless, in some cases their mechanism of action is still unclear and a high resolution structures of the AMP interacting with the bacterial membrane are still not available. [74]

Magainin, the AMP whose structure has inspired our design, acts through the formation of membrane pores, therefore it is reasonable to consider that the newly synthesized molecules follow a similar behaviour. To corroborate this hypothesis, and with the aim of obtaining an in-depth biological evaluation of the molecules prepared, so as to gain a more complete set of information, I have spent 4 months at the *Helmholtz Institute for Pharmaceutical Research Saarland* (HIPS) carrying out a series of experiments such as: MIC analysis, membrane depolarization assay, time-kill assay, ATP assay, scanning electron microscopy, lysis assay and affinity based proteomic.

Furthermore, I have endeavored to elucidate the mode of action of the chosen molecules, aiming to compare it with melittin and ascertain whether non-specific membrane disruption or interaction with specific intracellular targets occurred.

[This page is intentionally left blank]

4.3.Results and discussion

4.3.1. Biological activity and structure activity relationship (SAR)

The synthesis of the molecules as reported in the previous section took advantage from the preliminary screening of their antibacterial activity. Feedback from the microbiology drove the iterative synthesis of several derivatives, and therefore a total of 16 compounds were preliminary tested at the *Helmholtz Institute for pharmaceutical research* (HIPS) in prof. Muller's lab. Along with the molecules showing a final structure as planned, also some intermediates endowed with structural features well-suited with a potential activity were evaluated ***(Table2).*** In order to have a more comprehensive set of information, a broad panel of bacteria was considered, with common Gram-positive and Gram-negative bacteria, several fungi, and two Mycobacteria. This way, either selectivity or broad-spectrum activity of the molecules could be appreciate

Compound	S. aureus [1]	E.coli WT [2]	E. coli [3]	B.subtilis[4]	P. aeruginosa [5]	M. Smegmatis [6]	A. baumannii [7]	P. anomala [8]	C.freundii [9]	M. hiemalis [10]	C. neoformans [11]	C. albicans [12]	M. tuberculosis [13]
49	≥ 64	≥ 64	≥ 64	≥ 64	≥ 64	≥ 64	≥ 64	≥ 64	≥ 64	≥ 64	≥ 64	≥ 64	16-32
51	≥ 64	≥ 64	≥ 64	≥ 64	≥ 64	≥ 64	≥ 64	≥ 64	≥ 64	≥ 64	≥ 64	≥ 64	32
52	≥ 64	≥ 64	≥ 64	≥ 64	≥ 64	≥ 64	≥ 64	≥ 64	≥ 64	≥ 64	≥ 64	≥ 64	≥ 64
53	≥ 64	≥ 64	≥ 64	≥ 64	≥ 64	≥ 64	≥ 64	≥ 64	≥ 64	≥ 64	≥ 64	≥ 64	4-8
54	≥ 64	≥ 64	≥ 64	≥ 64	≥ 64	≥ 64	≥ 64	≥ 64	≥ 64	≥ 64	≥ 64	≥ 64	≥ 64
55	≥ 64	≥ 64	≥ 64	≥ 64	≥ 64	≥ 64	≥ 64	≥ 64	≥ 64	≥ 64	≥ 64	≥ 64	≥ 64
56	≥ 64	≥ 64	≥ 64	≥ 64	≥ 64	≥ 64	≥ 64	≥ 64	≥ 64	≥ 64	≥ 64	≥ 64	4-8
57	≥ 64	≥ 64	≥ 64	≥ 64	≥ 64	≥ 64	≥ 64	≥ 64	≥ 64	≥ 64	≥ 64	≥ 64	≥ 64
72	8-16	≥ 64	≥ 64	≥ 64	≥ 64	≥ 64	≥ 64	≥ 64	≥ 64	≥ 64	≥ 64	≥ 64	32-64
74	16	32	32	2	2	1	16	>64	16	≥ 64	≥ 64	≥ 64	≥ 64
73	8	≥ 64	≥ 64	4	≥ 64	≥ 64	32	≥ 64	≥ 64	≥ 64	≥ 64	≥ 64	32-64
75	1	8-16	4-8	1	8	≥ 64	16-32	≥ 64	16-32	≥ 64	≥ 64	≥ 64	8--16
77	8	≥ 64	8-16	1	16-32	8-16*	≥ 64	≥ 64	≥ 64	≥ 64	≥ 64	≥ 64	32
78	4	32	8-16	1	16-32	≥ 64	nt	≥ 64	16-32	≥ 64	≥ 64	≥ 64	16
80	32-64	32	32-64	4	≥ 64	≥ 64	≥ 64	≥ 64	64	≥ 64	≥ 64	≥ 64	nd
81	8	32	8	1	≥ 64	4	64	≥ 64	32	64	8-16	≥ 64	nd

Table2. *MIC values against a pannel of clinically relevant patogens. Higligthed in green all the MIC values lower than 64 µg/mL. [1]Newman, [2]BW25113,[3] JW0451-2 (ΔacrB),[4]DSM-10,[5] PA14- DSM-19882, [6]MC2155,[7]DSM-30008,[8] DSM-6766,[9] DSM-30039,[10]DSM-2656,[11]DSM-11959,[12] DSM-1665,[13] H37Ra.*

From this preliminary investigation, some interesting structure-activity relationships hints could be retrieved. The majority of the intermediates tested failed to show any activity against the whole panel of bacteria selected for this study. On the other hand, we were very pleased to notice that those molecules having an arginine as positively charged portion were all endowed with a broad antibacterial activity, although the potency in some cases was not remarkable. Since this was our first attempt to design magainin-related peptidomimetics, we considered these encouraging results a solid base for further research development.

To further comment the antibacterial activity of these compounds, it can be noticed that, in general, all of the tested compounds are devoid of activity toward fungi, whereas promising activity was noticed toward the small set of Gram positive and Gram negative bacteria used. In general, Gram-positive bacteria were more affected by the inhibitory activity of these peptidomimetics, with *B. subtilis* being the most susceptible to the antibacterial action of almost all the arginine-containing compounds. Interestingly, the majority of compounds tested, both intermediates and final derivatives, showed some measurable activity toward *M. tuberculosis*, paving the way for additional investigations. Moreover, taking into consideration the fact that intermediates (**52**,**56**) are more active than the arginine-containing molecules, it can be roughly speculated that their weak action might be due not to the interaction with the mycobacterial cell wall but rather to the inhibition of an internal target.
From this preliminary investigation, two derivatives (**74** and **75**) clearly emerged as hit compounds, since their broad spectrum of activity coupled to intriguing antibacterial potency. To a lesser extent, also **78** and **81** show a decent antimicrobial profile.

Finally, the different antibacterial activity and potency appear to be associated with distinct structural characteristics of microorganisms. As noted, higher activity is observed against Gram-positive bacteria, while it is comparatively

lower for Gram-negative bacteria, and no activity is noted against fungi. This suggests a potential interaction between the compounds and the microorganism membrane, as hypothesized. Subsequent experiments will provide confirmation of this interaction.

SAR considerations

Based on the MIC analysis conducted, general considerations about the structure-activity relationships are summarized in this section**.** It is worth to remember that, to start, all of these molecules were tested against wild type strains.

As outlined in the previous chapter, I have identified three distinct segments of the molecule contributing to variability. These segments can be subject to further modifications for the purpose of SAR refining. To enhance clarity, I have summarized the SAR hints based on these specific segments.

As a general notion, all of the compounds lacking the arginine portion were inactive.

- **Same central core/ different aminoacidic branch**

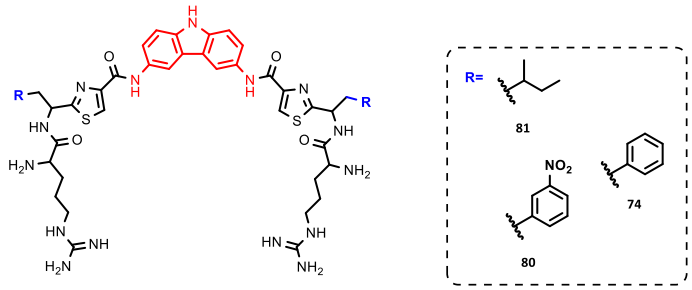

MIC(μg/mL)

Compound	*S. aureus*[1]	*E.coli* [2]	*E. coli* [3]	*B.subtilis*[4]	*P. aeruginosa* [5]
74	16	32	32	2	64
80	32-64	32-64	32-64	4	≥ 64
81	8	32	8	1	≥ 64
72*	8-16	≥ 64	≥ 64	4	≥ 64

Figure 45. **80, 81** *and* **72** *antimicrobial activity compared to* **74.** *[1]Newaman,[2]WT BW25223,[3] ΔacrB JW0451-2, [4] DSM10, [5]PA14. * Presenting the general structure h.1 previously described in chapter3.*

80 presents a nitro-phenyl portion while **81** presents a branched aliphatic substituent at positions R. The introduction of a less lipophilic moiety for **81** resulted in extending the activity to *S.aureus* and *E coli* if compared to **80** and **74**. On the other hand, compound **80,** presenting nitro-phenyl portion, maintains the activity against *B.subtilis* but it resulted totally inactive against *E.coli* and *S.aureus*. These molecules resulted inactive against all the efflux systems deficient strains. Thereby, maintaining the carbazole as central core, the replacement of the phenyl portion of **74** with a less lipophilic moiety **81** lead to an increase of the antimicrobial activity, while increasing the lipophilic character is detrimental.

- **Different central core/same aminoacidic branch**

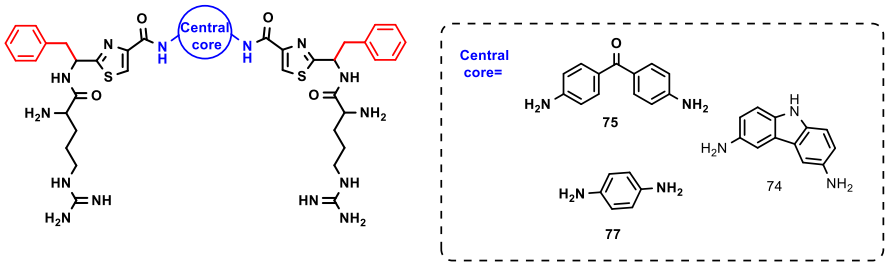

MIC(µg/mL)

Compound	*S. aureus*[1]	*E.coli* [2]	*E. coli* [3]	*B.subtilis*[4]	*P. aeruginosa* [5]
74	16	32	32	2	64
75	1	8-16	4-8	1	8
77	8	≥ 64	8-16	1	32

Figure 46. **75** *and* **77** *structures and antimicronial activity compared to* **74**.
[1]*Newaman,*[2]*WT BW25223,*[3] *ΔacrB JW0451-2,* [4] *DSM10,* [5]*PA14*

Compounds **74, 75 and 77** are all characterized by the same aminoacidic branch on the thiazole moiety, which is the benzylic portion of phenylalanine, while the central core has been modified. This modification is able to confer suitable activity against Gram-positive, indeed **75** and **77**resulted active against *S.aureus* while **75** showed activity against *P.aeruginosa* as well. As noted before, both **74** and **75** are active against both gram positive and negative, with the first being in general more promising. As a hypothesis, this distinction could be attributed to the diverse central cores. Specifically, the rotatable bond in the benzophenone central core of **75** may contribute to a unique spatial arrangement that is unattainable by the planar and rigid structure of the carbazole central core in**74**.

- **Different central core/ different aminoacidic branch**

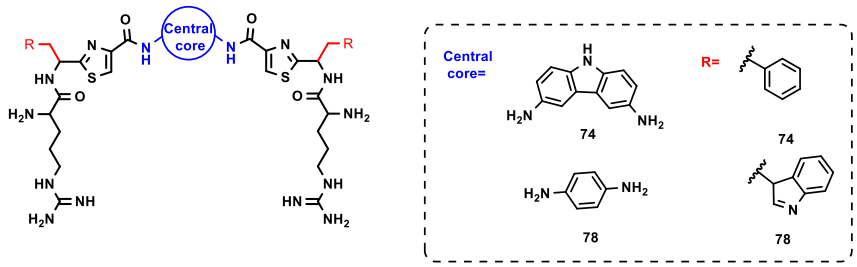

MIC(μg/mL)

Compound	*S. aureus*[1]	*E.coli* [2]	*E. coli* [3]	*B.subtilis*[4]	*P. aeruginosa* [5]
74	16	32	32	2	64
78	1	8-16	4-8	1	8

Figure 47. 78 *structure and antimicrobial activity compared to* **74**. *[1]Newaman,[2]WT BW25223,[3] ΔacrB JW0451-2, [4] DSM10, [5]PA14*

Among the molecules in the panel, **78** is the only compound with modifications to both the central core and side portion when compared to **74**. Overall, it is noteworthy that these modifications did not result in significant variations in activity, as the range of activity overlaps with that of the hit compounds **74** and **75.**

4.3.2. Preliminary metabolic stability analysis

In order to determine the stability to phase I metabolism and the consequent half-life time and internal clearance, I carried out at the University of Parma in the lab of Prof Vacondio the metabolic stability in the presence of **Human Liver Microsomal (HLM)** fractions for two intermediates (**49** and **51**) and two final compounds (**73** and **74**). Sample aliquots were collected at different time points up to 60 min to evaluate the percentage of remaining test sample over the time.

As reported by ***Table 3*** compound **49**, **74** and **73** showed a great stability since the percentage of remaining tested sample after 60 min was 86%,84% and 76% respectively. Moreover, compound **51** shows a linear decreasing in the percentage of concentration since after 60 mins it is 18%, consequently it is possible to define the half-life ($t_{1/2}$) which is 27,5 min and the internal clearance (Cl_{int}) as 24,45 microL/min·mgprotein. As in the case of activity, also this result aligned with the expectations of synthesizing stable structures, as initially planned.

Compound	% 60 min	T ½ (min)	Cl_{int} (µL/min·mg_{prot})
Diclofenac *(Cntrl)*	4.5	9.3	73.13
51	18	27.5	24.45
49	86	/	/
73	60	/	/
74	84	/	/

Table 3 *Comparison between remaining compound concetration at 60 min, half-life time and internal clearance for selected compounds.*

4.3.3. Extended analysis of the minimum inhibitory concentration (MIC)

In previous section **(4.3.1),** a preliminary MIC investigation was carried out on a limited panel of bacteria such as Gram-positives, Gram-negatives, fungi, and Mycobacteria. From one side, the information obtained were used to rationally design and synthesize novel analogues to test; on the other hand, this preliminary investigation prompted us to undertake more elaborated experiments to refine the biological characterization of the compounds prepared.

Unfortunately, it was impossible to further characterize the representative **74** as its MIC values against *P. Aeruginosa* obtained in the preliminary assay were not reproducible. This discrepancy might be due to the activation of specific efflux systems as well as to the sensibility of the bacterial strain to the cultivation conditions (use of outdated bacterial culture) or to loss on the oxygen supply.

To gain more hints concerning these hypotheses, the antimicrobial activity of **74** was tested on *E. coli* Δ*tolC and* Δ*acr*B strains, which are *E. coli* modified strains where genes encoding the TolC and the AcrB subunit of RND efflux systems are deleted. Ciprofloxacin (CIP) was used as control since it is one of the antibacterials most affected by the action of these efflux pumps.

	MIC [µg/mL]	
E. coli	**74**	**CIP**
BW25113 (WT)	≥ 64	0.002
Δ*tolC*	16	0.005
Δ*acrB*	≥ 64*	0.00125

Table4. *MIC values for* **74** *against E.coli WT and two mutant strains E. coli ΔtolC and ΔacrB compared to ciprofloxacin (CIP) as reference.*

Only deletion of *tolC* had a positive effect on the activity of **74** ***(Table4),*** meaning efflux might play a role in its activity, although of minor importance. Also, this suggests that the compound might be substrate of the **TolC** portion of the RND pump. Of note, we did also observe a reduced growth of *E. coli* Δ*acrB* strain compared to the wild type, but not enough to affect the MIC determination. Therefore, as a first take-home message, we can say that **74** is endowed with a weak antibacterial activity, which is however affected by the fact that it might be a substrate of the RND pump. This information should be taken into consideration in the next round of molecules design.

On a similar vein, other compounds were analyzed as well **(*Table* 5).**

	MIC [µg/mL]	
Compound	***E. coli*** [1]	***E. coli*** [2]
49	≥ 64	≥ 64
51	≥ 64	≥ 64
72	≥ 64	≥ 64
74	≥ 64	16
52	≥ 64	≥ 64
73	≥ 64	≥ 64
53	≥ 64	≥ 64
54	≥ 64	≥ 64
55	≥ 64	≥ 64
56	≥ 64	≥ 64*
57	≥ 64	≥ 64
80	≥ 64	≥ 64*
81	≥ 64	4
75	≥ 64	4
77	≥ 64	4
78	≥ 64	4
CIP	0.002	0.006

Table5. *Comparison of MIC values against [1]E.coli WT BW25113 and [2]E.coli ΔtolC.*

Despite the fact that the majority of compounds tested did not show any antibacterial activity against *E.coli* Δ*tolC*, we were pleased to notice that compounds **81**, **75,** **77**, and **78** exhibited a good activity, in some cases higher than that of **74**, suggesting the reliability of the rational design.

Considering these results particularly encouraging, these selected compounds were also tested on a number of additional Gram-negative and Gram-positive strains either knock-out for efflux pumps, or lacking specific regulators responsible for the overexpression of efflux systems ***(Table* 6).**

The following deletions were taken under consideration for *E.coli*:

- Δ*ompC or* Δ*ompF*, which are deficient for the subunit C or F of the *omp* influx/porins;
- Δ*bas*R *and E. Coli* Δ*bas*S deficient for *basR* and *basS*, known iron- and zinc-sensing transcription regulators involved in resistance to colistin[137];
- Δ*mdt*B, *E. Coli* Δ*mdt*C, *E. Coli* Δ*mdt*F, which are deficient for the relative subunit of the MdtABC/tolC MDR pump;
- Δ*mar*R which is deficient for the *mar* transcriptional repressor which regulates the expression of the acrA/B subunit of the tolC MDR efflux pump.

Concerning *P. Aeruginosa*, the following strains were taken into consideration: *Pa* Δ*mexAB, Pa* Δ*mexCD, Pa* Δ*mexEF and Pa* Δ*mexXY* are strains deficient for different *mex* operons responsible for the expression of RND mex efflux pump causing resistance to several antibiotics. Finally, also *E.faecium, K.pneumoniae and K.oxytoca* wild type strains were introduced in the panel of bacteria to expand the set of information and with the aim of finding molecules more active than **74** and **75** to be used for proteomic studies.

Strain	74	73	81	77	75	78	Ctr (CIP)
Pa WT[1]	64	≥ 64	≥ 64	≥ 64	32	≥ 64	1
Pa ΔmexAB[1,a]	64	≥ 64	≥ 64	≥ 64	32	64	1
Pa ΔmexCD[1,a]	64	≥ 64	≥ 64	≥ 64	64	≥ 64	0.5
Pa ΔmexEF[1,a]	64	≥ 64	64	64	32	64	1
Pa ΔmexXY[1,a]	32	≥ 64	≥ 64	≥ 64	32	≥ 64	1
E. coli [2]	32	≥ 64	64	≥ 64	16	64	8
E. coli ΔbasR[2,b]	64	≥ 64	32	≥ 64	32	32	8
E. coli ΔbasS[2,b]	64	≥ 64	64	≥ 64	16	64	8
E. coli ΔmarR[2,b]	32	≥ 64	64	≥ 64	32	x	8
E.coli ΔompC[2,a]	32	≥ 64	64	≥ 64	16	64	16
E.coli ΔompF[2,a]	64	≥ 64	64	≥ 64	32	64	8
E. coli mdtE[2,a]	32	≥ 64	64	≥ 64	32	≥ 64	4
E. coli mdtF[2,a]	64	≥ 64	64	≥ 64	16	64	16
E. coli mdtC[2,a]	64	≥ 64	64	≥ 64	32	64	8
E. coli mdtB[2,a]	64	≥ 64	64	≥ 64	16	64	16
E. faecium[3]	≥ 64	8	≥64	≥ 64	32	≥ 64	≥ 64
E. faecium[4]	64	≥ 64	64	64	32	64	0.125
K. pneumoniae[5]	≥ 64	≥ 64	≥ 64	≥ 64	64	64	4
K. oxytoca[6]	64	≥ 64	64	≥ 64	64	64	4
S. enterica[7]	≥ 64	≥ 64	≥ 64	≥ 64	64	64	8

Table 6. *Antibacterial activity on selected bacteria strains of compounds presenting structure **i**, reported as minimal inhibitory concentrations (MICs) in mg/mL. CIP= ciprofloxacin, [1]PA14, [2] BW25113, [3] DSM 20477, [4]DSM 17050, [5]DSM 30104, [6]ATCC 13182,[7]SB300. [a] Efflux systems, [b] Gene regulators.*

As a first take-home message, considering activity on *E.coli* Δ*Tol*C, we were pleased to notice that, as planned, the proper arrangement of structural features might exert good activity, and the replacement of the peptide bond with a thiazole surrogate proved to be functional. As for many AMPs and

peptidomimetics reported in literature, the positively charged branches play a determinant role in the activity, as compounds devoid of the arginine appendage lack antibacterial activity both in wild type and knock-out strains. The symmetric amino groups of compounds such as **51**, lacking the arginine but still showing basic character, are apparently not sufficient to hold the positive charge and correctly interact with the bacterial membrane. Moreover, Boc protection of the arginine residues led to loss of antibacterial potency (**74** *vs* **72** and **75** *vs* **73**). It can be speculated that the hindrance generated by the protective group prevent the molecule from interacting properly with the cellular membrane.

Concerning the portion of the molecule that is seems to be more important to confer antibacterial potency, the central core seems to play a role. Indeed, carbazole central core appears to be detrimental for activity especially if compared to analogues having as central nucleus a benzophenone (**75**) and a benzene (**77** and **78**). Interestingly, all these molecules have an aromatic moiety attached to the thiazole peptide-bond surrogate, mimicking a phenylalanine or tryptophan branch. However, also the isoleucine mimic was found to exert good activity on this strain, also coupled to the carbazole central core. Therefore, it can be speculated that less constrained central nuclei are able to confer good activity, and aliphatic branches such isoleucine are as well tolerated and suitable for activity.

When tested against other bacterial strains, either wild type or knock-out for some genes, the following general considerations based on the obtained MIC values can be made.

In general, contrary to what was observed with *E coli* Δ*tol*C, **73, 81**, **77** and, to a lesser extent, **78**, failed to show any hint of activity (with the only possible exception being represented by **73** against *E.faecium*). On the contrary, **74** and **75**, despite the MIC values are far from being optimal in a drug discovery campaign, were found to show a measurable improvement of activity toward all the strains being evaluated. Between the two, **75** surely emerged as the hit compound to be used for further structural refinement. More in details, **75** showed to be slightly active on *E.coli* Δ*mdt*E, Δ*mdt*F. This MIC value is the

same obtained against *E.coli* WT, meaning the compound is only partially substrate of the mdtE and mdtF efflux systems. Similarly, the compound is moderately active against *E.coli* Δ*omp*C underling as it might be substrate of these porins system(MIC=16μg/mL). On the contrary, it is inactive against E.coli Δ*mar*R lacking the mar repressor and consequently characterized by over expression of tolC. This result suggest as the compound might not be substrate of this subunit of the tolC efflux pump. To be noticed, both compounds showed a slight selectivity toward *E.coli* strains rather than for *P. aeruginosa* and *E fecium*, highlighting that this selectivity might be due to the structural features of the molecules. These results also confirm the superiority of the benzophenone core compared to the carbazole. In addition, phenylalanine seems to be the best amino acid mimic to attach to the thiazole. These considerations may help in the synthesis of ameliorated analogues.

In summarizing the information gathered at this moment, it can be affirmed that arginine plays a crucial role in the activity against both Gram-positive and Gram-negative bacteria, and its absence results in a loss of activity. Assuming its presence, cyclic structures such as the more constrained carbazole, or benzophenone and benzene, prove suitable for antibacterial activity in the central core. While the differences in activity are relatively negligible, it appears that central cores allowing for a higher degree of rotational freedom (such as benzophenone and benzene) compared to carbazole exhibit better antibacterial activity. Additionally, **74**, **77**, and **78** show slight activity against *M. tuberculosis*.

Moreover, the amino acid branch attached to the thiazole peptide bond surrogate does not seem to significantly influence the antibacterial activity of the compounds. However, it appears that the benzyl appendage might impart a slightly higher potency against Gram-negative bacteria. Further modifications may offer the potential to achieve selectivity of action for these molecules.

4.3.4. Cytotoxicity assay

A preliminary investigation on the cytotoxicity of the synthesized compounds was carried out to determine if intermediate and final molecules might have toxic effects on selected cell models, such as HEPG2 ***(Table7).***

Compound	HepG2	Compound	HepG2
49[1]	36.2 ± 1.1	**74**[2]	33.4 ± 0.4
51[1]	11.3 ± 1.5	**73**[2]	>37
52[1]	>37	**80**[2]	>37
53[1]	5.6 ± 0.1	**81**[2]	>37
54[1]	>37	**75**[2]	>37
55[1]	12.7 ± 3.2	**77**[2]	>37
56[1]	34.7 ± 0.3	**78**[2]	>37
57	>37		

Table 7. *Cytotoxicity results (IC_{50}) for compounds presenting [1]intermediate general structure **g** and [2]final structure **i***

It was very encouraging to assess that all of those compounds showing an inhibitory activity on bacterial cell line, and in particular our hit derivatives **74** and **75**, were able to combine an acceptable antibacterial profile with moderate-to-low toxicity. Unfortunately, compound **53** showing a promising activity toward *M.tuberculosis,* resulted to be among the most toxic ones. Under the structural point of view, it is reasonable to assume that compounds bearing the arginine moiety as charged portion have less propensity to be cytotoxic to eukaryotic HepG2 cells. These encouraging results confirmed that the rationale design based on the maintenance of a specific equilibrium between lipophilic and hydrophobic portions is a focal point to obtain molecules endowed with good antimicrobial activity and low toxicity. Since only one eukaryotic cell line was considered, additional evaluations on different cytotoxicity models need to be reported.

4.3.5. Lysis assay

Based on the results above described and compound availability, **74** was selected for further analysis. First, a lysis assay was performed in order to determine if the compound displays its antimicrobial activity through a bactericidal or bacteriostatic mode of action. The assay was performed on the bacterial strains of interest, *E. coli*, *S. aureus*, *B. subtilis*. Since melittin served as basis for the peptidomimetic design and due to its mode of action, it was used as a control antibiotic.

	MIC (µg/mL)		
	Melittin	**74**	**CIP 0.5**
E.coli ΔtolC	2	64	0,025
S.Aureus	8	2-4	0,16
B.Subtilis	8	0,5	0,4

Table 8. *MIC values for melittin and **74** against E.coli ΔtolC, S.aureus Newman and B.subtilis DSM10*

Figure 48. clearly shows melittin arresting growth in the first 5h after exposure for both *B.subtilis* ***(Figure 48A)*** and *S.aureus* ***(Figure 48B)*** at both tested concentrations (2xMIC and 4xMIC). However, in both cases we observe regrowth, meaning that the compound is either acting as a bacteriostatic or concentration-depended bactericidal, and we would need to increase the exposure concentration to observe full lysis with no regrowth. Contrarily to melittin, **75** acts as a concentration-depending bactericidal on *S.aureus* ***(Figure 48D)*** and bactericidal on *B.subtilis* ***(Figure 48C).*** As per *E.coli*, no arresting in the growth was detected for both melittin ***(Figure 48E)*** and **75** ***(Figure 48F),*** even though a time-dependent bacteriostatic effect can be observed at both concentration for **74.**

From the results obtained, we can conclude that both melittin and **74** result in a different lytic effect on Gram-positive and Gram-negative bacteria. However, whereas melittin show a bacteriostatic behaviour, **74** exerts its action through a highly desirable bactericidal mechanism of action toward Gram-positive bacteria, although the same clear results is not seen in the case of *E.coli* Δ*tol*C , a Gram-negative microorganism. It is reasonable to speculate that the different membrane structures of the two bacterial strains play a role in this difference, especially in the case of molecules that have bacterial membrane as the primary target.

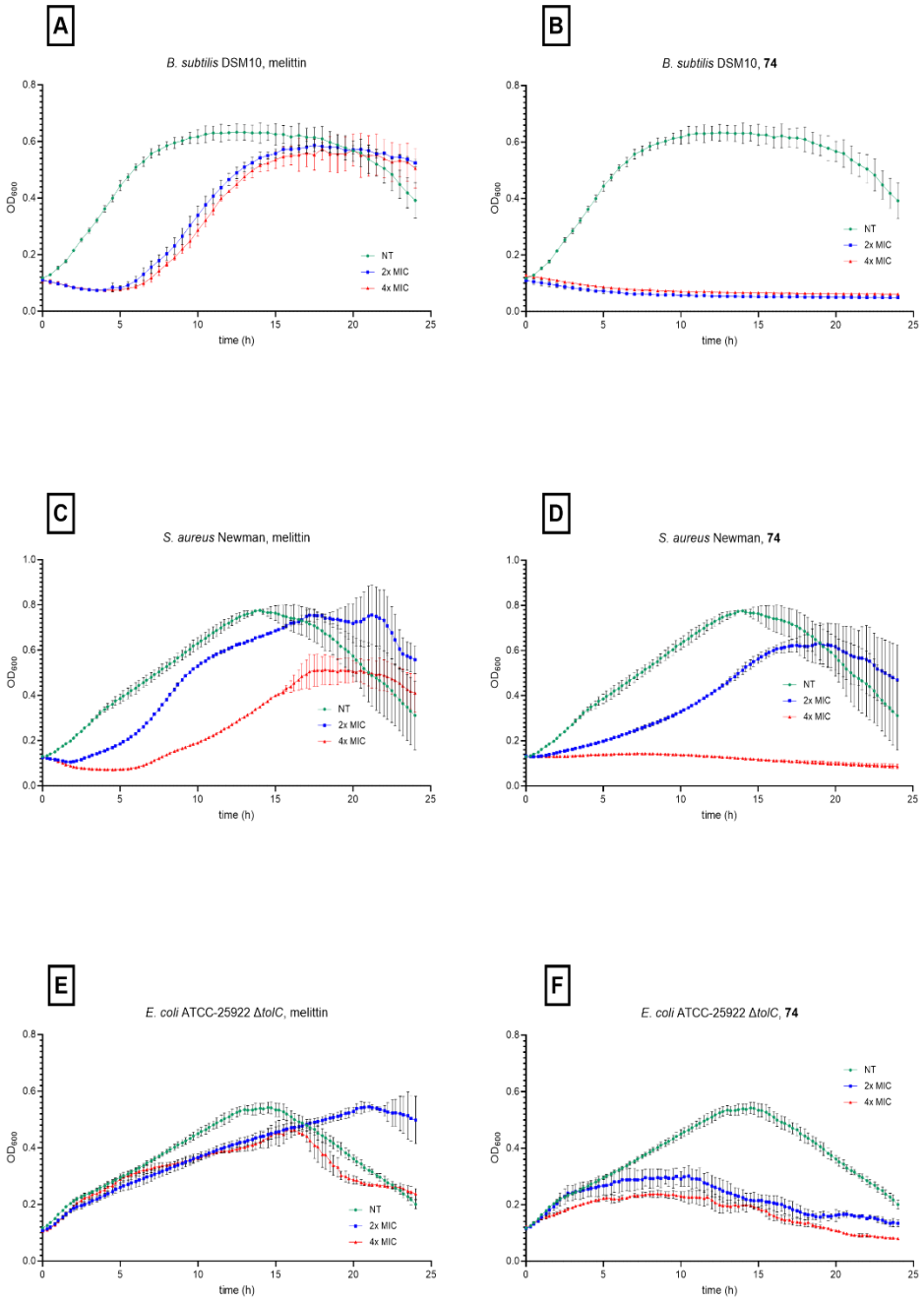

Figure 48. *Lysis curves for melittin (A,C, and E) and for* **74** *(B,D, and F) against B.subtilis (A and B), S.aureus (C and D) and E.coli Δ tolC (E and F).*

4.3.6. Time -kill curves (TKC) assay

After assessed the bactericidal activity of **74**, its killing kinetics was evaluated. Both melittin and **74** have a fast bactericidal effect against *B.subtilis*, with an effect that is practically overlapping ***(Figure49A,B).*** Concerning the other strains, melittin was found to be bacteriostatic against *S.aureus* at 8xMIC, ***(Figure 49C)*** whereas it fails to show bactericidal effect on *E.coli* Δ*tol*C at both the tested concentrations ***(Figure 49E).*** On the other hand, **75** showed a fast bactericidal effect on *E.coli* Δ*tolC* strain ***(Figure 49B,F)*** without any regrowth in the following 24hs. Concerning *S.aureus*, after a quick bactericidal behaviour at both concentrations, bacterial regrowth ***(Figure 49D)*** was detected after 10 hours. These data do not correlate perfectly with the lysis assay, and the reason of this discrepancy can be due either to resistance development or to bacterial persistence. As such, a resistance development analysis was conducted (see next section), demonstrating that this peculiar behavior should be due to intrinsics persistence rather than acquired resistance.

Summing up, with regards to **74**, killing kinetics correlate partially well with the data on lysis obtained against both Gram-positive and Gram-negative bacteria. On the contrary, melittin results fast bactericidal against *B.subtilis* and *S.aureus* at 8xMIC **(*Figure 49A,C*)** *but* no effect is reported for *E.coli* Δ*tol*C ***(Figure 49E).***

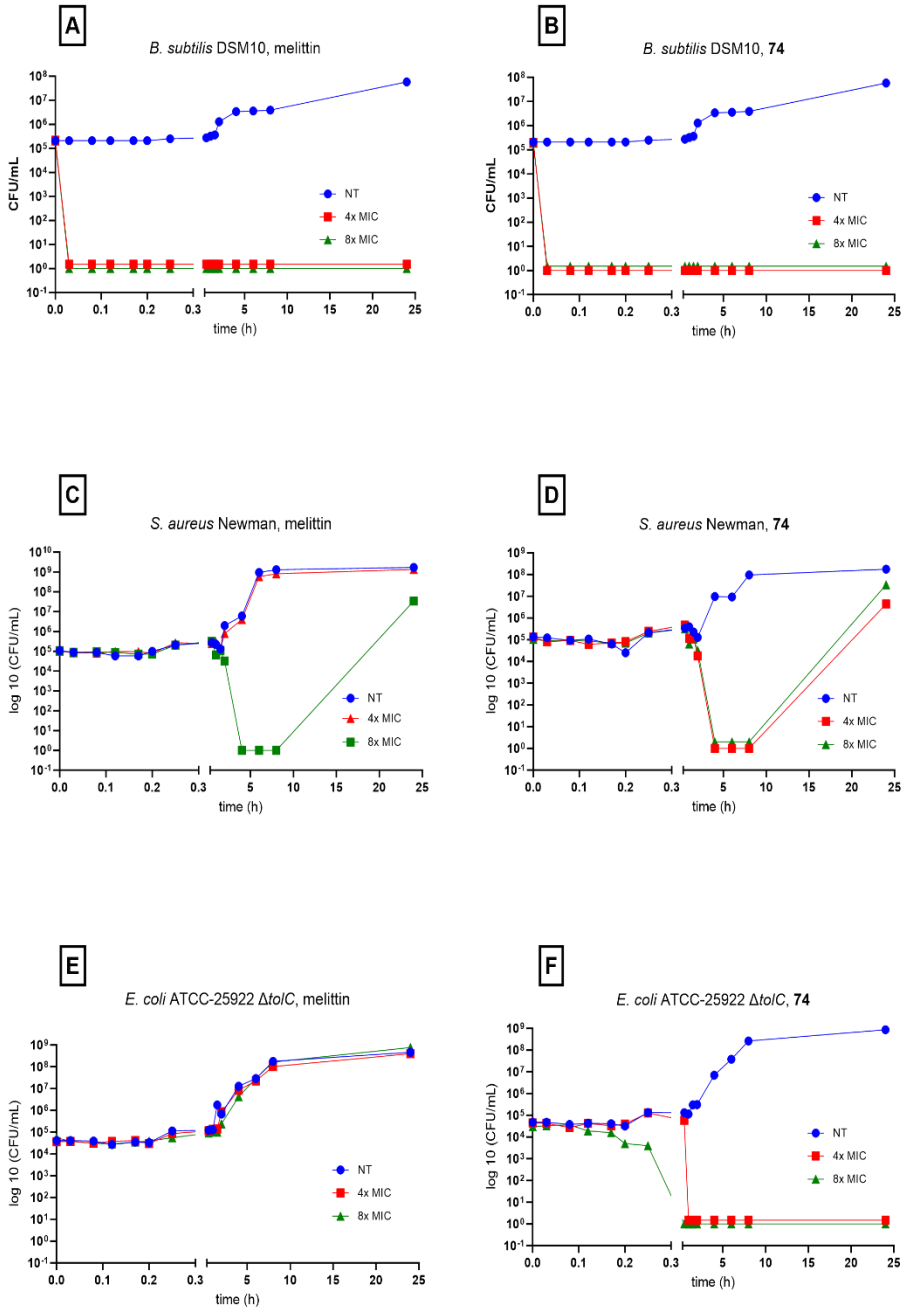

Figure 49. *Time-killing curves for melittin (A,C, and E) and for* **74** *(B,D, and F) against B.subtilis (A and B), S.aureus (C and D) and E.coli Δ tolC (E and F).*

4.3.7. Resistance development

A resistance development analysis was carried out with the aim to identify an additional target and to evaluate how quickly bacteria become resistant to our molecules. At first, this study was carried out on **74**, since, as above reported, it was accidentally taken as the hit compound. We therefore determined the frequency of resistance (FoR) after 48h (no colonies observed after the first 24h) to be 2.4 x 10^{-6} at 4x MIC and 3.5 x 10^{-8} at 8x MIC. MIC shift showed that the clones obtained from selective plates are not resistant to **74 (*Table* 8).** Afterward, a liquid resistance development was performed for **75** against the selected strains and no regrowth was observed after 48h against *B.subtilis* and E.coli, while a slight turbidity was detected on *S.aureus* liquid culture. This led us us to choose this culture to perform a FoR after 48h for **75**. Since no colonies were observed after 48h, we were pleased to conclude that the selected strains are not resistant to **75**.

Strain	SRM	X x MIC	MIC [µg/mL] **74** to confirm R	MIC [µg/mL] CIP
B. subtilis DSM10	WT	-	2	0.2
	74^{R} #1	4	4	0.4
	74^{R} #2		2	0.2
	74^{R} #3	8	2	0.4
	74^{R} #4	8	1	0.2
	74^{R} #5	8	1	0.2
	74^{R} #7	4	1	0.2
	74^{R} #10	4	2	0.2

Table 9. *Determination of MIC shift for clones obtained from selective plates during resistance development. SRM, spontaneous resistant mutant; R, resistance; CIP, ciprofloxacin.*

4.3.8. Membrane depolarization assay

In order to determine if **75** leads to membrane depolarization and study its interaction with the bacterial membrane, a comprehensive analysis of the depolarization effect of the cytoplasmic membranes of both Gram-positive and Gram-negative bacteria was conducted for **75** and then a comparison with melittin was carried out. The bacterial membrane potential was determined according to the procedure reported by Epand et al.[138]

Figure 50 clearly shows that both melittin and **75** lead to a membrane depolarization in the selected bacterial strains which occurs in a concentration dependent manner ***(Figure 50A,F).*** Melittin seems to have a stronger depolarization effect on *B.subtilis* and *E.coli* Δ*tol*C compared to **75** ***(Figure 50A,B,E,F),*** whereas the depolarization effect is the same for both the tested molecules in the case of S.aureus ***(Figure 50C,D).*** Of note, in this latter case, **75** shows a faster depolarization effect if compared to melittin ***(Figure 50C,D)*** based on the time points at which the fluorescence is detected.

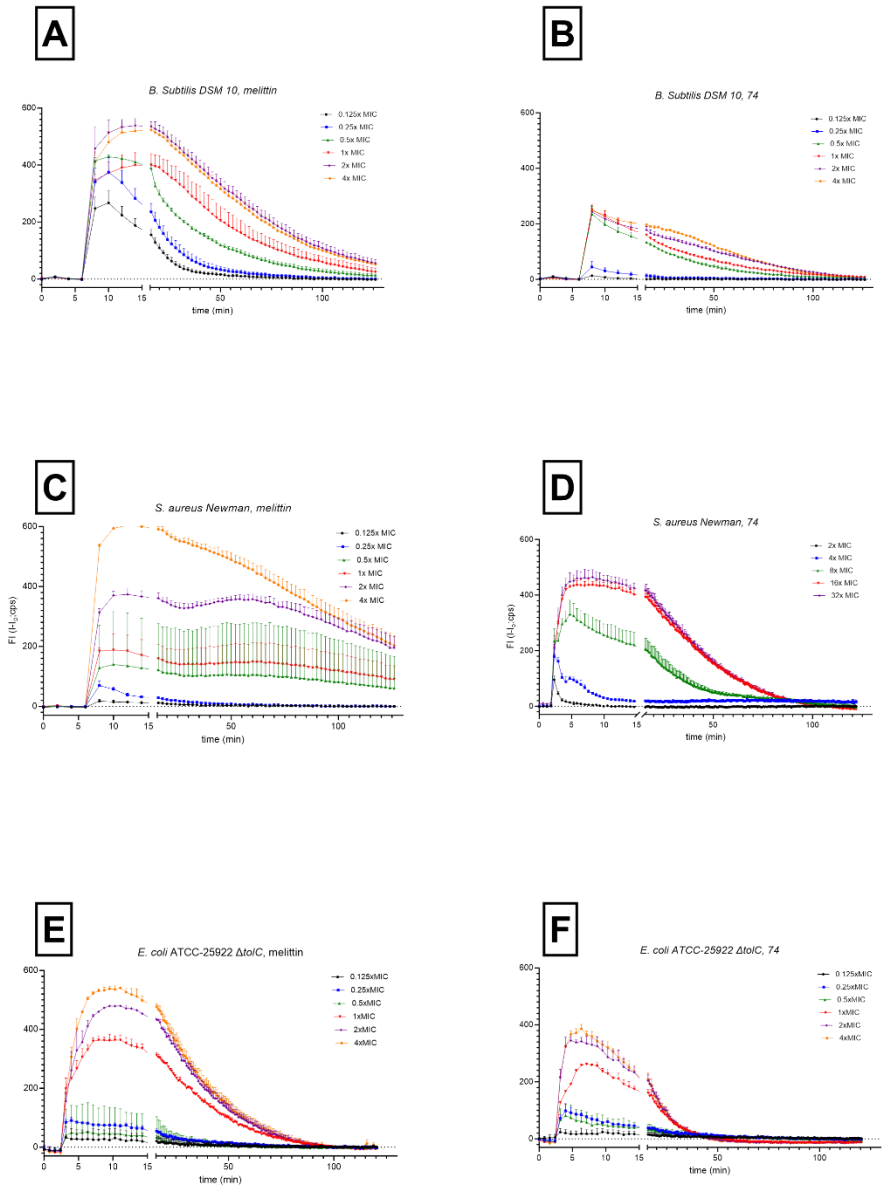

Figure 50. *Membrane depolarization curves for melittin (A,C, and E) and for 75 (B,D, and F) against B.subtilis (A and B), S.aureus (C and D) and E.coli Δ tolC (E and F).*

Overall, **75** induces fast membrane depolarization in all the three analysed bacterial strains proving as the tested compound alter the membrane potential leading to the membrane cell disruption. However, others specific experiments are required to define the exact mode of action which lead to the bacterial

membrane potential alteration and if the leakage of intracellular ions is related to the direct disruption of bacterial cell membrane or to the formation of pores on the membrane.

4.3.9. Electron microscopy analyses

Since AMPs are reported to act forming pores in the membrane, and with the aim of gaining deeper insight into the precise mechanism responsible for the lytic effect of compound **75**, a comprehensive set of analyses utilizing scanning electron microscopy (SEM) and transmission electron microscopy (TEM) was undertaken. Based on the previous results related to the antimicrobial activity of this compound, the *S. aureus* strain was chosen as reference strain to conduct the electron microscopy analysis. First a preliminary SEM analysis was carried out comparing the effect of compound **75** and melittin on *S. aureus* by using different concentration (2xMIC and 4xMIC) of compound. Unfortunately, no holes were identified neither in samples treated with compound **75** nor with melittin which has been used as control compound since it is known to act by forming pores in the bacterial membrane as reported in **Chapter 2**. The extracellular material which is visible is connecting material which is not treatment-specific since it is present in both treated and untreated samples. We can clearly affirm that no relevant differences could be spotted from the images since different concentration of compound **75** or melittin do not seem to affect the bacteria structure at different time points up to 60 min (15 min **Figure 51**, 30 min **Figure 52**, 60 min **Figure 53**).

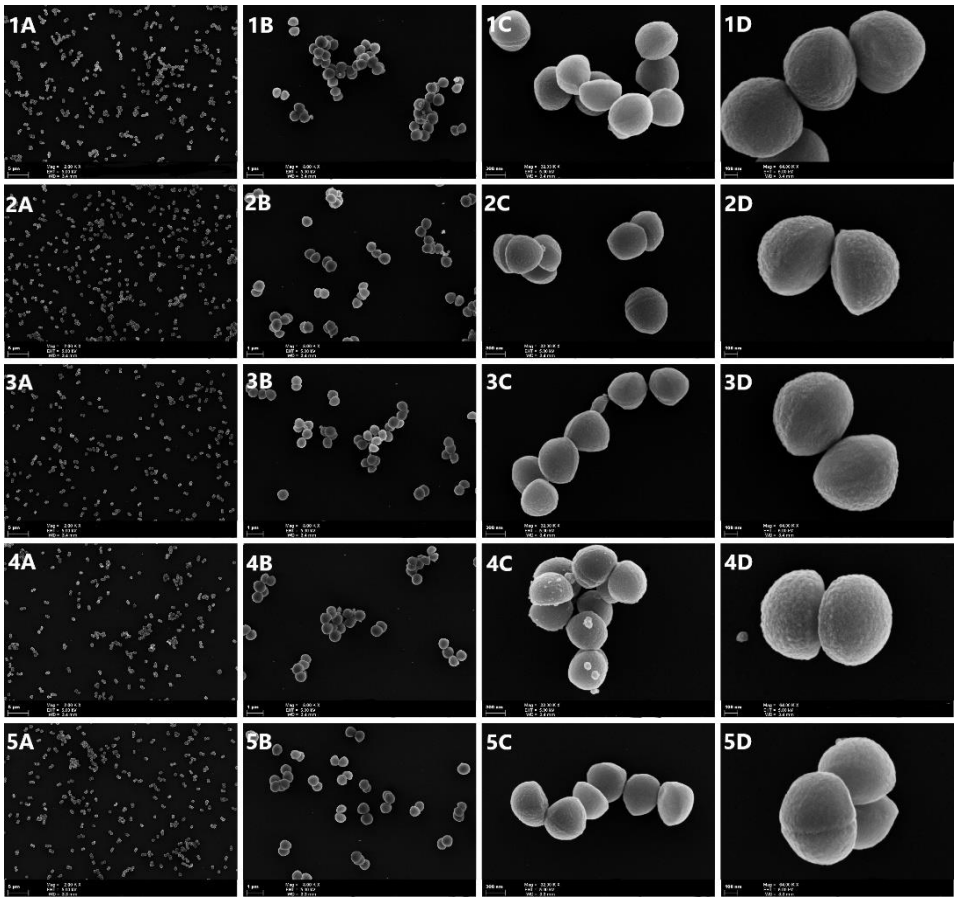

Figure 51. *SEM micrographs of S.aureus bacteria at **15 mins** after addition of compound 75 compared to the non treated samples at different magnifications.* **1**=*non-treted,***2**=*2x MIC 75,* **3**=*2X MIC melittin,* **4**=*4x MIC 75,* **5**=*4x MIC melittin.* **A**= *5µm,* **B**=*1µm,* **C**=*300nm,* **D**=*100nm.*

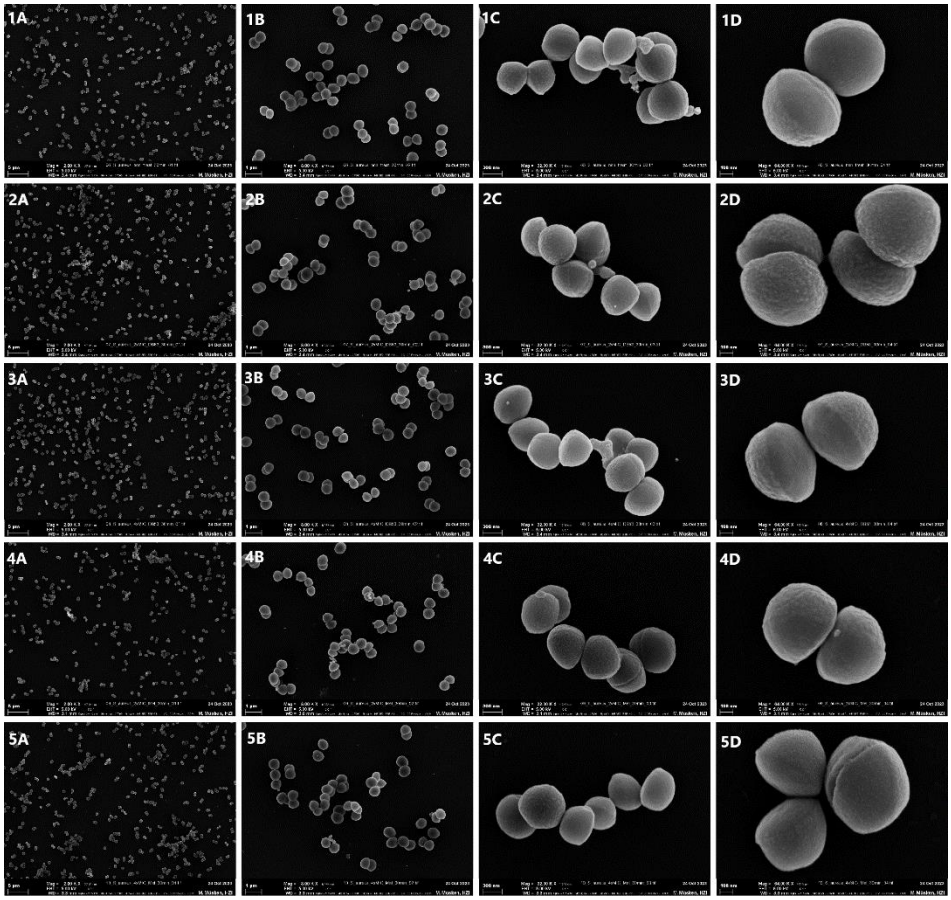

Figure 52 *SEM micrographs of S.aureus bacteria at **30 mins** after addition of compound* **75** *compared to the non-treated samples at different magnifications. 1=non-treted,2=2x MIC* **75** *3=2X MIC melittin, 4=4x MIC* **75**, *5=4x MIC melittin. A= 5µm, B=1µm, C=300nm, D=100nm.*

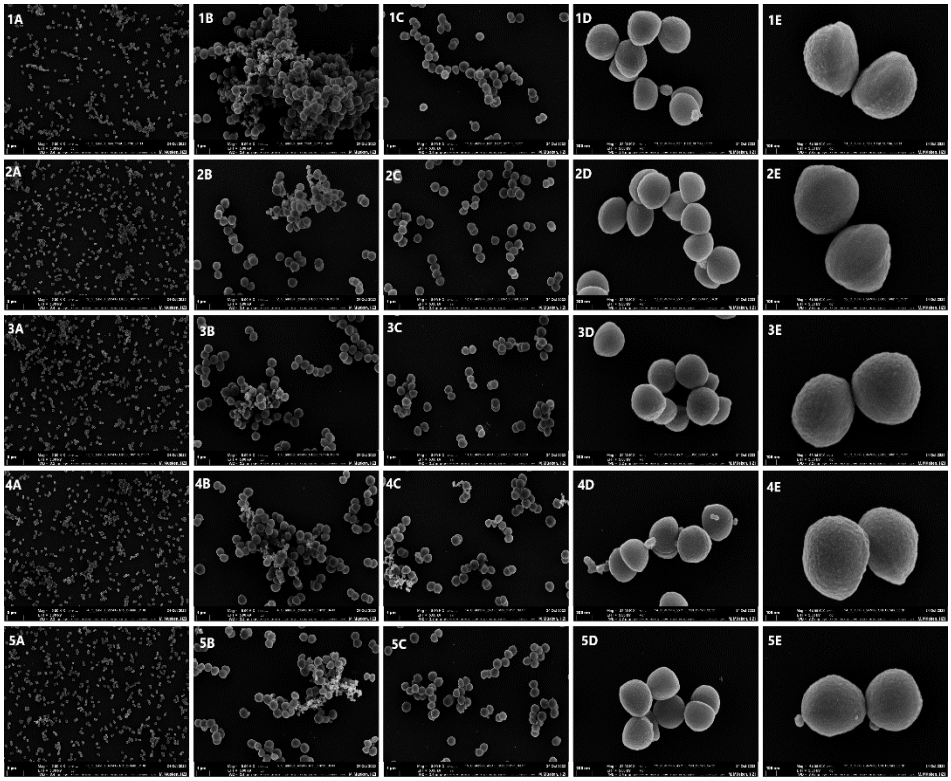

Figure 53 *SEM micrographs of S.aureus bacteria at 60 mins after addition of compound* **75** *compared to the non-treated samples at different magnifications. 1=non-treted,2=2x MIC* **75***, 3=2X MIC melittin, 4=4x MIC* **75***, 5=4x MIC melittin. A= 5µm, B=1µm, C=300nm, D=100nm.*

To confirm that neither compound **75** nor melittin had any effect on the membrane structure of *S. aureus* at these concentrations, a more detailed analysis was conducted through TEM analysis of the *S. aureus* samples treated with compound **75** and melittin at 4xMIC at 60 min. Unfortunately, also in this case no significant results could be identified comparing untreated and treated samples **(Figure 54).**

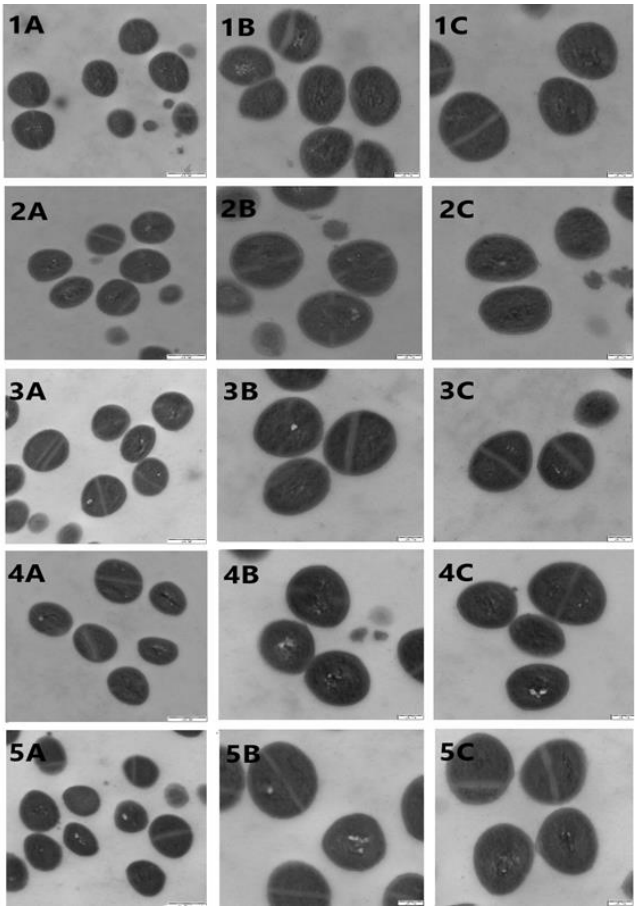

Figure 54. *TEM micrographs of S.aureus bacteria at 60 mins after addition of compound* **75** *and melittin compared to the non treated samples at different magnifications.* **1**=*non-treted,***2**=*2x MIC* **75***,* **3**=*2X MIC melittin,* **4**=*4x MIC* **75***,* **5**=*4x MIC melittin*. **A**= *500nm,* **B**=*200nm,* **C**=*200nm.*

To investigate more in depth, SEM analysis was performed increasing the concentration of the treated samples up to 10x MIC of both compound **75** and melittin and analysed at 15min, 30 min and 60 min **(Figure 55).** As reported in **Figure 55-2B,D** some extra cellular material can be distinguished but it is difficult to identify it as cytosolic material or as material shading off the cell surface since no clearly damaged cells are visible. It is not connecting material as seen in the previous experiment **(Figures 51, 52 ,53)** since it is not present in the untreated samples but only visible in samples treated with compound **75**

both at 15 min **(Figure 55-2A-D)** and 60 min **(Figure 55-5A-D).** Surprisingly more evident differences between the untreated and treated samples were detected after 15 min than after 60 min**.**

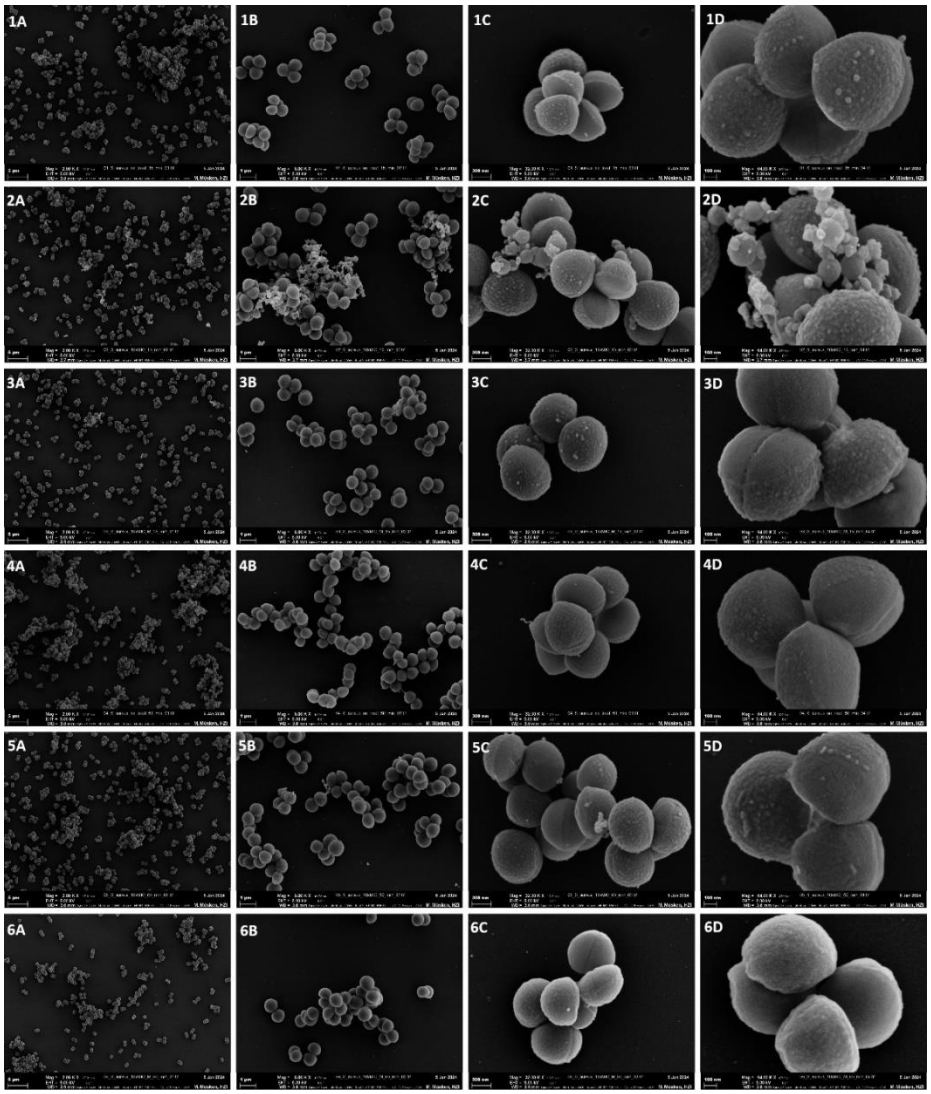

Figure 55 *SEM micrographs of S.aureus bacteria at 15 min and 60 min after addition of compound* **75** *or melittin compared to untreated samples at the same time points and different magnifications.* **1**=*non-treted at 15 min,***2**=*10x MIC* **75** *at 15min,* **3**=*10x MIC melittin at 15min,* **4**= *non-treted at 60 min,* **5**=*10x MIC* **75** *at 60 min,* **6**=*10x MIC melittin at 60 min.* **A**= *5µm,* **B**=*1µm,* **C**=*300nm,* **D**=*100nm.*

These first encouraging results led us to conduct a further TEM analysis on these samples (10x MIC compound **75** and melittin at 15 min and 60 min after treatment). In this case, both compound **75** and melittin seem to have an effect on the plasma membrane if compared to the untreated samples, although there is a slight difference on their mode of action **(Figure 56** and **Figure 57).**

Melittin after 15 min from treatment seems to determine the formation of electron-dense, membrane-like structures **(Figure 56-3C,3D)** while treatment with compound **75** after 15 min results in some brighter events in the cell **(Figure 56-2C,2D).** Additionally, compound **75** leads to the formation of vesicle-like structures which appear empty **(Figure 56-2C).** This last result is in line with what observed in the previous SEM experiment **(Figure 55-2D)** which identified some extracellular material which can be now defined as vesicles formed after treatment with compound **75**, not with melittin.

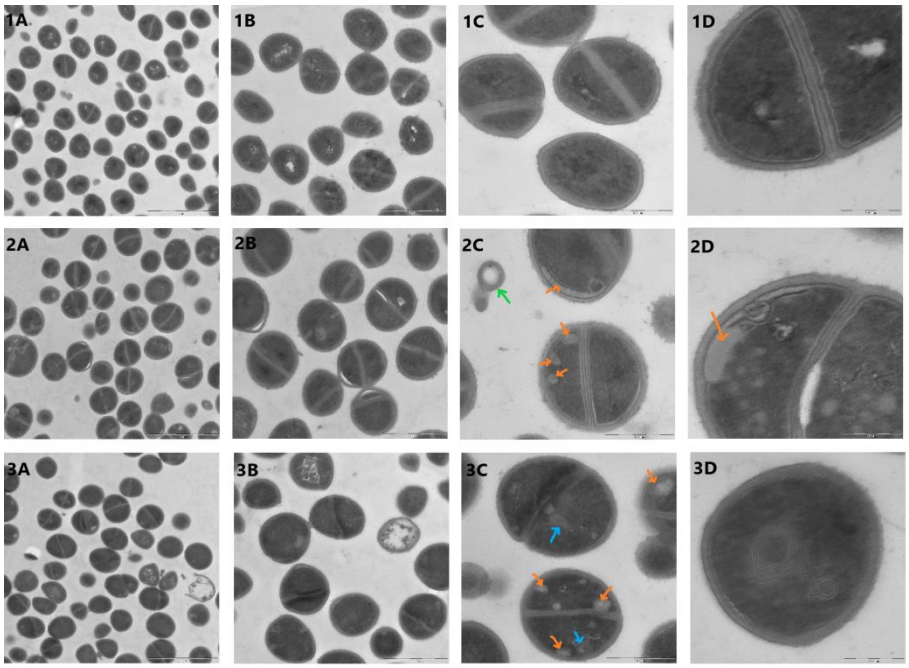

Figure 56 *TEM micrographs of S.aureus bacteria at 15 mins after addition of compound* **75** *or melittin compared to untreated samples at different magnifications.* **1**=*non-treted,***2**=*10x MIC* **75**, **3**=*10x MIC melittin,* **4**. **A**= *2µm,* **B**=*1µm,* **C**=*500nm,* **D**=*200nm. Green arrows=vesicle-like structures, Orange arrows= vacuole-like structure, Ble arrows= electron-dense, membrane-like structures.*

Following 60 minutes of treatment, vacuole-like structures became notably more pronounced in samples treated with compound **75** (**Figure 57-2C and 2D**), whereas they were only marginally present in samples treated with melittin (**Figure 57-3C**).

Vesicle like structures are still present in samples treated with compound **75 (Figure 57-2B)** while electron-dense, membrane-like structure are visible only in samples treated with melittin **(Figure 57-3C)** and not present in samples treated with compound **75 (Figure 57-2C)**

These preliminary results allow us to affirm that compound **75,** which showed a better antimicrobial activity compared to the reference compound melittin, acts in a different way. It leads to the formation of vacuole like structures which are slightly present in samples treated with melittin, whereas they are characterized by the presence of electron-dense, membrane-like structures which are not present in samples treated with compound **75**. The exact mode of action of compound **75** still needs to be deeply investigated, but the formation of vesicles is a peculiar characteristic of compound **75**, which cannot be detected after treatment with melittin.

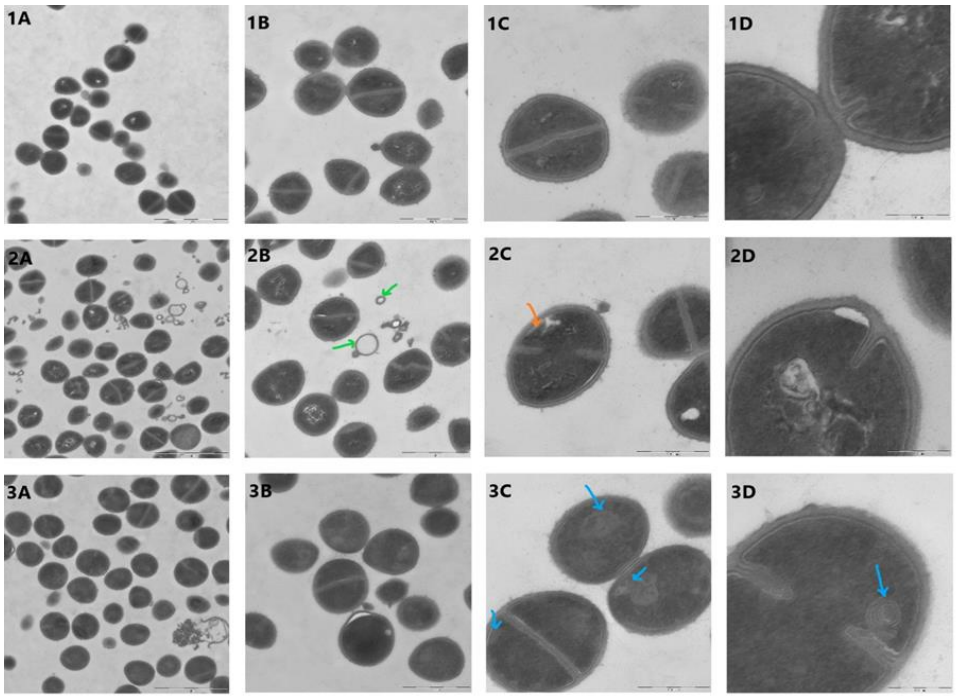

Figure 57 *TEM micrographs of S.aureus bacteria at 60 mins after addition of compound* **75** *or melittin compared to untreated samples at different magnifications.* **1**=*non-treted,****2***=*10x MIC* **75**, **3**=*10x MIC melittin,* **4**. **A**= *2µm,* **B**=*1µm,* **C**=*500nm,* **D**=*200nm. Green arrows=vesicle-like structures, Orange arrows= vacuole-like structure, Ble arrows= electron-dense, membrane-like structures.*

4.3.10. Tag-74 design, synthesis and antimicrobial activity evaluation

As previously reported, in order to perform an affinity based proteomic analysis, the tagged form of **74** was synthetized. Based on literature evidence[132,139], an aryl-diaziridine fluorescent probe has been chosen for the proteomic analysis.

A coupling reaction was carried out using HATU and DIPEA as coupling reagents. Reaction occurred between the activated carboxylic moiety of the diaziridine probe and the free amine group in **74** structure. Since in this structure two symmetric amine groups are available for the coupling reaction two different tagged derivatives of **74** were synthetized: **tag-74 -H1** bearing the diaziridine probe only on one side and **tag-74-H2** bearing the probe at both the amine sides.

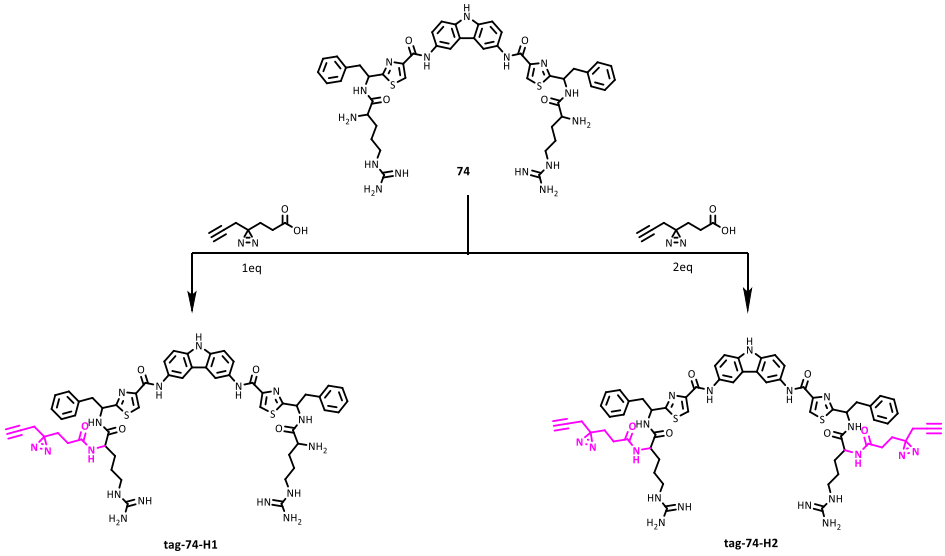

Scheme 5 *Synthetic route for tag-74-H1 and tag-74-H2*

In order to verify if the new tagged compounds maintained the same antimicrobial activity of the parent peptide and if they could consequently be used in further proteomics analysis, the MIC was evaluated ***(Table 9)***. Both of

them showed an antimicrobial activity comparable to **74** against *B.Subtilis*, *S.Aureus* and E.Coli Δ*tolC*. **tag-74-H2** was easier to synthetize and was therefore chosen to be used in proteomic studies.

	MIC (µg/mL)				
	B. Subtilis	*S. Aureus*	*E.coli WT*	*E.coli* Δ*tol*C	*E. Coli* Δ*acr*B
CIP	0.05	0.2	0.1	0.05	0.1
74	1	16	64	16	32
tag-74-H1	4	4-8	≥ 64	8	32
tag-74-H2	4-8	8	≥ 64	64	≥ 64

Table 10. *MIC evaluation for tag-***74***-H1 and tag-***74***-H2 compared to 74 and CIP.*

4.3.11. Proteomic approaches to 74 target identification

One of the aims of this project was the mode of action determination of the identified leading compound. Based on the positive results initially obtained for **74** against *B.Subtilis*, *S.Aureus*, *E.coli ΔtolC* and *P.aeruginosa* a comprehensive affinity/activity based proteomic analysis was planned.

This technique requires to tag the compound of interest with a fluorescent probe, represented in this case by the aryl-diaziridine portion consequently the parent compound **74** was synthetized in great amount then functionalized by adding the probe portion in prof. Hirsh lab, obtaining the **tag-74** A general workflow for this approach is reported in ***Figure 54***. [140]

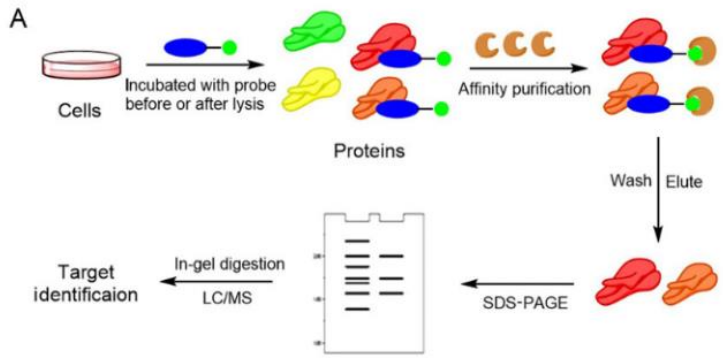

Figure 58. *General affinity based proteomic workflow.*

The tagged compound is first incubated with cell lysates to facilitate the covalent attach of the tagged compound to its target proteins. This step is followed by a purification step by using affinity chromatography in order to selectively bind the probe-protein complexes to collum beads. Then non bound proteins are selectively removed through washing steps consequently followed by target proteins elution. The obtained target proteins are then identified by using gel electrophoresis methods and digested in order to be analysed by LC–

MS/MS.Unfortunately, the affinity based proteomic analysis hasn't been conducted on **tag-74**, since the antimicrobial activity initially reported for the parent compound **74** wasn't reproducible and further biological analysis underline as this compound (**74**) is fast bactericidal consequently excluding the possibility of an antimicrobial activity related to membrane target interaction. For these reasons, a global proteomic approach has been chosen. Cells are treated with the compound of interest, then proteins are extracted, digested to peptides, and analysed by LC-MS.

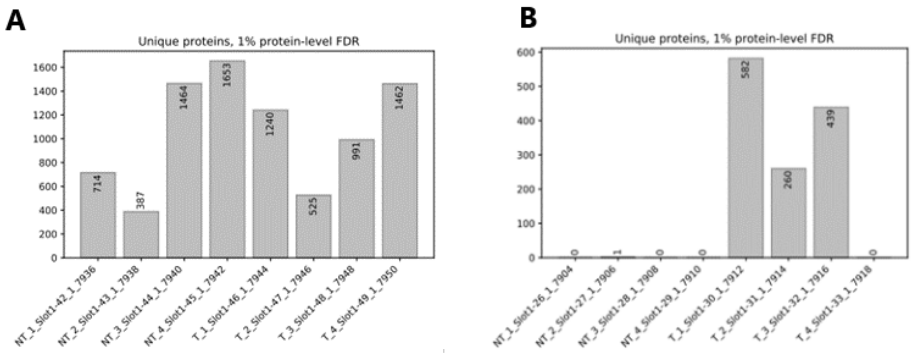

Figure 59. *Unclassifiable results from global proteomic assay. Amount of detected proteins in treated (T) and non-treated (NT) samples of E.coli* **(A)** and *B.subtilis* **(B)**.

The analysis of the whole proteome has been conducted on the three bacterial strains of interest against which **75** showed activity (*B.subtilis*, *S.aureus* and *E.coli ΔtolC*). Unfortunately, I could not obtain any relevant results, since, in some of the analysed samples of treated and non-treated *B.subtilis* ***(Figure 55B),*** no proteins fragments could be detected and other samples showed such a low amount of proteins that are not sufficient for reliable analytical considerations ,. Similarly, this happened for the *E.coli* Δ*tol*C samples ***(Figure 55A).*** Additionally, a final report for the analysis conducted on *S.aureus* hasn't been produced by the instrument since there were no proteins fragments detected in any sample. These unclassifiable results prevented a further and deep analysis and might depend on systematic errors on the analysis development leading to plan to repeat the experiment.

4.4.Conclusion

During the period spent at HIPS, I have tried to collect information on the biological activity of the compounds synthesized and also to define the mode of action of some of the most promising compounds such as **74** and **75**. First and foremost, the majority of the synthesized compounds demonstrated activity against both Gram-positive and Gram-negative bacteria, albeit in the medium micromolar range. This confirms the rationale behind the design. Notably, the most active compounds did not exhibit significant activity against fungal species or mycobacteria. Given the different structure of the bacterial cell wall for these microorganisms, this data may somehow corroborate the action of my molecules on bacterial membrane. In terms of Structure-Activity Relationship (SAR), the presence of arginine is crucial to ensuring sufficient antibacterial activity. Conversely, the central core and the thiazole branch appear to have a lesser impact. This information is valuable and represents a positive aspect, as this part of the molecule, especially the thiazole portion, can be strategically exploited in the hit-to-lead optimization process to modulate physicochemical characteristics and/or ADMET properties. In addition to the activity against wild strains, a minimal effect of efflux pumps, regulators, and porins was revealed through comprehensive Minimum Inhibitory Concentration (MIC) analysis against strains lacking specific efflux systems.

Cytotoxicity evaluation was also carried out for all the tested compounds, highlighting the lack of relevant toxicity. Moreover, these compounds have also a remarkable stability, again complying with the design rationale Lysis assays allowed to define the lytic character of **74** which leads to direct bacterial lysis within half an hour with no recover. Furthermore, a membrane depolarization assay was conducted to determine the membranolytic properties of the compound. As anticipated, the results indicated rapid membrane depolarization, signifying that the compound interacts with the membrane and leads to its complete disruption. Additionally, a time-killing assay demonstrated the compound's fast bactericidal effect against the three selected bacterial species.

In a resistant development assay, it was revealed that the compound does not induce resistant development in the tested strains. According to these assays, this compound clearly shows a different behaviour against Gram-positive and Gram-negative bacteria, resulting in a faster bactericidal and increased lytic effect for Gram positive instead of Gram-negative. Therefore, the obtained results allowed us to define the selected compound as a fast bactericidal compound, which induce cells death through the disruption of the bacterial membrane through a membranolytic mechanism of action without interaction with specific membrane or intracellular targets.

As a support to the investigation of the mechanism of action for these compounds more in-depth analyses like global proteomic investigation were performed. Unfortunately, it failed in confirming the previous results, prompting us to repeat the assays.

Moreover, the effects of representative **75** and melittin on the *S. aureus* cells were characterized by SEM and TEM. Differently from melittin, compound **75** induces the formation of vacuoles within the cell structure. This peculiar characteristic represents a significant information in favor of further investigations of these peptidomimetics.

4.5.Experimental procedures

4.5.1. Chemicals and general methods for purification and analysis

Commercial reagents were purchased as reagent grade and used without further purification. Solvents for RP-HPLC were purchased as HPLC grade and used without further purification. Solvents and chemicals were all purchased from Sigma–Aldrich (St Louis, MO, USA).

Analytical HPLC

The analytical HPLC was performed by UPLC-MS (ThermoScientific Dionex Ultimate 3000 UHPLC System coupled to a ThermoScientific Q Exactive Focus with an electrospray ion source) using an Acquity Waters Column (BEH, C8 1.7 µm, 2.1 × 150 mm, Waters, Germany) at a flow rate of 0.250 mL/min with detection set at 210, 254, 290, and 310 nm, and the mass spectrum recorded in a positive mode in the range of 100−700 m/z. The solvent system was 0.1% formic acid in H_2O (Solvent-A) and 0.1% formic acid in MeCN (Solvent-B). The gradient program began with 10% of Solvent-B for 1 min and was then increased to 95% of Solvent-B over 5 min and held for 1 min, followed by a decrease of Solvent-B to 10% over 0.3 min, where it was held for 1 min.

Preparative RP-HPLC

Preparative RP-HPLC was performed on Waters 600E System equipped with a Waters 2487 dual wavelength absorbance detector at 210 and 254 nm using a DAICEL EC NUCLEODUR HILIC column (5 µm; 100 x 2mm). The gradient (solvent A=0.1% TFA in water and solvent B=0.1% TFA in ACN) began with 5% B for 5 min and was then increased to 30%B over 25 min and held for 5 min, followed by a further inclease to 100%B in 5 min and held for 6 min. Then Solvent-B was decreased to 5% over 0.1 min, where it was held for 1 min. A flow rate of 5.0 mL/min was employed as specified.

Nuclear magnetic resonance (NMR)

Spectra were recorded on a Bruker AVANCE 400 spectrometer at 400 MHz for ^{1}H nuclei and 100 MHz for ^{13}C nuclei at rt in $CDCl_3$. All chemical shifts are reported in parts per million (ppm) and refers to the residual chloroform peak (δ 7.26 ppm) for ^{1}H NMR or the residual chloroform peak (δ 77.1 ppm) for ^{13}C NMR. The ^{1}H NMR shift values are reported as chemical shift δ, multiplicity (s=singlet, d= doublet, t=triplet, q=quartet, m=multiplet, dd=doublet of doublets, td=triplet of doublets, qd=quartet of doublets) and coupling constant (J inHz). ^{13}C NMR values are reported as chemical shift δ.

4.5.2. Synthesis of tag-74-H1 and tag-74-H2

Synthesis of tag-74-H1

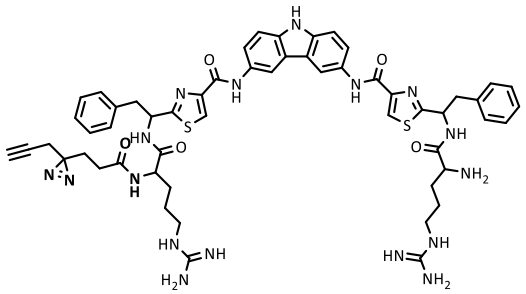

tag-74-H1

To a solution of 3-(3-(but-3-yn-1-yl)-3H-diazirin-3-yl)propanoic acid (0,0017g, 0.001 mmol, 1 eq.) in $DMF_{dry,}$ under a nitrogen atmosphere at rt were added HATU (0.004 g, 0.001 mmol 1 eq.) and DIPEA (0.008 mL,0.005mmol,5eq.). The mixture was stirred at RT for 10 min. Then **74** (0.010g, 0.001 mmol, 1 eq.) was added and the solution stirred at rt for 1h. The solvent was removed under reduced pressure and the product was purified by using preparative HPLC (Dionex UltiMate 3000 UHPLC+ focused, Thermo Scientificand and a Daicel column (5 µm; 250 x 10mm), gradient 30%B in 30min then100 %B in 5 min (1% B/min), flow rate 5mL/min. Elution peaks were collected manually and

analysed by analytical MS-HPLC. Pure fractions were combined and lyophilised obtaining the product as a white powder (1.9 mg, 58% yield).

ESI-MS (m/z): 1103.44$[M+H]^+$; $[M+2H]^{2+}$: 552.72

Synthesis of tag-74-H2

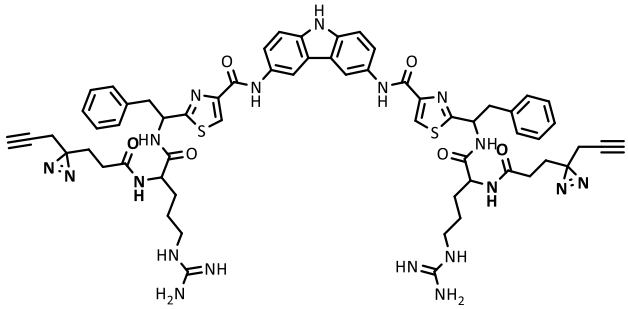

tag-74-H2

To a solution of 3-(3-(but-3-yn-1-yl)-3H-diazirin-3-yl)propanoic acid (0.0025 g, 0.015 mmol, 2 eq.) in $DMF_{dry,}$ under a nitrogen atmosphere at rt were added HATU (0.0057 g, 0.015 mmol 2.2 eq.) and DIPEA (0.013 mL, 0.075 mmol, 5 eq.). The mixture was stirred at rt for 10 min. Then **74** (0.015g, 1 eq.) was added and the solution stirred at rt for 1h. The solvent was removed under reduced pressure and the product was purified by using preparative HPLC (Dionex UltiMate 3000 UHPLC+ focused, Thermo Scientificand and a Daicel column (5 µm; 250 x 10mm), gradient 30%B in 30min then100 %B in 5 min (1% B/min), flow rate 5mL/min. Elution peaks were collected manually and analysed by analytical MS-HPLC. Pure fractions were combined and lyophilised obtaining the product as a white powder (1.9 mg, 10 % yield).

ESI-MS (m/z): 1237.49 $[M+H]^+$; $[M+2H]^{2+}$: 619.74

4.5.3. General methods for biological analysis

MIC evaluation

Minimal inhibitory concentration (MIC) was determined accordingly to the Hancock's protocol.[141] The experiment was conducted on three selected bacteria strains: B.Subtili, S. Aureus and E.Coli *ΔtolC* .

The above-mentioned method requires to first fill a 96-well microtiter plate with 75µL of media (Mueller Hinton II Broth_MHIIB). Then tested compounds are added and serial dilutions are carried out. Finally, bacterial culture adjusted to 5x 10^9 CFU/mL was added and the plates were incubated overnight at 30 °C for B.Subtilis and 37 °C E.Coli *ΔtolC* and S. Aureus. The MIC was then determined by observing the well turbidity and it is considered as the lowest concentration at which no bacterial growth was detected.

In vitro stability evaluation

Metabolic stability assays on compounds **49**, **51**, **74** and **75** were performed in the presence of human liver microsomal (HLM) fractions. Enzymatic co-factors (glucose-6-phosphate (10 mM), NADP+ (2 mM), MgCl2 (5 mM) and glucose-6-phosphate-dehydrogenase (0.4 U/mL)) were dissolved in 100 mM of PBS pH 7.4. HLMs (15 µL) were then added to a solution of 60 µL of co-factors solution and 222 µL of PBS buffer. 3 µL of the tested compound 100nM were added to the samples pre-incubated at 37 ◦C for 5 min. Sample aliquots (50 µL or 100 µL) were collected at 0,5,15,30 and 60 min then the enzymatic reaction was stopped by addition of a solution of internal standard (IS) (100 nM) in ANC (100µL or 200 µL). Samples were centrifuged (16 000 rpc, 10 min, 4 ◦C) and the supernatant directly analysed by HPLC-ESI-MS/MS to progressively evaluate the percentage of remaining tested compound.

Cell Lysis assay

Cell lysis was determined by evaluating optical density (OD) of the three selected bacterial strains during their logarithmic phase growth. The overnight culture of the selected bacteria where firstly diluted to adjust the OD_{600} to 0.5 and treated with 2-fold MIC and 4-fold MIC of tested compounds. The $OD_{600}$was then monitored at different time point (t=0,0.25,0.5,1,2,3,4,6,24,48h)

Time killing kinetics

TKCs were performed by using B.Subtilis, S.Aureus and E.Coli *ΔtolC* cultured overnight in MHBII.

Briefly, the overnight culture was diluted 1:10 to define OD_{600} then used to make a diluted bacterial solution with a starting bacterial count of $1x10^6$ CFU/mL. Compounds were added to to reach the final concentration of 4-fold and 8-fold MIC.

All tested conditions were ran in duplicates in a 96-well plate and incubated at 30°C (B.Subtilis) or 37°C (for S.Aureus and E.coli *ΔtolC*) in a shaking incubator. Samples were taken at 0, 0.25, 0.5, 1, 1.5, 2, 4, 6, 8, 24h and serial diluted in a 96-well plate. Dillution were then spotted on a CASO agar plate (modified Miles and Misra). After drying at room temperature, plats were moved to a 30°C or 37 °C static incubator and colonies were counted by visual observation after overnight incubation.

Frequency of resistance (FoR) determination

Bacterial cultures were plated at different concentration on CASO agar plates containing the antibacterial agent at 4x MIC. Plates were incubated for 24 or 48 hours at 30 or 37°C. Frequency of resistance was determined as ratio between number of bacteria growing divided by number of bacteria in the inoculum.

Resistance development

Bacterial strains were plated on CASO agar plates and incubated in a static incubator at 30° (*B.Subtilis*) or 37° (for *S.Aureus* and *E.coli* Δ*tol*C) overnight. A single colony was then inoculated in tubes containing fresh MHIIB and the liquid culture was incubated in a shaking incubator (180 rmp) at 30° or 37°C overnight with 4-fold and 8-fold MIC concentrations of tested compound.

Based on the OD_{600} of the overnight culture, the volume of culture required to achieve a 5 x 10^9 CFU/plate concentration was calculated and then uniformly spread on the agar plates that were incubated in a static incubator for 24 hours at 30/37 °C. Serial dilution of the overnight cultures was then carried out by plating them on non-selective CASO agar plates and the bacterial growth was then observed leading to determine frequency of resistance related to the number of bacteria on the plate and on the inoculum.

Membrane depolarization assay

Membrane depolarization assay was carried out according to Epand et al.[138]

Gram positive strains: Bacterial cultures were grown overnight in MHBII at 30°C. Cells were collected by centrifugation and washed in a buffer of 250mM sucrose, 5mM and 10mM potassium phosphate (pH 7.0). The supernactant was removed and after three washings, pellets were resuspended in the fresh buffer and futher diluted in buffer 1:10 and used to obtain a suspension with OD_{600} = 0.085 to which a solution of DiS-C_2(5) at a final concentration of 1μM was added. The solution of bacteria and fluorophore was then sampled in a 96-well plate and incubated at room temperature for 7 min, followed by an incubation at 30°C for 7 min, followed by fluorescent measurement at 30-s intervals, which gave a stable baseline. Compounds (0.5 mM stock) were then added at 0.25-, 0.5-, 1-, 2- and 4- fold MIC then fluorescence measurements were taken at 30-s

intervals for 2 hours. Samples were shaken at a stable temperature of 30°C during the experiment where an excitation wavelength of 600 nm and an emission wavelength of 660 nm were used to monitor depolarization.

Gram-negative strains: Bacterial cultures were grown overnight in MHBII at 37°C. Cells were collected by centrifugation, washed and resuspended in MHBII. After three more washings, pellets were resuspended in a buffer containing 20 mM glucose and 5 mM HEPES (pH 7.3). The suspension was diluted in buffer 1:10 and used to obtain a suspension with OD_{600} = 0.085 to which was then added a solution of DiS-C_2(5) at a concentration of 1μM. The solution of bacteria and fluorophore was then sampled in a 96-well plate and incubated at 37°C for 1 hour to equilibrate to a stable baseline. Compounds (0.5 mM stock) were then added at 0.5-, 1-, 2- and 4- fold MIC then fluorescence measurements were taken at 30-s intervals for 2 hours. Samples were shaken at a stable temperature of 37°C during the experiment where an excitation wavelength of 600 nm and an emission wavelength of 660 nm were used to monitor depolarization.

Scanning electron microscopy (SEM)

Bacteria were cultured overnight and diluted in fresh media 1:100 then grown at 30/37 °C until it reached OD_{600}=1. Compounds were then added, the suspension was incubated at 30/37 °C and sampled at 15 min, 30 min and 60 min. 720 µL of this suspension was treated with 80 µL of glutaraldehyde solution Grade I, 25% in H_2O and 200 µL of PFA 25%. Samples where then keep at room temperature for 1 hour and stored at 4 °C.

After two washings in TE buffer (20 mM TRIS, 1 mM EDTA, and pH 6.9), cells were incubated on a Poly-L-Lysine pretreated coverslip for 10 minutes at room temperature. The coverslip was then transferred to 1% glutaraldehyde TE buffer, incubated 10 min at room temperature and washed with the same buffer. Graded dehydration (10%, 30%, 50%, 70%, and 90%) of samples in acetone was carried out for 10 min each, followed by two steps in 100% acetone at

room temperature before critical point drying with liquid CO_2 in a CPD300 (Leica). Coverslips were arranged on aluminium stubs equipped with carbon adhesive discs and covered by sputter coating with a gold palladium film for 55 seconds at 45 mA with a SCD 500 (Bal-Tec).
The analysis was carried out by using a field emission scanning electron microscope Merlin (Zeiss) endowed of Everhart Thornley HESE2 detector and inlens SE detector in a 25:75 ratio with an acceleration voltage of 5 kV.

Global proteomic profiling

Overnight cultures of *B.Subtilis, S.Aureus* and *E.coli* Δ*tol*C were diluted in fresh media 1:100, 0.25-fold MIC of tested compound was added and they were grown at 30/37 °C until early stationary phase (OD_{600} ~1). A control sample was also prepared without addition of compound.

Suspension was centrifuged and surfactant was removed then cell pellets were resuspended in lysis buffer I (470µL, 100mM Tris-HCl, 0.4%SDS in H2O, pH7) and sonicated by using SONOPLUS sonication probe (3x20s, 80% int.). Lysis buffer II (188µL, 100mM Tris-HCl, 9.6%SDS, 1.25% sodium deoxycholate in H2O, pH7) was then added and the samples were sonicated once again (1x10s, 80%int.), followed by incubation at 90 °C for 10 min at 400 rmp and centrifuging at 13000g, 10 min, 4 °C. The supernatant was then transferred to new Eppendorf tubes.

A bicinchoninic acid (BCA) assay using the BCA protein assay kit was then carried out in order to determine proteins concentration (between 50/100µg) in each sample. Dilution series of BSA were prepared in Eppendor tubes (400, 200, 100, 50, 25, 0 µg/mL, 100µL each) and sampled to a 96-well plate. Proteome samples were then diluted 1:20 and 3x25 µL of each sample were then added to the 96-well plate. Working solution (50 parts of reagent A, 1 part of reagent B) was then prepared and 200 µL were added to each well. The plate was then incubated at 30/37 °C for 30 min then the absorption was measured at

562 nm using a TECAN microplates reader. Finally, the proteome concentration was adjusted to the lowest sample concentration by using 0.4% SDS in PBS and samples were transferred in LoBind Eppendorf tubes.

Samples were precipitated by adding 5x volume ice cold acetone (-80°C) and stored overnight at -20°C. Precipitated protein were centrifuged (16900g, 15 min, 4°C) and supernatant was removed. Samples were washed with 1 mL of cold ice methanol (-80°C), resuspended by sonication (1x10s, 10%int) and centrifuged (16900g, 15 min, 4°C). Supernatant was then discarded and samples were stored at -80 °C overnight.

Proteins digestion was then carried out. Pellets were resuspended in 200 µL X-buffer (300 µL, 7 M urea, 2 M thiourea in 20 mM 4 HEPES buffer, pH 7.5). Then 0.8 µL DTT 250mM was added to reduce proteins and after vortexing the samples were incubated at 25°C, 45 min, 450 rmp. Proteins alkylation was carried out by adding 2 µL of 550 mM IAA the solution was then incubated for 45 min at 25 °C, 450 rpm. The reaction was stopped by adding 3.2 µL of 250 mM DTT and incubating 30 min at 25 °C, 450 rpm. 600 µL of 50 mM Triethylammonium bicarbonate (TEAB , pH 8-8.5) was added and proteins were digested by adding 1 µL trypsin (0.5 µg/ µL, Promega VA9000, Trypsin Platinum). Samples were then incubated overnight, 37°C, 450 rpm. Digestion was stopped by adding 8 µL of formic acid 0.1%.

Samples were then desalted by using 50 mg Sep-Pak C18 columns which were first equilibrated by washing the resin with ACN (1 mL), 0.5 mL of elution buffer (80% ACN, 0.5% formic acid) and with 3mL of 0.1% trifluoroacetic acid. Samples were then loaded to the colums , bound peptides were washed with 0.1% TFA (3x1 mL) and 0.5% FA (0.5 mL), eluted with elution buffer (0.75 mL) and collected in 2 mL LoBind Eppendorf. Peptides were dried using a centrifugal vacuum concentrator.

Samples were prepared to be analysed by solving in 1 %FA (1 µg/ µL), sonicating in sonication bath for 10 min and filtration with 0.22µm Ultrafree-MC centrifugal filters.

Analytical analysis

Samples were analysed by using a nano-HPLC system (nanoElute Bruker, Germany) coupled with a timsTOF Pro (Bruker, Germany) and an analytical column Aurora Ultimate CSI 25 cm x 75 µm ID, 1.6 µm FSC C18, gradient 0-85%B in 90 min (A: H_2O + 0.1% FA, B: ACN + 0.1% FA), flow rate 400 nL/min.

Data were processed using DIA-NN (version 1.8.1) and Perseus (version 2.0.5.0). Result values were analysed as log2-values, cut-off for –log p-value was set to 1.3 (p-value = 0.05) and t-test difference >1.0. Proteins which suited these limits were considered as significantly over- or under expressed compared to the wild type.

Chapter5_Synthesis and biological characterization of polymyxin B S-lipidated derivatives

[This page is intentionally left blank]

5.1.Background

5.1.1. Structural features and mechanism of action

Polymyxins are natural lipopeptides produced by *Paenibacillus polymyxa,* a Gram-positive soil bacterium[142] , which were discovered in the 1940s [143]and approved as antibiotics in the late 1950s.[144] They exhibit inhibitory activity towards most Gram-negative bacteria, while gram positive are intrinsically resistant. Nowadays about 37 polymyxin congeners have been isolated[143] despite their use rapidly decreasing in the 1970s because of their nephrotoxicity[144] which results in tubular necrosis aided by accumulation in kidney and brain tissues. Additionally, they can bind to neurons affecting the muscular system. For these reasons, for many decades they have been considered the last resort choice to treat those pathogens which are resistant to the main antibiotic classes such as β-lactams, aminoglycosides and fluoroquinolones. [145] Their use was restricted to the treatment of cystic fibrosis and ophthalmic persistent infections. Otherwise, the recent rise in antibiotic resistance has seen in an increase on the use of polymyxins and despite toxicity issues, indeed they are now employed in the treatment of serious infections caused by multidrug-resistant (MDR) Gram negative pathogens, such as *Pseudomonas aeruginosa, Acinetobacter baumannii, and Klebsiella pneumoniae*.[146]

Polymyxins are cyclic lipopeptides which are produced non-ribosomally and are structurally similar to cationic antimicrobial peptides naturally produced by eukaryotic cells as an innate immune defence against pathogens.[145] From a structural point of view, they are decapeptides characterized by the presence of a distinctive aminoacidic ring and a N-terminal fatty acyl tail The ring is made up of 7 aminoacidic residues forming a loop between the ɤ-amino group of the Dab residue at position 4 and the carboxyl group of the threonine residue at the

C-terminal position. The N-terminal exocyclic tail is constituted by three aminoacidic residues linked to a fatty acid portion.[143,145]

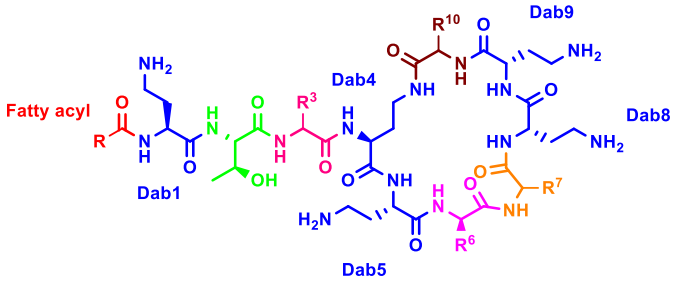

Polymyxin	Fatty acyl	R3	R6	R7	R10
A	(S)-6- methyloctanoyl	D-Dab	D-Leu	Thr	Leu
B1	(S)-6- methyloctanoyl	Dab	D-Phe	Leu	Thr
B2	6-methylhexanoyl	Dab	D-Phe	Leu	Thr
B3	Octanoyl	Dab	D-Phe	Leu	Thr
C	(S)-6- methyloctanoyl	Dab	D-Phe	Thr	Thr
D1	(S)-6- methyloctanoyl	D-Ser	D-Leu	Thr	Thr
E1	(S)-6- methyloctanoyl	Dab	D-Leu	Leu	Thr
E2	6-methylhexanoyl	Dab	D-Leu	Leu	Thr
E3	Octanoyl	Dab	D-Leu	Leu	Thr
M	(S)-6- methyloctanoyl	Dab	D-Leu	Thr	Thr
S1	(S)-6- methyloctanoyl	D-Ser	D-Phe	Thr	Thr
T	(S)-6- methyloctanoyl	Dab	D-Phe	Leu	Leu

Figure 60. *Structure of some of the most studied polymyxins.*

As mentioned, there are many different congeners of the polymyxin family which can be grouped into ten different classes, all of them characterized by the presence of a cyclic heptapeptide and exocyclic tripeptide linked to an N-terminal fatty acyl tail. Position 3 includes a D/L-Dab or D-Ser residue and position 6 contains a hydrophobic residue which can be Phe or Leu. Position 7 is the one that varies the most, indeed it can contain different residues like leucine, isoleucine, valine, norvaline or threonine which always maintain a L-stereochemistry. Position 10 contains L-threonine or L-leucine residues.

Additionally, they showed common features such as the presence of four L-Dab residues always located at position 1,5,8,9 positively charged at physiological pH and at position 2 there is always a L-Thr residue. The N-terminal fatty acid tail can be constituted of one of six fatty acyl groups distinguished by their length which varies from 7 to 9 carbons.[143] These structural features result in amphipathic molecules where the Dab residues provide hydrophilicity and cationic charge, while the fatty acid tail and residue in positions 6 and 7 confer hydrophobicity. These general characteristics result in the ability to bind to Lipid A of Gram-negative bacteria and insert into the membranes hydrophobic core, leading to its permeabilization and disruption, being at the same time responsible for the toxicity against eukaryotic cells.[145]

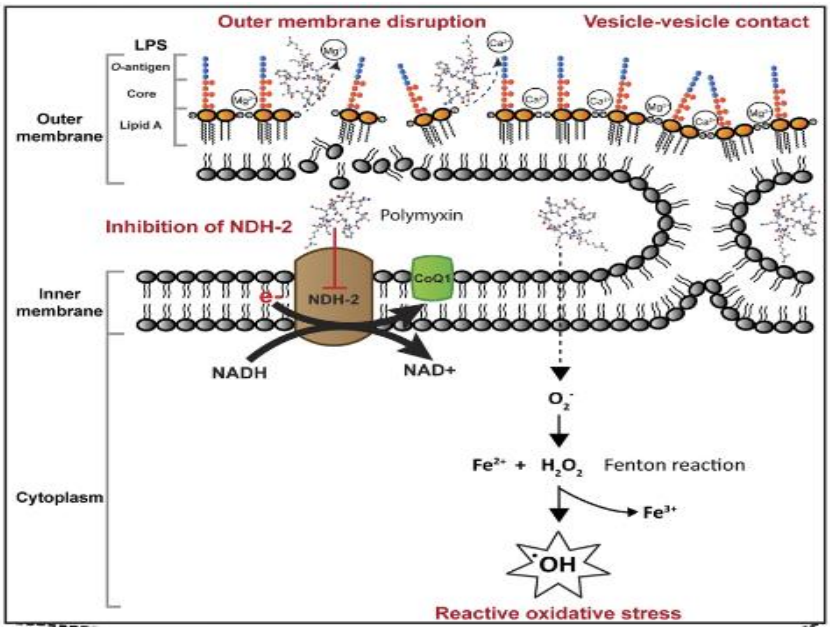

Figure 61. *Mechanisms of antibacterial activity of polymyxins in Gram negative bacteria. Adapted from Ref.144.*

The selectivity for gram-negative bacteria is mainly due to the presence of the outer membrane (OM) which is mostly composed by the negatively charged lipopolysaccharide (LPS). Consequently, the initial polymyxins binding to the OM is due to electrostatic interactions between the positively charged Dab residues of the polymyxin and the negative phosphate groups on the lipid A constituting the LPS. These interactions result in the displacement of the Ca^{2+} and Mg^{2+} ions from the negative charged lipid A phosphates allowing the hydrophobic fatty acid tail of the polymyxin to interact with the LPS's hydrophobic portions inserting deeply into the membrane and enhancing a "self-promoted uptake". The structural integrity of the outer membrane is consequently altered resulting in the leakage of the periplasmic proteins. After that the polymyxin molecules reach the cell membrane (CM) interacting and disrupting it , leading to the release of the cytoplasmic content and the cell death.[144,145,147,148]This mechanism is nowadays still not completely understood, but is now believe to occur similarly to outer membrane permeabilization, where PMB can bind to LPS molecules present at the inner membrane, where

they are assembled by Gram-negative bacteria before transport to their ultimate location at the outer membrane by the lipopolysaccharide transport system (LPT). [149]

Despite the interaction and disruption of the Gram-negative bacterial membrane having been considered as the main mechanism, and the LPS is the initial target, a precise mechanism of action is still partially unclear especially in relation to the interaction with the CM, indeed many hypotheses/models about multiple modes of activity of polymyxins have been proposed.[144] Currently many research groups are indeed working on the identification of secondary mechanisms of action such as the vescicle-vescicle contact pathway which promotes the phospholipids diffusion between inner and outer membrane mediated by vesicles, the inhibition of bacterial respiration related to the effect on the NADH enzyme or the inhibition of reproduction caused by the interaction with specific factors involved in cell division and, the generation of reactive oxygen species which damage the cellular components.[148,150]

5.1.2. Polymyxin B: Structure-activity features

Among the different types of polymyxins discovered, polymyxin B and E (also known as colistin) are the only two used clinically. From a chemical point of view the only difference is the different aminoacidic residue at position 6 which is D-Phe for polymyxin B and D-Lue for Colistin. The commercially available formulations can be administered by different ways including intravenous, intramuscular, inhalational, intrathecal or topical and, only colistin is indicated for oral use in its prodrug form methansulfonate.[151]

Initially, polymyxin B was considered more nephrotoxic than colistin but over the years it was demonstrated that a larger amount of colistin was necessary to equal polymyxin B's efficacy and that both the polymyxins induce renal failure and neuromuscular alteration in the same way. [151] Additionally, it has now been

proven that polymyxin B is less nephrotoxic than colistin and for this reason it has been employed in the treatment of MDR infections in many clinical situations.[152,153]

Polymyxin B is an amphipathic molecule characterized by a cationic cyclic peptide with a lipophilic side tail obtained from *Paenibacillus polymyxa*. It is a mixture of four polymyxin components (B1, B2, B3, and B4) which differ for the fatty acid constituting the side chain and the main components are polymyxin B1 and polymyxin B2.[152]

As previously reported polymyxin B has a poor oral availability which prevents it from oral administration, additionally drug elimination involves renal and non-renal routes but it preferentially accumulates in renal tissue consequently resulting in nephrotoxicity given by oxidative stress, apoptosis, cell cycle arrest, and autophagy.[152]

Based on this evidence, over the past decades many attempts have been made to develop new polymyxins analogues to maintain similar or provide better efficacy avoiding the side effects of nephrotoxicity. Most of them have centred on the modification of the fatty acid attached to the side tail at the N-terminal portion, although aminoacidic residues substitution or modification have also been investigated.[154] Most of them have been extensively described in different reviews.[155–157]

5.1.3. Solid phase peptide synthesis (SPPS)

Two different strategies can be employed for peptide synthesis which are the in-solution synthesis or the solid-phase peptide synthesis (SPPS). The in-solution peptide synthesis involves a coupling reaction between two amino acids, one protected at the C-terminus and the other at the N-terminus. The formed dipeptide undergoes a deprotection step followed by another coupling reaction. Consequently, repeated cycles of coupling and deprotection lead to obtain a

long-protected peptide that can be finally fully deprotected. Unfortunately, this approach requires a purification and characterization step after each coupling or deprotection passage leading to a laborious and time consuming process. [158] Additionally, the activation of the C-terminal COOH moiety in the peptide often promotes the racemization of this C-terminal amino acid. Other issues are related to the poor solubility of the fully protected peptides which lead to reduce the amount of reacting peptides resulting in incomplete coupling reactions.[159,160]

These issues have been overcome by the development of SPPS approach which is based on anchoring *N*-protected amino acids through their C-terminus on a solid support represented by a resin. First step in the solid phase synthesis includes the attachment of the *N*-protected amino acid to the solid support followed by repeated cycles of *N*-terminus deprotection and coupling of the incoming *N*-protected amino acids. Finally, the fully protected peptide is cleaved from the resin and the simultaneous removal of the protecting groups is carried out by treatment with an acidic solution. [158]

SPPS has been introduced for the first time by Merrifield in 1963 and it was a **Boc-SPPS** strategy which includes the use of Boc and Cbz *N*-protected amino acids in the coupling steps, 30% HBr solution for the protecting group removal and NaOH for peptide cleavage from the resin. [161] Over the years many adjustments to this initial procedure have been made in particular Sakakibara in 1967 introduced the HF mediated cleavage which allow the contemporary removal of the acidic labile protecting groups.[162] Unfortunately, the extremely toxic and corrosive nature of HF limited the use of these approach that has been overcome by the discovery of a new base labile protecting group by Caprino et al.[163] in 1970. This laid the foundation of a new strategy introduced by Sheppard et al. in 1978[164] based on the use of Fmoc protecting group which is orthogonal to the Boc and Cbz protecting groups and can be easily removed by using 20% piperidine in DMF. Moreover, the final peptide cleavage is carried out by using a cleavage cocktail made of TFA and specific scavengers such as triisopropylsilane (TIPS) or 1,2-ethanedithiol(EDT) to prevent the reactive

species (e.g. trityl cation) liberated from undergoing undesired side reactions with nucleophilic peptide functional groups. This strategy is known as the **Fmoc-SPPS** synthesis and is the most commonly used approach for peptide synthesis in recent decades.[158]

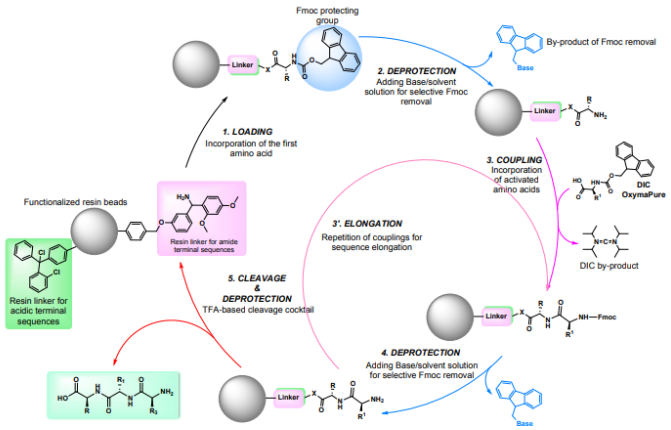

Figure 62. *General scheme of solid-phase peptide synthesis (spps) steps. Adapted from Ref. 158.*

SPPS is the result of the use of many combined elements which have been deeply studied in the past decades to develop different combinations which are best suited for the synthesis of specific peptides. These characteristic components are briefly described below:

- **Resin**

A resin includes a **polymeric solid support** covalently bonded to a **linker** which promotes the first amino acid anchoring to the polymeric solid support. The most common solid supports are the polystyrene and polyethylene glycol(PEG) resins even though many other alternatives are available with different swelling factors which determine the successful obtainment of the final peptide since an high swelling factor results in faster and more complete reactions through enhanced diffusion of reagents and minimized peptide aggregation. On the other hand, the linker is extremely important as well since

it has to be characterized by the ability to link the first amino acid residue in a manner that is highly stable during peptide synthesis but allowing at the same time the final peptide cleavage. It has to be stabile to all the reagents employed in the synthetic procedure leading to obtain a final product in high yield without considerable side products formation. [158] Different linkers are used in both SPPS strategies which allow to define different type of resins for instance Wang resin SASRIN resin, HMBA resin, 2-chlorotrityl resin are used in the Fmoc-SPPS strategy while Merrifield resin, PAM resin, MBPA resin, sulfhydryl resin are employed in the Boc-SPPS strategy.[158,165]

- **Protecting groups**

Appropriate amino acids side chain protecting groups have to be stable to the reaction conditions and consequently chosen based on that. The most common protecting groups used in the Fmoc-SPPS strategy are tert-butyl (tBu), trityl (Trt), tertbutoxycarbonyl (Boc) which are stable in basic environment used for recurring Fmoc removals, but can be removed by acidic conditions given by TFA and the N-1-(4,4-dimethyl-2,6-dioxocyclohexylidene)ethyl (Dde) group which is removed by using hydrazine, providing orthogonality with typical protecting strategies, enabling modifications such as branching or cyclisation of peptide chains on-resin.[166]

- **Coupling reagents**

Coupling reagents are electrophilic activators essential for the amide bond formation in the peptide synthesis, indeed they act by activating the ammino acid carboxylic group to provide a leaving group which is then attacked by the nucleophilic amine.[167] Coupling reagents include different classes even though the main representatives are carbodiimides, phosphonium and aminium/uranium salts.

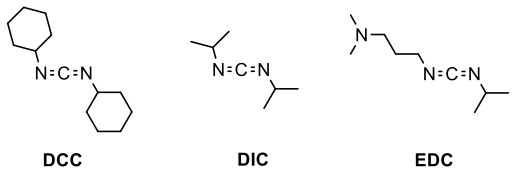

Figure 63. *Carbodiimides as coupling agents..*

The carbodiimide reagent *N,N′*-Dicyclohexylcarbodiimide (DCC) was used for the first time in the peptides synthesis in 1955 by Sheehan et al.[168] The use of this coupling reagent leads to the formation of dicyclohexylurea (DCU) byproduct which is insoluble in most of the organic solvents, consequently reducing the use of DCC as a coupling agent and leading to the development of other derivatives such as DIC, which is soluble in organic solvents and EDC which is a water soluble derivative. The insoluble byproduct formation and the possible epimerization are the main issues in the use of these reagents which can slightly reduce by adding specific additives such as 1-hydroxybenzotriazole

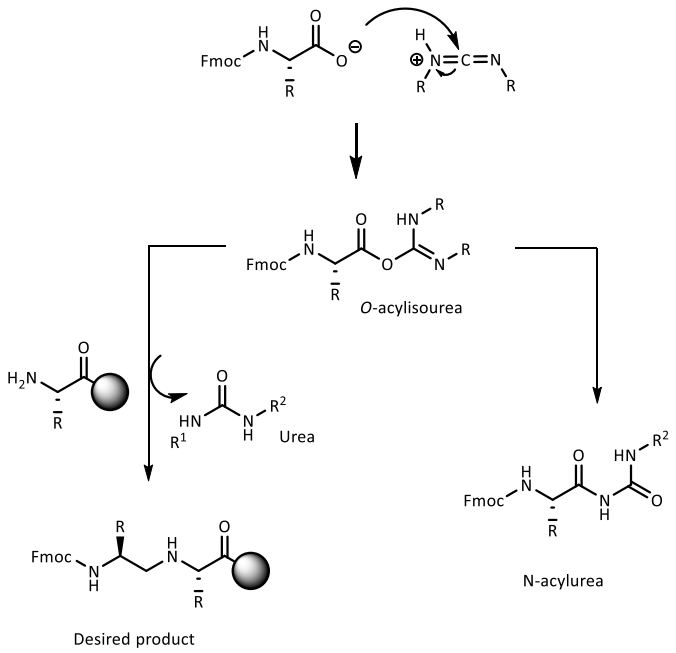

Scheme 6. *Carbodiimide coupling reaction and byproduct formation..*

(HOBt) or 1-hydroxy-7-azabenzotriazole (HOAt) which interact with the *O*-acylisourea intermediate leading to the formation of OBt and OAt esters which are less prone to epimerisation or rearrangement to non-reactive species.[169]

	Aminium/uronium salts	***Phosphonium salts***
HOAt derivates	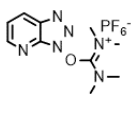 HATU	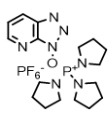 PyAOP 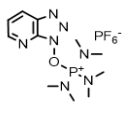 AOP
HOBt derivates	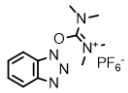 HBTU	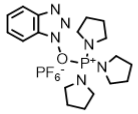 PyBOP 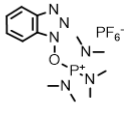 BOP

To overcome the issues related to carbodiimides, aminium /uranium salts (HBTU,HATU), based on HOAt and HOBt structures, have been introduced as coupling reagents becoming the most used even if one of their main issue is

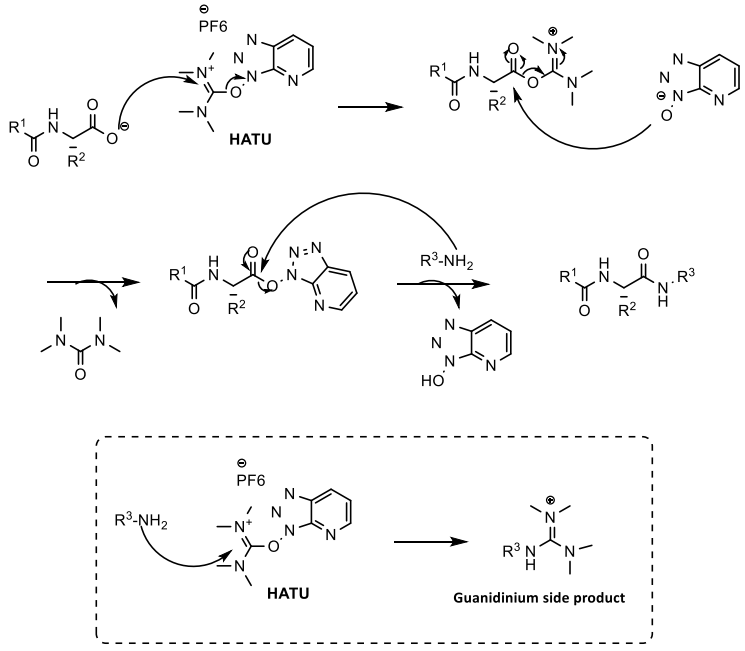

Scheme 7. *Mechanism of coupling reaction with HATU and guanidinium side product formation..*

related to a possible side chain reaction which results in the formation of a guanidinium by-product responsible for the chain elongation interruption. For this reason the incoming amino acids are typically preactivated and the provided in slight excess to the uronium agent to avoid termination side reactions. [169]

The side reaction doesn't occur in presence of phosphonium coupling reagents which includes BOP and PyBOP based on HOBt structure and AOP and PyAOP derived from HOAt. They react with the carboxylic portion of the substrate releasing HOAt or HOBt which then react with the urea derivate leading to obtain Oat or OBt, less reactive esters, as previously described. This property makes them useful for certain reactions such as cyclisation where the C-terminal carboxyl group cannot be pre-activated in the absence of the amino component of the reaction. It is worth nothing that the coupling reaction using BOP generates the human carcinogen hexamethylphosphoramide (HMPA) leading to prefer PyBOP or PyAOP instead of BOP.[170]

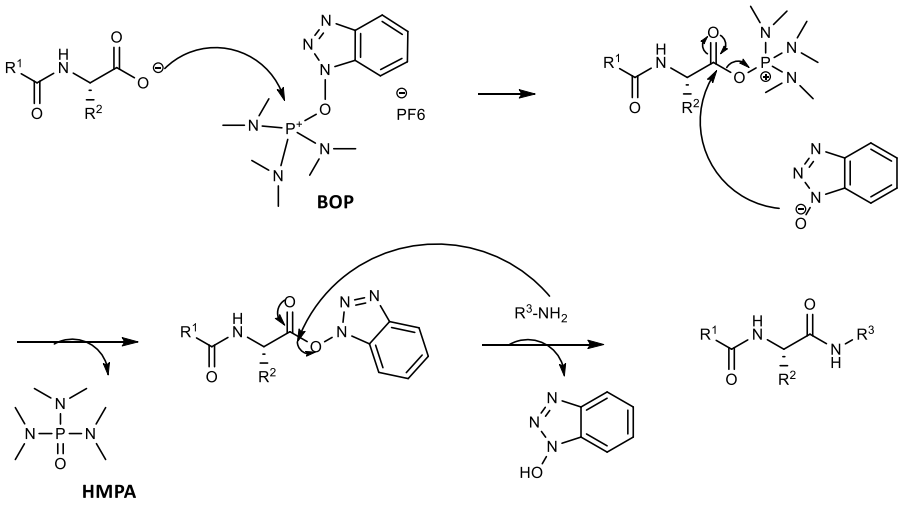

Scheme 8. *Amide bond formation with BOP as coupling agent.*

5.1.4. Synthetic strategies for Polymyxin B total synthesis

Over the years different synthetic polymyxins derivatives have been synthetized. Various synthetic approaches have been employed included in solution synthesis and semi-solid synthesis which is partially in solution and partially solid phase synthesis, even though most of the time the solid phase peptide synthesis (SPPS) was carried out. The different approaches to their preparation can be grouped into three main categories[157]

- *In solution peptide synthesis*→ this approach represents the first attempt of polymyxin total synthesis and has been carried out by Vogler et al. in 1965 based on a condensation approach of three peptide segments. [171] This approach has been soon superseded by the advent of SPPS which offers a more efficient production of synthetic polymyxins.[172]

- *Peptide solid synthesis followed by in solution cyclization*→ many research groups focused on this method, using Thr^{10} residue as anchoring point to the resin.

  First, *Sharma et al.* in 1999 by using the Sasrin resin and protecting the Dab_4 by Dde protecting group obtained the linear peptide by the Fmoc-SPPS technique. The Dde protecting group was then removed by using hydrazine, the protected peptide was cleaved from the resin by using 1% TFA and cyclized in solution using diphenylphosphorazide (DPPA) as a coupling reagent. Finally, the fully deprotected peptide has been obtained after treatment with TFA.[173]

  In 2000 *Tsubery et al*. obtained the polymyxin nonapeptide (PMBN) by using two different approaches. One included the protection of Dab^4 by using Mtt protecting group and the 2-chlorotrityl resin, enabling

cleavage of the Mtt group and C-terminus from the resin with dilute acid while the other Boc/*t*Bu based groups were retained, the other included the use of Wang resin and Dab[4] protected with Boc while the others Dab residues bared the TFA stable Cbz. The linear peptide synthesis was then followed by cleavage, cyclization by using PyBOP and deprotection with TFA.[174]

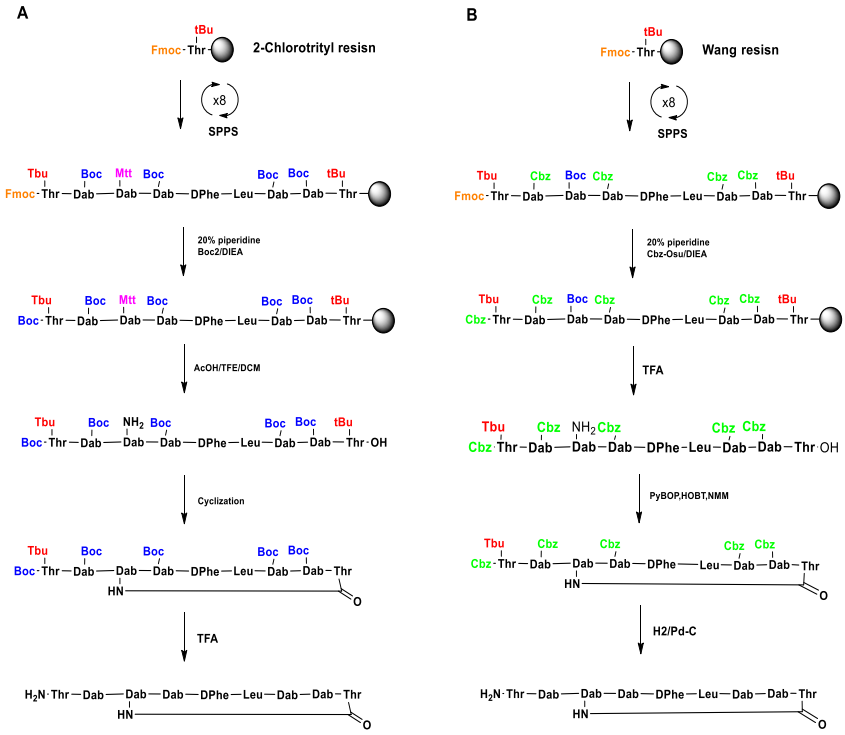

Scheme 9. *Two different synthetic routes to PMBN. Adapted from Ref.174.*

Kline et al. in 2001 used as anchoring point on the resin Leu[7] instead of Thr[10] and experimented the use of 2-chlorotrityl resin, additionally they used Alloc as protecting group on Dab[4]. Then a branched strategy in which the α-amino group of Dab[4] was used as the branch point was carried out followed by in solution cyclization with DPPA and TEA. This strategy allowed to obtain less side products, but the main disadvantage was that position 7 couldn't be modified.[175]

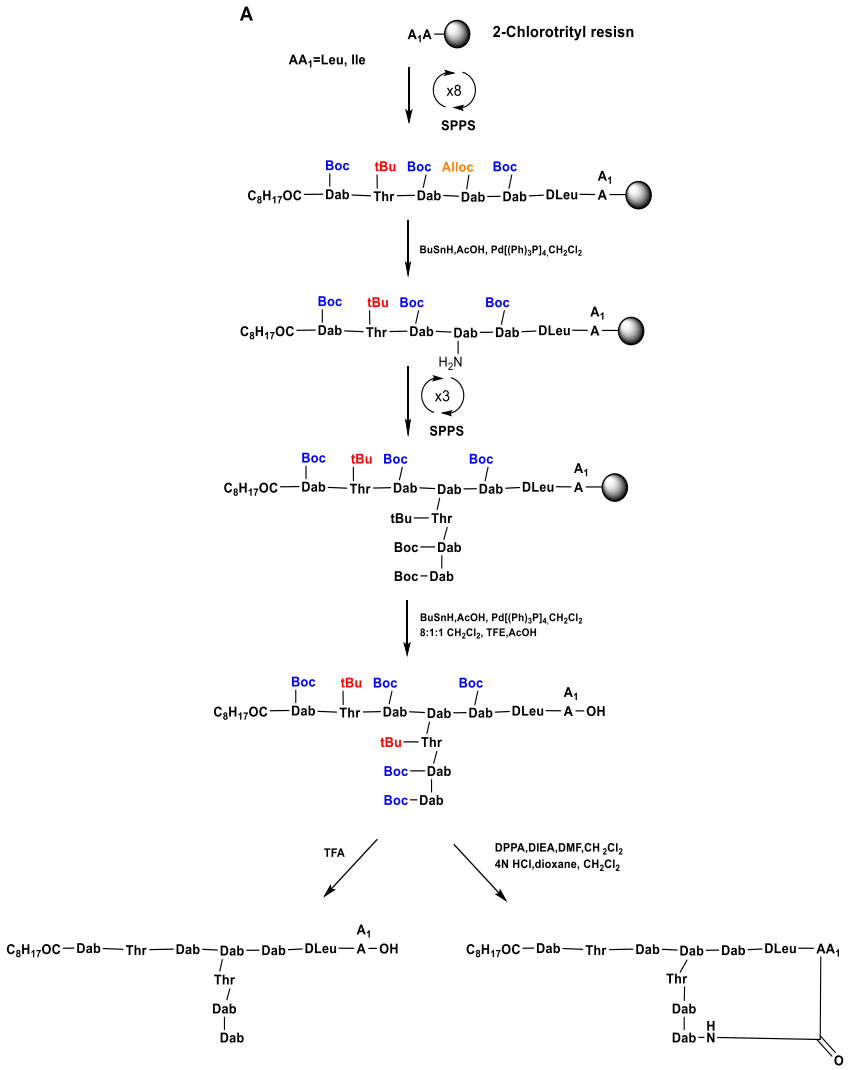

Scheme 10. *Polymyxins SPPS developed by Kline et al. using a branched strategy in which the α-amino group of Dab [4] was used as the branch point. Adapted from Ref. 175..*

Sakura et al. and Vaara et al. in 2009 achieved the total synthesis by using Wang resin and substituting tBu protecting group on Thr10 with a Bzl protecting group. The cleavage performed by using TFA led to obtain the partially protected peptide, consequently cyclization was carried out by using DPPA or PyBOP and global deprotection was achieved with HF or catalytic dehydrogenation.[176,177]

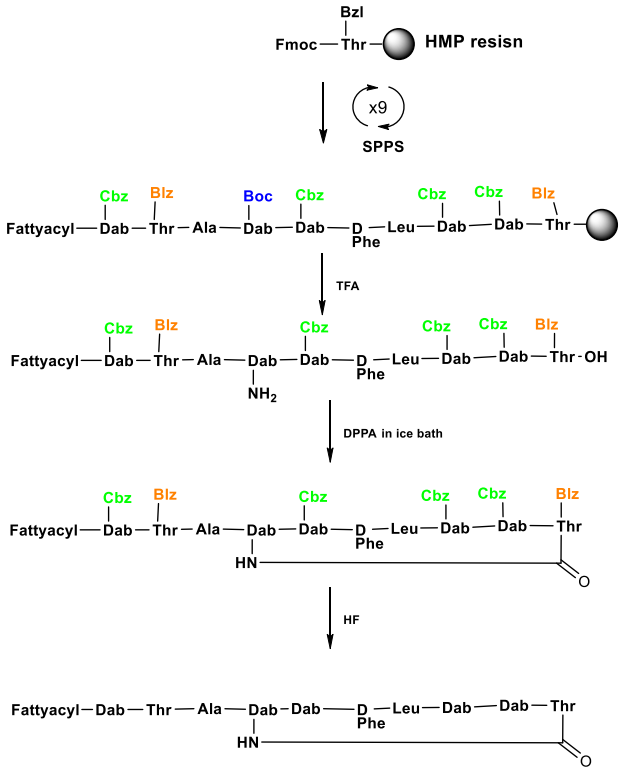

Scheme 11. *Polymyxin B synthetic route developed by Skura et al. Adapted from Ref. 176.*

- *On resin peptide synthesis and cyclization*→ this route was initially explored in order to avoid deprotection issues responsible for side products development during solution cyclization.[157]

Pioneers on this strategy were *Tsubery et al*. which first achieved the synthesis of PMBN derivatives starting by coupling a dipeptide Fmoc-

Dab-Thr(tBu)-OtBu on benzyl chloroformate resin. Boc and tBu protecting groups were then removed by TFA and cyclization was performed on resin by using PyBOP or HATU. The final cleavage was carried out employing TMSBr/TFA getting to the final unprotected nonapeptide. Unfortunately, this method was abandoned since it was arduous, slow, and not efficient enough. [174]

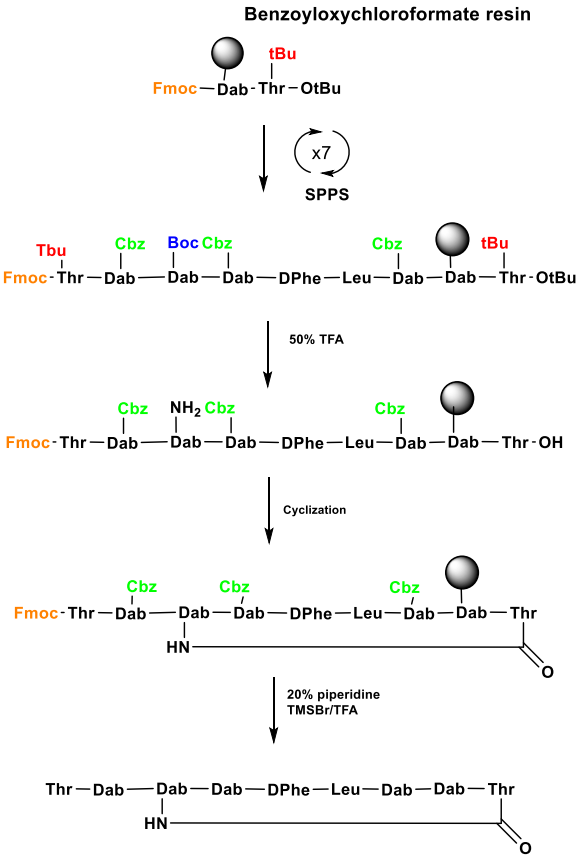

Scheme 12. *Cyclization on the solid support developed by Tsubery et al. Adapted from Ref.174.*

In 2015 *Xu et al.* developed one of the most efficient methods on the SPPS of polymyxins (the synthesis performed in this project is based on this method). They first anchored Dab[9] by its side chain ɤ- amino

groupon 2-chlorotrityl chloride resin as Fmoc-Dab-OAll to avoid side reactions between Dab amine or carboxylic group and the resin. Then a total Fmoc-SPPS synthesis was performed by using 20% piperidine in DMF for Fmoc removal and HCTU as coupling agent. The Dde protecting group used for Dab^4 was then removed orthogonally and Fmoc-Thr(tBu)-OH was coupled at the same position. Then the allyl ester was removed from Dab^9 using $Pd(PPh_3)_4$ and $PhSiH_3$, followed by Fmoc removal from Thr^{10}. Cyclization between Dab^9 and Thr^{10} was conducted on-resin using PyAOP, *N*-methyl morpholine (NMM) and HOAt and the cleavage was performed by using the cleavage cocktail TFA/H_2O/ TIPS allowing the contemporary deprotection of the acidic labile groups.[178]

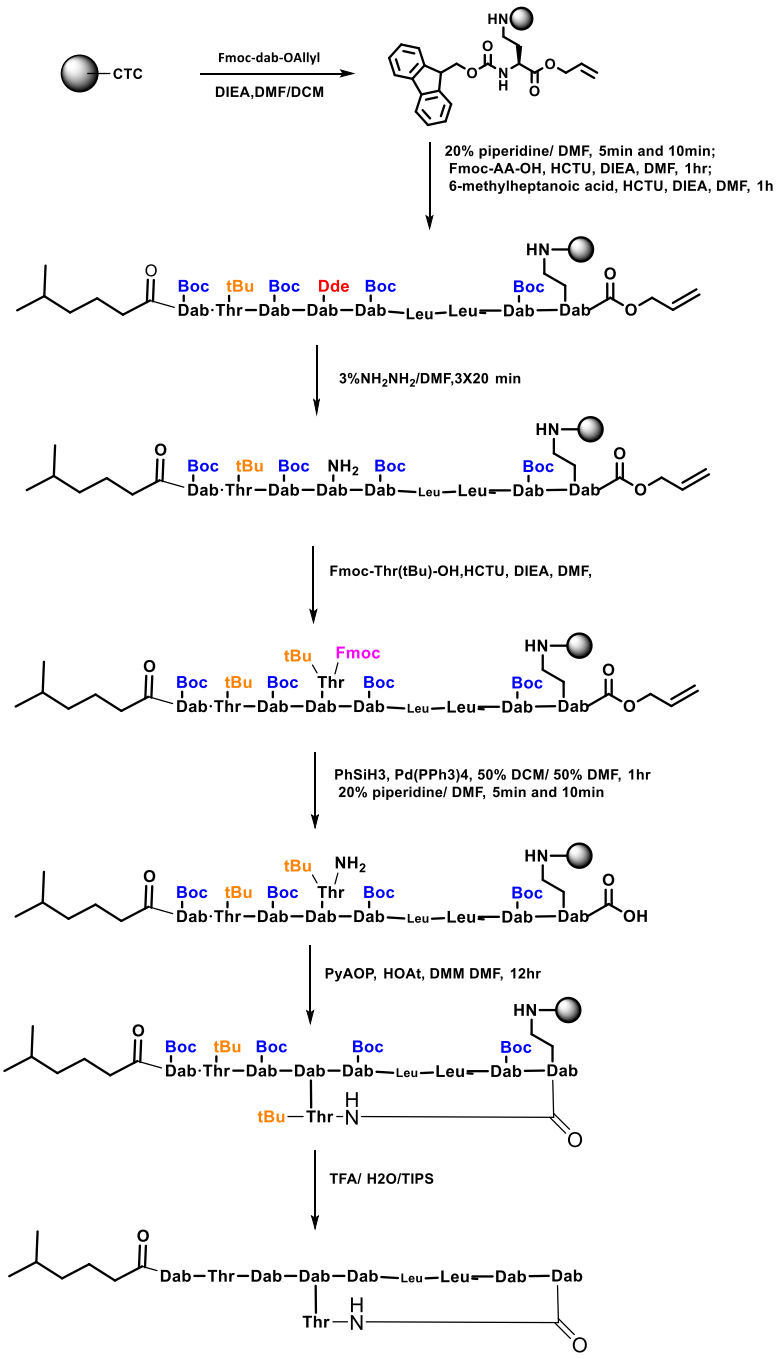

Scheme 13.-*SPPS od polymyxin B using chlorotrityl chloride resin and Fmoc-Dab-OAllyl as anchoring point, developed by Xu et al. Adapted from Ref. 178.*

In 2016 *Cooper et al*. investigated another SPPS based on the anchoring of an *O*-allyl ester Dab[9] to the 4-dihydropyran-2-yl-methoxymethyl polystyrene resin. After Fmoc-threonine O-allyl ester anchoring on the resin, a typical Fmoc chemistry was employed using Boc as protecting group for Dab residues and Alloc for Dab[4] residue. This allow to remove the Allyl-ester portion and deprotect Dab-Alloc residue at the same time, then followed by DPPA on-resin cyclization and TFA mediated cleavage which allow to the total peptide deprotection.[179]

5.1.5. Polymyxin B derivatives

Over the years, due to the increasing emergence of novel MDR bacterial pathogens, many attempts have been made to develop polymyxin derivatives with the purpose of increasing antimicrobial activity and reducing toxicity.[145] Different types of modifications have been investigated at different polymyxin structure levels including modifications at *N*-terminal fatty acyl chain, Dab side chains, Phe[6] and Leu[7] hydrophobic moieties, size of the cyclic peptide ring and, *N*-terminal linear tripeptide segment.[172]

For the purpose of this project, attention will be given to previous works focused on modifications at fatty acyl chain and at Phe[6] and Leu[7] residues.

- **The *N*-terminal fatty acyl chain** of PMB's structure has been demonstrated as essential for the antimicrobial activity. This results in researchers focusing the attention on the development of various derivatives with different *N*-terminal fatty acyl tails. [172]
  Chihara et al.[180] were the first investigating these modifications indeed they found out as derivatives with C_9-C_{12} *N*-terminal fatty acyl tail were more active then shorter ones against polymyxin resistant strains.

Clausell et al. experimented the substitution of the native fatty acyl tail with a pyrene group, resulting in reduced antimicrobial activity.[181]

De Visser et al. developed PMB analogues with fatty acyl chains shorter than C_7, demonstrating hexanoyl and 1-adamantane analogues had a potent antimicrobial activity while pentanoyl and butanoyl where responsible for a reduction in the activity.[182]

Tsubery et al. explored the synthesis of polymyxin nonapeptides (PMBN) analogues were the N-terminus was substituted with oligoalanyl portions or with the hydrophobic Fmoc group and, the latter showed increased antimicrobial activity and reduced toxicity.[183]

In the following years *Sakura et al*. [184]identified the octanoyl fatty acid tail as the optimal substituent while most recent studies[185] underlined cyclohexylbutanoyl, 4-biphenylacetyl- and 1-adamantaneacetyl analogues showed to possess interesting antimicrobial activity.

Then the *Pfizer group* focused the attention on the synthesis of PMBN derivatives proving as linear octanoyl fatty acyl tails showed increased activity while nonanoyl and decanoyl displayed decreased activity.[186]

- Modifications at **Phe6 and Leu7 portions** have also been investigated. These two portions contribute to the hydrophobicity of the molecule and they are believed to play a pivotal role in the stabilization of the molecule into the bacterial membrane due to hydrophobic interactions with the lipidic portions of the LPS. [172]

  Tsubery et al. first analysed the effect of substituting D-Phe^6 with D-Trp or D-Tyr and L-Leu^7 with L-Phe or L-Ala on PMBN analogues: lipophilic substituents did not affect the activity significantly while hydrophilic substituents reduced it drastically. [187]

  Sakura et al. synthetized PMB analogues substituting position 6 with D-Trp, D-Ala, and L-Phe or position 7 with L-Ala and L-Trp preserving both antimicrobial activity and LPS binding. [177]

de Visser et al. developed a series of analogues where the dipeptide Phe^6-Leu^7 was substituted by a dipeptide mimic leading to totally inactive compounds.[182]

5.1.6. ClipPA technology an innovative thiol-ene click chemistry

Over the years Brimble and co-workers developed a wealth of experience in the total synthesis and derivatization of antimicrobial lipopeptides indeed battacin analogues[188], iturin A analogues[189], teixobactin analogues[190], paenipeptin analogues[191] and polymyxins analogues have been successfully synthesized by using thiol-ene click chemistry to introduce novel lipids. [192] It is known also as hydrothiolation or thiol-ene coupling and it consists of a radical mediated alkylation of a thiol with an unsaturated portion (usually an alkene).[193,194]

The thiol–ene reaction is well known since the early 1900's even though an increased application was reported in the last decades in relation to cysteine alkylation/lipidation reactions. The first attempt on the synthesis of *S*-alkylated cysteine was performed by Waldmann et al. and it resulted in a low yield since most of the product was constituted by the disulfide byproduct. [195]

Based on this evidence, Brimble et al. initiated the development of an appropriate thiol-ene reaction procedure to incorporate it in the synthesis of *S*-lipidated peptides. They first performed *S*-alkylation of *N*-Fmoc-protected cysteine using thermal conditions reported by Waldmann which included the use of AIBN as radical initiator obtaining the *S*-lipidated cysteine in a low yield. Consequently, they investigated the use of a different radical initiator (DMPA) activated by UV light (365 nm), avoiding the use of high temperature which might not suit with the substrate, resulting in reaction completion in 1h and increased yield (44%). [196]

In the following years detailed studies on the reaction conditions have been carried out by Brimble and coworkers to develop *S*-lipidated building blocks

and to define the optimal conditions for the S-lipidation of any peptide containing cysteine. Consequently, different combination of *N*-protecting groups, radical initiators, activation method and radical quenchers have been investigated. [192,196]

This resulted in the definition of the optimal S-lipidation conditions. An N-methyl2-pyrrolidone (NMP) solution of vinyl ester and DMPA as photo initiator is treated under UV irradiation.

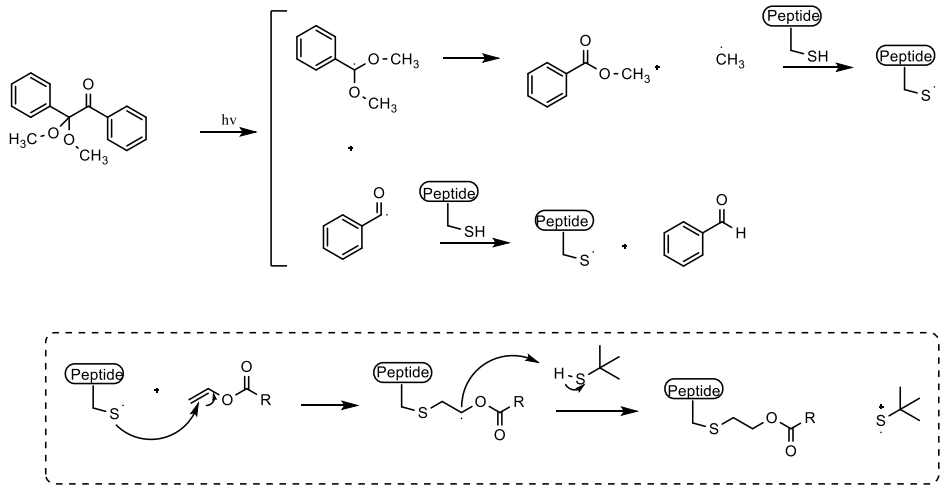

Scheme 14. *ClipPA S-Lipidation mechanism.*

The obtained sulphur radical quickly reacts with the vinyl group to give a radical intermediate. Then tert-butyl thiol (tBuSH) or tert-nonyl thiol (tNonylSH) and triisopropylsilane (TIPS) which are reducing agents incorporated in the reaction, act as radical scavengers to promote hydrogen transfer to the radical intermediate avoiding the production of disubstituted byproduct. TFA is added as well to protonate reactive species such as amines and alcohols consequently avoiding the interference with the radical process.[188]

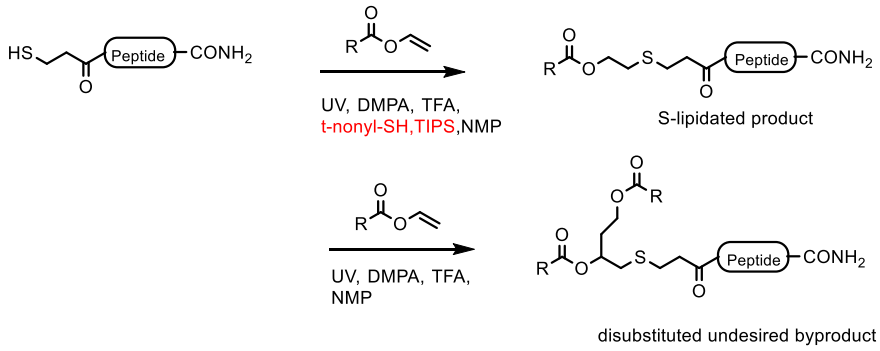

Scheme 15. *The role of scavenger agents in avoiding the formation of disubstituted by product.*

Finally, the term "CLipPA" — **C**ysteine **Li**pidation on a **P**eptide or **A**mino acid" was then coined by Brimble and coworkers to describe the radical-initiated thiol−ene reaction between the thiol group of a cysteine and the terminal carbon atom of a vinyl ester. The new discovered technology was then patented and extensively used in the S-lipidation of many lipidated peptides as previously described.[194]

5.1.7. Previous works on polymyxins by Brimble group

Based on previous reported literature underlining the important role of hydrophobic moieties at N-terminus, position 6 and position 7 in conferring proper features to exert antimicrobial activity,[172] Brimble and coworkers

focused on the SPPS of S-lipidated polymyxin by using the 'CLipPA' technology above described.

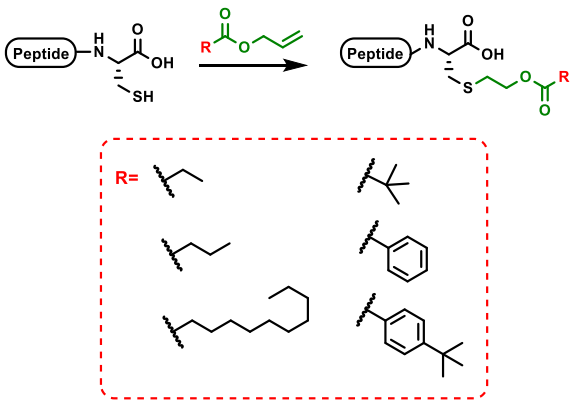

Scheme 16. *Polymyxin B analogues synthetized by the described work.*

The synthetic approach adopted for the synthesis of polymyxins is based on the synthetic strategy developed by Xu et al. as described in previous section (see ***Scheme13***).[178] Polymyxin B derivatives have been obtained by incorporating the appropriate lipidated amino acid at N-terminus, at position 6 and position 7. The lipidated amino acid building blocks have been synthesized by adopting the 'CLipPA' reaction previously described which occurs between a cysteine and a vinyl ester (***Scheme 16***). [197]

The general synthetic strategy started by anchoring the Fmoc-Dab-O-Allyl building block to the trityl chloride resin (***Scheme 17***). Fmoc amino acids were then added by Fmoc-SPPS method by using 20% piperidine in DMF for Fmoc removal and the incoming Fmoc amino acids (including the last S-lipidated building block) were coupled by using HATU/ DIPEA. The N-terminal Fmoc protecting group was then replaced with a Boc group and Dde protecting group was then removed by hydrazine from the amino acid at position 4 (Dab or Lys). The free amine group in position 4 was then acylated by coupling Fmoc-Thr(tBu)-OH. The C-terminal allyl ester of Dab_9 was removed using $Pd(PPh_3)$ and PhSiH and after proving by mass spectronmety the reaction completion,

Fmoc protecting group on Thr_{10} was removed. The cyclic peptide was then obtained by on-resin cyclisation using PyBOP and HOAt followed by global sidechain deprotection given by cleavage cocktail (90% TFA, 5%TIPS, 5%H_2O). The cyclic lipopeptides were then purified by HPLC.[197]

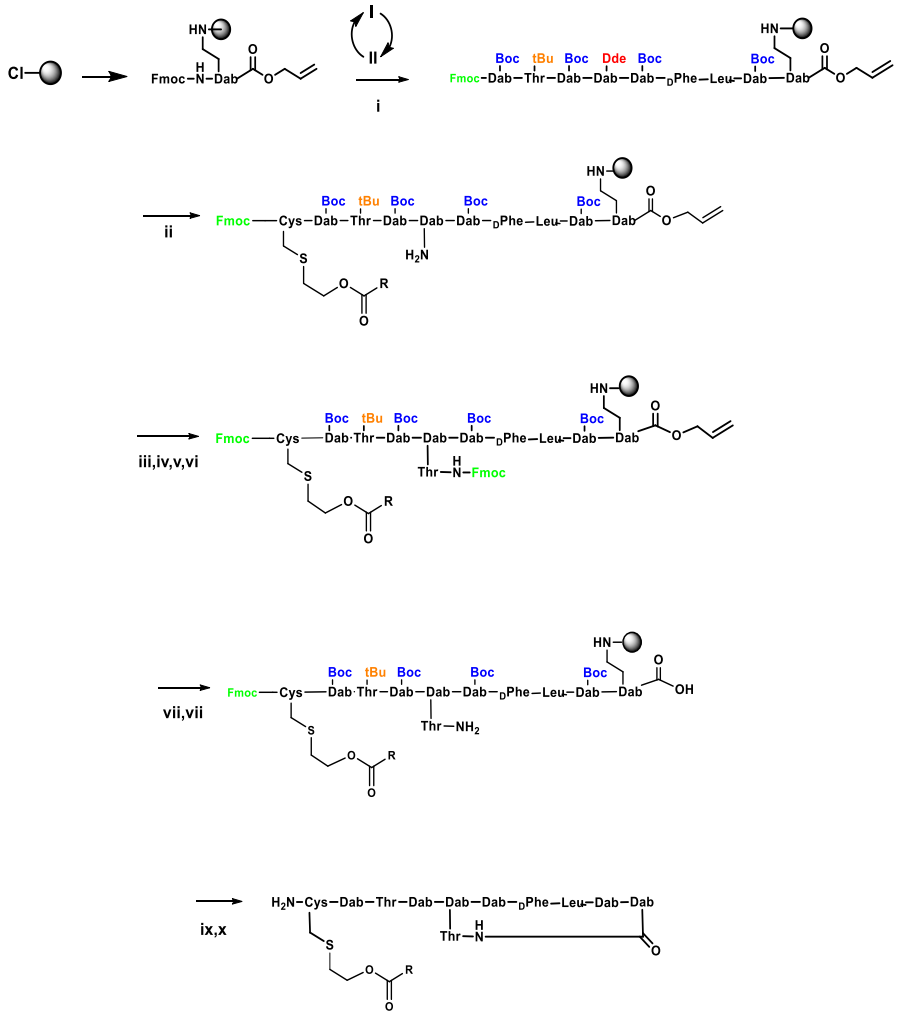

Scheme 17. *Synthetic Strategy for the Solid-Phase Synthesis of S-Lipidated Polymyxins*

This pioneer synthesis of polymyxins analogues based on the above-described conditions led to the development of two series of different derivatives

- Mono-S-Lipidated Polymyxin B Analogues (9a-9l)→ prepared by incorporating at the N-terminus aromatic, short, long, or branched chain lipids **(*Figure 60*)**

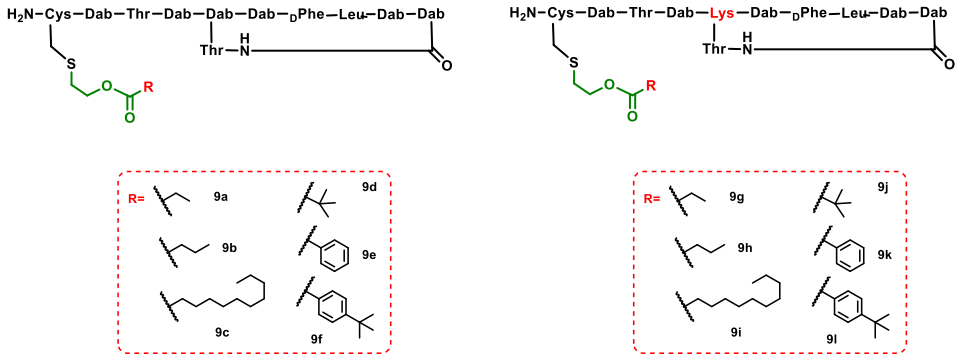

Figure 64. *Mono-S-Lipidated Polymyxin B Analogues*

- Multiple S-Lipidated Polymyxin B analogues in two series **(*Figure* 61):**

    1. both N-terminal fatty acid and Leu7 were substituted with a S-lipidated Cys building block
    2. both N-terminal fatty acid and D-Phe6 were substituted with a S-lipidated Cys building block

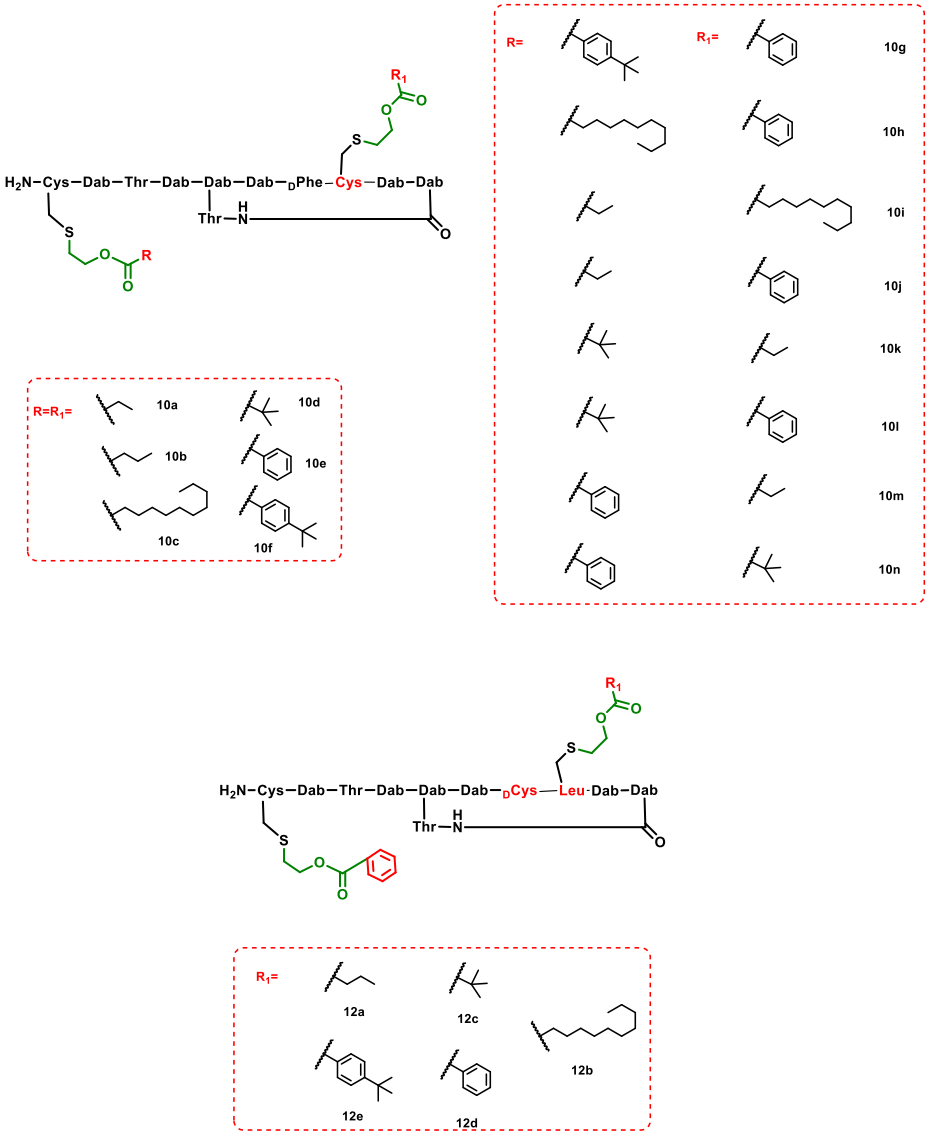

Figure 65. •*Multiple S-Lipidated Polymyxin B.*

All the synthetized compounds were then tested on a panel of 7 species of representative Gram-negative pathogens and most of them showing a maintained activity against MDR *Enterobacteriacea* and *A. baumannii*, while the activity against other species varied based on their structural features. Among them some have been selectively chosen to test their toxicity on Vero and HaCaT cell lines and nephrotoxicity on kidney organoids. Based on these results two S-lipidated polymyxins derivates emerged as promising compounds which became the reference point for further investigation.[197]

[This page is intentionally left blank]

5.2. Aim of the project

During my PhD secondment, I had the opportunity to join the group of Professor Margareth Brimble at the University of Auckland, New Zealand. Although not directly related to the synthesis of melittin analogues, this experience provided me with the chance to further broaden my knowledge in the field of peptides and peptidomimetic synthesis and characterization, which are reported herein.

According to the above-described background the development of new polymyxin S-lipidated analogues was undertaken, therefore leading to obtain two interesting compounds, **9g** and **9k** which, based on the *in vitro* encouraging results, have been chosen for carrying out further biological in vivo analysis.

Consequently, one of the aims of the period spent at Brimble's lab was to resynthesize the two compounds in a greater amount to allow in vivo biological studies.

Furthermore, based on in vitro toxicity/stability analysis of compounds 9g and **9k**, to expand the library of polymyxins *S*-lipidated compounds, two more compounds **AC4.107/DB7** and **AC4.106/DB8** bearing different fatty acid lipid

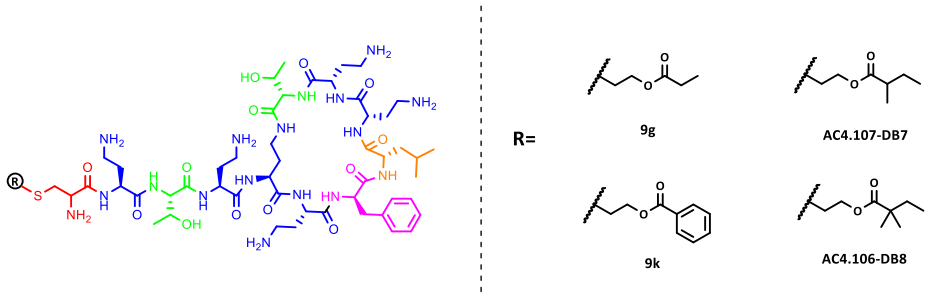

Figure 66. *Synthesized polymyxins S-lipidated compounds*.

tails, have planned to be synthesized as reported in ***Figure 62.*** Previous studies have shown **9g** has promising bioactivity profile with similar efficacy to PMB but reduced nephrotoxicity. However, it degrades rapidly in human serum at the ester linkage. By introducing additional steric hinderance, it was hypothesised that analogues **AC4.107/DB7** and **AC4.106/DB8** would increase the stability but may afford similar favourable biological properties.

From a chemical perspective, the main purpose was to synthesise the compounds through a different synthetic strategy already designed by the research group which includes the total on-resin synthesis of the native polymyxins, including cyclization and, the consequent in-solution derivatization by using the previously described 'CLipPA' technology.

Finally, with the purpose to verify that the resynthesized **9k** and **9g** compounds had same biological activity of the previously synthetized batches their antimicrobial activity has been tested on the same bacteria strains, additionally a preliminary analysis of the in vitro antimicrobial activity of the two new compounds **AC4.107/DB7** and **AC4.106/DB8** has been carried out.

5.3.Results and discussion

5.3.1. Synthetic strategy

As previously described the synthetic strategy employed in this project was aimed to replace the prior synthesis which relied on including S-lipidated building blocks on the synthesis of S-lipidated polymyxin derivatives, thereby leading to employ many steps on the total synthetic procedure. This work adopts a new strategy which leans on the use of commercially available or easily obtainable vinyl esters which are simply linked to the sulphur group of the N terminus Cys by using the above described 'CLipPA' technique. This results in a single synthesis of the peptide and subsequent lipid derivatization allowing to reduce the synthetic steps and increasing the total yield.

The new strategy involves the Fmoc-SPPS protocol as for the previous one and the first steps are the same indeed they both have been developed based on Xu et al. synthesis and start with anchoring the Fmoc-Dab-*O*Allyl on the 2-chlortrityl chloride polystyrene resin through a S_N1 substitution mechanism.[198] The Fmoc-Dab-*O*Allyl **2** has been separately synthetized in-solution from the commercially available Fmoc-Dab(Boc)-OH **1**.

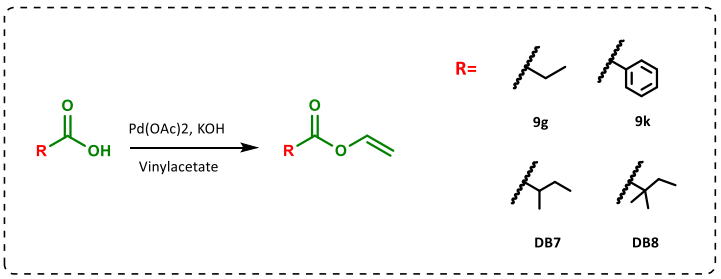

Figure 67. *Vinyl esters synthesis*

Considering that the resin loading is almost never 100%, after the determination of the exact loading percentage, to avoid the formation of side products in the sites not loaded with the Fmoc-Dab-OAllyl, a capping step was performed by

treatment of the resin with methanol followed by the addition of the incoming commercially available protected amino acids by using the classic Fmoc-SPPS

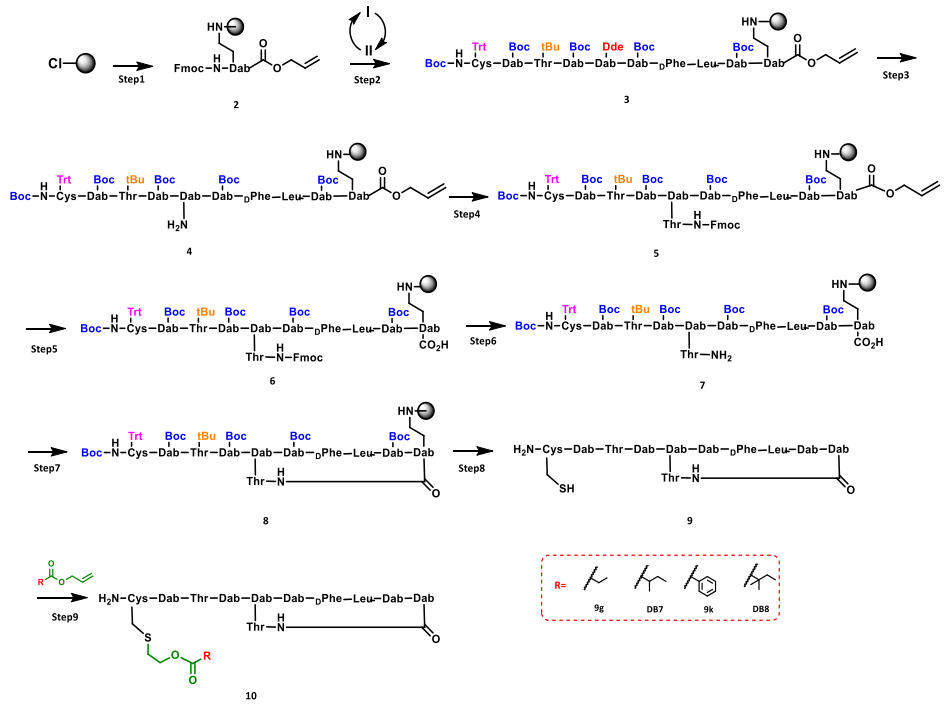

Scheme 18 *General synthetic procedure for the synthesis of polymyxins B derivatives. Reagents and conditions.* **Step1,2.** *Fmoc SPPS, 20% piperidine in DMF (v/v), 2 × 5min, rt then Fmoc-Xaa-OH, HATU, DIPEA, DMF, 20 min, rt.* **Step3**. *2%$N_2H_4{\cdot}H_2O$ in DMF (v/v), 3×5min, rt;* **Step4**. *Fmoc-Thr(tBu)-OH, HATU, DIPEA, DMF, 20min then 20% piperidine in DMF (v/v), 2×5min, rt.* **Step5**. *Pd$(PPh_3)_4$, $PhSiH_3$, CH_2Cl_2/DMF (1:1,v/v), 3h, rt;* **Step6** *20% piperidine in DMF (v/v), 2×5min, rt;* **Step7**. *PyAOP, NMM, DMF, 12h, rt;* **Step8**. *90% TFA, 5%TIPS, 5%H_2O(v/v/v), 2h, rt.* **Step9.** $Pd(OAc)_2$, KOH, vinyl derivate, UV, DMPA, TFA, t-nonyl-SH, TIPS, NMP.

method (20% piperidine in DMF for Fmoc removal and with HATU as coupling reagent, activated by DIPEA as the base) to get to the final linear sequence **3 (*Scheme* 18).** It worth nothing as a *N*-terminal Cys was installed which would subsequently enable the *S*-lipidation by ClipPA to be effected in solution.

After assembling the linear peptide **3** the Dde protecting group on Dab^4 was then removed by using hydroxylamine and imidazole in NMP for 5h at rt

(Method 5) obtaining peptidyl resin **4** and the free amine at that position was coupled with Fmoc-Thr(tBu)-OH to get peptidyl resin **5.**

The C-terminal allyl ester of Dab^9 was removed using $Pd(PPh_3)$ and PhSiH getting to peptidyl resin **6**. This step was monitored by RP-HPLC after cleaving the resulting product from a small portion of the resin beads from the first attempt to prove the deprotection was totally complete since, based on previous experience, the incomplete reaction results in a deletion which led to challenging purification after the cyclization step. Despite these precautions, as reported more in detail in the following sections, the first synthetic attempts led to obtain a product with many impurities responsible for the yield reduction of the final synthetic step.

With resin **6** in hand, the Fmoc protecting group on Thr^{10} was removed to afford peptidyl resin **7** and the cyclic peptide **8** was obtained by on-resin cyclisation using PyAOP as coupling reagent. The solid phase synthesis was followed by the cleavage of the polymyxin from the resin using the cleavage cocktail 94% TFA, 1%TIPS, 2,5% DODT, 2,5%H_2O which allowed at the same time the total deprotection giving final polymyxin B **9.** It then underwent the in solution ClipPA reaction getting to *S*-Lipidated PMB analogue **10** which was purified using semipreparative HPLC.

Four compounds have synthetized according to the reported procedure: the previously synthetised **9g** and **9k** to carry out further in vivo studies and two new compounds **AC4.107-DB7** and **AC4.106-DB8** characterized by an aliphatic branched portion linked to the sulfur group of the terminal cysteine residue. The two new compounds were designed and synthesized in line with toxicity studies conducted on 9g and 9k compounds which underlined as **9k**, bearing the benzyl group at this position, resulted more toxic than **9g** bearing the aliphatic propyl chain.

5.3.2. Detailed analysis of the synthetic procedure

During the synthesis of final compounds some issues have been encountered specifically related to amino acid deletions and cyclization step as following reported:

- ***Amino acid deletions***

As already introduced many attempts to obtain the final polymyxin structure have been performed considering that on many occasions some amino acids deletions showed up.

At the beginning each amino acid coupling step was monitored through the Kaiser test **(*Method* 10)** and a small sample of the cleaved peptide was then analysed by using mass spectrometry and analytical HPLC.

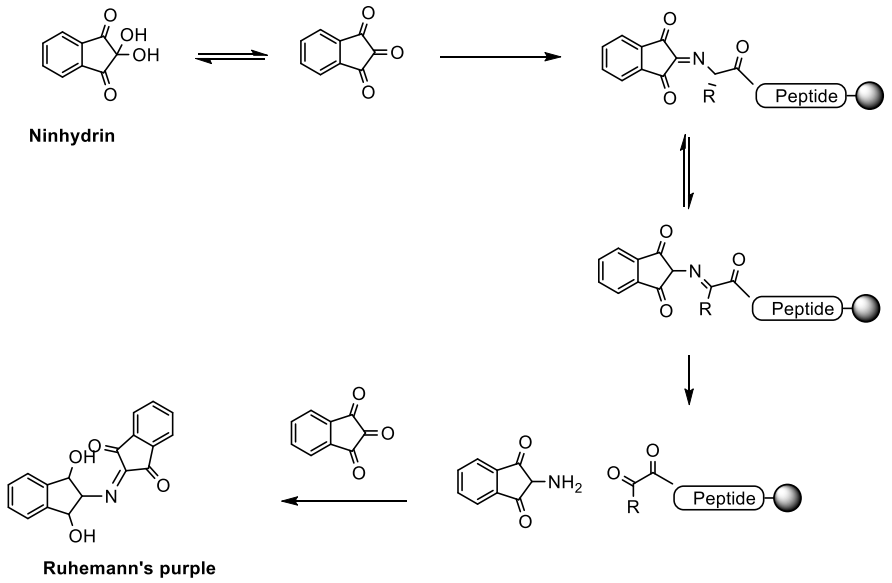

Scheme 19. *Colorimetric amino groups detection by kaiser test*

The kaiser test was developed to avoid formation of incomplete peptide chains during the peptide synthesis indeed the terminal amino group on the resin should be completely coupled with the incoming amino acids. To monitor the completion of the coupling reaction, treatment of a few beads of peptidyl resin with ninhydrin was performed. If free amino group are present on the resin a strong blue coloration is detected which is related to the generation of Ruhemann's purple. This result is considered as "positive" while if the terminal amino groups are completely coupled due to a successful coupling reaction, the beads result colourless and the test is perceived as "negative". [199]

It is worth mentioning that in one of the first attempts the linear peptide sequence has been checked after the addition of the 5th amino acid (Dab-Dde) cleaving a small portion of the resin beads (mini-cleavage step) to enable analysis by the analytical HPLC and ESI-MS analysis which showed positive results indicating as the aminoacidic sequence until that point was the correct one.

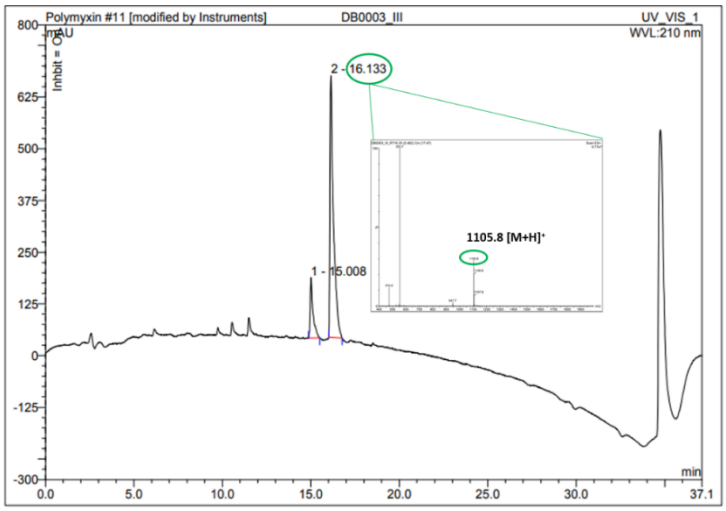

Figure 68 *Analytical RP-HPLC (214 nm) monitoring Dab-Dde coupling Phenomenex Luna C18 column (100Å, 5 µm, 4.6 mm x 250 mm), linear gradient of 5%B to 45%B over 40 min (ca. 1%/min) at 1 ml/min. * denotes the resin cleaved product of the respective peptidyl resin.*

The sequence has been analysed one more time after the Cys coupling reaction only through the kaiser test which showed a negative result allowing us to continue the synthesis coupling the Thr residue to the side chain of Dab[6] leading to peptidyl resin **5**. Unexpectedly, a mini-cleavage performed after this step evidenced the occurrence of amino acids deletions in the linear sequence. The required mass value was m/z=1123.6 while the observed mass values were *m/z*=923.6 and *m/z*=1023.6, which reflect as two coupling steps didn't get to completion based on the mass values obtained (923 and 1023 instead of 1123) which means the Kaiser test previously performed has failed.

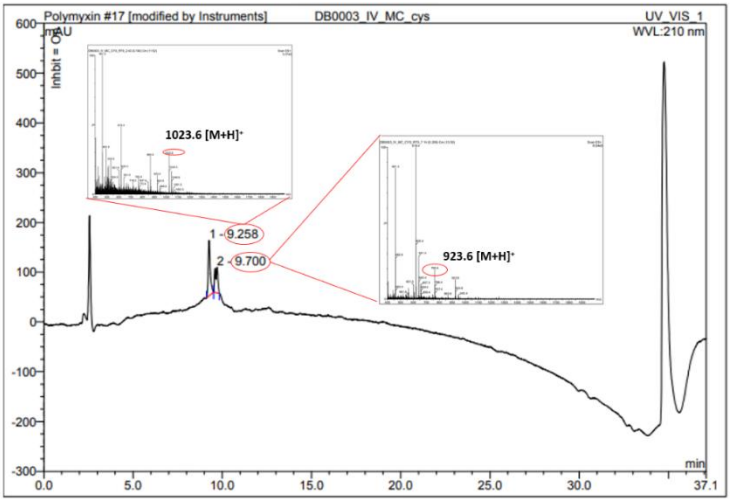

Figure 69 *Analytical RP-HPLC (214 nm) monitoring Cys coupling Phenomenex Luna C18 column (100Å, 5 µm, 4.6 mm x 250 mm), linear gradient of 5%B to 45%B over 40 min (ca. 1%/min) at 1 ml/min. * denotes the resin cleaved product of the respective peptidyl resin.*

Repeat failed attempts at different coupling steps in the synthesis of the linear sequence led us to verify every single coupling reaction status to clarify which could have been the issue. It has been found as most of the times deletions involved Fmoc-Dab(Boc) or Fmoc-Dab(Dde) residues based on the difference in mass values. Modifications to the coupling procedure were required, leading us to attempt the coupling reagent substitution of O-(6-chlorobenzotriazol-1-yl)-*N,N,N',N'*-tetramethyluronium (HCTU) for HATU, for all the coupling

reactions, finally leading to obtain the linear desired aminoacidic sequence free of the previously observed deletion byproducts.

.Compared to previous work by this group[197] a different type of resin has been involved: ChemPep brand polystyrene resin has been used instead of Trityl-ChemMatrix®, which is a PEG based resin. The use of a different resin could be reflected in different swelling properties that could enable reagent diffusion and avoid peptide aggregation or lead to a different orientation of the aminoacidic chains on the resin. After different coupling reactions this could result in a particular stereometric orientation of the building up aminoacidic chain that reduce the availability of the active sites involved in the next coupling reactions with a consequent failure of the step and a deletion.

The challenging synthesis of the linear sequence allowed us to establish that to avoid amino acid deletion the best coupling reagent to use in each step is HATU instead of HCTU.

This is related to the different structural nature of HATU and HCTU. The first is an HOAt derivate with pka=3.28 due to the presence of the nitrogen, makes it a better leaving group if compared to HCTU which is a 6-Cl-HOBt derivate with pka=3.35. Additionally, the aza nitrogen in position 6 facilitates the formation of a hydrogen bond with the nucleophilic amino group, that results in the formation of a transition state which cannot be achieved by HCTU which promote the reaction. [200]

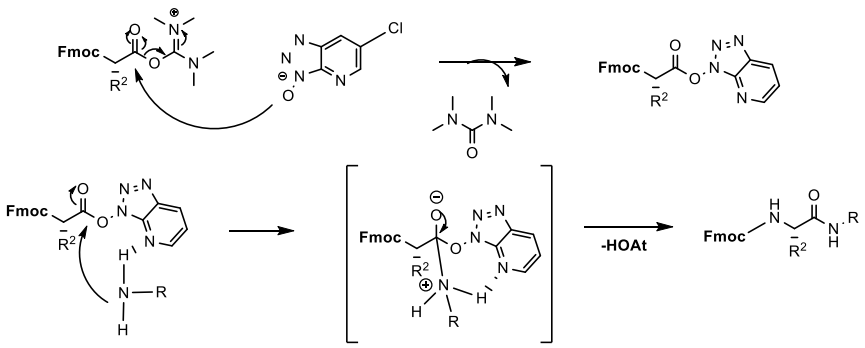

Scheme 20. *Formation of 1-hydroxybenzotriazole esters and stabilization by neighbouring effect by using HCTU as coupling agent.*

Moreover, the Kaiser Test cannot be used as the unique confirmation test to monitor the coupling reaction considering that even though it showed a clearly negative result, for various reasons, it could fail preventing us from identifying the presence of incomplete coupling to resin bound amino group.

- ***Cyclization***

Having identified the best reagents for the synthesis of the linear peptide sequence, the following steps did not present any unexpected challenges except for the cyclization step. The reagents and the reaction scale have been outlined as the most challenging aspects.

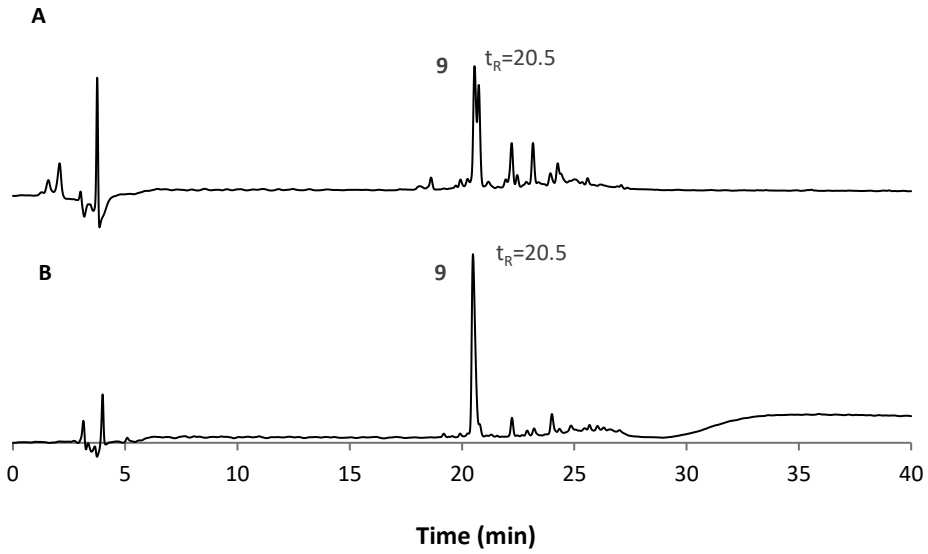

Figure 70.. *Comparison between BOP/ HOAt cyclization* **(A).** *and PyAOP cyclization* **(B)**. *Analytical RP-HPLC (214 nm) monitoring. Phenomenex Luna C18 column (100Å, 5 µm, 4.6 mm x 250 mm), linear gradient of 5%B to 45%B over 40 min (ca. 1%/min) at 1 ml/min.*

Firstly, it has been demonstrated that the purity of the crude product depends on the type of coupling reagents involved in the reaction, particularly ***Figure 70*** shows the analytical HPLC chromatogram of the reaction in which BOP/DIPEA/HOAt have been used as coupling reagents. Chromatogram at the top shows the analytical chromatogram of the crude cyclic product obtained by PyAOP and DIPEA as coupling reagents. Comparing the two figures a clear difference in the purity of the two different batches of resin **8** can be observed,

underlining as the most appropriate combination of coupling reagents is represented by PyAOP and DIPEA.

In previous works the solid phase synthesis of this linear sequence has already been carried out using PyBOP/DIPEA/HOAt. With the purpose to increase the yield and reduce the side products formation, PyAOP has been preferred instead of PyBOP. Iindeed some studies underline that azabenzotriazole based phosphonium salts (PyAOP, AOP) are as effective as the analogous uronium salts (HATU) but superior to the corresponding benzotriazole derivatives (PyBOP, BOP)[201]

Moreover, another important factor is related to the synthetic scale. Unfortunately, a larger synthesis scale **(*Figure* 71B)** led to a final product with more impurities indeed the lower is the scale the higher is the purity of the crude product **(*Figure* 71A)**.

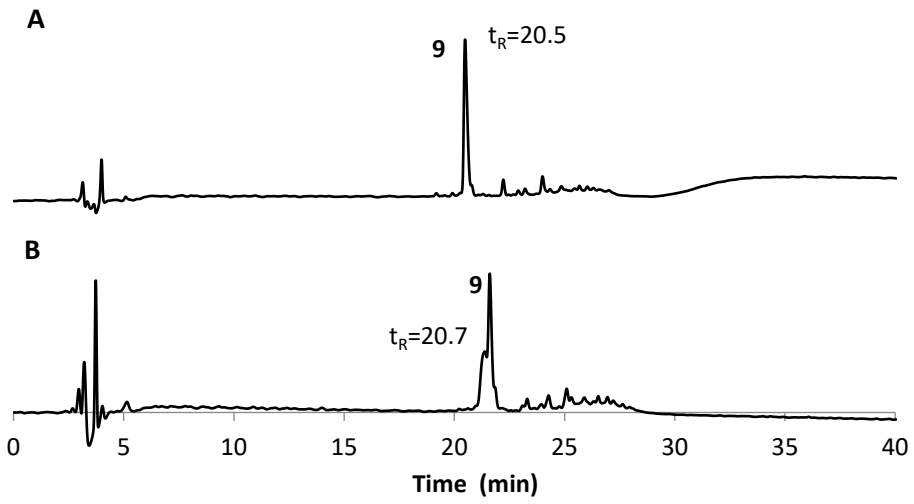

Figure 71. *Comparison between cyclization. at scale 0.04* **(A)** *and scale 0.3* **(B).** *Analytical RP-HPLC (214 nm) monitoring Phenomenex Luna C18 column (100Å, 5 µm, 4.6 mm x 250 mm), linear gradient of 5%B to 45%B over 40 min (ca. 1%/min) at 1 ml/min.*

- ***Piperidine adduct***

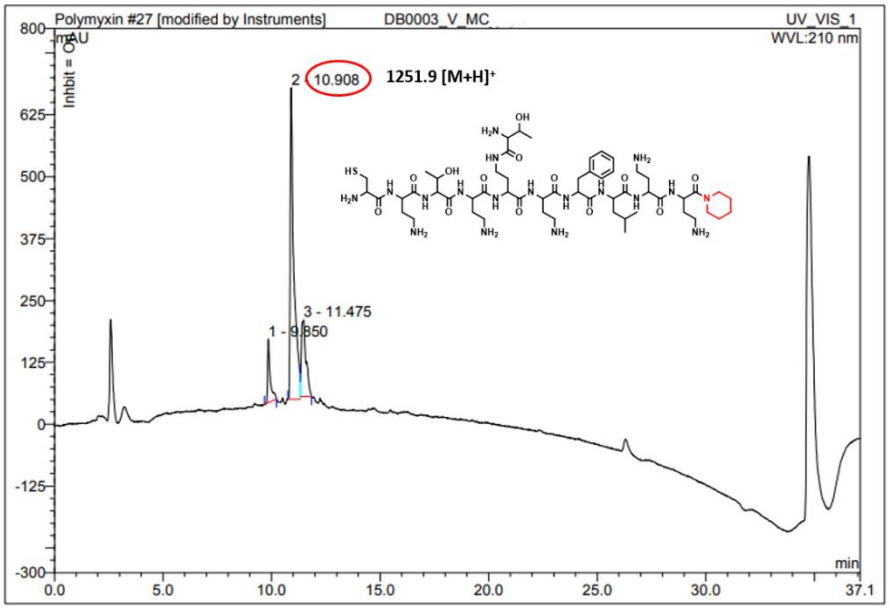

Figure 72. *Analytical RP-HPLC (214 nm) monitoring after Fmoc deprotection and piperidine adduct detection. Phenomenex Luna C18 column (100Å, 5 µm, 4.6 mm x 250 mm), linear gradient of 5%B to 45%B over 40 min (ca. 1%/min) at 1 ml/min.*

It was also observed ***(Figure* 72*)*** that a piperidine adduct can been obtained as a result of the Fmoc deprotection step (step6) which follows allyl ester deprotection.. This adduct results from a side coupling reaction occurring between the carboxylic group of Dab1 residue and piperidine used in the Fmoc-deprotection step and, it is mediated by the presence of coupling agents used during the cyclization step, thereby blocking further cyclization of the PMB product. It has consequently been proved that increasing the washing steps with DCM and Et_2O after Fmoc deprotection facilitates the elimination of residual piperidine, reducing the probability to obtain a piperidine adduct and improving the quality of the final product. Additionally, higher scale leads to higher amount of piperidine derivate..

- ***ClipPA***

During the synthesis of *S*-lipidated peptides by using 'CLipPA' technology it has been found that the purity of the starting material is extremely important to avoid the formation of side products that could lead to a challenging purification, This is due to overlapping retention times and it is explicated by the following chromatograms: ***Figure* 73** shows the chromatogram of the compound obtained from a starting material not previously purified compared to the product obtained from a starting material (cyclic peptide) previously purified.

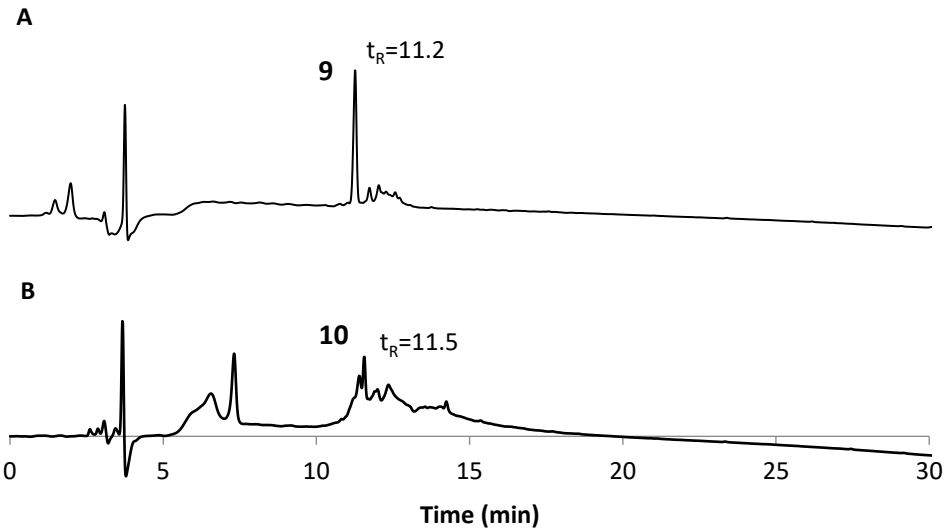

Figure 73. *Comparison between non purified starting cyclic compound and product after ClipPA reaction.Analytical RP-HPLC (214 nm) monitoring Phenomenex Luna C18 column (100Å, 5 µm, 4.6 mm x 250 mm), linear gradient of 5%B to 45%B over 40 min (ca. 1%/min) at 1 ml/min.*

Comparing the two chromatograms **(*Figure* 74)** it's clear as the retention time of the final product (t_R=11.6min) moves to the right side after the ClipPA reaction if compared with the starting material (t_R=11.2min). This means that if a crude starting material is employed in the CLipPA reaction, the product peak perhaps will present the same retention time of the impurities. Upon lipidation the final product peak shifts to exactly where the impurities are, consequently leading to a final product which is extremely difficult to isolate. For these reasons we chose to purify the cyclized starting material, to avoid a challenging purification and thereby increasing the final yield, that changed from 8% using the non-purified starting material to 25% using the purified one.

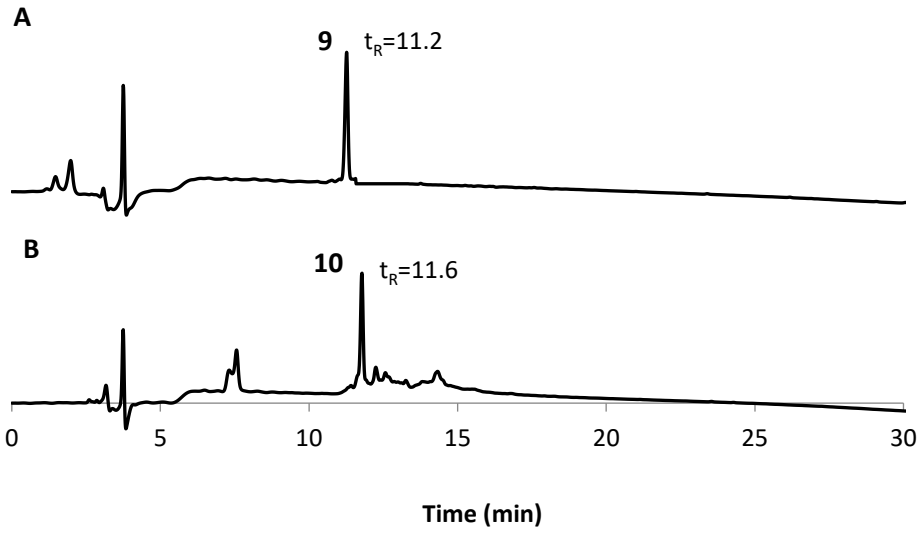

Figure 74 *Comparison between purified starting cyclic compound and product after ClipPA reaction. Analytical RP-HPLC (214 nm) monitoring Phenomenex Luna C18 column (100Å, 5 µm, 4.6 mm x 250 mm), linear gradient of 5%B to 45%B over 40 min (ca. 1%/min) at 1 ml/min.*

5.3.3. Biological results

State of the art on biological results for 9g and 9k

Compounds 9g and 9k were previously proven to be extremely active against *E.coli ATCC25922* with a MIC value for **9k** of 0.25 μg/mL and for **9g** of 0.5 μg/mL.

Moreover antimicrobial activity of **9g** and **9k** against other relevant gram negative strains was already known from the previous work, indeed **9k** resulted the most active compound against most of the tested strains, while both of them resulted inactive against *K.pneumoniae* MS6671 (MIC up to 32 μg/mL), a pan-drug strain resistant to 31 known antibiotics[202] Additionally, the two compounds **9g** and **9k**, along with others from that series, have been previously tested on *E.coli* MS8345, an MDR pathogen which presents the mcr-1 resistance gene encoding for modification of lipid A and it has been demonstrated as **9k,** bearing the aromatic lipids ethyl benzoate, performs an improved activity (2 μg/mL) compared to PMB (4 μg/mL).

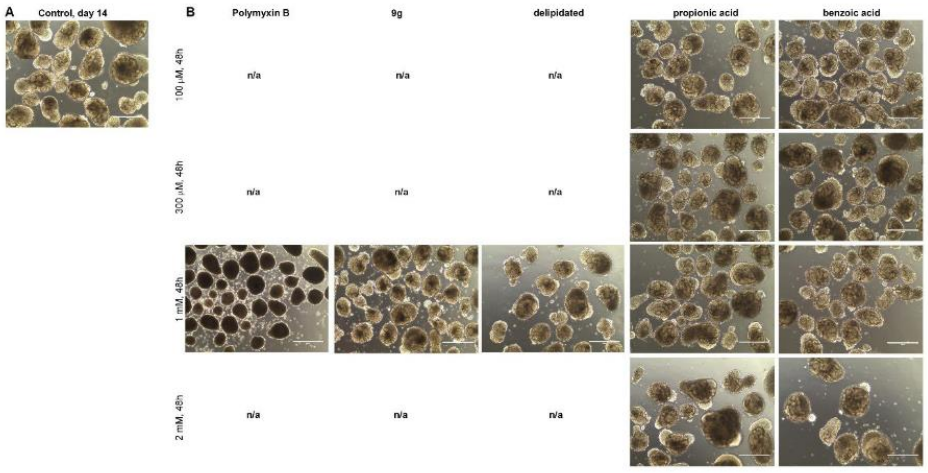

Figure 75. *Comparison of polymyxin 9g, an ester hydrolysed 9g (delipid) and the lipids arising from hydrolysis of 9g (propionic acid) and 9k (benzoic acid)*

The nephrotoxicity of **9g** and **9k** was evaluated as well by using human kidney organoids which derived from human-induced pluripotent stem cells and have been used as model since they include renal tubules presenting typical features of human kidney. 9g and 9k have been successfully evaluated by these assays, resulting in a dose dependent degradation of organoids after treatment with compound **9k** (bearing the benzene group) while compound **9g** (characterized by the propyl portion) did not affect the organoid cells which maintained a normal appearance up to 1 mM concentration. Therefore, **9g** has a significantly reduced toxicity compared to PMB (approx.10-fold), but only moderately reduced for **9k**

Consequently, to verify if the toxicity of **9k** was due to the hydrolysed benzene portion, the organoids were exposed to benzoic acid resulting in any organoid deterioration up to 2mM (***Figure 75).***

This lead to speculate that **9k** is probably faster assimilate by organoids increasing the nephrotoxicity. Indeed, the stability of **9g**, **9k**, and PMB in the organoids assay was analysed to verify if the toxicity was related to high concentrations of the compounds resulting in a similar rates degradation for **9g** and **9k** consequently the **9k** toxicity previously observed cannot be related to its higher concentration.

The stability of compound **9g** and **9k** was also evaluated at different pH values and compared to PMB after 24h and 48h. At pH 1 ,5 or 9 compound **9k** was the more stable, while both **9g** and **9k** undergo a rapid degradation at higher pH value (pH 13). At pH7 all the three compounds where intact after 48h (***Figure* 76**).

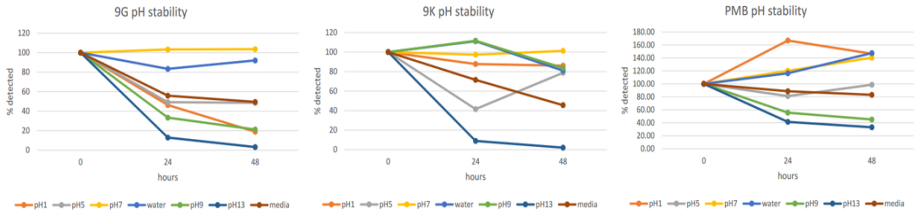

Figure 76. *pH stability for compounds **9g,9k** and PMB*

Degradation in human serum was also detected, revelling as PMB levels were unaltered after 24 h, while **9g** and **9k** where rapidly degraded within 4 h and were undetectable after 24 h (***Figure* 77**). In particular, **9g** was more stable since after 4h a remaining 9% was detected, while **9 k** was 1%.

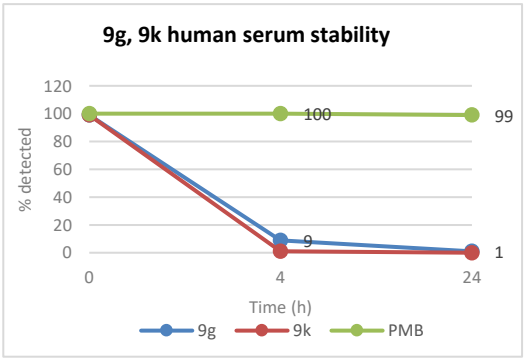

Figure 77. *Human serum stability for compounds **9g**, **9k** and PMB*

Antimicrobial activity evaluation

Antimicrobial activity of the four synthetized compounds **9g**, **9k**, **AC4.107-DB7** and **AC4.106-DB8** was evaluated with selected bacterial strains. Particularly all of them have been preliminary tested on the *E.coli* ATCC 25922 strain, even the new batches of compounds **9g** and **9k** to reconfirm the antimicrobial activity. Compounds were tested using Minimum Inhibitory Concentration (MIC) assay following the CLSI guidelines[203] and compared with native polymyxin B (PMB) as a reference.

MIC (µg/mL)	
Cmpd	*E.coli*[1]
PMB	0.25
9g	2
9k	0.25
AC4.107-DB7	0.1-0.25
AC4.106-DB8	0.25

Table 11 *MIC values of AC4.107-DB7 and AC4.106-DB8 compared to* ***9g*** *and* ***9k.*** [1] *ATCC 25922.*

As reported in ***Table* 11** the four compounds demonstrated excellent potency towards *E.coli,* additionally the MIC value for **9k** (0.25 µg/mL) has been totally proven while the MIC value for **9g** (0.5 µg/mL) resulted slightly lower than the one reported on the previous analysis (2 µg/mL)

Compounds **AC4.107-DB7** and **AC4.106-DB8** were tested on the same gram negative strain *E.coli ATCC25922*, demonstrating generally greater activity compared to **9g** but less active if compared to **9k.**

We were then interested to compare with **9g** and **9k** the activity of **AC4.107-DB7** and **AC4.106-DB8** towards this larger list of pathogens based on their promising initial results towards E.coli ATCC 25922.They showed a comparable activity for A. baumannii ATCC25922 and against all the *K.Pneuoniae* strains. However, like **9g**, they are also inactive as well against the pan-drag resistant *K.pneumoniae* MS6671 with a MIC value >16 for both of them ***(Table* 12*)***

	MIC (µg/mL)						
Cmpd	*E.coli*[1]	*A.baumannii*[2]	*P.aeruginosa*[3]	*K.pneumoniae*[4]	*K.pneumoniae*[5]	*E.coli*[6]	*K.pneumonia*[7]
PMB	0.25	0.5	0.25	0.25	0.5	4	>32
9g	2	2	0.5	0.125	0.5	32	>32
9k	0.25	0.5	0.125	0.0625	0.25	2	>32
AC4.107- DB7	0.5	2	1	0.25-0.5	1	16	>16
AC4.106- DB8	0.5	2	1	0.5	0.5-1	8	>16

Table 12 *MIC values on an extended panel of bacteria.[1] ATCC25922, [2]ATCC 19606, [3]ATCC 27853, [4]ATCC 33495, [5]ATCC 700603, [6]MS8345, [7]MS6671.*

Nephrotoxicity and organoids stability evaluation

Given the promising antimicrobial activity and based on the well- known nephrotoxicity effects of polymyxins, previously described in ***section 5.1***, we were interested to evaluate the nephrotoxicity of **AC4.107-DB7** and **AC4.106-DB8.** Therefore, they were subjected to evaluation in kidney organoids as per **9g** and **9k** previously reported. According to previous established toxicity protocols **AC4.107-DB7**, **AC4.106-DB8** and commercially available PMB were tested by adding 100 µM, 300 µM, 1mM, or2mM to the organoids at day 12. Toxicity was then monitored at 48 h determining the renal tubules deterioration by bright-field imaging.

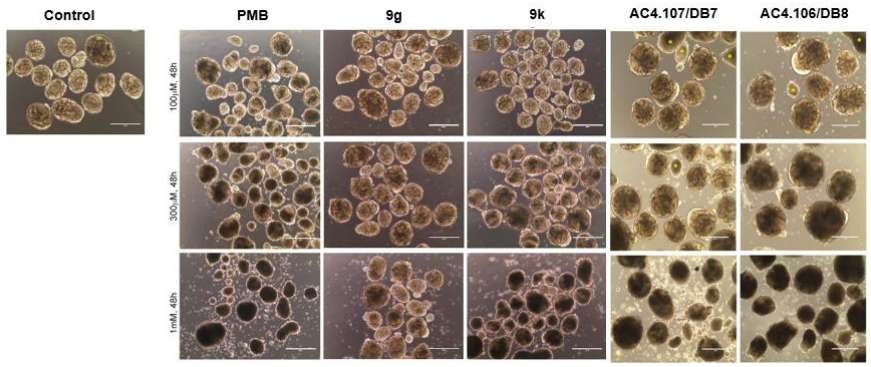

Compound	Deterioration of kidney organoids		
	100 µM	300 µM	1 mM
Polymyxin B	Mild	Severe	Complete
R =			
	Unaffected	Unaffected	mild
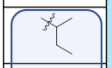	Unaffected	Mild	Severe
	Unaffected	Severe	Complete
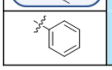	Unaffected	Mild	Complete

Figure 78 *Summary of nephrotoxicity of Polymyxin B and S-Lipidated Analogues on Kidney organoids.*

It resulted in a dose dependent degradation of organoids after treatment with compound **AC4.106-DB8** (dimethyl branched group) comparable to the effect of compound **9k** (bearing the benzene group) and PMB, indeed for all of them loss of tubular structures and defined edges, floating debris, and dark colouring of the organoid are observed, resulting in a severe deterioration of the organoids at 300 µM and in a complete deterioration at 1 mM **(*Figure* 78).** Treatment with compound **AC4.107-DB7** (monomethyl branched group) resulted in a mild deterioration at 300 µM and a severe deterioration at 1 mM, slightly different from compound **9g which** did not affect the organoid cells with a normal appearance up to 1 mM concentration.

pH and human serum stability

Previous results on **9g** and **9k** pH stability inspired stability studies on **AC4.107-DB7** and **AC4.106-DB8,** indeed the low stability of 9g has been on of the drivers of the design of the two new branched compounds **AC4.107-DB7** and **AC4.106-DB8.** This was based on the hypothesis would have reduced the rate of ester hydrolysis by steric interference.

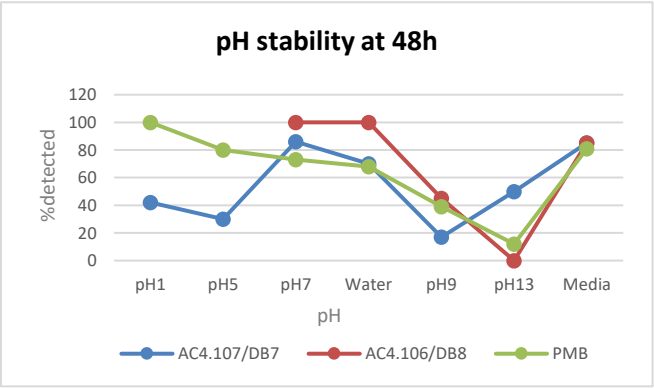

Figure 79. *pH stability for AC4.107-DB7 and AC4.106-DB8*

The pH stability was evaluated for compounds **AC4.107-DB7** and **AC4.106-DB8** at 48h, resulting in **AC.106-DB8** totally stable at pH 7 after 48h while compound **AC4.107-DB7** resulted slightly less stable leading to speculate that an increased branched feature increases the stability at this pH value. On the other hand, they resulted instable at basic pH values (pH9 and 13) in line with the obtained results for **9g** and **9k** and the PMB stability used as reference **(*Figure* 79).**

Additionally, compound **AC4.107-DB7** resulted less stable than PMB and **9k** after 48h at acidic pH values, but comparably stable to **9g**. This seems to underline as aliphatic linear or branched mojeties (for **9g** and **AC4.107-DB7** respectively) are responsible for less stable compounds than aromatic moieties (as for **9k**). The stability of compound **AC.106-DB8** has to be repeated.

Stability in human serum has been evaluated for compounds **AC4.107-DB7** and **AC4.106-DB8** as well (***Figure* 80)** resulting in a greater stability for the two new compounds if compared to compounds **9g** and **9k** as reported in graph x, since 39% and 16% respectively is the percentage of compound detected after 24h that underline as aliphatic branched lipid moieties might be preferred to aromatic or linear aliphatic lipid to increase the molecule stability.

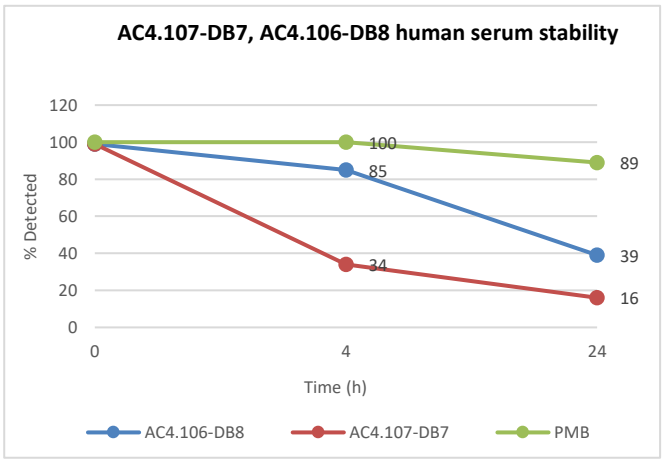

Figure 80. *Human serum stability for AC4.107-DB7 and AC4.106-DB8.*

[This page is intentionally left blank]

5.4.Conclusion

During the period spent at Brimble's lab, an innovative synthesis of four S-lipidated polymyxins derivates was successfully carried out, confirming as HATU is the most efficient coupling reagent for the coupling of incoming amino acids and PyAOP is the most efficient reagent that can be employed in the cyclization step. Additionally, the yield was optimized over various synthetic attempts, leading to affirm as the optimal yield is reached when the purified cyclic peptide is used as substrate for the consequent CLipPA functionalization. This information is crucial to scale up products of interest for biological studies. The four compounds have then been tested and based on the combined results of antimicrobial activity, toxicity in human organoids and serum/pH stability, **AC4.107-DB7** resulted the compound with the best balance between all these parameters. Indeed, even if compound **9g** showed a lower toxicity in human organoids, on the other side it resulted less stable in human serum with a 9% less after 4h, and a total degradation after 24h, while 34% of compound **AC4.107-DB7** has been detected after 4h and 16% still determined at 24h. Additionally, these results allow us to make some SAR consideration, as the presence of a lipid with aliphatic structure at the cysteine terminus leads to compounds less toxic even if slightly less active than aromatic lipids, as resulted by comparing compound **9g** and **9k**. On the other hand, this evidence led us to believe an aliphatic portion at that position would be better for the activity/toxicity balance. Consequently, other compounds with an aliphatic branched lipid portion were synthetized (**AC4.107-DB7** and **AC4.106-DB8**) but this resulted in the evidence that the higher is the branching the higher is the toxicity, which is comparable to PMB for compound **AC4.106-DB8** presenting the dimethyl branched group.

[This page is intentionally left blank]

5.5.Experimental procedures

5.5.1. Solvents and chemicals

All solvents and reagents used in the synthesis are high purity commercial products utilized without further purifications. For MS, NMR and HPLC analysis were used only solvents with a purity level certified for respective techniques. Milli-Q water was obtained through Millipore purification system of distilled water. Main solvents and reagents are here reported: 2-Chlorotrityl chloride polystyrene resin was purchased from ChemPep Inc. (Wellington, FL, USA). Fmoc-DPhe-OH, Fmoc-Trh(tBu), Fmoc-Dab(Boc), Fmoc-Leu-OH, Fmoc-Dab(Dde) and Fmoc-Cys(Trt) were purchased from GL Biochem. Tetrakis(triphenylphosphine)palladium(0) **($Pd(PPh_3)_4$),** triisopropylsilane (**TIPS**) were purchased from AK Scientific (Union City, CA, USA). O-(6-chlorobenzotriazol-1-yl)-N,N,N′,N′- tetramethyluronium hexafluorophosphate (**HCTU**), benzotriazol-1-yloxytripyrrolidinophosphonium hexafluorophosphate**(PyBOP**),(benzotriazol-1-yloxy)tris(dimethylamino) phosphoniumhexafluorophosphate (**BOP**) and 1-[bis(dimethylamino)methylene]-1H-1,2,3-triazolo[4,5-b]pyridinium 3-oxide hexafluorophosphate **(HATU**) were purchased from Aapptec (Louisville, KY, USA). N,N'-diisopropylethylamine (**DIPEA**), piperidine, phenylsilane (**PhSiH3**), sodium diethyldithiocarbamate, 1-methyl-2-pyrrolidinone (**NMP**), tert-nonyl mercaptan, vinyl acetate, vinyl propionate, vinyl benzoate, 2,2-dimethoxy-2-phenylacetophenone (**DMPA**), were purchased from Sigma-Aldrich (St Louis, MO, USA). 1-Hydroxy-7-azabenzotriazole (**HOAt**) was purchased from Manchester Organics (Manchester, England). Trifluoroacetic acid (**TFA**) was purchased from Oakwood Chemicals (Estill, SC, USA). N,N-Dimethylformamide (**DMF**), Petrolium ether (**PE**), Ethyl acetate (**EtOAc**) and acetonitrile (**CH3CN**) were purchased from Scharlau (Barcelona, Spain). Dichloromethane (**CH2Cl2**) was purchased from ECP Limited (Auckland, New

Zealand). Diethyl ether (Et2O) was purchased from Avantor Performance Materials (Center Valley, PA, USA).

5.5.2. General methods for purification and analysis

Flash column chromatography

Flash chromatography is performed packing silica gel (Grace Davison Discovery Sciences, Davasil LC60A 40−63 μm Chromatographic Silica Media) in a variable size glass column and flushing with air. The final product is purified from the reaction mixture by using an eluent mixture optimized through TLC analysis.

Analytical thin-layer chromatography (TLC)

TLC was performed using Kieselgel F254 200 μm(Merck) silica plates. In order to enhance the difference of Rf between reagents, products and any possible impurity, mobile phases have been optimized and EP/EtOAc was identified as the best solvents combination for the synthesized molecules. TLC spots were then visualized by UV florescence lamp at 254 nm and 365 nm or by $KMnO_4$ staining followed by heating of the plate.

Nuclear magnetic resonance (NMR)

Spectra were recorded on a Bruker AVANCE 400 spectrometer at 400 MHz for 1H nuclei and 100 MHz for 13C nuclei at RT in CDCl3. All chemical shifts are reported in parts permillion (ppm) and refers to the residual chloroform peak (δ 7.26 ppm) for ^{1}H NMR or the residual chloroform peak (δ 77.1 ppm) for ^{13}C NMR. The ^{1}H NMR shift values are reported as chemical shift δ, multiplicity (s=singlet, d= doublet, t=triplet, q=quartet, m=multiplet, dd=doublet of doublets, td=triplet ofdoublets, qd=quartet ofdoublets) and coupling constant (J inHz). ^{13}C NMR values are reported as chemical shift δ.

Mass spectrometry

Tandem mass spectrometry (MS/MS) was recorded on a Waters QSTAR XL Quadrupole-Time-of-Flight instrument.

Analytical reverse-phase high-performance liquid chromatography (RP-HPLC)

Analytical RP-HPLC was performed on a Waters Alliance 2695 System equipped with a Luna® column LC C18(2) 100Å (5 µm; 150 mm x 4.6mm), A: 0.1% TFA in H2O, and B: 0.1%TFA in ACN. Gradient 5-65%B over 60 min (1%B/min), flow rate 1 mL/min.

Semi-preparative RP-HPLC

Semi-preparative RP-HPLC was performed on Waters 600E System equipped with a Waters 2487 dual wavelength absorbance detector at 210 and 254 nm using a semi-preparative Gemini_NX C18 110 Å column (5 µm; 250 x 10mm). Solvent gradients (solvent A=0.1% TFA in water and solvent B=0.1% TFA in ACN) were designed according to the elution time obtained from the analytical RP-HPLC and a flow rate of 5.0 mL/min was employed as specified.

5.5.3. Synthetic procedures

Method 1: Loading of Fmoc-Dab-NH_2-OAllyl

2-Chlorotrityl chloride polystyrene resin (1g, 0,86 mmol/g loading) was pre-swollen at room temperature in DCM (10 mL, 20 min) in a solid phase reaction vessel then washed with DCM/DMF. A solution of Fmoc-Dab-OAll (2.5 mmol,3eq) and DIPEA (5.2 mmol, 6eq) in DCM/DMF (5 mL) was added and the reaction mixture was agitated for 4 h at rt. Methanol (1 mL) was added to quench any unbound resin sites and the reaction was agitated for 20 additional mins at rt. The resin was drained and washed with DCM (3 x 5 mL) and DMF (3 x 5 mL).

Method 2: Loading Test

To a sample (~2 mg) of dry loaded resin is added a solution of piperidine in DMF (20% v/v, 1mL). The suspension is shaken for 5 min at rt and centrifuged then 100µL of supernatant is diluted in 1.9 mL of DMF. Absorbance at 290 nm is measured against a blank containing 100 µL of 20% piperidine in DMF diluted with 1.9 mL of DMF. Loading was determined through the equation:

$$L = 1000 \times \frac{D(As - Ab) \times V}{\varepsilon_{290} \times m_r \times \mathrm{I}}$$

L = the experimental loading ($\frac{mmol}{g}$),

1000 = conversion factor to obtain L in $\frac{mmol}{g}$

D= dilution factor (D = 20)

As= absorbance of the sample solution at 290 nm

Ab=absorbance of the blank at 290 nm

V= volume of reaction (V = 1 mL),

ε_{290} = molar extinction coefficient of dibenzofulvene at 290 nm (ε_{290} = 6089 $\frac{L}{mol \times cm}$),

m_r=mass of the resin sample (mg)

l = path length of the UV cuvette (l = 1 cm).

Method 3: Fmoc protecting group removal

The peptidyl resin is treated with a solution of 20% piperidine in DMF (5mL) and agitated at rt for 5 min. The solution is then removed in vacuo and the resin is washed with DMF (3x5 mL). Then the piperidine solution is added one more time and the reaction mixture agitated for further 10 min. The resin is filtered

and washed with DMF (3x5 mL). Finally, the complete Fmoc removal is confirmed by a positive Kaiser test.

Method 4: Amino acid coupling

To the peptidyl resin was added a solution of Fmoc-AA-OH (3 equiv.), HCTU (2.7 equiv.) and DIPEA (8 equiv.) in DMF. The reaction mixture was agitated for 30 min at RT, then the resin was washed with DMF. The coupling of cysteine residue was slightly different since DIPEA was substituted by 2,4,6-collidine and performed in DCM/DMF for 1 h at rt. The resin was washed with DCM (3x5 mL) and DMF (3x5 mL) and the coupling was repeated. The coupling reaction was monitored via Kaiser test or HPLC analysis.

Method 5: Dde Protecting Group removal

The peptidyl resin was treated with a solution of hydroxylamine hydrochloride (1eq) and imidazole (0,7 eq) in NMP (10 mL) and agitated for 5 h at rt. Then the solution was drained and the resin was rinsed with DMF (3x5 mL).

Method 6: Allyl ester protecting group removal

To the peptidyl resin was added tetrakis(triphenylphosphine) palladium (0) ($Pd(PPh_3)_4$, 0.25 equiv.) and phenylsilane (PhSiH3, 15 equiv.) in DCM. The reaction was agitated at RT for 3h, then the resin was filtered and washed with DCM (2x5mL) and a solution of sodium diethyldithiocarbamate in DMF (0.5 % w/v) and DMF (2x5mL). The successful deprotection was monitored by cleavage of a small portion of peptidyl resin and analysis via MS spectrometry.

Method 7: On-Resin Cyclisation

Peptidyl resin was treated with a solution of PyAOP (3 eq.) and DIPEA (6 eq.) in DMF. Cyclisation was performed for 2 h at RT. The solution was drained, and the resin was washed with DMF (3 × 5 mL) and DCM (3 × 5 mL). Cyclization completion was then monitored by Kaiser test.

Method 8: Cleavage

To the peptidyl resin was added a solution of TFA/TIPS/DODT/H2O (94/1/2.5/2.5) and the reaction was carried out for 2 h at RT. The reaction mixture was then filtered, and the resin washed with TFA which was evaporated by N_2. The crude peptide was precipitated by addition of ice-cold Et_2O, centrifuged and washed with additional Et2O. It was then dissolved in ACN/H2O+ 0,1%TFA and lyophilised.

CLipPA S-Lipidation (Method 9)

The peptide (1eq.) was dissolved in a solution of DMPA (0.5 equiv.) in argon degassed NMP. Tertnonyl mercaptan (80 equiv.), TIPS (80 equiv.), vinyl ester (70 equiv.) and TFA (5% final reaction volume) were added and the reaction volume was adjusted to a final peptide concentration of 10 mg/mL by adding NMP. The reaction mixture was stirred for 1 h at room temperature under UV irradiation (365 nm). Cold Et_2O was added to precipitate the lipidated peptide which was then recovered by centrifugation. The precipitate was dissolved in DCM/H2O + 1% TFA and lyophilized.

Kaiser Test (Method 10)

Peptidyl resin was washed with DCM (3 x 5 mL). A small amount was dried under vacuum and transferred to a vial. Then solution 1 (ninhydrin in isopropanol_0.05 g/mL), solution 2 (80% phenol in ethanol) and solution 3 (1 mM aqueous potassium cyanide in pyridine (1/50, v/v)) were added 1 drop each. The resulting mixture was heated at 100 °C for 2 min and the colour development was analysed. Colourless resin and yellow solution referred to a negative test, while blue resin and/or blue solution resulted in a positive test.

General method for vinyl esters synthesis (Method 11)

The acid starting material (2-methylbutyric acid or 2,2-dimethylbutiric acid) (1eq), $Pd(OAc)_2$ 0,156 eq) and KOH (0.1 eq) were dissolved in vinylacetate (20 mL).The reaction mixture was stirred at RT for 24h under nitrogen then it was filtered through a pad of Celite and the solvent evaporated in vacuo (400atm, T<35). The crude product was purified by flash column chromatography on silica gel (9:1 EP/ET2O) obtaining the final product as a yellow liquid and volatile oil.

5.5.4. general methods for biological analysis

MIC Evaluation

Antimicrobial activity evaluation was carried out by using broth microdilution according to the Clinical and Laboratory Standard Institute (CLSI) Guidelines.[203] Derivatives were tested at a maximum final concentration of 64 μg/mL diluting a stock solution of the peptide (20 mg/mL) with sterile calcium-adjusted Mueller-Hinton broth (CAMHB) to the desired concentration and plating it in a 96-well polypropylene plate. Each well was inoculated with a freshly grown culture of *E. coli* ATCC® 25922 at a concentration of 5 x 10^5 CFU/ mL (evaluated by measuring the optical density at 600 nm). A negative (no inoculate) and a positive (untreated) control as well as a control experiment with commercial polymyxin B were included. All series were performed in triplicate for each experiment. The plates were cultivated overnight at 37 ºC. Then the minimal inhibitory concentration (MIC) was determined as the lowest analyte concentration where no bacterial growth was observed.

5.5.5. Synthetic procedures

Synthesis of allyl 2-((((9H-fluoren-9-yl)methoxy)carbonyl)amino)-4-((tert-butoxycarbonyl)amino)butanoate

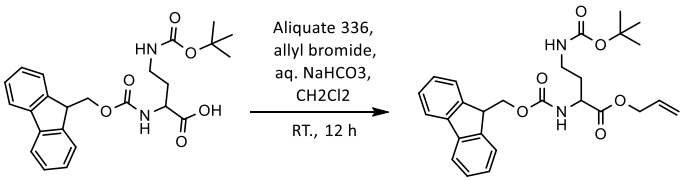

Fmoc-Dab(Boc)-OH (1 eq, 4 g, 8.8 mmol) was added to a solution of sodium bicarbonate (1eq, 0.7 g, 8.8 mmol) in water (18 mL). Then a solution of Aliquat 336 (0.8eq, 3 g, 7.4 mmol) and allyl bromide (5.3 eq, 4 mL, 46 mmol) in DCM (4.0mL) was added dropwise. The reaction was stirred overnight at rt. Subsequently, distilled water (90mL) was added before transferring to a separating funnel where the reaction mixture was extracted with DCM (3×100 mL) and washed with brine (2×50 mL). The mixture was then dried over Na_2SO_4 and the solvent was removed in vacuo. The raw product was purified by flash chromatography on silica gel (EP/EtOAc 8:2) to give a white powder (3.4g, 80% yield).

ESI-MS (m/z): 480.5 $[M+H]^+$

^{1}HNMR (400 MHz CD_3OD):δ 7.78 (d,J=8 Hz,2H), 7.62 (d,J=8.2Hz,2H), 7.42-7.38 (m,2H), 7.34-7.30 (m,2H), 5.95-5.87 (m,1H), 5.60 (d,J=7.8 Hz,1H), 5.35-5.26 (m,2H), 5.60 (s,1H), 4.66 (d,J=6.9 Hz,2H), 4.48-4.41 (m,2H), 4.24 (t,J=6.8 Hz,1H), 2.14-2.05 (m,1H), 1.80-1.76 (m,1H), 1.45 (s,9H).

Synthesis of allyl 2-((((9H-fluoren-9-yl)methoxy)carbonyl)amino)-4-aminobutanoate

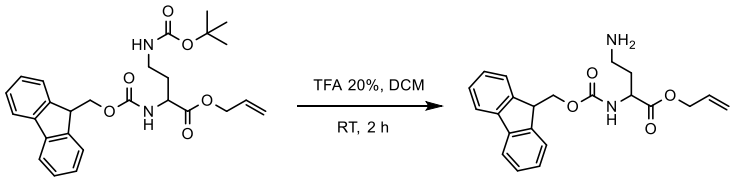

Fmoc-Dab(Boc)-OAllyl was dissolved in DCM containing 20% TFA (60 mL). The mixture was stirred at RT for 2 hours then the solvent was evaporated in vacuo and the product was obtaining after precipitation with cold diethyl ether. The obtained solid was washed with water, filtrated, dried under vacuum and lyophilized to give the final compound as a white solid (3.4 g, 98 % yield).

ESI-MS (m/z): 380.2 $[M+H]^+$

^{1}HNMR(400MHz,CD_3OD):δ8.13(s,2H),7.72(d,J=8Hz,2H),7.54(d,J=8.2Hz,2H), 7.37 (t,J=7.8,Hz,2H), 7.28-7.25 (m,2H), 5.92 (d,J=7.8 Hz,1H), 5.84-5.76 (m,2H), 5.28-5.19 (m,2H), 4.59-4.56 (m,2H), 4.39-4.34 (m,2H), 4.16 (t,J=7.9 Hz,1H), 3.10-2.77 (m,4H), 2.35-2.29 (m,1H), 1.94-1.89 (m,1H).

Synthesis of vinyl 2-methylbutanoate

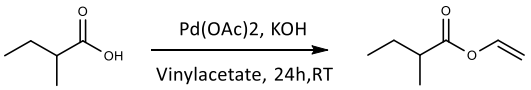

Vinyl 2-methylbutanoate was obtained as a yellow oil (0.7 mL, 76% yield) through the above reported general method for vinyl esters synthesis using 2-methylbutyric acid as starting material.

ESI-MS (m/z): 128.2 $[M+H]^+$

^{1}H NMR (400MHz, CD_3OD):δ 7.32 (q,J=8.0Hz,2H), 4.90 (dd,J=8,8 Hz, 14 Hz, 1H), 2.49-2.40 (m,1H), 1.77-1.67 (m,1H), 1.58-1.50 (m,1H), 1.20 (d,J=7.8 Hz,3H), 0.95 (t,J=7.8 Hz,3H).

Synthesis of vinyl 2,2-dimethylbutanoate

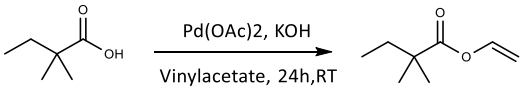

Vinyl 2,2-dimethylbutanoate was obtained as a yellow oil (0.8 mL, 67% yield) through the above reported general method for vinyl esters synthesis using 2-2-dimethylbutyric acid as starting material.

ESI-MS (m/z): 142.1 $[M+H]^+$

1H NMR (400 MHz, CD_3OD):δ 7.31-7.26 (m, ,1H), 4.91-4.88 (m, ,1H), 4.59-4.57 (m, ,1H), 1.65 (q,J=7.9 Hz,2H), 1.22 (s,6H), 0.89 (t,J=7.9,3H).

Synthesis of intermediate 9 (DB3)

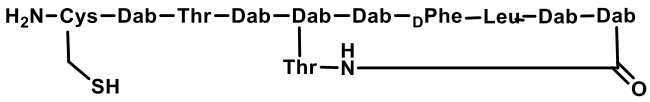

The 2-chlorotrityl polystyrene resin was loaded with Fmoc-Dab-OAll as reported in **Method 1** to assemble the peptide sequence on a 0.3 mmol scale (339 mg resin). Solid-phase peptide synthesis was performed using **Methods 3** and **4** for the coupling of Fmoc-Dab(Boc), Fmoc-Leu, Fmoc-D-Phe, Fmoc-Dab(Boc), Fmoc-Dab(Dde), Fmoc-Dab(Boc), Fmoc-Thr(tBu), Fmoc-Dab(Boc) and Fmoc-Cys(Trt). The Dde protecting group on Dab^4 was removed by **Method 5** followed by Fmoc-Thr(tBu) coupling carried out by using **Method 4**. The C-terminal allyl ester was removed using **Method 6** and the Thr Fmoc protecting group was removed by using **Method 3.** Cyclisation was then carried out by using **Method 7** followed by cleavage using **Method 9** leading to obtain raw intermediate as a white solid The obtained peptide was then purified by using a Waters 600E System and a Gemini_NX C18 110 Å column (5 μm; 250 x 10mm), gradient 17-47% B in 60 min (1% B/min), flow rate 5.0 mL/min. Elution peaks were collected manually and analysed by analytical RP-HPLC and ESI-MS. Pure fractions were combined and lyophilised obtaining the pure intermediate **9** (560 mg, 73 % yield).

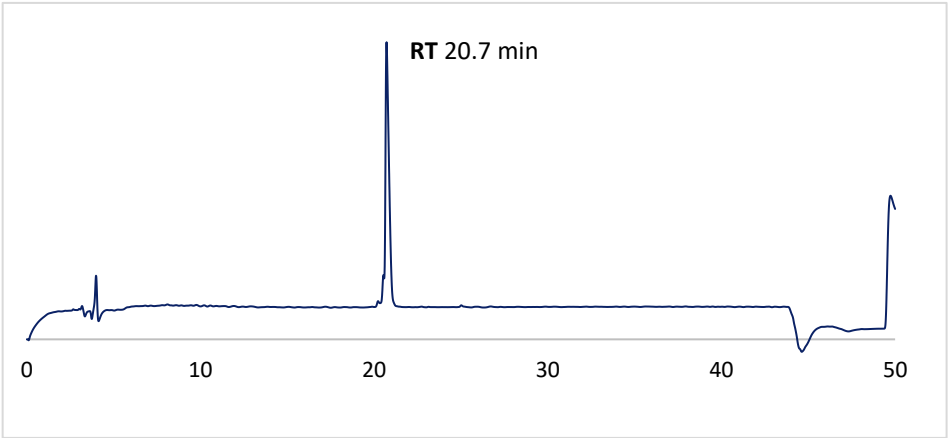

Figure 81. *Analytical RP-HPLC profile of intermediate 9. Luna® column LC C18(2) 100Å (5 µm; 150 mm x 4.6mm), A: 0.1% TFA in H2O, and B: 0.1%TFA in ACN. Gradient 5-65%B over 60 min (1%B/min), 1 mL/min, room temperature.*

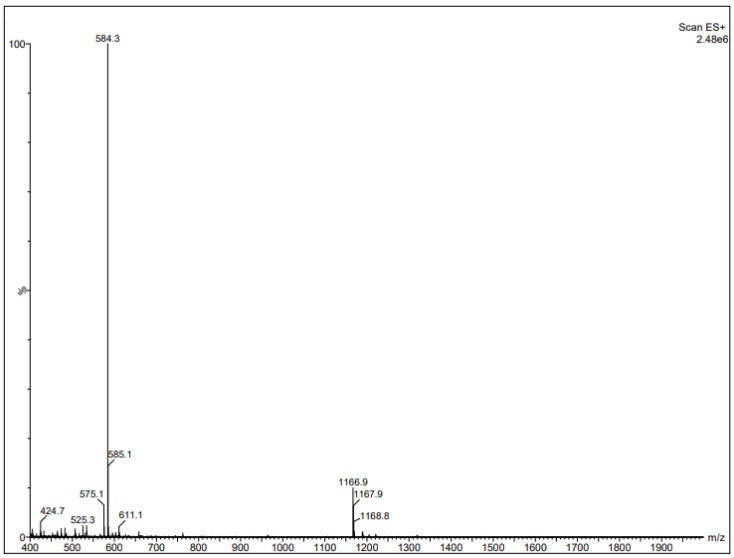

Figure 82. *ESI-MS of intermediate 9 [M+H]+ requires 1165.57 (observed 1166.9); [M+2H]2+ requires 583.7 (observed 584.3).*

Synthesis of analogue 9g

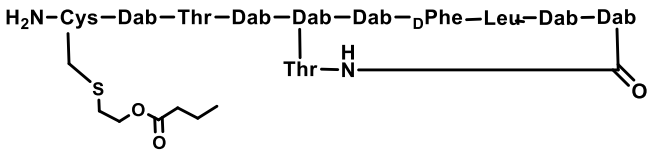

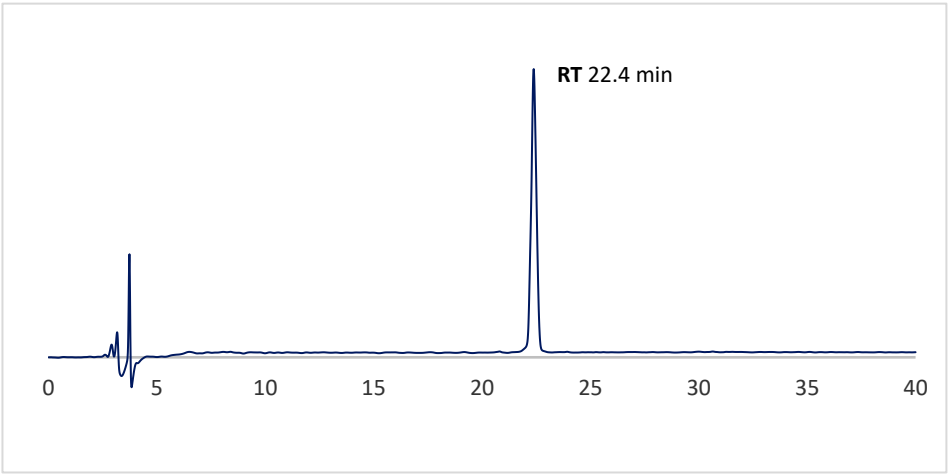

Figure 83. *Analytical RP-HPLC profile of analogue 9g. Luna® column LC C18(2) 100Å (5 µm; 150 mm x 4.6mm), A: 0.1% TFA in H2O, and B: 0.1%TFA in ACN. Gradient 5-65%B over 30 min (1%B/min), 1 mL/min, room temperature.*

S-lipidation of purified intermediate 9 (1eq, 15 mg) was performed as described in previous section using vinyl propionate (70eq, 90mg). The S-lipidated peptide was then precipitated with Et_2O and purified using a Waters 600E System and a Gemini_NX C18 110 Å column (5 µm; 250 x 10mm), gradient 5-95% B in 60 min (1% B/min), flow rate 5.0 mL/min. Elution peaks were collected manually and analysed by analytical RP-HPLC and ESI-MS. Pure fractions were combined and lyophilised obtaining the pure **9g** (3.7 mg, 23 % yield).

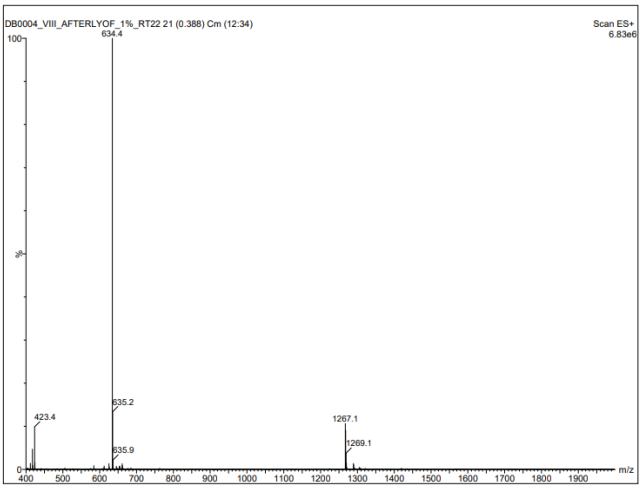

Figure 84. *ESI-MS of analogue 9g [M+H]+ observed 1267.1; [M+2H]2+ observed 634.4; [M+3H]3+ observed 423.4.*

Synthesis of analogue 9k

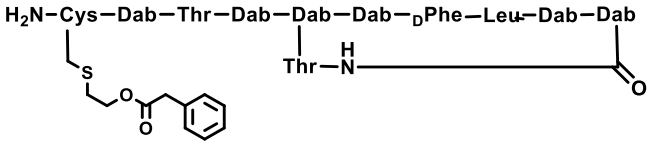

S-lipidation of purified intermediate 9 (1eq, 18 mg) was performed as described in previous section using vinyl benzoate (70eq, 150µL). The S-lipidated peptide was then precipitated with Et_2O and purified using a Waters 600E System and a Gemini_NX C18 110 Å column (5 µm; 250 x 10mm), gradient 5-95% B in 60 min (1% B/min), flow rate 5.0 mL/min. Elution peaks were collected manually and analysed by analytical RP-HPLC and ESI-MS. Pure fractions were combined and lyophilised obtaining the pure **9k** (5.2 mg, 26 % yield)

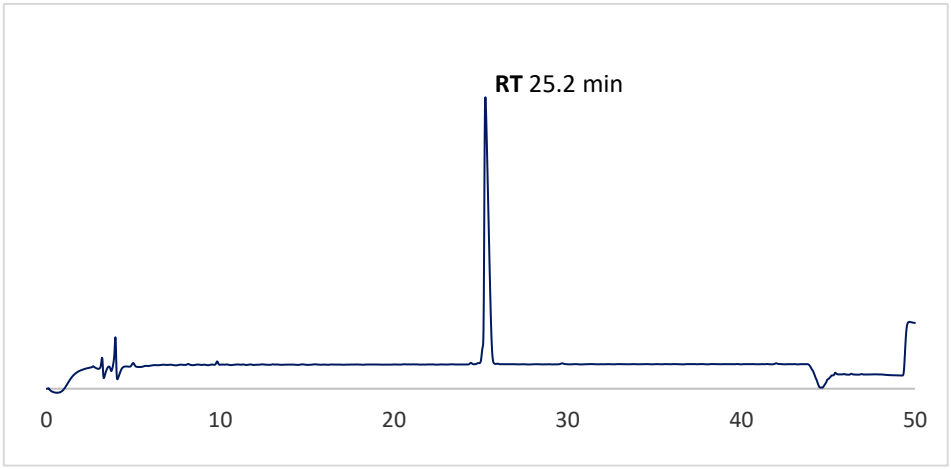

Figure 85.. *Analytical RP-HPLC profile of analogue 9k. Luna® column LC C18(2) 100Å (5 µm; 150 mm x 4.6mm), A: 0.1% TFA in H2O, and B: 0.1%TFA in ACN. Gradient 5-65%B over 60 min (1%B/min), 1 mL/min, room temperature.*

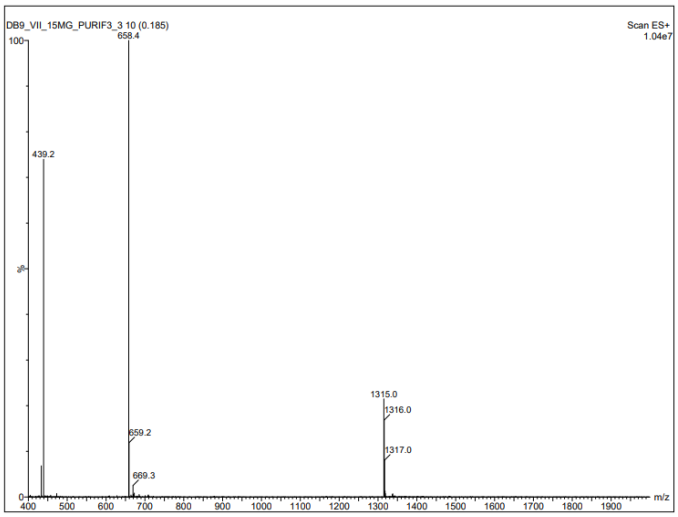

Figure 86. *ESI-MS of analogue 9k [M+H]+ observed 1315.01; [M+2H]2+ observed 658.4; [M+3H]3+ observed 423.4.*

Synthesis of analogue AC4.107/DB7

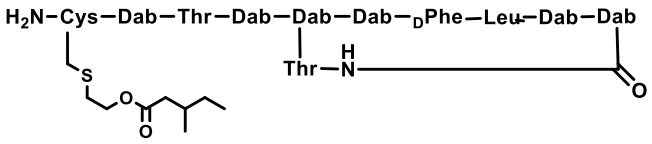

S-lipidation of purified intermediate 9 (1eq, 14 mg) was performed as described in previous section using Vinyl 2-methylbutanoate (70eq, 115mg) previously synthetized. The S-lipidated peptide was then precipitated with Et_2O and purified using a Waters 600E System and a Gemini_NX C18 110 Å column (5 µm; 250 x 10mm), gradient 5-95% B in 60 min (1% B/min), flow rate 5.0 mL/min. Elution peaks were collected manually and analysed by analytical RP-HPLC and ESI-MS. Pure fractions were combined and lyophilised obtaining the pure **AC4.107/DB7** (3.3 mg, 20 % yield)

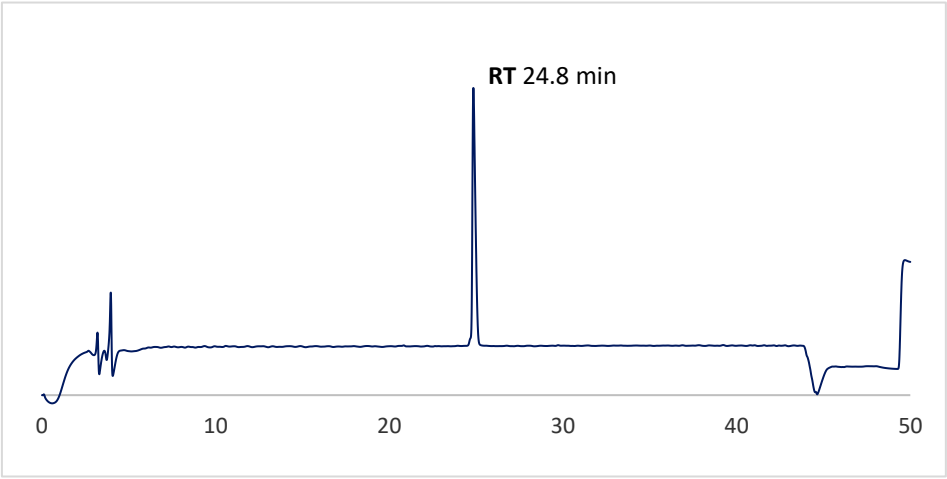

Figure 87. *Analytical RP-HPLC profile of analogue AC4.107/DB7. Luna® column LC C18(2) 100Å (5 µm; 150 mm x 4.6mm), A: 0.1% TFA in H2O, and B: 0.1%TFA in ACN. Gradient 5-65%B over 60 min (1%B/min), 1 mL/min,*

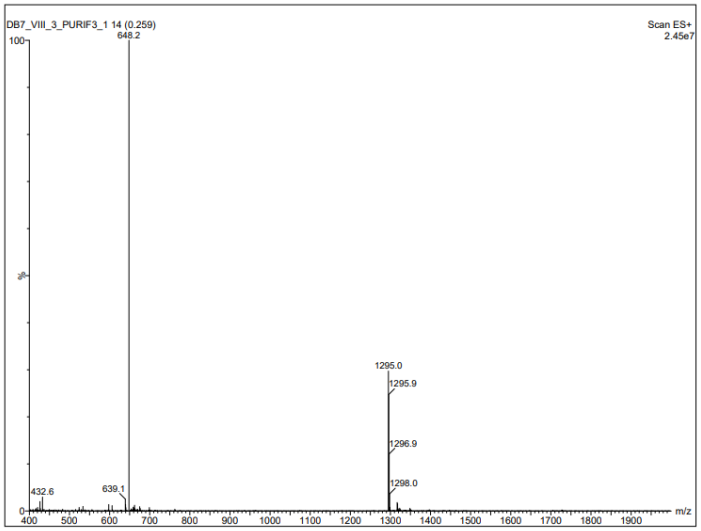

Figure 88. *ESI-MS of analogue AC4.107/DB7. [M+H]+ observed 1295.0; [M+2H]2+ observed 648.2; [M+3H]3+ observed 432.6.*

Synthesis of analogue AC4.106/DB8

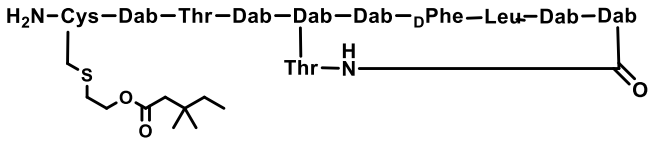

S-lipidation of purified intermediate 9 (1eq, 15 mg) was performed as described in previous section using vinyl 2,2-dimethylbutanoate (70eq, 127 mg) previously synthetized. The S-lipidated peptide was then precipitated with Et_2O and purified using a Waters 600E System and a Gemini_NX C18 110 Å column (5 µm; 250 x 10mm), gradient 5-95% B in 60 min (1% B/min), flow rate 5.0 mL/min. Elution peaks were collected manually and analysed by analytical RP-HPLC and ESI-MS. Pure fractions were combined and lyophilised obtaining the pure **AC4.106/DB8** (3.4 mg, 20 % yield).

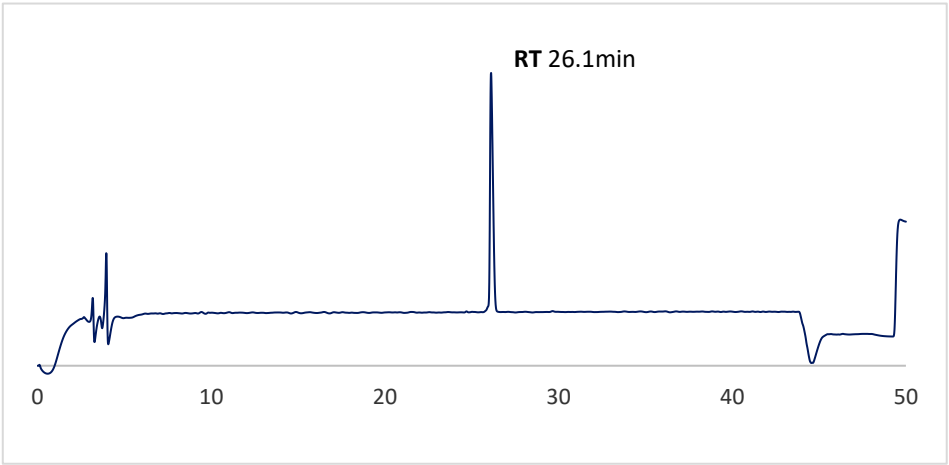

Figure 89. *Analytical RP-HPLC profile of analogue AC4.106/DB8. Luna® column LC C18(2) 100Å (5 µm; 150 mm x 4.6mm), A: 0.1% TFA in H2O, and B: 0.1%TFA in ACN. Gradient 5-65%B over 60 min (1%B/min), 1 mL/min, room temperature.*

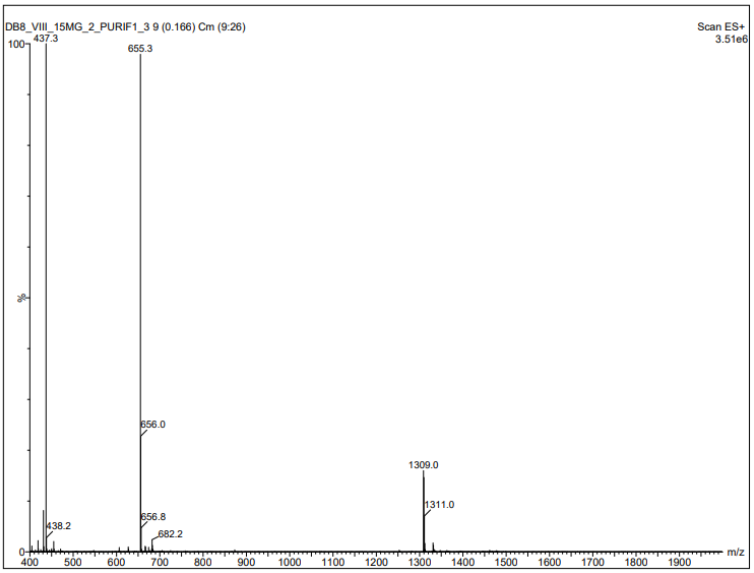

Figure 90. *ESI-MS of analogue AC4.106/DB8. [M+H]+ observed 1309.0; [M+2H]2+ observed 655.3; [M+3H]3+ observed 437.3.*

[This page is intentionally left blank]

References

(1) Durand, G. A.; Raoult, D.; Dubourg, G. Antibiotic Discovery: History, Methods and Perspectives. *International Journal of Antimicrobial Agents* **2019**, *53* (4), 371–382. https://doi.org/10.1016/j.ijantimicag.2018.11.010.

(2) Hutchings, M. I.; Truman, A. W.; Wilkinson, B. X Antibiotics: Past, Present and Future. *Current Opinion in Microbiology* **2019**, *51*, 72–80. https://doi.org/10.1016/j.mib.2019.10.008.

(3) Uddin, T. M.; Chakraborty, A. J.; Khusro, A.; Zidan, B. R. M.; Mitra, S.; Emran, T. B.; Dhama, K.; Ripon, Md. K. H.; Gajdács, M.; Sahibzada, M. U. K.; Hossain, Md. J.; Koirala, N. Antibiotic Resistance in Microbes: History, Mechanisms, Therapeutic Strategies and Future Prospects. *Journal of Infection and Public Health* **2021**, *14* (12), 1750–1766. https://doi.org/10.1016/j.jiph.2021.10.020.

(4) Nicolaou, K. C.; Rigol, S. A Brief History of Antibiotics and Select Advances in Their Synthesis. *J Antibiot* **2018**, *71* (2), 153–184. https://doi.org/10.1038/ja.2017.62.

(5) Gould, K. Antibiotics: From Prehistory to the Present Day. *Journal of Antimicrobial Chemotherapy* **2016**, *71* (3), 572–575. https://doi.org/10.1093/jac/dkv484.

(6) Ribeiro da Cunha, B.; Fonseca, L. P.; Calado, C. R. C. Antibiotic Discovery: Where Have We Come from, Where Do We Go? *Antibiotics* **2019**, *8* (2), 45. https://doi.org/10.3390/antibiotics8020045.

(7) Brown, E. D.; Wright, G. D. Antibacterial Drug Discovery in the Resistance Era. *Nature* **2016**, *529* (7586), 336–343. https://doi.org/10.1038/nature17042.

(8) Andrei, S.; Droc, G.; Stefan, G. FDA Approved Antibacterial Drugs: 2018-2019. *Discoveries (Craiova)* *7* (4), e102. https://doi.org/10.15190/d.2019.15.

(9) Chahine, E. B.; Dougherty, J. A.; Thornby, K.-A.; Guirguis, E. H. Antibiotic Approvals in the Last Decade: Are We Keeping Up With Resistance? *Ann Pharmacother* **2022**, *56* (4), 441–462. https://doi.org/10.1177/10600280211031390.

(10) Lee, H.-J.; Lee, D.-G. Urgent Need for Novel Antibiotics in Republic of Korea to Combat Multidrug-Resistant Bacteria. *Korean J Intern Med* **2022**, *37* (2), 271–280. https://doi.org/10.3904/kjim.2021.527.

(11) Acar, J.; Röstel, B. Antimicrobial Resistance: An Overview. *Revue scientifique et technique (International Office of Epizootics)* **2002**, *20*, 797–810. https://doi.org/10.20506/rst.20.3.1309.

(12) Kupferschmidt, K. Resistance Fighters. *Science* **2016**, *352* (6287), 758–761. https://doi.org/10.1126/science.352.6287.758.

(13) D'Costa, V. M.; King, C. E.; Kalan, L.; Morar, M.; Sung, W. W. L.; Schwarz, C.; Froese, D.; Zazula, G.; Calmels, F.; Debruyne, R.; Golding,

G. B.; Poinar, H. N.; Wright, G. D. Antibiotic Resistance Is Ancient. *Nature* **2011**, *477* (7365), 457–461. https://doi.org/10.1038/nature10388.
(14) English, B. K.; Gaur, A. H. The Use and Abuse of Antibiotics and the Development of Antibiotic Resistance. In *Hot Topics in Infection and Immunity in Children VI*; Finn, A., Curtis, N., Pollard, A. J., Eds.; Advances in Experimental Medicine and Biology; Springer: New York, NY, **2010**; pp 73–82. https://doi.org/10.1007/978-1-4419-0981-7_6.
(15) Li, B.; Webster, T. J. Bacteria Antibiotic Resistance: New Challenges and Opportunities for Implant-Associated Orthopedic Infections. *Journal of Orthopaedic Research* **2018**, *36* (1), 22–32. https://doi.org/10.1002/jor.23656.
(16) European Centre for Disease Prevention and Control.; World Health Organization. *Antimicrobial Resistance Surveillance in Europe 2023: 2021 Data.*; Publications Office: LU, **2023.**
(17) Contained and Controlled: The UK's 20-Year Vision for Antimicrobial Resistance.
(18) AMR-Tackling-the-Burden-in-the-EU-OECD-ECDC-Briefing-Note-2019.Pdf.
(19) Cassini, A.; Hopkins, S. Attributable Deaths and Disability-Adjusted Life-Years Caused by Infections with Antibiotic-Resistant Bacteria in the EU and the European Economic Area in 2015: A Population-Level Modelling Analysis. *The Lancet Infectious Diseases* **2019**, *19* (1), 56–66. https://doi.org/10.1016/S1473-3099(18)30605-4.
(20) Davies, J.; Davies, D. X Origins and Evolution of Antibiotic Resistance. *Microbiology and Molecular Biology Reviews* **2010**, *74* (3), 417–433. https://doi.org/10.1128/MMBR.00016-10.
(21) Vikesland, P.; Garner, E.; Gupta, S.; Kang, S.; Maile-Moskowitz, A.; Zhu, N. Differential Drivers of Antimicrobial Resistance across the World. *Acc. Chem. Res.* **2019**, *52* (4), 916–924. https://doi.org/10.1021/acs.accounts.8b00643.
(22) Meek, R. W.; Vyas, H.; Piddock, L. J. V. Nonmedical Uses of Antibiotics: Time to Restrict Their Use? *PLOS Biology* **2015**, *13* (10), e1002266. https://doi.org/10.1371/journal.pbio.1002266.
(23) Tang, K. W. K.; Millar, B. C.; Moore, J. E. Antimicrobial Resistance (AMR). *Br J Biomed Sci* **2023**, *80*, 11387. https://doi.org/10.3389/bjbs.2023.11387.
(24) Cella, E.; Giovanetti, M.; Benedetti, F.; Scarpa, F.; Johnston, C.; Borsetti, A.; Ceccarelli, G.; Azarian, T.; Zella, D.; Ciccozzi, M. Joining Forces against Antibiotic Resistance: The One Health Solution. *Pathogens* **2023**, *12* (9), 1074. https://doi.org/10.3390/pathogens12091074.
(25) Global increase and geographic convergence in antibiotic consumption between 2000 and 2015. https://doi.org/10.1073/pnas.1717295115.
(26) Samreen; Ahmad, I.; Malak, H. A.; Abulreesh, H. H. Environmental Antimicrobial Resistance and Its Drivers: A Potential Threat to Public

Health. *Journal of Global Antimicrobial Resistance* **2021**, *27*, 101–111. https://doi.org/10.1016/j.jgar.2021.08.001.

(27) Crofts, T. S.; Gasparrini, A. J.; Dantas, G. Next-Generation Approaches to Understand and Combat the Antibiotic Resistome. *Nat Rev Microbiol* **2017**, *15* (7), 422–434. https://doi.org/10.1038/nrmicro.2017.28.

(28) Reygaert, W. C. An Overview of the Antimicrobial Resistance Mechanisms of Bacteria. *AIMS Microbiol* **2018**, *4* (3), 482–501. https://doi.org/10.3934/microbiol.2018.3.482.

(29) Christaki, E.; Marcou, M.; Tofarides, A. Antimicrobial Resistance in Bacteria: Mechanisms, Evolution, and Persistence. *J Mol Evol* **2020**, *88* (1), 26–40. https://doi.org/10.1007/s00239-019-09914-3.

(30) Smith, W. P. J.; Wucher, B. R.; Nadell, C. D.; Foster, K. R. Bacterial Defences: Mechanisms, Evolution and Antimicrobial Resistance. *Nat Rev Microbiol* **2023**, *21* (8), 519–534. https://doi.org/10.1038/s41579-023-00877-3.

(31) Larsson, D. G. J.; Flach, C.-F. Antibiotic Resistance in the Environment. *Nat Rev Microbiol* **2022**, *20* (5), 257–269. https://doi.org/10.1038/s41579-021-00649-x.

(32) Vikesland, P. J.; Pruden, A.; Alvarez, P. J. J.; Aga, D.; Bürgmann, H.; Li, X.; Manaia, C. M.; Nambi, I.; Wigginton, K.; Zhang, T.; Zhu, Y.-G. Toward a Comprehensive Strategy to Mitigate Dissemination of Environmental Sources of Antibiotic Resistance. *Environ. Sci. Technol.* **2017**, *51* (22), 13061–13069. https://doi.org/10.1021/acs.est.7b03623.

(33) Holmes, A. H.; Moore, L. S. P.; Sundsfjord, A.; Steinbakk, M.; Regmi, S.; Karkey, A.; Guerin, P. J.; Piddock, L. J. V. Understanding the Mechanisms and Drivers of Antimicrobial Resistance. *The Lancet* **2016**, *387* (10014), 176–187. https://doi.org/10.1016/S0140-6736(15)00473-0.

(34) Lee, J.-H. Perspectives towards Antibiotic Resistance: From Molecules to Population. *J Microbiol.* **2019**, *57* (3), 181–184. https://doi.org/10.1007/s12275-019-0718-8.

(35) Blair, J. M. A.; Webber, M. A.; Baylay, A. J.; Ogbolu, D. O.; Piddock, L. J. V. Molecular Mechanisms of Antibiotic Resistance. *Nat Rev Microbiol* **2015**, *13* (1), 42–51. https://doi.org/10.1038/nrmicro3380.

(36) Brenciani, A.; Morroni, G.; Schwarz, S.; Giovanetti, E. Oxazolidinones: Mechanisms of Resistance and Mobile Genetic Elements Involved. *Journal of Antimicrobial Chemotherapy* **2022**, *77* (10), 2596–2621. https://doi.org/10.1093/jac/dkac263.

(37) Redgrave, L. S.; Sutton, S. B.; Webber, M. A.; Piddock, L. J. V. Fluoroquinolone Resistance: Mechanisms, Impact on Bacteria, and Role in Evolutionary Success. *Trends in Microbiology* **2014**, *22* (8), 438–445. https://doi.org/10.1016/j.tim.2014.04.007.

(38) Bebear, C. M.; Pereyre, S. Mechanisms of Drug Resistance in Mycoplasma Pneumoniae. *Current Drug Targets - Infectious Disorders* **2005**, *5* (3), 263–271.

(39) Miller, W. R.; Munita, J. M.; Arias, C. A. Mechanisms of Antibiotic Resistance in Enterococci. *Expert Review of Anti-infective Therapy*

2014, *12* (10), 1221–1236. https://doi.org/10.1586/14787210.2014.956092.

(40) Potter, R. F.; D'Souza, A. W.; Dantas, G. The Rapid Spread of Carbapenem-Resistant Enterobacteriaceae. *Drug Resistance Updates* **2016**, *29*, 30–46. https://doi.org/10.1016/j.drup.2016.09.002.

(41) Lavigne, J.-P.; Sotto, A.; Nicolas-Chanoine, M.-H.; Bouziges, N.; Pagès, J.-M.; Davin-Regli, A. An Adaptive Response of Enterobacter Aerogenes to Imipenem: Regulation of Porin Balance in Clinical Isolates. *International Journal of Antimicrobial Agents* **2013**, *41* (2), 130–136. https://doi.org/10.1016/j.ijantimicag.2012.10.010.

(42) Denissen, J.; Reyneke, B.; Waso-Reyneke, M.; Havenga, B.; Barnard, T.; Khan, S.; Khan, W. Prevalence of ESKAPE Pathogens in the Environment: Antibiotic Resistance Status, Community-Acquired Infection and Risk to Human Health. *International Journal of Hygiene and Environmental Health* **2022**, *244*, 114006. https://doi.org/10.1016/j.ijheh.2022.114006.

(43) Asokan, G. V.; Ramadhan, T.; Ahmed, E.; Sanad, H. WHO Global Priority Pathogens List: A Bibliometric Analysis of Medline-PubMed for Knowledge Mobilization to Infection Prevention and Control Practices in Bahrain. *Oman Med J* **2019**, *34* (3), 184–193. https://doi.org/10.5001/omj.2019.37.

(44) Mulani, M. S.; Kamble, E. E.; Kumkar, S. N.; Tawre, M. S.; Pardesi, K. R. Emerging Strategies to Combat ESKAPE Pathogens in the Era of Antimicrobial Resistance: A Review. *Frontiers in Microbiology* **2019**, *10*.

(45) Knight, G. M.; Costelloe, C.; Murray, K. A.; Robotham, J. V.; Atun, R.; Holmes, A. H. Addressing the Unknowns of Antimicrobial Resistance: Quantifying and Mapping the Drivers of Burden. *Clinical Infectious Diseases* **2018**, *66* (4), 612–616. https://doi.org/10.1093/cid/cix765.

(46) *Global Antimicrobial Resistance and Use Surveillance System (GLASS)*. https://www.who.int/initiatives/glass (accessed 2023-11-15).

(47) Ferri, M.; Ranucci, E.; Romagnoli, P.; Giaccone, V. Antimicrobial Resistance: A Global Emerging Threat to Public Health Systems. *Critical Reviews in Food Science and Nutrition* **2017**, *57* (13), 2857–2876. https://doi.org/10.1080/10408398.2015.1077192.

(48) Wang, J.; Dou, X.; Song, J.; Lyu, Y.; Zhu, X.; Xu, L.; Li, W.; Shan, A. Antimicrobial Peptides: Promising Alternatives in the Post Feeding Antibiotic Era. *Medicinal Research Reviews* **2019**, *39* (3), 831–859. https://doi.org/10.1002/med.21542.

(49) Moretta, A.; Scieuzo, C.; Petrone, A. M.; Salvia, R.; Manniello, M. D.; Franco, A.; Lucchetti, D.; Vassallo, A.; Vogel, H.; Sgambato, A.; Falabella, P. Antimicrobial Peptides: A New Hope in Biomedical and Pharmaceutical Fields. *Frontiers in Cellular and Infection Microbiology* **2021**, *11*.

(50) Zhong, C.; Zhang, F.; Yao, J.; Zhu, Y.; Zhu, N.; Zhang, Y.; Liu, H.; Gou, S.; Ni, J. Antimicrobial Peptides with Symmetric Structures against

Multidrug-Resistant Bacteria While Alleviating Antimicrobial Resistance. *Biochemical Pharmacology* **2021**, 114470. https://doi.org/10.1016/j.bcp.2021.114470.

(51) Erak, M.; Bellmann-Sickert, K.; Els-Heindl, S.; Beck-Sickinger, A. G. Peptide Chemistry Toolbox – Transforming Natural Peptides into Peptide Therapeutics. *Bioorganic & Medicinal Chemistry* **2018**, *26* (10), 2759–2765. https://doi.org/10.1016/j.bmc.2018.01.012.

(52) Huan, Y.; Kong, Q.; Mou, H.; Yi, H. Antimicrobial Peptides: Classification, Design, Application and Research Progress in Multiple Fields. *Frontiers in Microbiology* **2020**, *11*, 2559. https://doi.org/10.3389/fmicb.2020.582779.

(53) Nakatsuji, T.; Gallo, R. Antimicrobial Peptides: Old Molecules with New Ideas. *The Journal of investigative dermatology* **2012**. https://doi.org/10.1038/jid.2011.387.

(54) Seyfi, R.; Kahaki, F. A.; Ebrahimi, T.; Montazersaheb, S.; Eyvazi, S.; Babaeipour, V.; Tarhriz, V. Antimicrobial Peptides (AMPs): Roles, Functions and Mechanism of Action. *Int J Pept Res Ther* **2020**, *26* (3), 1451–1463. https://doi.org/10.1007/s10989-019-09946-9.

(55) Zhang, Q.-Y.; Yan, Z.-B.; Meng, Y.-M.; Hong, X.-Y.; Shao, G.; Ma, J.-J.; Cheng, X.-R.; Liu, J.; Kang, J.; Fu, C.-Y. Antimicrobial Peptides: Mechanism of Action, Activity and Clinical Potential. *Military Med Res* **2021**, *8* (1), 48. https://doi.org/10.1186/s40779-021-00343-2.

(56) Erdem Büyükkiraz, M.; Kesmen, Z. Antimicrobial Peptides (AMPs): A Promising Class of Antimicrobial Compounds. *Journal of Applied Microbiology* **2022**, *132* (3), 1573–1596. https://doi.org/10.1111/jam.15314.

(57) Tossi, A.; Sandri, L.; Giangaspero, A. Amphipathic, α-Helical Antimicrobial Peptides. *Peptide Science* **2000**, *55* (1), 4–30. https://doi.org/10.1002/1097-0282(2000)55:1<4::AID-BIP30>3.0.CO;2-M.

(58) Ceremuga, M.; Stela, M.; Janik, E.; Gorniak, L.; Synowiec, E.; Sliwinski, T.; Sitarek, P.; Saluk-Bijak, J.; Bijak, M. Melittin—A Natural Peptide from Bee Venom Which Induces Apoptosis in Human Leukaemia Cells. *Biomolecules* **2020**, *10* (2), 247. https://doi.org/10.3390/biom10020247.

(59) Hong, J.; Lu, X.; Deng, Z.; Xiao, S.; Yuan, B.; Yang, K. How Melittin Inserts into Cell Membrane: Conformational Changes, Inter-Peptide Cooperation, and Disturbance on the Membrane. *Molecules* **2019**, *24* (9), 1775. https://doi.org/10.3390/molecules24091775.

(60) Terwilliger, T. C.; Weissman, L.; Eisenberg, D. The Structure of Melittin in the Form I Crystals and Its Implication for Melittin's Lytic and Surface Activities. *Biophysical Journal* **1982**, *37* (1), 353–361. https://doi.org/10.1016/S0006-3495(82)84683-3.

(61) Degrado, W. F. Design of Peptides and Proteins. *Adv Protein Chem* **1988**, *39*, 51–124. https://doi.org/10.1016/s0065-3233(08)60375-7.

(62) Pincus, M. R. Chapter 2 - Physiological Structure and Function of Proteins. In *Cell Physiology Source Book (Fourth Edition)*; Sperelakis, N., Ed.; Academic Press: San Diego, **2012;** pp 19–47. https://doi.org/10.1016/B978-0-12-387738-3.00002-0.

(63) Giacometti, A.; Cirioni, O.; Kamysz, W.; D'Amato, G.; Silvestri, C.; Del Prete, M. S.; Łukasiak, J.; Scalise, G. Comparative Activities of Cecropin A, Melittin, and Cecropin A-Melittin Peptide CA(1-7)M(2-9)NH2 against Multidrug-Resistant Nosocomial Isolates of Acinetobacter Baumannii. *Peptides* **2003**, *24* (9), 1315–1318. https://doi.org/10.1016/j.peptides.2003.08.003.

(64) Zasloff, M. Magainins, a Class of Antimicrobial Peptides from Xenopus Skin: Isolation, Characterization of Two Active Forms, and Partial cDNA Sequence of a Precursor. *Proceedings of the National Academy of Sciences* **1987**, *84* (15), 5449–5453. https://doi.org/10.1073/pnas.84.15.5449.

(65) Juretić, D.; Chen, H.-C.; Brown, J. H.; Morell, J. L.; Hendler, R. W.; Westerhoff, H. V. Magainin 2 Amide and Analogues Antimicrobial Activity, Membrane Depolarization and Susceptibility to Proteolysis. *FEBS Letters* **1989**, *249* (2), 219–223. https://doi.org/10.1016/0014-5793(89)80627-1.

(66) Hasan, M.; Islam, M. M.; Rahman, M. M. A Review on Structure - Activity Relationship of Antimicrobial Peptide Magainin 2. *Dhaka Univ. J. Pharm. Sci* **2022**, 427–434. https://doi.org/10.3329/dujps.v20i3.59806.

(67) Ebenhan, T.; Gheysens, O.; Kruger, H. G.; Zeevaart, J. R.; Sathekge, M. M. Antimicrobial Peptides: Their Role as Infection-Selective Tracers for Molecular Imaging. *BioMed Research International* **2014**, *2014*, e867381. https://doi.org/10.1155/2014/867381.

(68) Dathe, M.; Wieprecht, T.; Nikolenko, H.; Handel, L.; Maloy, W. L.; MacDonald, D. L.; Beyermann, M.; Bienert, M. Hydrophobicity, Hydrophobic Moment and Angle Subtended by Charged Residues Modulate Antibacterial and Haemolytic Activity of Amphipathic Helical Peptides. *FEBS Letters* **1997**, *403* (2), 208–212. https://doi.org/10.1016/S0014-5793(97)00055-0.

(69) Bechinger, B.; Zasloff, M.; Opella, S. J. Structure and Orientation of the Antibiotic Peptide Magainin in Membranes by Solid-State Nuclear Magnetic Resonance Spectroscopy. *Protein Science* **1993**, *2* (12), 2077–2084. https://doi.org/10.1002/pro.5560021208.

(70) Chen, H.-C.; Brown, J. H.; Morell, J. L.; Huang, C. m. Synthetic Magainin Analogues with Improved Antimicrobial Activity. *FEBS Letters* **1988**, *236* (2), 462–466. https://doi.org/10.1016/0014-5793(88)80077-2.

(71) Wieprecht, T.; Dathe, M.; Epand, R. M.; Beyermann, M.; Krause, E.; Maloy, W. L.; MacDonald, D. L.; Bienert, M. Influence of the Angle Subtended by the Positively Charged Helix Face on the Membrane Activity of Amphipathic, Antibacterial Peptides. *Biochemistry* **1997**, *36* (42), 12869–12880. https://doi.org/10.1021/bi971398n.

(72) McMillan, K. A. M.; Coombs, M. R. P. Review: Examining the Natural Role of Amphibian Antimicrobial Peptide Magainin. *Molecules* **2020**, *25* (22), 5436. https://doi.org/10.3390/molecules25225436.
(73) Lee, W.; Lee, D. G. Magainin 2 Induces Bacterial Cell Death Showing Apoptotic Properties. *Curr Microbiol* **2014**, *69* (6), 794–801. https://doi.org/10.1007/s00284-014-0657-x.
(74) Magana, M.; Pushpanathan, M.; Santos, A. L.; Leanse, L.; Fernandez, M.; Ioannidis, A.; Giulianotti, M. A.; Apidianakis, Y.; Bradfute, S.; Ferguson, A. L.; Cherkasov, A.; Seleem, M. N.; Pinilla, C.; de la Fuente-Nunez, C.; Lazaridis, T.; Dai, T.; Houghten, R. A.; Hancock, R. E. W.; Tegos, G. P. The Value of Antimicrobial Peptides in the Age of Resistance. *The Lancet Infectious Diseases* **2020**, *20* (9), e216–e230. https://doi.org/10.1016/S1473-3099(20)30327-3.
(75) Wu, D.; Gao, Y.; Qi, Y.; Chen, L.; Ma, Y.; Li, Y. Peptide-Based Cancer Therapy: Opportunity and Challenge. *Cancer Letters* **2014**, *351* (1), 13–22. https://doi.org/10.1016/j.canlet.2014.05.002.
(76) Sato, H.; Feix, J. B. Peptide–Membrane Interactions and Mechanisms of Membrane Destruction by Amphipathic α-Helical Antimicrobial Peptides. *Biochimica et Biophysica Acta (BBA) - Biomembranes* **2006**, *1758* (9), 1245–1256. https://doi.org/10.1016/j.bbamem.2006.02.021.
(77) Annunziato, G.; Costantino, G. Antimicrobial Peptides (AMPs): A Patent Review (2015–2020). *Expert Opinion on Therapeutic Patents* **2020**, *30* (12), 931–947. https://doi.org/10.1080/13543776.2020.1851679.
(78) Kumar, P.; Kizhakkedathu, J. N.; Straus, S. K. Antimicrobial Peptides: Diversity, Mechanism of Action and Strategies to Improve the Activity and Biocompatibility In Vivo. *Biomolecules* **2018**, *8* (1), 4. https://doi.org/10.3390/biom8010004.
(79) Brogden, K. A. 12/11 Antimicrobial Peptides: Pore Formers or Metabolic Inhibitors in Bacteria? *Nature Reviews Microbiology* **2005**, *3* (3), 238–250. https://doi.org/10.1038/nrmicro1098.
(80) Dijksteel, G. S.; Ulrich, M. M. W.; Middelkoop, E.; Boekema, B. K. H. L. Review: Lessons Learned From Clinical Trials Using Antimicrobial Peptides (AMPs). *Front Microbiol* **2021**, *12*, 616979. https://doi.org/10.3389/fmicb.2021.616979.
(81) Molchanova, N.; Hansen, P. R.; Franzyk, H. Advances in Development of Antimicrobial Peptidomimetics as Potential Drugs. *Molecules* **2017**, *22* (9), 1430. https://doi.org/10.3390/molecules22091430.
(82) Koo, H. B.; Seo, J. X Antimicrobial Peptides under Clinical Investigation. *Peptide Science* **2019**, *111* (5), e24122. https://doi.org/10.1002/pep2.24122.
(83) Bellotti, D.; Remelli, M. Lights and Shadows on the Therapeutic Use of Antimicrobial Peptides. *Molecules* **2022**, *27* (14), 4584. https://doi.org/10.3390/molecules27144584.
(84) Mahlapuu, M.; Björn, C.; Ekblom, J. Antimicrobial Peptides as Therapeutic Agents: Opportunities and Challenges. *Critical Reviews in*

Biotechnology **2020**, *40* (7), 978–992. https://doi.org/10.1080/07388551.2020.1796576.

(85) Lienkamp, K.; Madkour, A. E.; Tew, G. N. Antibacterial Peptidomimetics: Polymeric Synthetic Mimics of Antimicrobial Peptides. In *Polymer Composites – Polyolefin Fractionation – Polymeric Peptidomimetics – Collagens*; Abe, A., Kausch, H.-H., Möller, M., Pasch, H., Eds.; Advances in Polymer Science; Springer: Berlin, Heidelberg, **2013**; pp 141–172. https://doi.org/10.1007/12_2010_85.

(86) Vagner, J.; Qu, H.; Hruby, V. J. Peptidomimetics, a Synthetic Tool of Drug Discovery. *Current Opinion in Chemical Biology* **2008**, *12* (3), 292–296. https://doi.org/10.1016/j.cbpa.2008.03.009.

(87) Lenci, E.; Trabocchi, A. Peptidomimetic Toolbox for Drug Discovery. *Chem. Soc. Rev.* **2020**, *49* (11), 3262–3277. https://doi.org/10.1039/D0CS00102C.

(88) Floris, M.; Moro, S. Mimicking Peptides… In Silico. *Molecular Informatics* **2012**, *31* (1), 12–20. https://doi.org/10.1002/minf.201100093.

(89) Pelay-Gimeno, M.; Glas, A.; Koch, O.; Grossmann, T. N. Structure-Based Design of Inhibitors of Protein–Protein Interactions: Mimicking Peptide Binding Epitopes. *Angewandte Chemie International Edition* **2015**, *54* (31), 8896–8927. https://doi.org/10.1002/anie.201412070.

(90) Trabocchi, A. Chapter 6 - Principles and Applications of Small Molecule Peptidomimetics. In *Small Molecule Drug Discovery*; Trabocchi, A., Lenci, E., Eds.; Elsevier, 2020; pp 163–195. https://doi.org/10.1016/B978-0-12-818349-6.00006-6.

(91) Tew, G. N.; Liu, D.; Chen, B.; Doerksen, R. J.; Kaplan, J.; Carroll, P. J.; Klein, M. L.; DeGrado, W. F. ORIGINI BRILACIDINA_De Novo Design of Biomimetic Antimicrobial Polymers. *Proceedings of the National Academy of Sciences* **2002**, *99* (8), 5110–5114. https://doi.org/10.1073/pnas.082046199.

(92) Palermo, E. F. Antimicrobial Polymers: Peptide-Mimetic Design and Mechanism of Action.

(93) Ghosh, C.; Haldar, J. 24/11 Membrane-Active Small Molecules: Designs Inspired by Antimicrobial Peptides. *ChemMedChem* **2015**, *10* (10), 1606–1624. https://doi.org/10.1002/cmdc.201500299.

(94) Liu, D.; Choi, S.; Chen, B.; Doerksen, R. J.; Clements, D. J.; Winkler, J. D.; Klein, M. L.; DeGrado, W. F. Nontoxic Membrane-Active Antimicrobial Arylamide Oligomers. *Angewandte Chemie International Edition* **2004**, *43* (9), 1158–1162. https://doi.org/10.1002/anie.200352791.

(95) Choi, S.; Isaacs, A.; Clements, D.; Liu, D.; Kim, H.; Scott, R. W.; Winkler, J. D.; DeGrado, W. F. X De Novo Design and in Vivo Activity of Conformationally Restrained Antimicrobial Arylamide Foldamers. *PNAS* **2009**, *106* (17), 6968–6973. https://doi.org/10.1073/pnas.0811818106.

(96) Tang, H.; Doerksen, R. J.; Jones, T. V.; Klein, M. L.; Tew, G. N. Biomimetic Facially Amphiphilic Antibacterial Oligomers with Conformationally Stiff Backbones. *Chemistry & Biology* **2006**, *13* (4), 427–435. https://doi.org/10.1016/j.chembiol.2006.02.007.
(97) Host Defense Protein Mimetics for Prophylaxis.
(98) Tew, G. N.; Scott, R. W.; Klein, M. L.; DeGrado, W. F. De Novo Design of Antimicrobial Polymers, Foldamers, and Small Molecules: From Discovery to Practical Applications. *Acc. Chem. Res.* **2010**, *43* (1), 30–39. https://doi.org/10.1021/ar900036b.
(99) Jamieson, A. G.; Boutard, N.; Sabatino, D.; Lubell, W. D. Peptide Scanning for Studying Structure-Activity Relationships in Drug Discovery. *Chemical Biology & Drug Design* **2013**, *81* (1), 148–165. https://doi.org/10.1111/cbdd.12042.
(100) Nagarajan, K.; Kapoor, G. Peptidomimetics in Medicinal Chemistry: The Art of Transforming Peptides to Drugs. In *Recent Advances in Pharmaceutical Innovation and Research*; Singh, P. P., Ed.; Springer Nature: Singapore, 2023; pp 215–242. https://doi.org/10.1007/978-981-99-2302-1_9.
(101) Gante, J. Peptidomimetics—Tailored Enzyme Inhibitors. *Angew. Chem. Int. Ed. Engl.* **1994**, *33* (17), 1699–1720. https://doi.org/10.1002/anie.199416991.
(102) Kumari, S.; Carmona, A. V.; Tiwari, A. K.; Trippier, P. C. Amide Bond Bioisosteres: Strategies, Synthesis, and Successes. *J Med Chem* **2020**, *63* (21), 12290–12358. https://doi.org/10.1021/acs.jmedchem.0c00530.
(103) Boström, J.; Hogner, A.; Llinàs, A.; Wellner, E.; Plowright, A. T. Oxadiazoles in Medicinal Chemistry. *J. Med. Chem.* **2012**, *55* (5), 1817–1830. https://doi.org/10.1021/jm2013248.
(104) Gerecke, M. Chemical Structure and Properties of Midazolam Compared with Other Benzodiazepines. *British Journal of Clinical Pharmacology* **1983**, *16* (S1), 11S-16S. https://doi.org/10.1111/j.1365-2125.1983.tb02266.x.
(105) Choudhary, A.; Raines, R. T. An Evaluation of Peptide-Bond Isosteres. *ChemBioChem* **2011**, *12* (12), 1801–1807. https://doi.org/10.1002/cbic.201100272.
(106) White, C. J.; Yudin, A. K. Contemporary Strategies for Peptide Macrocyclization. *Nature Chem* **2011**, *3* (7), 509–524. https://doi.org/10.1038/nchem.1062.
(107) Avan, I.; Dennis Hall, C.; R. Katritzky, A. Peptidomimetics via Modifications of Amino Acids and Peptide Bonds. *Chemical Society Reviews* **2014**, *43* (10), 3575–3594. https://doi.org/10.1039/C3CS60384A.
(108) Lobo-Ruiz, A.; Tulla-Puche, J. 2 - Synthetic Approaches of Naturally and Rationally Designed Peptides and Peptidomimetics. In *Peptide Applications in Biomedicine, Biotechnology and Bioengineering*; Koutsopoulos, S., Ed.; Woodhead Publishing, **2018**; pp 23–49. https://doi.org/10.1016/B978-0-08-100736-5.00002-8.

(109) Bolarinwa, O.; Nimmagadda, A.; Su, M.; Cai, J. Structure and Function of AApeptides. *Biochemistry* **2017**, *56* (3), 445–457. https://doi.org/10.1021/acs.biochem.6b01132.
(110) Matsuzaki, K.; Nakamura, A.; Murase, O.; Sugishita, K.; Fujii, N.; Miyajima, K. Modulation of Magainin 2−Lipid Bilayer Interactions by Peptide Charge. *Biochemistry* **1997**, *36* (8), 2104–2111. https://doi.org/10.1021/bi961870p.
(111) Wieprecht, T.; Dathe, M.; Beyermann, M.; Krause, E.; Maloy, W. L.; MacDonald, D. L.; Bienert, M. Peptide Hydrophobicity Controls the Activity and Selectivity of Magainin 2 Amide in Interaction with Membranes. *Biochemistry* **1997**, *36* (20), 6124–6132. https://doi.org/10.1021/bi9619987.
(112) Torres, M. D. T.; Sothiselvam, S.; Lu, T. K.; de la Fuente-Nunez, C. Peptide Design Principles for Antimicrobial Applications. *Journal of Molecular Biology* **2019**, *431* (18), 3547–3567. https://doi.org/10.1016/j.jmb.2018.12.015.
(113) Bacalum, M.; Janosi, L.; Zorila, F.; Tepes, A.-M.; Ionescu, C.; Bogdan, E.; Hadade, N.; Craciun, L.; Grosu, I.; Turcu, I.; Radu, M. Modulating Short Tryptophan- and Arginine-Rich Peptides Activity by Substitution with Histidine. *Biochimica et Biophysica Acta (BBA) - General Subjects* **2017**, *1861* (7), 1844–1854. https://doi.org/10.1016/j.bbagen.2017.03.024.
(114) Li, L.; Vorobyov, I.; Allen, T. W. The Different Interactions of Lysine and Arginine Side Chains with Lipid Membranes. *J. Phys. Chem. B* **2013**, *117* (40), 11906–11920. https://doi.org/10.1021/jp405418y.
(115) Aguilar, E.; Meyers, A. I. Reinvestigation of a Modified Hantzsch Thiazole Synthesis. *Tetrahedron Letters* **1994**, *35* (16), 2473–2476. https://doi.org/10.1016/S0040-4039(00)77147-4.
(116) Wu, Y.-J. Chapter 5.5 - Five-Membered Ring Systems: With N and S Atom. In *Progress in Heterocyclic Chemistry*; Gribble, G. W., Joule, J. A., Eds.; Elsevier, **2015**; Vol. 27, pp 287–303. https://doi.org/10.1016/B978-0-08-100024-3.00009-X.
(117) Bertram, A.; Blake, A. J.; Turiso, F. G.-L. de; Hannam, J. S.; Jolliffe, K. A.; Pattenden, G.; Skae, M. Concise Synthesis of Stereodefined, Thiazole—Containing Cyclic Hexa- and Octapeptide Relatives of the Lissoclinums, via Cyclooligomerisation Reactions. *Tetrahedron* **2003**, *59* (35), 6979–6990. https://doi.org/10.1016/S0040-4020(03)00821-4.
(118) Bertram, A.; Hannam, J. S.; Jolliffe, K. A.; González-López De Turiso, F.; Pattenden, G. The Synthesis of Novel Thiazole Containing Cyclic Peptides *via* Cyclooligomerisation Reactions. *Synlett* **1999**, *1999* (11), 1723–1726. https://doi.org/10.1055/s-1999-2942.
(119) Wahyudi, H.; Tantisantisom, W.; Liu, X.; Ramsey, D. M.; Singh, E. K.; McAlpine, S. R. Synthesis, Structure–Activity Analysis, and Biological Evaluation of Sanguinamide B Analogues. *J. Org. Chem.* **2012**, *77* (23), 10596–10616. https://doi.org/10.1021/jo3017499.

(120) Jiménez-Jiménez, C.; Moreno, V.; Vallet-Regí, M. Bacteria-Assisted Transport of Nanomaterials to Improve Drug Delivery in Cancer Therapy. *Nanomaterials* **2022**, *12*, 288. https://doi.org/10.3390/nano12020288.
(121) Silhavy, T. J.; Kahne, D.; Walker, S. The Bacterial Cell Envelope. *Cold Spring Harb Perspect Biol* **2010**, *2* (5), a000414. https://doi.org/10.1101/cshperspect.a000414.
(122) Chapter 1 - Basic Biology of Oral Microbes. In *Atlas of Oral Microbiology*; Zhou, X., Li, Y., Eds.; Academic Press: Oxford, **2015**; pp 1–14. https://doi.org/10.1016/B978-0-12-802234-4.00001-X.
(123) Schulz, G. E. The Structure of Bacterial Outer Membrane Proteins. *Biochimica et Biophysica Acta (BBA) - Biomembranes* **2002**, *1565* (2), 308–317. https://doi.org/10.1016/S0005-2736(02)00577-1.
(124) Rollauer, S. E.; Sooreshjani, M. A.; Noinaj, N.; Buchanan, S. K. Outer Membrane Protein Biogenesis in Gram-Negative Bacteria. *Philosophical Transactions of the Royal Society B: Biological Sciences* **2015**, *370* (1679), 20150023. https://doi.org/10.1098/rstb.2015.0023.
(125) Sun, J.; Deng, Z.; Yan, A. Bacterial Multidrug Efflux Pumps: Mechanisms, Physiology and Pharmacological Exploitations. *Biochemical and Biophysical Research Communications* **2014**, *453* (2), 254–267. https://doi.org/10.1016/j.bbrc.2014.05.090.
(126) Du, D.; Wang-Kan, X.; Neuberger, A.; van Veen, H. W.; Pos, K. M.; Piddock, L. J. V.; Luisi, B. F. Multidrug Efflux Pumps: Structure, Function and Regulation. *Nat Rev Microbiol* **2018**, *16* (9), 523–539. https://doi.org/10.1038/s41579-018-0048-6.
(127) JMA Blair1, G E Richmond, LJV Piddock Multidrug Efflux Pumps in Gram-Negative Bacteria and Their Role in Antibiotic Resistance, *Future Microbiol*. 2014, 9(10), 1165 –1177
(128) Du, D.; Wang, Z.; James, N. R.; Voss, J. E.; Klimont, E.; Ohene-Agyei, T.; Venter, H.; Chiu, W.; Luisi, B. F. Structure of the AcrAB–TolC Multidrug Efflux Pump. *Nature* **2014**, *509* (7501), 512–515. https://doi.org/10.1038/nature13205.
(129) Piddock, L. J. V. Clinically Relevant Chromosomally Encoded Multidrug Resistance Efflux Pumps in Bacteria. *Clinical Microbiology Reviews* **2006**, *19* (2), 382–402. https://doi.org/10.1128/cmr.19.2.382-402.2006.
(130) Li, X.-Z.; Plésiat, P.; Nikaido, H. The Challenge of Efflux-Mediated Antibiotic Resistance in Gram-Negative Bacteria. *Clin Microbiol Rev* **2015**, *28* (2), 337–418. https://doi.org/10.1128/CMR.00117-14.
(131) Savino, R.; Paduano, S.; Preianò, M.; Terracciano, R. The Proteomics Big Challenge for Biomarkers and New Drug-Targets Discovery. *International Journal of Molecular Sciences* **2012**, *13* (11), 13926–13948. https://doi.org/10.3390/ijms131113926.
(132) Burton, N. R.; Kim, P.; Backus, K. M. Photoaffinity Labelling Strategies for Mapping the Small Molecule–Protein Interactome. *Org. Biomol. Chem.* **2021**, *19* (36), 7792–7809. https://doi.org/10.1039/D1OB01353J.

(133) Bantscheff, M.; Scholten, A.; Heck, A. J. R. Revealing Promiscuous Drug–Target Interactions by Chemical Proteomics. *Drug Discovery Today* **2009**, *14* (21), 1021–1029. https://doi.org/10.1016/j.drudis.2009.07.001.
(134) Köcher, T.; Superti-Furga, G. Mass Spectrometry–Based Functional Proteomics: From Molecular Machines to Protein Networks. *Nat Methods* **2007**, *4* (10), 807–815. https://doi.org/10.1038/nmeth1093.
(135) Dadvar, P.; O'Flaherty, M.; Scholten, A.; Rumpel, K.; J.R. Heck, A. A Chemical Proteomics Based Enrichment Technique Targeting the Interactome of the PDE5 Inhibitor PF-4540124. *Molecular BioSystems* **2009**, *5* (5), 472–482. https://doi.org/10.1039/B815709J.
(136) Bantscheff, M.; Drewes, G. Chemoproteomic Approaches to Drug Target Identification and Drug Profiling. *Bioorganic & Medicinal Chemistry* **2012**, *20* (6), 1973–1978. https://doi.org/10.1016/j.bmc.2011.11.003.
(137) Ogasawara, H.; Shinohara, S.; Yamamoto, K.; Ishihama, A. Novel Regulation Targets of the Metal-Response BasS-BasR Two-Component System of Escherichia Coli. *Microbiology (Reading)* **2012**, *158* (Pt 6), 1482–1492. https://doi.org/10.1099/mic.0.057745-0.
(138) Epand, R. F.; Pollard, J. E.; Wright, J. O.; Savage, P. B.; Epand, R. M. Depolarization, Bacterial Membrane Composition, and the Antimicrobial Action of Ceragenins. *Antimicrob Agents Chemother* **2010**, *54* (9), 3708–3713. https://doi.org/10.1128/AAC.00380-10.
(139) P. Conway, L.; M. Jadhav, A.; A. Homan, R.; Li, W.; Sanchez Rubiano, J.; Hawkins, R.; Michael Lawrence, R.; G. Parker, C. Evaluation of Fully-Functionalized Diazirine Tags for Chemical Proteomic Applications. *Chemical Science* **2021**, *12* (22), 7839–7847. https://doi.org/10.1039/D1SC01360B.
(140) Chen, X.; Wong, Y. K.; Wang, J.; Zhang, J.; Lee, Y.-M.; Shen, H.-M.; Lin, Q.; Hua, Z.-C. Target Identification with Quantitative Activity Based Protein Profiling (ABPP). *PROTEOMICS* **2017**, *17* (3–4), 1600212. https://doi.org/10.1002/pmic.201600212.
(141) Wiegand, I.; Hilpert, K.; Hancock, R. E. W. Agar and Broth Dilution Methods to Determine the Minimal Inhibitory Concentration (MIC) of Antimicrobial Substances. *Nat Protoc* **2008**, *3* (2), 163–175. https://doi.org/10.1038/nprot.2007.521.
(142) Velkov, T.; Roberts, K. D.; Thompson, P. E.; Li, J. Polymyxins: A New Hope in Combating Gram-Negative Superbugs? *Future Medicinal Chemistry* **2016**, *8* (10), 1017–1025. https://doi.org/10.4155/fmc-2016-0091.
(143) Velkov, T.; Thompson, P. E.; Azad, M. A. K.; Roberts, K. D.; Bergen, P. J. History, Chemistry and Antibacterial Spectrum. In *Polymyxin Antibiotics: From Laboratory Bench to Bedside*; Li, J., Nation, R. L., Kaye, K. S., Eds.; Advances in Experimental Medicine and Biology; Springer International Publishing: Cham, **2019**; pp 15–36. https://doi.org/10.1007/978-3-030-16373-0_3.

(144) Nang, S. C.; Azad, M. A. K.; Velkov, T.; Zhou, Q. (Tony); Li, J. Rescuing the Last-Line Polymyxins: Achievements and Challenges. *Pharmacol Rev* **2021**, *73* (2), 679–728. https://doi.org/10.1124/pharmrev.120.000020.
(145) Mohapatra, S. S.; Dwibedy, S. K.; Padhy, I. Polymyxins, the Last-Resort Antibiotics: Mode of Action, Resistance Emergence, and Potential Solutions. *J Biosci* **2021**, *46* (3), 85. https://doi.org/10.1007/s12038-021-00209-8.
(146) Trimble, M. J.; Mlynárčik, P.; Kolář, M.; Hancock, R. E. W. Polymyxin: Alternative Mechanisms of Action and Resistance. *Cold Spring Harb Perspect Med* **2016**, *6* (10), a025288. https://doi.org/10.1101/cshperspect.a025288.
(147) Kaye, K. S.; Pogue, J. M.; Tran, T. B.; Nation, R. L.; Li, J. Agents of Last Resort: Polymyxin Resistance. *Infectious Disease Clinics* **2016**, *30* (2), 391–414. https://doi.org/10.1016/j.idc.2016.02.005.
(148) Poirel, L.; Jayol, A.; Nordmann, P. Polymyxins: Antibacterial Activity, Susceptibility Testing, and Resistance Mechanisms Encoded by Plasmids or Chromosomes. *Clinical Microbiology Reviews* **2017**, *30* (2), 557–596. https://doi.org/10.1128/cmr.00064-16.
(149) Sabnis, A.; Hagart, K. L.; Klöckner, A.; Becce, M.; Evans, L. E.; Furniss, R. C. D.; Mavridou, D. A.; Murphy, R.; Stevens, M. M.; Davies, J. C.; Larrouy-Maumus, G. J.; Clarke, T. B.; Edwards, A. M. Colistin Kills Bacteria by Targeting Lipopolysaccharide in the Cytoplasmic Membrane. *eLife* **2021**, *10*, e65836. https://doi.org/10.7554/eLife.65836.
(150) Ayoub Moubareck, C. Polymyxins and Bacterial Membranes: A Review of Antibacterial Activity and Mechanisms of Resistance. *Membranes* **2020**, *10* (8), 181. https://doi.org/10.3390/membranes10080181.
(151) Kwa, A.; Kasiakou, S. K.; Tam, V. H.; Falagas, M. E. Polymyxin B: Similarities to and Differences from Colistin (Polymyxin E). *Expert Review of Anti-infective Therapy* **2007**, *5* (5), 811–821. https://doi.org/10.1586/14787210.5.5.811.
(152) Avedissian, S. N.; Liu, J.; Rhodes, N. J.; Lee, A.; Pais, G. M.; Hauser, A. R.; Scheetz, M. H. A Review of the Clinical Pharmacokinetics of Polymyxin B. *Antibiotics* **2019**, *8* (1), 31. https://doi.org/10.3390/antibiotics8010031.
(153) Zavascki, A. P.; Goldani, L. Z.; Li, J.; Nation, R. L. Polymyxin B for the Treatment of Multidrug-Resistant Pathogens: A Critical Review. *Journal of Antimicrobial Chemotherapy* **2007**, *60* (6), 1206–1215. https://doi.org/10.1093/jac/dkm357.
(154) Tang, H.; Zhang, Y.; Ma, J.; Dong, Y.; Gao, Q.; Feng, J. Design, Synthesis and Antimicrobial Studies of Some Polymyxin Analogues. *J Antibiot* **2020**, *73* (3), 158–166. https://doi.org/10.1038/s41429-019-0262-0.
(155) Handzlik, J.; Matys, A.; Kieć-Kononowicz, K. Recent Advances in Multi-Drug Resistance (MDR) Efflux Pump Inhibitors of Gram-Positive

Bacteria S. Aureus. *Antibiotics* **2013**, *2* (1), 28–45. https://doi.org/10.3390/antibiotics2010028.
(156) Vaara, M. Polymyxins and Their Potential Next Generation as Therapeutic Antibiotics. *Frontiers in Microbiology* **2019**, *10*.
(157) Brown, P.; Dawson, M. J. Development of New Polymyxin Derivatives for Multi-Drug Resistant Gram-Negative Infections. *J Antibiot* **2017**, *70* (4), 386–394. https://doi.org/10.1038/ja.2016.146.
(158) Jaradat, D. M. M. Thirteen Decades of Peptide Synthesis: Key Developments in Solid Phase Peptide Synthesis and Amide Bond Formation Utilized in Peptide Ligation. *Amino Acids* **2018**, *50* (1), 39–68. https://doi.org/10.1007/s00726-017-2516-0.
(159) Kent, S. B. H. Chemical Synthesis of Peptides and Proteins. *Annual Review of Biochemistry* **1988**, *57* (1), 957–989. https://doi.org/10.1146/annurev.bi.57.070188.004521.
(160) H. Kent, S. B. Total Chemical Synthesis of Proteins. *Chemical Society Reviews* **2009**, *38* (2), 338–351. https://doi.org/10.1039/B700141J.
(161) Merrifield, R. B. Solid Phase Peptide Synthesis. I. The Synthesis of a Tetrapeptide. *J. Am. Chem. Soc.* **1963**, *85* (14), 2149–2154. https://doi.org/10.1021/ja00897a025.
(162) Sakakibara, S.; Shimonishi, Y.; Kishida, Y.; Okada, M.; Sugihara, H. Use of Anhydrous Hydrogen Fluoride in Peptide Synthesis. I. Behavior of Various Protective Groups in Anhydrous Hydrogen Fluoride. *Bulletin of the Chemical Society of Japan* **1967**, *40* (9), 2164–2167. https://doi.org/10.1246/bcsj.40.2164.
(163) Carpino, L. A.; Han, G. Y. 9-Fluorenylmethoxycarbonyl Function, a New Base-Sensitive Amino-Protecting Group. *J. Am. Chem. Soc.* **1970**, *92* (19), 5748–5749. https://doi.org/10.1021/ja00722a043.
(164) Atherton, E.; Fox, H.; Harkiss, D.; J. Logan, C.; C. Sheppard, R.; J. Williams, B. A Mild Procedure for Solid Phase Peptide Synthesis: Use of Fluorenylmethoxycarbonylamino-Acids. *Journal of the Chemical Society, Chemical Communications* **1978**, *0* (13), 537–539. https://doi.org/10.1039/C39780000537.
(165) Shelton, P. T.; Jensen, K. J. Linkers, Resins, and General Procedures for Solid-Phase Peptide Synthesis. In *Peptide Synthesis and Applications*; Jensen, K. J., Tofteng Shelton, P., Pedersen, S. L., Eds.; Methods in Molecular Biology; Humana Press: Totowa, NJ, **2013**; pp 23–41. https://doi.org/10.1007/978-1-62703-544-6_2.
(166) Orain, D.; Ellard, J.; Bradley, M. Protecting Groups in Solid-Phase Organic Synthesis. *J. Comb. Chem.* **2002**, *4* (1), 1–16. https://doi.org/10.1021/cc0001093.
(167) Albericio, F.; El-Faham, A. Choosing the Right Coupling Reagent for Peptides: A Twenty-Five-Year Journey. *Org. Process Res. Dev.* **2018**, *22* (7), 760–772. https://doi.org/10.1021/acs.oprd.8b00159.
(168) Sheehan, J. C.; Hess, G. P. A New Method of Forming Peptide Bonds. *J. Am. Chem. Soc.* **1955**, *77* (4), 1067–1068. https://doi.org/10.1021/ja01609a099.

(169) Valeur, E.; Bradley, M. Amide Bond Formation: Beyond the Myth of Coupling Reagents. *Chemical Society Reviews* **2009**, *38* (2), 606–631. https://doi.org/10.1039/B701677H.
(170) Hudson, D. Methodological Implications of Simultaneous Solid-Phase Peptide Synthesis. 1. Comparison of Different Coupling Procedures. *J. Org. Chem.* **1988**, *53* (3), 617–624. https://doi.org/10.1021/jo00238a026.
(171) Vogler, K.; Studer, R. O.; Lanz, P.; Lergier, W.; Böhni, E. Synthesen in Der Polymyxin-Reihe 9. Mitteilung. Synthese von Polymyxin B1. *Helvetica Chimica Acta* **1965**, *48* (5), 1161–1177. https://doi.org/10.1002/hlca.19650480523.
(172) Velkov, T.; Thompson, P. E.; Nation, R. L.; Li, J. Structure−Activity Relationships of Polymyxin Antibiotics. *J. Med. Chem.* **2010**, *53* (5), 1898–1916. https://doi.org/10.1021/jm900999h.
(173) Sharma, S. k.; Wu, A. d.; Chandramouli, N.; Fotsch, C.; Kardash, G.; Bair, K. w. Solid-Phase Total Synthesis of Polymyxin B1. *The Journal of Peptide Research* **1999**, *53* (5), 501–506. https://doi.org/10.1034/j.1399-3011.1999.00045.x.
(174) Tsubery, H.; Ofek, I.; Cohen, S.; Fridkin, M. Structure−Function Studies of Polymyxin B Nonapeptide: Implications to Sensitization of Gram-Negative Bacteria. *J. Med. Chem.* **2000**, *43* (16), 3085–3092. https://doi.org/10.1021/jm0000057.
(175) Kline, T.; Holub, D.; Therrien, J.; Leung, T.; Ryckman, D. Synthesis and Characterization of the Colistin Peptide Polymyxin E1 and Related Antimicrobial Peptides. *The Journal of Peptide Research* **2001**, *57* (3), 175–187. https://doi.org/10.1111/j.1399-3011.2001.00835.x.
(176) Vaara, M.; Fox, J.; Loidl, G.; Siikanen, O.; Apajalahti, J.; Hansen, F.; Frimodt-Møller, N.; Nagai, J.; Takano, M.; Vaara, T. Novel Polymyxin Derivatives Carrying Only Three Positive Charges Are Effective Antibacterial Agents. *Antimicrobial Agents and Chemotherapy* **2008**, *52* (9), 3229–3236. https://doi.org/10.1128/aac.00405-08.
(177) Kanazawa, K.; Sato, Y.; Ohki, K.; Okimura, K.; Uchida, Y.; Shindo, M.; Sakura, N. Contribution of Each Amino Acid Residue in Polymyxin B3 to Antimicrobial and Lipopolysaccharide Binding Activity. *Chem. Pharm. Bull.* **2009**, *57* (3), 240–244. https://doi.org/10.1248/cpb.57.240.
(178) Xu, W.-L.; Cui, A.-L.; Hu, X.-X.; You, X.-F.; Li, Z.-R.; Zheng, J.-S. A New Strategy for Total Solid-Phase Synthesis of Polymyxins. *Tetrahedron Letters* **2015**, *56* (33), 4796–4799. https://doi.org/10.1016/j.tetlet.2015.06.056.
(179) Gallardo-Godoy, A.; Muldoon, C.; Becker, B.; Elliott, A. G.; Lash, L. H.; Huang, J. X.; Butler, M. S.; Pelingon, R.; Kavanagh, A. M.; Ramu, S.; Phetsang, W.; Blaskovich, M. A. T.; Cooper, M. A. Activity and Predicted Nephrotoxicity of Synthetic Antibiotics Based on Polymyxin B. *J. Med. Chem.* **2016**, *59* (3), 1068–1077. https://doi.org/10.1021/acs.jmedchem.5b01593.
(180) Chihara, S.; Ito, A.; Yahata, M.; Tobita, T.; Koyama, Y. Chemical Synthesis and Characterization of *n*-Fattyacyl Mono-Aminoacyl

Derivatives of Colistin Nonapeptide. *Agricultural and Biological Chemistry* **1974**, *38* (10), 1767–1777. https://doi.org/10.1271/bbb1961.38.1767.

(181) Clausell, A.; Rabanal, F.; Garcia-Subirats, M.; Asunción Alsina, M.; Cajal, Y. Membrane Association and Contact Formation by a Synthetic Analogue of Polymyxin B and Its Fluorescent Derivatives. *J. Phys. Chem. B* **2006**, *110* (9), 4465–4471. https://doi.org/10.1021/jp0551972.

(182) de Visser, P. c.; Kriek, N. m. a. j.; van Hooft, P. a. v.; Van Schepdael, A.; Filippov, D. v.; van der Marel, G. a.; Overkleeft, H. s.; van Boom, J. h.; Noort, D. Solid-Phase Synthesis of Polymyxin B1 and Analogues via a Safety-Catch Approach. *The Journal of Peptide Research* **2003**, *61* (6), 298–306. https://doi.org/10.1034/j.1399-3011.2003.00061.x.

(183) Tsubery, H.; Ofek, I.; Cohen, S.; Fridkin, M. N-Terminal Modifications of Polymyxin B Nonapeptide and Their Effect on Antibacterial Activity. *Peptides* **2001**, *22* (10), 1675–1681. https://doi.org/10.1016/S0196-9781(01)00503-4.

(184) Sakura, N.; Itoh, T.; Uchida, Y.; Ohki, K.; Okimura, K.; Chiba, K.; Sato, Y.; Sawanishi, H. The Contribution of the N-Terminal Structure of Polymyxin B Peptides to Antimicrobial and Lipopolysaccharide Binding Activity. *Bulletin of the Chemical Society of Japan* **2004**, *77* (10), 1915–1924. https://doi.org/10.1246/bcsj.77.1915.

(185) Okimura, K.; Ohki, K.; Sato, Y.; Ohnishi, K.; Uchida, Y.; Sakura, N. Chemical Conversion of Natural Polymyxin B and Colistin to Their N-Terminal Derivatives. *Bulletin of the Chemical Society of Japan* **2007**, *80* (3), 543–552. https://doi.org/10.1246/bcsj.80.543.

(186) O'Dowd, H.; Kim, B.; Margolis, P.; Wang, W.; Wu, C.; Lopez, S. L.; Blais, J. Preparation of Tetra-Boc-Protected Polymyxin B Nonapeptide. *Tetrahedron Letters* **2007**, *48* (11), 2003–2005. https://doi.org/10.1016/j.tetlet.2007.01.071.

(187) Tsubery, H.; Ofek, I.; Cohen, S.; Eisenstein, M.; Fridkin, M. Modulation of the Hydrophobic Domain of Polymyxin B Nonapeptide: Effect on Outer-Membrane Permeabilization and Lipopolysaccharide Neutralization. *Mol Pharmacol* **2002**, *62* (5), 1036–1042. https://doi.org/10.1124/mol.62.5.1036.

(188) Yim, V.; Kavianinia, I.; K. Knottenbelt, M.; A. Ferguson, S.; M. Cook, G.; Swift, S.; Chakraborty, A.; R. Allison, J.; J. Cameron, A.; R. Harris, P. W.; A. Brimble, M. "CLipP"Ing on Lipids to Generate Antibacterial Lipopeptides. *Chemical Science* **2020**, *11* (22), 5759–5765. https://doi.org/10.1039/D0SC01814G.

(189) V. Yim, V.; Kavianinia, I.; J. Cameron, A.; R. Harris, P. W.; A. Brimble, M. Direct Synthesis of Cyclic Lipopeptides Using Intramolecular Native Chemical Ligation and Thiol–Ene CLipPA Chemistry. *Organic & Biomolecular Chemistry* **2020**, *18* (15), 2838–2844. https://doi.org/10.1039/D0OB00203H.

(190) Yim, V. V.; Cameron, A. J.; Kavianinia, I.; Harris, P. W. R.; Brimble, M. A. Thiol-Ene Enabled Chemical Synthesis of Truncated S-Lipidated Teixobactin Analogs. *Frontiers in Chemistry* **2020**, *8*.
(191) W. Tong, J. T.; Kavianinia, I.; A. Ferguson, S.; M. Cook, G.; R. Harris, P. W.; A. Brimble, M. Synthesis of Paenipeptin C′ Analogues Employing Solution-Phase CLipPA Chemistry. *Organic & Biomolecular Chemistry* **2020**, *18* (23), 4381–4385. https://doi.org/10.1039/D0OB00950D.
(192) Ahangarpour, M.; Kavianinia, I.; Harris, P. W. R.; Brimble, M. A. Photo-Induced Radical Thiol–Ene Chemistry: A Versatile Toolbox for Peptide-Based Drug Design. *Chem. Soc. Rev.* **2021**, *50* (2), 898–944. https://doi.org/10.1039/D0CS00354A.
(193) Hoyle, C. E.; Bowman, C. N. Thiol–Ene Click Chemistry. *Angewandte Chemie International Edition* **2010**, *49* (9), 1540–1573. https://doi.org/10.1002/anie.200903924.
(194) Yang, S.-H.; Harris, P. W. R.; Williams, G. M.; Brimble, M. A. Lipidation of Cysteine or Cysteine-Containing Peptides Using the Thiol-Ene Reaction (CLipPA). *European Journal of Organic Chemistry* **2016**, *2016* (15), 2608–2616. https://doi.org/10.1002/ejoc.201501375.
(195) Triola, G.; Brunsveld, L.; Waldmann, H. Racemization-Free Synthesis of S-Alkylated Cysteines via Thiol-Ene Reaction. *J. Org. Chem.* **2008**, *73* (9), 3646–3649. https://doi.org/10.1021/jo800198s.
(196) Wright, T. H.; Brooks, A. E. S.; Didsbury, A. J.; Williams, G. M.; Harris, P. W. R.; Dunbar, P. R.; Brimble, M. A. Direct Peptide Lipidation through Thiol–Ene Coupling Enables Rapid Synthesis and Evaluation of Self-Adjuvanting Vaccine Candidates. *Angewandte Chemie International Edition* **2013**, *52* (40), 10616–10619. https://doi.org/10.1002/anie.201305620.
(197) Brimble, M. Synthesis, Antibacterial Activity and Nephrotoxicity of Novel Polymyxin B Analogues Modified at Leu-7, D-Phe-6 and the N-Terminus Enabled by Cysteine Lipidation.
(198) Chatzi, K. Barlos. O.; Gatos, D.; Stavropoulos, G. 2-Chlorotrityl Chloride Resin: Studies on Anchoring of Fmoc-Amino Acids and Peptide Cleavage. *International Journal of Peptide and Protein Research* **2009**, *37* (6), 513–520. https://doi.org/10.1111/j.1399-3011.1991.tb00769.x.
(199) Kaiser, E.; Colescott, R. L.; Bossinger, C. D.; Cook, P. I. Color Test for Detection of Free Terminal Amino Groups in the Solid-Phase Synthesis of Peptides. *Analytical Biochemistry* **1970**, *34* (2), 595–598. https://doi.org/10.1016/0003-2697(70)90146-6.
(200) Carpino, L. A. 1-Hydroxy-7-Azabenzotriazole. An Efficient Peptide Coupling Additive. *J. Am. Chem. Soc.* **1993**, *115* (10), 4397–4398. https://doi.org/10.1021/ja00063a082.
(201) Albericio, F.; Cases, M.; Alsina, J.; Triolo, S. A.; Carpino, L. A.; Kates, S. A. On the Use of PyAOP, a Phosphonium Salt Derived from HOAt, in Solid-Phase Peptide Synthesis. *Tetrahedron Letters* **1997**, *38* (27), 4853–4856. https://doi.org/10.1016/S0040-4039(97)01011-3.

(202) Zowawi, H. M.; Forde, B. M.; Alfaresi, M.; Alzarouni, A.; Farahat, Y.; Chong, T.-M.; Yin, W.-F.; Chan, K.-G.; Li, J.; Schembri, M. A.; Beatson, S. A.; Paterson, D. L. Stepwise Evolution of Pandrug-Resistance in Klebsiella Pneumoniae. *Sci Rep* **2015**, *5* (1), 15082. https://doi.org/10.1038/srep15082.

(203) Performance Standards for Antimicrobial Susceptibility Testing, 26th Ed.,CLSI Document M100S; Clinical andLaboratory Standards Institute: Wayne, PA,**2016.** In *erformance Standards for Antimicrobial Susceptibility Testing*; Clinical andLaboratory Standards Institute: Wayne, 2016.